

Lancaster Environment Centre
Faculty of Science and Technology
Lancaster University

Exploiting diversity in the
regulation of carbon
assimilation to improve wheat productivity

Gustaf E. Degen BSc MSc

This thesis is submitted in partial fulfilment of the requirements for the degree of Doctor of Philosophy

September 2020



This work is my own work and has not been submitted in any form for the award of a higher degree elsewhere. For work that has been published or will be submitted to a journal, author contributions have been described.


Gustaf E. Degen

September 2020

Summary

Rubisco activase (Rca) is a key regulator of carbon assimilation. It removes inhibitory sugar phosphate derivatives from the active site of Rubisco by using the energy from ATP hydrolysis. However, Rca is thermosensitive and limits photosynthesis at moderately high temperatures and during photosynthetic induction. A better understanding of the properties of Rca isoforms present in wheat, a staple crop for human nutrition, will unlock the potential to improve the efficiency and resilience of carbon assimilation to meet future food demands in the face of climate change.

The three wheat Rca isoforms were found to vary in the capacity to activate Rubisco *in vitro*. Rca1 β had lower Rubisco activation activity than Rca2 β and Rca2 α . Ratios of Rubisco active sites to Rca above 6-11:1 resulted in maximal Rubisco activation. Furthermore, residues that conferred ADP sensitivity of Rca1 β were identified using site-directed mutagenesis of the ADP-insensitive Rca2 β isoform. These findings can inform future efforts to optimise Rubisco activation during shade to sun transitions in crops.

To investigate the thermotolerance of native wheat Rca isoforms, temperature responses of ATP hydrolysis and Rubisco activation were assessed. Rca1 β exhibited increased thermotolerance but reduced Rubisco activation activity, in contrast to Rca2 β . An isoleucine residue was shown to confer thermostability in the mutant Rca2 β -M159I, whilst maintaining high Rubisco activation rates and efficiency.

To expand the understanding of thermotolerance and isoform abundance *in planta*, the effect of heat stress on wheat plants was investigated. The thermotolerant Rca1 β increased to 6% of the total Rca protein pool after 5 days of heat stress, but Rubisco activation state remained reduced in heat stressed plants. Furthermore, activity of CA1Pase, which metabolises Rubisco inhibitors, increased in plants in recovery conditions (4 h after relief from heat stress), suggesting a build-up of inhibitors during heat stress and a wider role of this enzyme in Rubisco regulation.

Exploiting diversity of wheat wild relatives have been suggested as a strategy for improving modern wheat cultivars. Rca in wild relatives was

highly conserved and highly similar to the donor-species of the three wheat sub-genomes. Despite the small differences, the observed variation in Rca expression and protein levels might be associated with the ability of these species to adapt to high temperatures.

Overall the results from this thesis suggest that engineering thermo-tolerant Rca isoforms into wheat to improve carbon assimilation will be the most promising way to make Rubisco regulation in wheat more resilient to heat stress in changing environments.

Acknowledgements

First of all, I would like to thank my supervisors Elizabete Carmo-Silva and Martin Parry. Elizabete in particular supported me from the beginning to the end and was always available to talk to and was supportive of letting me give this thesis my own direction. I would also like to thank the photosynthesis group at the Lancaster Environment Centre for making my PhD a truly enjoyable time. I'd like to thank Dawn for co-authoring my first paper and Doug for helping me with my (hopefully) second paper. I'd like to thank Cris for being a good friend in the lab and outside of work. Thanks to Jack who made my time in office B31a much more enjoyable and for being a good friend. Thanks to Maddie and Tom for taking me wild swimming in the Lakes, a good relief from PhD stress. Thanks to my partner Annabelle for making my life outside the PhD so much better, which helped when PhDing didn't go as planned. Thanks to my parents Karl and Ulla and my sisters Antonia and Luise for supporting me during my PhD and *Bjarne* and the Edwards family. I'd also like to thank people I met along the way without which I wouldn't have come this far. My high school teacher Frau Fenzl who encouraged me to study biology, Prof. Andreas Weber who got me interested in plant science and allowed me to write my Bachelor's thesis in his lab. Thanks to David Kramer, Tom Sharkey and Sean Weise for teaching me a lot during my time at Michigan State and to Prof. Maria von Korff and Agatha Walla for supervising my Master's thesis. I couldn't have come this far without the help of all these brilliant people.

Table of contents	
List of figures and tables.....	8
List of abbreviations	11
1. Chapter 1: Introduction	13
1.1 The gap in future wheat yields and food security.....	13
1.2 Influence of climate change on crop yields.....	14
1.3 Photosynthesis	16
1.3.1 Basic concepts	16
1.3.2 Light reactions	16
1.3.3 Carbon reactions	19
1.4 Rubisco	21
1.4.1 Rubisco reactions	22
1.4.2 Regulation	24
1.5 Rubisco activase	25
1.5.1 The AAA+ protein family	25
1.5.2 Structure of Rubisco activase.....	27
1.5.3 The role and regulation of Rca in higher plants.....	29
1.6 Thesis aims	33
1.7 References	34
2. Chapter 2: Wheat Rca isoforms vary in their concentration- dependent activity and ADP sensitivity	44
2.1 Introduction.....	45
2.2 Results	46
2.2.1 Rca ATPase and Rubisco activation activities.....	46
2.2.2 Concentration-dependence of wheat Rca isoforms.....	50
2.2.3 ADP sensitivity of wheat Rca isoforms.....	52
2.3 Discussion	54
2.4 Material and Methods.....	57
2.5 References	61
3. Chapter 3: An isoleucine residue acts as a thermal and regulatory switch in wheat Rubisco activase.....	65
Graphical abstract	65
3.1 Introduction.....	66
3.2 Results	70
Identification of a residue putatively associated with the temperature optimum of Rca.....	70
Wheat Rca2 β -M159I exhibits higher temperature optima of ATP hydrolysis and Rubisco activation	71
M159I alters the regulatory properties of Rca	75
3.3 Discussion	78
3.4 Material and Methods.....	82

3.5 References	87
3.6 Supplementary information	92
4. Chapter 4: Heat-induced changes in the abundance of wheat Rubisco activase isoforms	104
4.1 Introduction	105
4.2 Materials and Methods	109
4.3 Results	115
4.4 Discussion	127
4.5 References.....	132
4.6 Supporting Information	145
5. Chapter 5: Low genetic diversity in cereal Rubisco activase might still offer scope for crop improvement	163
5.1 Introduction	164
5.2 Results	166
5.2.1 Wheat Rca gene expression	166
5.2.2 Rca genetic diversity in wheat and its wild relatives	168
5.3 Discussion	179
5.4 Material and Methods.....	182
5.5 References	185
6. General discussion.....	188
Conclusion	194
References.....	195
7. Complete reference list.....	199

List of figures and tables

1. Introduction

Fig.1: The basic system of photosynthesis.

Fig.2: Strategies to improve carbon fixation in crops.

Fig.3: Crystal structure of green-type L₈S₈ Rubisco.

Fig.4: Reactions of Rubisco.

Fig.5: Structural elements of the AAA+ domain.

Fig.6: Structure of green type Rca from *N. tabacum*.

2. Chapter 2: Wheat Rca isoforms vary in their concentration-dependent activity and ADP sensitivity

Fig.1: Rubisco activase activities.

Fig.2: Concentration-dependence of wheat Rca isoforms activity.

Fig.3: Alignment of mature Rca isoforms from wheat, tobacco and *Arabidopsis*.

Fig.4: ATPase activity and Rubisco activation in response to increasing ADP:ATP ratios relative to 0.00 ADP:ATP control of native wheat isoforms and three mutant proteins.

Table 1: ADP sensitivity of Rubisco activation by Rca in different species.

3. Chapter 3: An isoleucine residue acts as a thermal and regulatory switch in wheat Rubisco activase

Fig.1: Selection of residues putatively involved in the temperature response of Rca.

Fig.2: Temperature response of ATP hydrolysis and Rubisco activation by Rca.

Fig.3: The efficiency of Rubisco activation by Rca.

Table 1: Temperature optimum of Rca activity.

Table 2: ADP sensitivity of Rca2 β -M159I.

Fig.S1: Temperature response of ATP hydrolysis and Rubisco activation by Rca.

Fig.S2: The spontaneous release of RuBP from inhibited Rubisco (ER) increases with temperature.

Fig.S3: Amino acid sequence alignment of Rca isoforms from warm-adapted wild rice (*O. australiensis*, Oa), cultivated rice (*O. sativa*, Os) and bread wheat (*T. aestivum*, Ta).

Fig.S4: Separation of purified Rca and Rubisco proteins by SDS-Page.

Fig.S5: Temperature response of ATP hydrolysis by Rca proteins

Table S1: Modelling the temperature response of ATP hydrolysis and Rubisco activation by wheat Rca isoforms.

Table S2: Result of a Tukey's multiple comparison test of the Rca ATPase activity.

Table S3: Result of a Tukey's multiple comparison test of the Rubisco activation activity.

Table S4: Two-way ANOVA showed no significant differences between results obtained for ATPase activity using different preparations of Rca ($P > 0.05$).

4. Chapter 4: Heat-induced changes in the abundance of wheat Rubisco activase isoforms

Fig.1: Experimental design, air and leaf temperatures of wheat plants during heat stress.

Fig.2: (a) Net CO₂ assimilation (A), (b) stomatal conductance to water vapour (g_s), (c) vapour pressure deficit (VPD) based on leaf temperature, and (d) intercellular CO₂ concentration (C_i) in wheat plants under heat stress.

Fig.3: Rubisco activities and content in wheat plants under heat stress.

Fig.4: CA1Pase activity in wheat plants under heat stress.

Fig.5: Rca protein amounts in wheat plants under heat stress.

Fig.6: Relative abundance of Rca isoforms in wheat plants under heat stress.

Fig.7: Relative expression of *Rca*, *ca1pase*, *RbcL* and *RbcS* genes in wheat plants under heat stress.

Table 1: Final biomass and yield traits of wheat plants exposed to heat stress for five days during booting.

Fig. S1. Profile of relative humidity in the plant growth cabinets.

Fig. S2. Immunoblot detection and quantification of Rca using purified Rca standards.

Fig. S3. Rubisco activities, total soluble protein and Rubisco content in wheat plants under heat stress.

Fig. S4. Chlorophyll a, chlorophyll b and total carotenoids in wheat plants under heat stress.

Fig. S5. Relative Rca isoform abundance in wheat plants under heat stress.

Fig. S6. Location of heat responsive elements in wheat *Rca1β*.

Fig. S7. Phylogenetics of RbcS in wheat.

Fig. S8. *RbcS* gene expression in wheat.

Fig. S9. Alignment of RbcS protein sequences from rice and wheat.

Table S1. MIQE guidelines for gene expression analyses.

Table S2. Sequences of qPCR primers used in this study.

Table S3. Wheat *RbcS* gene groups.

Table S4. Comparison of wheat plants in the two cabinets prior to heat stress.

Table S5. Ratio of Rubisco active sites to Rca (R_{A.S.}:Rca) in wheat flag leaves.

5. Chapter 5: Low genetic diversity in cereal Rubisco activase might still offer scope for crop improvement

Fig.1: Gene expression of Rca isoforms of the three wheat sub-genomes A, B and D.

Fig.2: Alignment of mature protein sequences of A) Rca1 β , B) Rca2 β /Rca2 α of the three wheat sub-genomes and selected wheat wild relatives.

Fig.3: Phylogenetic trees of mature protein sequences.

Fig.4: Sequence analysis of Rubisco large subunits of wheat and related species.

Fig.5 Protein sequence flow of Rca from wild relatives to wheat.

Fig.6: Alignment of Rca protein sequences from selected grass species.

Table.S1: Primer sequences used for sequencing wheat wild relative Rubisco activase genes.

List of abbreviations

1,3-PGA	1,3-bisphosphoglycerate
2PG	2-phosphoglycolate
3-PGA	3-phosphoglycerate
ADP	Adenosine diphosphate
ATP	Adenosine triphosphate
CA1P	2-carboxy-D-arabinitol-1-phosphate
cDNA	Complementary DNA
Chl	Chlorophyll
CTBP	2-carboxytetritol-1,4-bisphosphate
Cytb6f	Cytochrome b6f
DHAP	dihydroxyacetone phosphate
DTT	Dithiothreitol
E4P	erythrose-4-phosphate
ECM	Rubisco carbamylated and stabilised by Mg ²⁺ (active)
EDTA	Ethylenediaminetetraacetic acid
ER	Rubisco enzyme uncarbamylated and bound to RuBP (inhibited)
F1,6P	fructose-1,6-bisphosphate
F6P	fructose-6-phosphate
FBA	fructose-1,6-bisphosphate aldolase
FBPase	fructose-1,6-bisphosphatase
G3P	glyceraldehyde-3-phosphate
GAPDH	glyceraldehyde-3-phosphate dehydrogenase
gs	Stomatal conductance
HEPES	(4-(2-hydroxyethyl)-1- piperazineethanesulfonic acid)
KABP	3-ketoarabinitol-1,5-bisphosphate
KOH	Potassium hydroxide
MgCl ₂	Magnesium Chloride
mRNA	messenger RNA
NADPH	Nicotinamide adenine dinucleotide phosphate
NaHCO ₃	Bicarbonate
NaOH	Sodium hydroxide
PDBP	D-glycero-2,3-pentodiulose-1,5-bisphosphate
PGK	phosphoglycerate kinase
Pi	Inorganic phosphate
PMSF	phenylmethylsulfonyl fluoride
PRK	phosphoribulokinase
PSI	Photosystem I
PSII	Photosystem II
qRT-PCR	quantitative Real Time

	Polymerase Chain Reaction
R5P	ribulose-5-phosphate
rbcL	large Rubisco subunit
RbcS	small Rubisco subunit
Rca	Rubisco activase
RPE	ribulose-5-phosphate 3-epimerase
RPI	ribose-5-phosphate isomerase
Rubisco	ribulose-1,5-bisphosphate carboxylase/oxygenase
RuBP	ribulose-1,5-bisphosphate
RuP	ribulose-5-phosphate
S1,7P	sedoheptulose-1,7-bisphosphate
S7P	sedoheptulose-7-phosphate
SBPase	sedoheptulose-1,7-bisphosphatase
SDS	Sodium dodecyl sulfate
SEM	Standard error of the mean
TER	Tris EDTA and RNase buffer
TK	transketolase
TPI	triose phosphate isomerase
TSP	Total Soluble Protein
Vi	Rate of CO ₂ assimilation by Rubisco
VPD	Vapour pressure deficit
X5P	xylulose-5-phosphate
XuBP	xylulose-5-phosphate

Figure 2 of the following chapter was published as Figure 1 in **Andralojc PJ, Carmo-Silva E, Degen GE, Parry MAJ. 2018**. Increasing metabolic potential: C-fixation. *Essays In Biochemistry* **62**: 109–118.

1. Chapter 1: Introduction

1.1 The gap in future wheat yields and food security

By 2050, the world population will have increased to 9.7 billion, with high population growth in Africa and Asia (United Nations, Department of Economic and Social Affairs, Population Division, 2015). Global crop production needs to double to ensure food security (Ray *et al.*, 2013), which is met when “all people, at all times, have physical and economic access to sufficient, safe, and nutritious food to meet their dietary needs and food preferences for an active and healthy life” (FAOSTAT 2014, 2014). Various climate related (temperature, precipitation, CO₂ and ozone) and non-climate factors (soil fertility, irrigation, fertilisers, demography and economics) can impact the food system (Porter *et al.*, 2014). These require certain responses, such as improving agriculture, livestock and fisheries, as well as non-production aspects, such as income, processing, transport, storage and retailing. Taken together, all these factors contribute to food security. Not only will demand for food increase, but the nature of demand itself will change. Due to increasing per capita GDP in currently less-developed countries, diets will likely change and become more calorie and protein rich (Tilman *et al.*, 2011). Together with already unsustainable lifestyles in developed countries, this will further put pressure on agriculture. Improvements in crop production are thus essential, not only to meet demands, but also to decrease environmental impact.

Wheat (*Triticum aestivum* (bread wheat), *Triticum durum* (pasta wheat)) is one of the major crops grown world-wide and provides 20 % of the calories of the world's population. However, the current trend of wheat yields is insufficient to double production by 2050 (Ray *et al.*, 2013). It is estimated that current wheat yields would result in a shortfall of 388 million tons/year by 2050 and in order to meet demands, an extra 95 million hectares of arable land would be required. Yet, world-wide area of arable land has remained at ca. 10 % since 1990 (Fedoroff *et al.*, 2010) and increasing this is not desirable, as it would put more pressure on ecosystems, which would ultimately be

unsustainable. Thus, crop productivity on current land has to be increased by adopting cultivars with enhanced genetic traits resulting in increased yield potential. Adopting cultivars that were developed during the green revolution, between 1965 and 2004, has successfully increased yields and thus saved an estimated 17.9-26.7 million hectares from being brought into agricultural production, especially in developing countries (Stevenson *et al.*, 2013). These past successes show that research can be brought to the field and have real world impact.

Due to the need for increased wheat yields, coordinated international research such as the International Wheat Yield Partnership (<http://www.iwyp.org>) and its collaboration with the International Maize and Wheat Improvement Centre (CIMMYT) have become crucial. CIMMYT was the cradle of the first green revolution, however, today climate change threatens wheat yield across the world and population growth increases demand, calling for a second green revolution, called “golden revolution” by some (Evans & Lawson, 2020)

1.2 Influence of climate change on crop yields

The effect climate change has and will have on wheat yields has been subject to some debate (Semenov *et al.*, 2012) and multiple studies have used a modelling approach with a general agreement that rising temperatures will reduce global wheat yields (Asseng *et al.*, 2013; 2014; Tack *et al.*, 2015; Tanaka *et al.*, 2015; Liu *et al.*, 2016). These studies predict that with every °C increase, global wheat production will fall between 4.1 and 6.4 % (Asseng *et al.*, 2014; Liu *et al.*, 2016). Major effects of temperature are expected in China, India and the US, the world’s largest wheat producers (Liu *et al.*, 2016). One reason given for this is the decrease of days between anthesis and maturity, resulting in a lower grain filling period (Gourdji *et al.*, 2013; Asseng *et al.*, 2014; Penacchi *et al.*, 2018). Pollen viability and key enzymes in carbon assimilation are sensitive to heat and will likely perform sub-optimally at higher temperatures (Dawson & Wardlaw, 1989; Salvucci & Crafts-Brandner, 2004). These studies also point out that cultivars respond differently to high temperatures

(Gourdji *et al.*, 2013; Asseng *et al.*, 2014), which suggests that natural genetic diversity can be a valuable resource for wheat improvement.

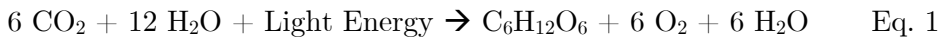
Predicting the effect of increasing atmospheric CO₂ (IPCC, 2014) on crop yields has been somewhat more challenging. Initially it was assumed that increased CO₂ would offset yield loss due to warming, but free-air concentration enrichment (FACE) experiments have shown that actual changes in crop production are much lower than theoretical values at a CO₂ concentration of 550 ppm (Long *et al.*, 2006a). At 25°C, yields should theoretically increase 36 %, but this study showed that for major crops, only a 13 % yield increase was observed in FACE experiments. For C4 crops (maize and sorghum), no yield increase using the FACE approach was observed, contrasting the yield increase measured in C4 plants grown in enclosures. For wheat specifically, yield and photosynthetic increase under FACE conditions was 13 %, whereas in enclosure wheat yield increased by 31 %. Another FACE study revealed that drought, which is likely to become more prevalent with climate change, offsets expected yield gains under elevated CO₂ for soybean (Gray *et al.*, 2016). In a survey of Australian wheat yields since 1990, the authors showed a 27 % decline in water-limited yield potential and attribute this to increased drought and temperatures (Hochman *et al.*, 2017). The authors also point out that national yields only increased due to increased use of technology, and it remains to be seen if this trend can continue.

These studies highlight the complexity of the effect of increased CO₂ under field conditions and further emphasise the need for improved photosynthesis in a changing environment.

1.3 Photosynthesis

1.3.1 Basic concepts

Photosynthesis is the process by which inorganic carbon enters the biosphere and can be summarised by the following equation 1 (reviewed in (Govindjee & Whitmarsh, 1999)) :



For each CO_2 , C3 plants would require eight electrons (e^-) (Zhu *et al.*, 2008) resulting in 48 e^- for Eq.1. Photosynthesis can be divided in two major reactions: the light reactions and the carbon reactions. These are interdependent, and one does not function without the other.

1.3.2 Light reactions

The electron transport chain (ETC) is located in the thylakoid membranes in plants. These are compartments found in chloroplasts and are the source of NADPH and ATP fuelling carbon assimilation. The ETC consists of two major reaction centres, Photosystem I (PSI) and Photosystem II (PSII), the Cytb_6/f complex and ATP synthase (reviewed in (Eberhard *et al.*, 2008)) (Fig. 1A) .

Water is split at the photosystem II water-oxidizing complex (reviewed in (Vinyard *et al.*, 2013)), which oxidizes H_2O and yields $\frac{1}{2} \text{O}_2$, two H^+ and two e^- . Electron flow begins when energy from light is funnelled into P680 Chlorophyll a. Excitonic energy is converted into chemical energy when an e^- is passed from P680^* (singlet excited state) to Pheophytin (Phe^-), a process called charge separation. P680^* recovers its lost e^- from the YZ, tyrosine-161 of the D1 protein and the process is repeated. Phe^- passes the e^- to the plastoquinone QA at the D2 protein, which, in turn, is passed onto QB at the D1 protein. QB is reduced to a plastoquinol ($\text{QB}(\text{H}_2)$) after a second e^- from P680 is accepted and it is exchanged with a mobile plastoquinone (PQ). One e^- is passed onto the FeS protein in the cytochrome b_6/f complex which in turn reduces Cytf . The second e^- from $\text{QB}(\text{H}_2)$ is passed into the Q-

cycle. While QB(H₂) is oxidised, protons are released into the thylakoid lumen which are, together with H⁺ from H₂O splitting, building up a proton gradient across the membrane. The e⁻ from Cyt_f is passed to P700⁺ via plastocyanin (PC) in PSI. The electron is excited again and from P700* it is passed to NADP⁺ via various phylloquinones (A0, A1), iron-sulphur clusters (Fx, Fa, Fb), ferredoxin (Fd) and ferredoxin-NADP⁺ reductase (FNR). The proton motive force, built up by the gradient, is used for ATP generation via ATP synthase.

In summary, 4 photons are required to reduce one molecule of NADPH, for which a maximum of 6 protons are moved to the thylakoid lumen: 4 via the cytochrome b₆f complex and 2 from water oxidation. For the production of 1 ATP, 4 protons are required.

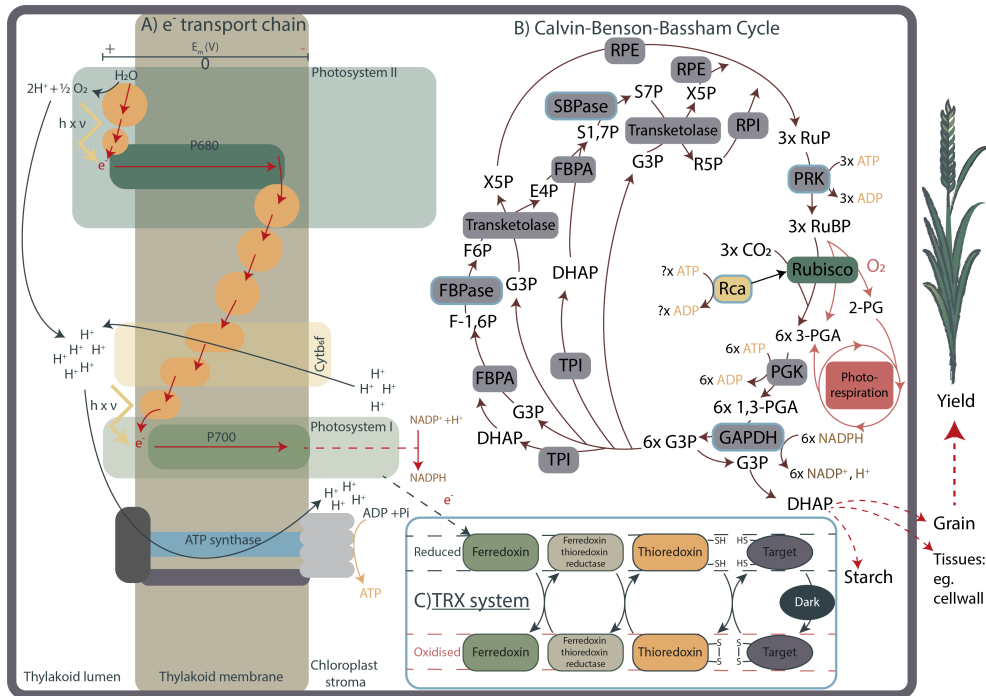


Fig. 1: The basic system of photosynthesis. A) Electron transport chain. An electron (e^-) is liberated from H_2O at the water-splitting complex, which produces $2H^+$ and $0.5 O_2$. In Photosystem II, light energy excites the electron, which is passed to the $Cytb_6f$ complex, where H^+ are pumped into the thylakoid lumen, and excited again in Photosystem I, where, finally, $NADP^+$ is reduced to $NADPH$. The proton gradient across the thylakoid membrane is used by ATP synthase to regenerate $ADP + Pi$ to ATP . B) Calvin-Benson-Bassham Cycle. Rubisco is activated by Rca, which uses the energy from ATP hydrolysis. Rubisco uses the substrate Ribulose-1,5-bisphosphate (RuBP) and can fix CO_2 or O_2 . The former yields 3-PGA, 2-PG, which is recycled via photorespiration. The latter yields 3-PGA which converted to 1,3-PGA via PGK, which consumes ATP . GAPDH converts 1,3-PGA to G3P, which is used in RuBP regeneration or exported and used for starch synthesis. G3P is converted to DHAP, and X5P via TPI and transketolase, respectively. In addition, FBPA converts G3P to F-1,6P and FBPase uses this to produce F6P, which is also a substrate for transketolase. X5P is converted to RuP via RPE and F6P to E4P via transketolase. FBPA, SBPase and Transketolase convert S1,7P and G3P to RuP, which is converted to RuBP via PRK. Enzymes: Rubisco, ribulose-1,5-bisphosphate carboxylase/oxygenase; PGK, phosphoglycerate kinase; GAPDH, glyceraldehyde-3-phosphate dehydrogenase; TPI, triose phosphate isomerase; FBA, fructose-1,6-bisphosphate aldolase; FBPase, fructose-1,6-bisphosphatase; TK, transketolase; SBPase, sedoheptulose-1,7-bisphosphatase; RPE, ribulose-5-phosphate 3-epimerase; RPI, ribose-5-phosphate isomerase; PRK, phosphoribulokinase. Blue boxes around enzyme names indicate know redox regulation. Metabolites, RuBP, ribulose-1,5-bisphosphate; 3-PGA, 3-phosphoglycerate; 2-PG, 2-phosphoglycolate; 1,3-PGA, 1,3-bisphosphoglycerate; G3P, glyceraldehyde-3-phosphate; DHAP, dihydroxyacetone phosphate; F1,6P, fructose-1,6-bisphosphate; F6P, fructose-6-phosphate; X5P, xylulose-5-phosphate;

E4P, erythrose-4-phosphate; S1,7P, sedoheptulose-1,7-bisphosphate; S7P, sedoheptulose-7-phosphate; R5P, ribulose-5-phosphate; RuP, ribulose-5-phosphate. C) The Thioredoxin system. Reduced ferredoxin reduces ferredoxin thioredoxin reductase, which in turn reduces disulfide bonds in thioredoxin. Thioredoxin reduces disulfide bonds in target proteins, such as Rca. Upon oxidation in the dark, disulphide bonds are formed again in the target proteins. Source: original figure

1.3.3 Carbon reactions

The Calvin-Benson-Bassham-Cycle (CBBC) (Calvin & Benson, 1948) is the pathway of carbon fixation in photosynthesis taking place in the chloroplast stroma (Fig.1B). Originally these reactions were termed “dark reactions” or “light-independent”, but as they are clearly neither happening in the dark, nor independent of light, the term “carbon reactions” is much more fitting and in line with the current understanding of its chemistry and regulation. The CBBC can be broken down into three phases: carboxylation, reduction and regeneration.

During the carboxylation reaction, ribulose-1,5-bisphosphate carboxylase/oxygenase (Rubisco), uses ribulose-1,5-bisphosphate (RuBP) and CO₂ to generate two 3-phosphoglycerate (3-PGA). Rubisco can also use O₂ instead of CO₂. This process, known as photorespiration (PR), is initiated by O₂ fixation and yields one 3PG and one 2-phospho-glycolate (2PG). At 380 ppm CO₂ and at 30°C, this process reduces the theoretical gross photosynthesis of C₃ plants by 48% (Zhu *et al.*, 2008; Walker *et al.*, 2016).

In the reduction phase, 3PGA is converted into glyceraldehyde-3-phosphate (G3P) by phosphoglycerate kinase (PGK) and glyceraldehyde-3-phosphate dehydrogenase (GAPDH). Most of the G3P is used to regenerate RuBP, but a fraction is converted into dihydroxy-acetone phosphate (DHAP), which is exported from the chloroplast via the Pi-triose phosphate antiporter and constitutes the building block of various cellular structures. Within the chloroplast, G3P and DHAP are used for starch synthesis. In the regeneration phase of the CBBC, G3P is converted back to RuBP via multiple pathways catalysed by 9 enzymes including fructose-1,6-bisphosphatase

(FBPase) and sedoheptulose-1,7-bisphosphatase (SBPase). Overall, to fix one CO₂ and regenerate one RuBP in one C3 cycle, 3 ATP and 2 NADPH are needed, requiring a total of 8 photons and 12 protons.

The reactions of the CBBC have been subject to much research in order to identify bottlenecks with the aim to improve carbon fixation (reviewed in (Long *et al.*, 2006b)). When a crop is light saturated, photosynthesis becomes limited by the speed of carbon fixation by Rubisco (V_{cmx}) and RuBP regeneration (J_{max}). With rising CO₂ and increasing carbon assimilation, RuBP regeneration also has to be increased to achieve a maximum benefit.

A reduction of SBPase has been shown to have a strong control over RuBP regeneration (Harrison *et al.*, 1997; 2001), as well as the Cytb6f complex in the electron transport chain (Price *et al.*, 1998; Ermakova *et al.*, 2019). Overexpressing SBPase has resulted in increased yield in greenhouse experiments (Driever *et al.*, 2017) and under fully open air CO₂ fumigation (Rosenthal *et al.*, 2011). Similarly, increasing FBPase has resulted in enhanced growth and photosynthesis (Uematsu *et al.*, 2012), as well as a combination of SBPase and FBPase (Simkin *et al.*, 2015).

Besides optimising RuBP supply by targeting key enzymes, other strategies can be implemented to improve carbon fixation, which are summarised in Fig.2, and reviewed in Andralojc *et al.* (2018). Increasing CO₂ supply to Rubisco can be achieved by concentrating mechanisms such as employing carboxysomes or pyrenoids. Furthermore, efforts are being made to convert C3 crops, such as rice, into C4 crops. Recently, understanding and optimising mesophyll conductance has also become of greater interest (Flexas *et al.*, 2016).

Improving Rubisco and its regulation is a promising strategy to improve carbon assimilation. As detailed below, the carboxylating enzyme Rubisco is characterised by a number of inefficiencies and subject to much research aimed at improving its function. Surveying Rubisco from wheat wild relatives has shown great diversity of catalytic rates (Prins *et al.*, 2016; Orr *et al.*, 2016), especially with regards to temperature response and these

isoforms can be used to replace native Rubisco. Furthermore, changing specific residues (Whitney *et al.*, 2011; Orr *et al.*, 2016) or transplanting Rubisco small subunits (Ishikawa *et al.*, 2011) are additional strategies, as well as improving Rubisco regulation by targeting its molecular chaperone, Rubisco activase (Rca) (Carmo-Silva *et al.*, 2015).

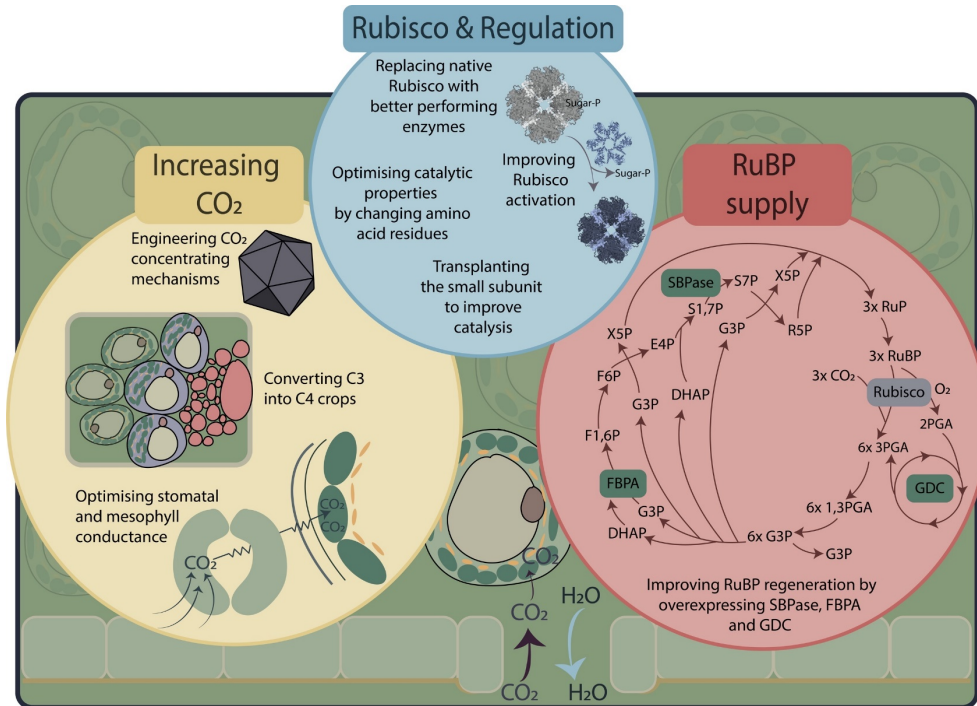


Fig.2: Strategies to improve carbon fixation in crops. Published in Andralojc *et al.* (2018)

1.4 Rubisco

Rubisco is a multimeric enzyme, consisting of eight large and eight small subunit L₈S₈ (Fig.3). The large subunit (rbcL) comprises the N-terminal α + β domain (ca. 150 residues) and the C-terminal domain (ca. 325 residues). RbcL is organised as an antiparallel dimer, containing two active sites. These are located between the C-terminal domain of one subunit and the N-terminal domain of the adjacent one. In addition, Rubisco contains small Rubisco subunits (RbcS) and the oligomeric L₈S₈ form of Rubisco contains eight active sites.

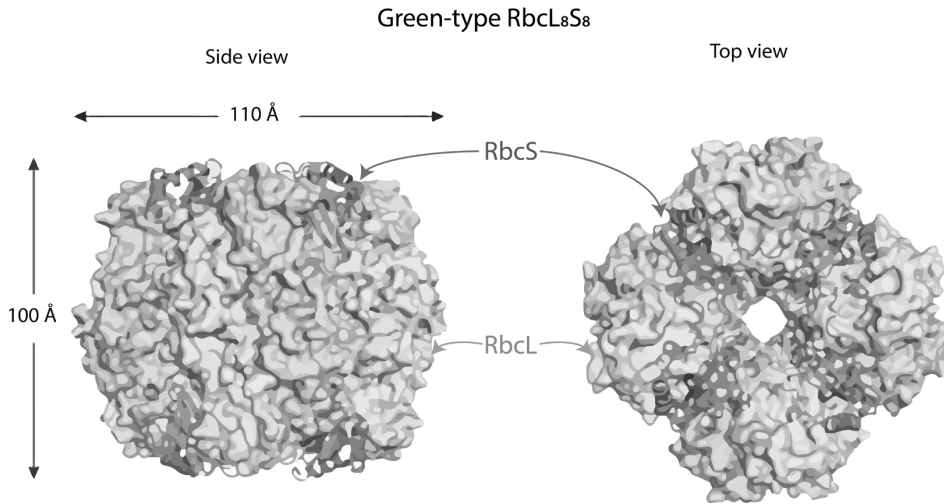


Fig.3: Crystal structure of green-type L₈S₈ Rubisco. Dark grey colour indicates the RbcS subunits, light grey the large RbcL subunits. Adapted from Bracher *et al.* (2017).

The large subunit is encoded by *rbcL* in the chloroplast genome. The small and much more divergent small subunit is encoded by a family of *RbcS* genes in the nuclear genome (Spreitzer, 2003). Its expression is regulated by several transcription factors, including GUN1/ABI4, which is in turn controlled by *rbcL* expression. The *RbcS* mRNA is imported to the chloroplast via the TOC/TIC mechanism. *rbcL* and RbcS are then assembled into the holoenzyme in the chloroplast (Jarvis & Soll, 2002).

In order for Rubisco to function, the active site requires carbamylation by binding non-substrate CO₂ to Lys₂₀₁, followed by Mg²⁺ binding to the carbamylated residue to stabilise it (Lorimer *et al.*, 1976; Lorimer & Miziorko, 1980). When RuBP binds the carbamylated active site, it is available for carboxylation or oxygenation. However, when RuBP binds to an inactivated, uncarbamylated site, for example under low CO₂, Rubisco becomes inhibited and the loop 6 of Rubisco closes and locks the enzyme into an inactive conformation (Parry *et al.*, 2008).

1.4.1 Rubisco reactions

Rubisco catalyses the carboxylation of RuBP, using atmospheric CO₂ as a carbon source via a series of complex reactions. The steps of Rubisco reactions are summarised in Fig.4 (Bracher *et al.*, 2017). The first step is the enolisation of RuBP by deprotonation. This highly reactive enediolate is then used as

the substrate for carboxylation and oxygenation. Hydration, bond cleavage and stereospecific protonation results in two molecules of 3 3-PGA. As a result of oxygenation, one 2PG and one 3PGA are produced in step 6. 2PG is toxic and has to be recycled via photorespiration (reviewed in Bauwe *et al.* (2010)). The inhibitor D-xylulose-1,5-bisphosphate (XuBP) can be formed when the enediolate is misprotonated (step 5), a reaction that increases with temperature (Schrader *et al.*, 2006). Steps 7-9 result in the formation of further inhibitory sugar-phosphates following oxygenation of RuBP.

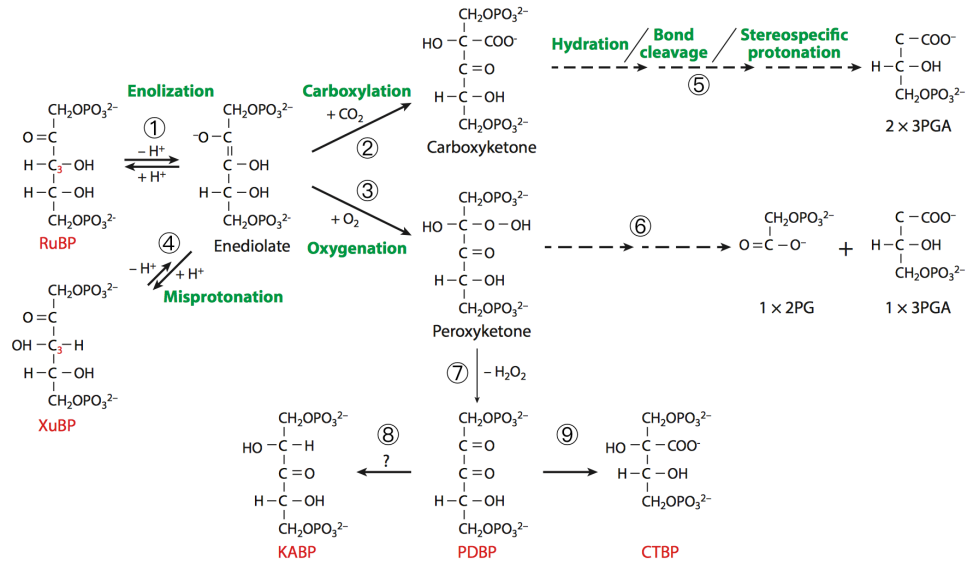


Fig.4: Reactions of Rubisco. Figure was taken from Bracher *et al.* (2017). RuBP, ribulose-1,5-bisphosphate; XuBP, xylulose-1,5-bisphosphate; 3PGA, 3-phosphoglycerate; 2PG, 2-phosphoglycolate; KABP, 3-ketoarabinitol-1,5-bisphosphate; PDBP, D-glycero-2,3-pentodiulose-1,5-bisphosphate; CTBP, 2-carboxytetritol-1,4-bisphosphate; H₂O₂, hydrogen peroxide

All of the described steps are catalysed by Rubisco during the complex reactions of carboxylation or oxygenation. The multistep processes are considerably slower than more straight-forward reactions in nature, which results in the slow catalytic turnover of Rubisco, with 2-5 molecules of CO₂ being fixed per second per enzyme (Bracher *et al.*, 2017). The slow turnover and the dual nature of Rubisco as a carboxylase/oxygenase limit photosynthetic efficiency and require high amounts of the enzyme to be present in leaves (ca. 50% of soluble leaf protein (Feller *et al.*, 2008)) to sustain adequate rates of photosynthesis (Carmo-Silva *et al.*, 2017).

Rubisco has been a target for modification and improvement over the past 4-5 decades, a goal that is hindered by the fact that the enzyme is encoded in two genomes, and chloroplast transformation is still difficult to achieve. However, natural variation in Rubisco can be exploited (Orr *et al.*, 2016; Prins *et al.*, 2016) (Sharwood *et al.*, 2016; Hermida-Carrera *et al.*, 2016), and gene editing could open new doors for crop improvement.

1.4.2 Regulation

The active site of Rubisco requires the formation of a carbamate by binding of non-substrate CO₂ before catalysis can occur. Therefore, Rubisco will only become active when CO₂ is present and will be inactive during the night or under stress, when no or less CO₂ is available (Lorimer *et al.*, 1976). In addition, Mg²⁺ is required to stabilise the carbamate (Lorimer & Miziorko, 1980), thus fluctuations of Mg²⁺ in the stroma can also impact Rubisco activity. The naturally occurring sugar-phosphate RuBP and its derivatives XuBP can bind to uncarbamylated sites and form a dead-end complex, whereas 2-Carboxy-D-arabinitol 1-phosphate (CA1P) and D-glycero-2,3-pentodiulose-1,5-bisphosphate (PDBP) can bind to the carbamylated active site of Rubisco and form a dead-end complex (Zhu & Jensen, 1991; Pearce, 2006).

2-Carboxy-D-arabinitol 1-phosphatase (CA1Pase) has been shown to regulate Rubisco by metabolising CA1P, 2-Carboxy-D-arabinitol 1,5-bisphosphate (CABP), 2-carboxy-D-ribitol-1,5-bisphosphate (CRBP) and D-glycero-2,3-pentodiulose-1,5-bisphosphate (PDBP), but this was only shown for French bean, tobacco and rice, while in *Arabidopsis* and wheat CA1P was not detected (Andralojc *et al.*, 2012). The Km for the sugar-phosphate derivatives CABP and CRBP is lower than for CA1P (Andralojc *et al.*, 2012), highlighting that CA1Pase metabolises other sugar-phosphate derivatives as well. Since CA1Pase is present in wheat and can metabolise other sugar phosphate-derivatives, it is likely that it is involved in Rubisco regulation, which has been shown by decreased Rubisco abundance and grain yield in a wheat CA1Pase overexpressor line (Lobo *et al.*, 2019).

Rubisco is not only regulated by cellular processes, but also by environmental factors, such as light. The availability of light to a plant varies greatly throughout the day, as clouds can block the sun, wheat leaves in a canopy can shade neighbouring plants and no light is available during the night. The thioredoxin system (Fig. 1C) is a way for a plant to regulate many enzymes in response to light availability (Michelet *et al.*, 2013). Under illumination, ferredoxin is reduced via Photosystem I (Fig. 1C), which in turn reduces ferredoxin-thioredoxin reductase. Following this, a disulphide bridge between two cysteine residues (Cys) in thioredoxin is reduced. Cys can be found in many redox responsive enzymes and provide a regulatory function in response to conditions affecting the redox status of the chloroplast, such as light intensity. Finally, the disulphide bridge of the target enzyme is reduced. In the dark, the target protein returns to its oxidised state. Under fluctuating light, the presence of oxidants in the chloroplast increases, resulting in the oxidation of many proteins, thus requiring the thioredoxin system to maintain functionality (Kaiser *et al.*, 2019). One such protein is Rubisco activase (Rca), a key regulator of Rubisco (Salvucci & Crafts-Brandner, 2004), which can be responsive to redox status of the chloroplast (Zhang & Portis, 1999), allowing for Rubisco regulation under fluctuating light. In addition, Rca has been shown to be regulated by Mg^{2+} availability (Hazra *et al.*, 2015). As an AAA+ ATPase, Rca uses the energy from ATP hydrolysis to remove inhibitory sugar-phosphate derivatives from Rubisco's active site (Somerville *et al.*, 1982; Salvucci *et al.*, 1985; 1986), making it catalytically competent. Because of the complexity of Rubisco activation, understanding Rca regulation and its role as a molecular chaperone is important in order to improve carbon assimilation.

1.5 Rubisco activase

1.5.1 The AAA+ protein family

ATPases associated with various cellular activities (AAA) constitute a large protein family and are found in all domains of life (Neuwald *et al.*, 1999). AAA+ proteins, a subsection of the AAA family containing certain distinguishing features, hydrolyse ATP and use the released energy to remodel the

structure of target proteins. The ATPase module is highly conserved between these proteins (Neuwalde *et al.*, 1999), making it feasible to use sequence alignment to identify new members of this family.

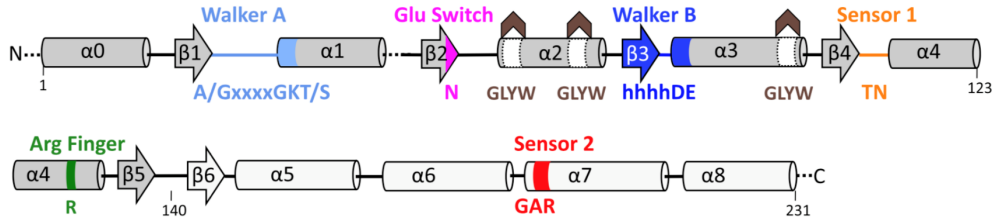


Fig.5: Structural elements of the AAA+ domain. Secondary structures (α -helices and β -sheets) are numbered in order of appearance from the N- to C-terminus. Pore loop insertions are indicated with brown arrows. Consensus sequences for various defining motifs are given. Taken from Wendler *et al.* (2012).

AAA+ proteins are members of the larger p-loop family and contain a unique α/β fold (Fig.5), termed α/β subdomain. This contains five α helices and five β sheets (dark grey Fig. 5), which forms an α - β - α sandwich. They contain a C-terminal α -helical bundle which forms a lid over the nucleotide binding site and mediates subunit interactions in complexes (Neuwalde *et al.*, 1999). In addition to these features, certain motifs are conserved amongst the AAA+ family members (Fig. 5).

Firstly, the Walker A motif, consisting of GXXXXGK[T/S]XX, where X can be any amino acid and the final one can be threonine or serine, is forming a loop between $\beta 1$ and $\alpha 1$, representing the p-loop, which is the defining structure for members of the p-loop family (Neuwalde *et al.*, 1999). The lysine residue in the Walker A motif interacts with the β and γ phosphates of ATP. The Walker B motif consists of hhhhD[D/E], where h can be any hydrophobic residue and the last amino acid can be either aspartate or glutamate. Mutations of the glutamate residue in the Walker B motif have been shown to abolish ATP hydrolysis (Neuwalde *et al.*, 1999), known as the glutamate switch. This glutamate interacts with an asparagine on the $\beta 2$ strand when ATP is bound. Upon binding of the target enzyme, the AAA+ protein

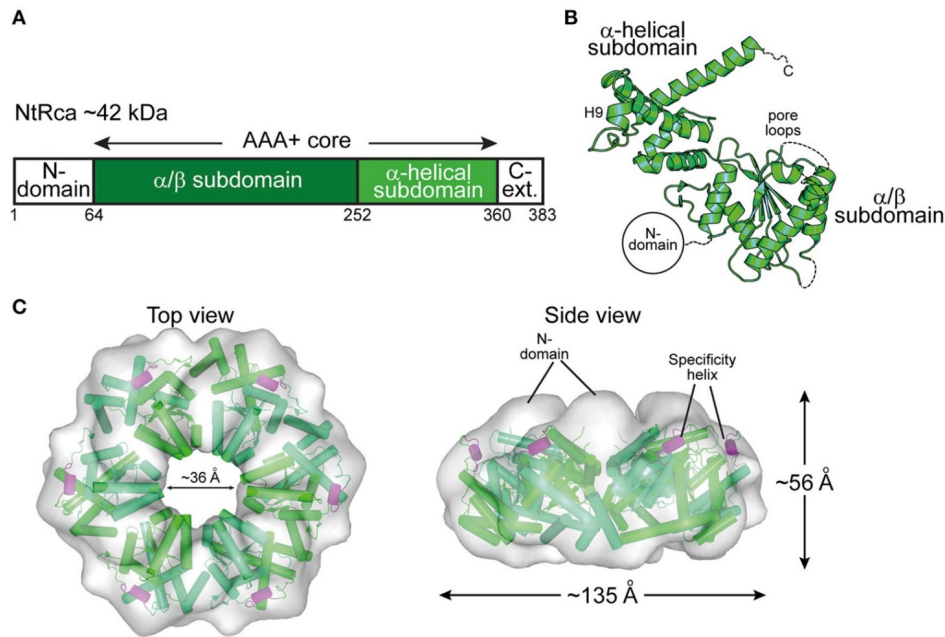
into the fully active ATPase configuration. Both Walker motifs are therefore essential for ATP binding.

Next to the Walker motifs, the second region of homology is a defining feature. This includes part of $\alpha 4$, partial $\beta 4$ and the loop connecting $\alpha 4$ to $\beta 5$ (Ogura *et al.*, 2004). This motif contains the Sensor 1 domain and the arginine finger, both of which are essential for ATP hydrolysis. In a protein complex, the WalkerA/B motifs and Sensor 1 are located on the same subunit, whereas the arginine finger can be found on the neighbouring one, contributing to the nucleotide binding site. Hence, two subunits are interacting in a protein complex. In addition, the sensor 2 domain facilitates conformational change during ATP hydrolysis and directly interacts with the α -phosphate of bound ATP (Ogura *et al.*, 2004). Finally, an N-linker, N-terminal to $\alpha 0$, runs perpendicular to the β strand of the α - β - α core and is involved in forming the ATP binding pocket and connects the ATPase module with other domains, such as the target protein recognition site. It also may play a role in coupling ATP hydrolysis to conformational changes (Neuwald *et al.*, 1999; Smith *et al.*, 2004; Judson, 2017).

AAA+ ATPase proteins are involved in many diverse cellular processes, such as DNA replication, transcription, proteolysis, protein disaggregation and repair (reviewed in Ogura and Wilkinson (2001)). Hence, improving understanding an ATPase like Rca, might help in understanding other cellular processes too. Furthermore, this knowledge can be applied elsewhere, for example in biotechnological processes where an ATPase is required to perform molecular processes. A substantial effort in the past has been made to understand Rca because of its key role in Rubisco regulation and its sensitivity to high temperatures (detailed below) or redox state of the chloroplast.

1.5.2 Structure of Rubisco activase

To date, three distinct types of Rca have been identified: the CBBQO-type of proteobacteria (Tsai *et al.*, 2015), the red-type (Mueller-Cajar *et al.*, 2011) and the green-type (Salvucci *et al.*, 1985) (Fig. 6). These types were recruited



from different areas of the AAA+ proteome and their AAA+ modules contain less than 25% sequence identity (Ammelburg *et al.*, 2006), suggesting a degree of convergent evolution. Although Rca types are very diverse, all contain a functionally similar AAA+ core and are organised as a functional hexamer and contain a Rubisco recognition domain and a C-terminus (Bhat *et al.*, 2017). These domains can be found in chlorophyte Rca and in all plants. During endosymbiosis, a chloroplast transit peptide and an N-terminal domain were added to Rca. Upon land colonisation of green algae, a C-terminal extension was added, and alternative splicing evolved (Nagarajan & Gill, 2018).

Fig.6: Structure of green type Rca from *N. tabacum*. A) Domain structure of tobacco Rca. B) Crystal structure of the Rca monomer. C) Model of the hexamer. Taken from Bhat et al (2017).

During the evolution of plants on land, monocot and dicot Rca copy number in the genome increased (Nagarajan & Gill, 2018). The Solanaceae crop *Solanum lycopersicum* (tomato) contains two Rca genes, while *Nicotiana tabacum* contains six copies. Interestingly, species of the Solanaceae family have lost the C-terminal extension of Rca (Nagarajan & Gill, 2018). In the monocot family poaceae, a tandem duplication of Rca occurred, resulting in *Rca1* and *Rca2* genes. *Rca2* is alternatively spliced and yields the longer redox-sensitive α -isoform and a shorter β -isoform which lacks the C-terminal

extension. A short β -isoform lacking the C-terminal extension is produced by *Rca1*. Within the poaceae, Rca continued to evolve. *O. sativa*, for example, does not express the *Rca1* gene and in sorghum, there is no alternative splicing, *Rca1* encodes the α -isoform, whilst *Rca2* only encodes the shorter β -isoform (Nagarajan & Gill, 2018). In hexaploid *Triticum aestivum*, three copies of *Rca1* and *Rca2* can be found in the A, B and D genomes. *Rca1* and *Rca2* produce 42kDa β -isoforms and *Rca2* also produces the 46 kDa α -isoform containing a C-terminal extension (Carmo-Silva *et al.*, 2015).

1.5.3 The role and regulation of Rca in higher plants

The role of Rca was first described in *Arabidopsis thaliana* (Somerville *et al.*, 1982; Salvucci *et al.*, 1985; Salvucci *et al.*, 1986) where it was shown that a *rca* mutant was incapable of activating Rubisco in the light. *In vitro* experiments showed that adding Rca and ATP to inactivated Rubisco restored its activity (Robinson & Portis, 1989). Rca has been found in many higher plant species, including the cereal grains oat, barley (Salvucci *et al.*, 1987) and wheat (Feller *et al.*, 1998), as well as in *Chlamydomonas reinhardtii* (Salvucci *et al.*, 1987) where it was shown to be located to the pyrenoid (McKay *et al.*, 1991). Rca is therefore a highly conserved regulator in photosynthetic eukaryotes and prokaryotes (Mueller-Cajar *et al.*, 2011; Tsai *et al.*, 2015).

When the active site of Rubisco is inhibited by RuBP or sugar phosphate-derivatives, Rca uses the energy from ATP hydrolysis to remodel the active site and subsequently inhibitors are released (Salvucci *et al.*, 1985; 1986). It is thought that the N-domain of green type Rca interacts with Rubisco and H9 helix recognises Arg89 on RbcL (Portis *et al.*, 2008). The inhibitory sugar-phosphates include Rubisco's substrate RuBP, as well as XuBP formed by misprotonation, a process increasing with temperature (Salvucci & Crafts-Brandner, 2004). Misfire products bind less tightly at higher temperatures to Rubisco because the enzyme structure becomes more mobile (Schrader *et al.*, 2006).

Activation at high temperatures, however, is reduced due to the heat sensitivity of Rca and not Rubisco activity, which is still functional at 50°C (Salvucci & Crafts-Brandner, 2004). Photosynthesis thus decreases at high temperature because Rca cannot remove inhibitors fast enough due to its impaired activity and consequently Rubisco deactivates (Salvucci *et al.*, 2006). *A. thaliana* mutants which expressed only the short β or long α Rca isoform individually still showed photosynthetic impairment under high temperature, supporting the concept of denaturation of Rca under high temperature (Salvucci *et al.*, 2006). Expression of *A. thaliana* Rca isoforms is not affected by heat (Kumar *et al.*, 2009), but heat stress induced *Rca1* expression in wheat (Scafaro *et al.*, 2019a). In that study, protein abundance was not quantified and it remains unclear how Rca gene expression and protein levels correlate. This shows, that the sensitivity of Rca to heat between species differs, as shown with an Australian wild rice species (Scafaro *et al.*, 2016) and Rca from the CAM plant *Agave tequilana* (Shivhare & Mueller-Cajar, 2017). Mutant screens have been developed to identify more thermostable Rca isoforms in *A. thaliana* by changing one amino acid residue (Kurek *et al.*, 2007). Overexpressing a more thermostable Rca variant from tobacco in Arabidopsis has been shown to increase photosynthesis at moderately high temperatures (Kumar *et al.*, 2009), highlighting the scope for improving Rubisco activation in a model species. However, to date this has not been successfully implemented in crops.

As shown above, Rca can limit photosynthesis at moderately high temperatures and more thermostable enzymes have been identified. Scafaro *et al.* (2019a) showed that Rca2 β from wheat became more thermostable by mutating 11 residues which were found in warm-adapted species and Degen *et al.* (2020) identified a single isoleucine residue that increase thermotolerance of Rca.

Rca is not only a limiting factor at high temperature, but also under fluctuating light. For wheat, slow induction of photosynthesis from shade to sun has been shown to limit carbon assimilation (Taylor & Long, 2017). The C-terminal extension of the longer α isoform contains two cysteine residues,

that respond to redox changes in the stroma. In the oxidised state, the extension can dock into the ATP binding pocket of Rca which prevents ATP from binding, but not ADP (Zhang *et al.*, 2001). By this mechanism, Rca activity is regulated by the redox state of the stroma. Arabidopsis plants with only the α isoform had reduced Rubisco activity under limiting light and activity was reduced and increased more slowly under saturating light, whereas lines with only the short β isoform had wild type levels of CO₂ assimilation (Zhang *et al.*, 2002). Furthermore, Arabidopsis plants lacking the redox-sensitive isoform produced higher biomass under fluctuating light (Carmo-Silva & Salvucci, 2013). This highlights the potentially limiting role of the α isoform under limiting light and in non-steady state conditions which crop plants experience in the field due to shade from the canopy and the moving sun.

A second mechanism linking Rubisco activation to light reactions is the sensitivity of some isoforms to the ATP:ADP ratio in the stroma. The β isoforms from tobacco and spinach have been shown to be partially inhibited by an ADP:ATP ratio of 0.11 and experience complete inhibition at a ratio of 0.33 (Salvucci *et al.*, 2003). The β isoform from Arabidopsis, however, is much less sensitive to ADP inhibition. A tobacco mutant which contained 17 residues from Arabidopsis showed reduced sensitivity to ADP inhibition (Carmo-Silva & Salvucci, 2013), yet, it remains to be elucidated which residues are responsible for this. The oxidised C-terminal extension of Arabidopsis has been shown to result in increased ADP sensitivity, likely because of increased cross linking of the oxidised extension in the presence of ADP and the ATP binding pocket (Wang & Portis, 2006). In Arabidopsis, the acetylated residue K474 has been implicated in ADP inhibition (Hartl *et al.*, 2017). Rca1 β and 2 α isoforms of wheat contain a lysine residue at this position as well, whilst it is lacking in the ADP-insensitive Rca2 β and the partial role of this residue in ADP sensitivity has recently been confirmed (Scafaro *et al.*, 2019b).

As a member of the AAA+ protein family, Rca functions as a hexamer, however some data suggests it might already be able to hydrolyse ATP as a dimer (Keown *et al.*, 2013). Furthermore, ATP has been identified as a

driving force of oligomerization (Wang *et al.*, 2018). ATP γ S (a form of ATP that cannot be hydrolysed) has been shown to promote tetramer/hexamer formation from dimers for concentrations between 1 and 10 μ M (Wang *et al.*, 2018). ADP on the other hand has been implicated in disassociating complexes by increasing the rate of subunit exchange >2 fold. Protein concentration and the multimeric state of Rca appears to influence ATPase activity, as current evidence suggests that 1-2 μ M subunit concentration results in a spike of activity and that higher concentrations reduce ATP hydrolysis (Keown *et al.*, 2013).

Finally, Rca requires Mg $^{2+}$ and excess binding increases the affinity for ATP and results in a hexameric assembly of Rca (Hazra *et al.*, 2015). Mg $^{2+}$ concentration varies in the stroma throughout the day and it is estimated to be 0.50 mM in the dark and 1.95 after 10 min illumination (Ishijima *et al.*, 2003). This links Rca activity to light availability and provides a plausible mechanism by which ATP hydrolysis by Rca in the dark is prevented.

Rca has been shown to repair Rubisco's active site with great selectivity, in order to prevent destabilization of other parts of Rubisco. Rca repairs one active site at a time by positioning the C-terminal of Rubisco in order to stabilise the catalytic centre so the hexamer pore of Rca can be accessed. In order to release inhibitory sugar-phosphates, Rca pulls on the C-terminal RbcL tail with great specificity (Bhat *et al.*, 2017).

As a key regulator of carbon assimilation, Rca of model species has been studied to a great extent. In order to understand and improve Rubisco regulation in crops, species-specific studies of Rca are needed. Since crops experience varying light environments in an agricultural setting, as well as increasing average temperatures, improving Rca activity has the potential to become a promising strategy to improve crop yields sustainably in the face of climate change.

This can be achieved by characterising the activity of wheat Rca isoforms *in vitro* and by understanding how gene expression and protein levels vary *in planta* under heat stress. Furthermore, variation in the regulation of carbon assimilation in wheat wild relatives that are adapted to diverse environments can be exploited to improve wheat productivity.

1.6 Thesis aims

This thesis is divided into four results chapters and addresses the following research hypotheses:

1. Rca isoforms from wheat differ in activity and is concentration-dependent and varies in its response to ADP inhibition.
2. Rca isoforms from wheat differ in their temperature response and individual amino acids contribute to thermostability.
3. Short-term heat stress induces Rca expression and changes the Rca protein pool and reduces Rubisco activation in wheat.
4. Wheat wild relatives offer genetic diversity in Rca sequences.

1.7 References

- Ammelburg M, Frickey T, Lupas AN. 2006.** Classification of AAA+ proteins. *Journal of Structural Biology* **156**: 2–11.
- Andralojc PJ, Carmo-Silva E, Degen GE, Parry MAJ. 2018.** Increasing metabolic potential: C-fixation. *Essays In Biochemistry* **62**: 109–118.
- Andralojc PJ, Madgwick PJ, Tao Y, Keys A, Ward JL, Beale MH, Loveland JE, Jackson PJ, Willis AC, Gutteridge S, et al. 2012.** 2-Carboxy-D-arabinitol 1-phosphate (CA1P) phosphatase: evidence for a wider role in plant Rubisco regulation. *Biochemical Journal* **442**: 733–742.
- Asseng S, Ewert F, Martre P, Rotter RP, Lobell DB, Cammarano D, Kimball BA, Ottman MJ, Wall GW, White JW, et al. 2014.** Rising temperatures reduce global wheat production. *Nature Climate Change* **5**: 143–147.
- Asseng S, Ewert F, Rosenzweig C, Jones JW, Hatfield JL, Ruane AC, Boote KJ, Thorburn PJ, Rotter RP, Cammarano D, et al. 2013.** Uncertainty in simulating wheat yields under climate change. *Nature Climate Change* **3**: 827–832.
- Bauwe H, Hagemann M, Fernie AR. 2010.** Photorespiration: players, partners and origin. *Trends in Plant Science* **15**: 330–336.
- Bhat JY, Miličić G, Miličić G, Thieulin-Pardo G, Bracher A, Maxwell A, Maxwell A, Ciniawsky S, Mueller-Cajar O, Engen JR, et al. 2017.** Mechanism of enzyme repair by the AAA(+) chaperone rubisco activase. *Molecular cell* **67**: 744–756.e6.
- Bracher A, Whitney SM, Hartl FU, Hayer-Hartl M. 2017.** Biogenesis and Metabolic Maintenance of Rubisco. *Annual Review of Plant Biology* **68**: 29–60.
- Calvin M, Benson AA. 1948.** The Path of Carbon in Photosynthesis. *Science* **107**: 476–480.
- Carmo-Silva E, Salvucci ME. 2013.** The regulatory properties of Rubisco activase differ among species and affect photosynthetic induction during light transitions. *Plant Physiology* **161**: 1645–1655.
- Carmo-Silva E, Andralojc PJ, Scales JC, Driever SM, Mead A, Lawson T, Raines CA, Parry MAJ. 2017.** Phenotyping of field-grown wheat in the UK highlights contribution of light response of photosynthesis and flag leaf longevity to grain yield. *Journal of Experimental Botany* **68**: 3473–3486.
- Carmo-Silva E, Scales JC, Madgwick PJ, Parry MAJ. 2015.** Optimizing Rubisco and its regulation for greater resource use efficiency. *Plant, Cell & Environment* **38**: 1817–1832.

- Dawson IA, Wardlaw IF. 1989.** The tolerance of wheat to high temperatures during reproductive growth. III. Booting to anthesis. *Australian Journal of Agricultural Research* **40**: 965–980.
- Degen GE, Worrall D, Carmo-Silva E. 2020.** An isoleucine residue acts as a thermal and regulatory switch in wheat Rubisco activase. *The Plant Journal* **103**: 742–751.
- Driever SM, Simkin AJ, Alotaibi S, Fisk SJ, Madgwick PJ, Sparks CA, Jones HD, Lawson T, Parry MAJ, Raines CA. 2017.** Increased SBPase activity improves photosynthesis and grain yield in wheat grown in greenhouse conditions. *Philosophical transactions of the Royal Society of London. Series B, Biological sciences* **372**: 20160384.
- Eberhard S, Finazzi G, Wollman F-A. 2008.** The dynamics of photosynthesis. *Annual Review of Genetics* **42**: 463–515.
- Evans JR, Lawson T. 2020.** From green to gold: agricultural revolution for food security. *Journal of Experimental Botany* **71**: 2211–2215.
- FAOSTAT 2014. 2014.** Food and Agriculture Organization of the United Nations Statistics Division.
- Fedoroff NV, Battisti DS, Beachy RN, Cooper PJM, Fischhoff DA, Hodges CN, Knauf VC, Lobell D, Mazur BJ, Molden D, et al. 2010.** Radically rethinking agriculture for the 21st century. *Science* **327**: 833–834.
- Feller U, Anders I, Mae T. 2008.** Rubiscolytics: fate of Rubisco after its enzymatic function in a cell is terminated. *Journal of Experimental Botany* **59**: 1615–1624.
- Feller U, Crafts-Brandner S, Salvucci M. 1998.** Moderately high temperatures inhibit Ribulose-1,5-Bisphosphate Carboxylase/Oxygenase (Rubisco) activase-mediated activation of Rubisco. *Plant Physiology* **116**: 539–546.
- Flexas J, Díaz-Espejo A, Conesa MA, Coopman RE, Douthe C, Gago J, Gallé A, Galmés J, Medrano H, Ribas-Carbo M, et al. 2016.** Mesophyll conductance to CO₂ and Rubisco as targets for improving intrinsic water use efficiency in C₃ plants. *Plant, Cell and Environment* **39**: 965–982.
- Gourdji SM, Mathews KL, Reynolds M, Crossa J, Lobell DB. 2013.** An assessment of wheat yield sensitivity and breeding gains in hot environments. *Proceedings. Biological sciences / The Royal Society* **280**: 20122190–20122190.
- Govindjee, Whitmarsh J. 1999.** Photosynthesis and Photomorphogenesis: Section I.2: The Photosynthetic process. *Concepts in Photobiology*: 13.
- Gray SB, Dermody O, Klein SP, Locke AM, McGrath JM, Paul RE, Rosenthal DM, Ruiz-Vera UM, Siebers MH, Strellner R, et al. 2016.** Intensifying

drought eliminates the expected benefits of elevated carbon dioxide for soybean. *Nature Plants* **2**: 16132.

Harrison EP, Olcer H, Lloyd JC, Long SP, Raines CA. 2001. Small decreases in SBPase cause a linear decline in the apparent RuBP regeneration rate, but do not affect Rubisco carboxylation capacity. *Journal of Experimental Botany* **52**: 1779–1784.

Harrison EP, Willingham NM, Lloyd JC, Raines CA. 1997. Reduced sedoheptulose-1,7-bisphosphatase levels in transgenic tobacco lead to decreased photosynthetic capacity and altered carbohydrate accumulation. *Planta* **204**: 27–36.

Hartl M, Füll M, Boersema PJ, Jost JO, Kramer K, Bakirbas A, Sindlinger J, Plöschinger M, Leister D, Uhrig G, et al. 2017. Lysine acetylome profiling uncovers novel histone deacetylase substrate proteins in Arabidopsis. *Molecular Systems Biology* **13**: 949–16.

Hazra S, Henderson JN, Liles K, Hilton MT, Wachter RM. 2015. Regulation of ribulose-1,5-bisphosphate carboxylase/oxygenase (rubisco) activase: product inhibition, cooperativity, and magnesium activation. *The Journal of Biological Chemistry* **290**: 24222–24236.

Hermida-Carrera C, Kapralov MV, Galmés J. 2016. Rubisco Catalytic Properties and Temperature Response in Crops. **171**: 2549–2561.

Hochman Z, Gobbett DL, Horan H. 2017. Climate trends account for stalled wheat yields in Australia since 1990. *Global Change Biology* **23**: 2071–2081.

IPCC. 2014. Climate change 2014. Mitigation of Climate Change—Working Group III Contribution to the Fifth Assessment Report of the Intergovernmental Panel on Climate Change. *Cambridge University Press*.

Ishijima S, Uchibori A, Takagi H, Maki R, Ohnishi M. 2003. Light-induced increase in free Mg²⁺ concentration in spinach chloroplasts: Measurement of free Mg²⁺ by using a fluorescent probe and necessity of stromal alkalization. *Archives of Biochemistry and Biophysics* **412**: 126–132.

Ishikawa C, Hatanaka T, Misoo S, Miyake C, Fukayama H. 2011. Functional Incorporation of Sorghum Small Subunit Increases the Catalytic Turnover Rate of Rubisco in Transgenic Rice. *Plant Physiology* **156**: 1603–1611.

Jarvis P, Soll J. 2002. Toc, Tic, and chloroplast protein import. *Biochimica et Biophysica Acta* **1590**: 177–189.

Kaiser E, Correa-Galvis V, Armbruster U. 2019. Efficient photosynthesis in dynamic light environments: a chloroplast's perspective. *Biochemical Journal* **476**: 2725–2741.

- Keown JR, Griffin MDW, Mertens HDT, Pearce FG. 2013.** Small oligomers of ribulose-bisphosphate carboxylase/oxygenase (Rubisco) activase are required for biological activity. *The Journal of Biological Chemistry* **288**: 20607–20615.
- Kumar A, Li C, Portis AR. 2009.** Arabidopsis thaliana expressing a thermostable chimeric Rubisco activase exhibits enhanced growth and higher rates of photosynthesis at moderately high temperatures. *Photosynthesis Research* **100**: 143–153.
- Kurek I, Chang TK, Bertain SM, Madrigal A, Liu L, Lassner MW, Zhu G. 2007.** Enhanced thermostability of Arabidopsis Rubisco activase improves photosynthesis and growth rates under moderate heat stress. *The Plant Cell* **19**: 3230–3241.
- Liu B, Asseng S, Müller C, Ewert F, Elliott J, Lobell DB, Martre P, Ruane AC, Wallach D, Jones JW, et al. 2016.** Similar estimates of temperature impacts on global wheat yield by three independent methods. *Nature Climate Change* **6**: 1130–1136.
- Lobo AKM, Orr DJ, Gutierrez MO, Andralojc PJ, Sparks C, Parry MAJ, Carmo-Silva E. 2019.** Overexpression of calpase Decreases Rubisco Abundance and Grain Yield in Wheat. *Plant Physiology* **181**: 471–479.
- Long SP, Ainsworth EA, Leakey ADB, Nösberger J, Ort DR. 2006a.** Food for thought: lower-than-expected crop yield stimulation with rising CO₂ concentrations. *Science* **312**: 1918–1921.
- Long SP, Zhu X-G, Naidu SL, Ort DR. 2006b.** Can improvement in photosynthesis increase crop yields? *Plant, Cell & Environment* **29**: 315–330.
- Lorimer GH, Mizioroko HM. 1980.** Carbamate formation on the epsilon-amino group of a lysyl residue as the basis for the activation of ribulose-bisphosphate carboxylase by CO₂ and Mg²⁺. *Biochemistry* **19**: 5321–5328.
- Lorimer GH, Badger MR, Andrews TJ. 1976.** The activation of ribulose-1,5-bisphosphate carboxylase by carbon dioxide and magnesium ions. Equilibria, kinetics, a suggested mechanism, and physiological implications. *Biochemistry* **15**: 529–536.
- McKay RML, Gibbs SP, Vaughn KC. 1991.** RuBisCo activase is present in the pyrenoid of green algae. *Protoplasma* **162**: 38–45.
- Michelet L, Zaffagnini M, Morisse S, Sparla F, Perez-Perez ME, Francia F, Danon A, Marchand CH, Fermani S, Trost P, et al. 2013.** Redox regulation of the Calvin-Benson cycle: something old, something new. *Frontiers in Plant Science* **4**: 470.
- Mueller-Cajar O, Stotz M, Wendler P, Hartl FU, Bracher A, Hayer-Hartl M. 2011.** Structure and function of the AAA+ protein CbbX, a red-type Rubisco activase. *Nature* **479**: 194–199.

- Nagarajan R, Gill KS. 2018.** Evolution of Rubisco activase gene in plants. *Plant Molecular Biology* **96**: 69–87.
- Neuwald AF, Aravind L, Spouge JL, Koonin EV. 1999.** AAA+: A class of chaperone-like ATPases associated with the assembly, operation, and disassembly of protein complexes. *Genome research* **9**: 27–43.
- Ogura T, Wilkinson AJ. 2001.** AAA+ superfamily ATPases: common structure–diverse function. *Genes to cells : devoted to molecular & cellular mechanisms* **6**: 575–597.
- Ogura T, Whiteheart SW, Wilkinson AJ. 2004.** Conserved arginine residues implicated in ATP hydrolysis, nucleotide-sensing, and inter-subunit interactions in AAA and AAA+ ATPases. *Journal of Structural Biology* **146**: 106–112.
- Orr DJ, Alcântara A, Kapralov MV, John Andralojc P, Carmo-Silva E, Parry MAJ. 2016.** Surveying rubisco diversity and temperature response to improve crop photosynthetic efficiency. *Plant Physiology* **172**: 707–717.
- Parry MAJ, Keys AJ, Madgwick PJ, Carmo-Silva AE, Andralojc PJ. 2008.** Rubisco regulation: a role for inhibitors. *Journal of Experimental Botany* **59**: 1569–1580.
- Pearce FG. 2006.** Catalytic by-product formation and ligand binding by ribulose biphosphate carboxylases from different phylogenies. *Biochemical Journal* **399**: 525–534.
- Porter JR, Xie L, Challinor AJ, Cochrane K, Howden SM, Iqbal MM, Lobell DB, Travasso MI. 2014.** Food security and food production systems. In: *Climate Change 2014: Impacts, Adaptation, and Vulnerability. Part A: Global and Sectoral Aspects. Contribution of Working Group II to the Fifth Assessment Report of the Intergovernmental Panel on Climate Change.*
- Portis AR, Li C, Wang D, Salvucci ME. 2008.** Regulation of Rubisco activase and its interaction with Rubisco. *Journal of Experimental Botany* **59**: 1597–1604.
- Prins A, Orr DJ, Andralojc PJ, Reynolds MP, Carmo-Silva E, Parry MAJ. 2016.** Rubisco catalytic properties of wild and domesticated relatives provide scope for improving wheat photosynthesis. *Journal of Experimental Botany* **67**: 1827–1838.
- Ray DK, Mueller ND, West PC, Foley JA. 2013.** Yield trends are insufficient to double global crop production by 2050. *PLoS ONE* **8**: e66428.
- Robinson SP, Portis AR. 1989.** Ribulose-1,5-bisphosphate carboxylase/oxygenase activase protein prevents the in vitro decline in activity of ribulose-1,5-bisphosphate carboxylase/oxygenase. *Plant Physiology* **90**: 968–971.

- Rosenthal DM, Locke AM, Khozaei M, Raines CA, Long SP, Ort DR. 2011.** Over-expressing the C₃ photosynthesis cycle enzyme Sedoheptulose-1-7 Bisphosphatase improves photosynthetic carbon gain and yield under fully open air CO₂ fumigation (FACE). *BMC Plant Biology* **11**: 123.
- Salvucci ME, Crafts-Brandner SJ. 2004.** Relationship between the heat tolerance of photosynthesis and the thermal stability of Rubisco activase in plants from contrasting thermal environments. *Plant Physiology* **134**: 1460–1470.
- Salvucci ME, DeRidder BP, Portis AR. 2006.** Effect of activase level and isoform on the thermotolerance of photosynthesis in Arabidopsis. *Journal of Experimental Botany* **57**: 3793–3799.
- Salvucci ME, Portis AR, Ogren WL. 1985.** A soluble chloroplast protein catalyzes ribulosebisphosphate carboxylase/oxygenase activation in vivo. *Photosynthesis Research* **7**: 193–201.
- Salvucci ME, Portis AR, Ogren WL. 1986.** Light and CO₂ Response of Ribulose-1,5-Bisphosphate Carboxylase/Oxygenase Activation in Arabidopsis Leaves. **80**: 655–659.
- Salvucci ME, van de Loo FJ, Stecher D. 2003.** Two isoforms of Rubisco activase in cotton, the products of separate genes not alternative splicing. *Planta* **216**: 736–744.
- Salvucci ME, Werneke JM, Ogren WL, Portis AR. 1987.** Purification and Species Distribution of Rubisco Activase. *Plant Physiology* **84**: 930–936.
- Scafaro AP, Bautsoens N, Boer den B, Van Rie J, Gallé A. 2019a.** A conserved sequence from heat-adapted species improves rubisco activase thermostability in wheat. *Plant Physiology* **181**: 43–54.
- Scafaro AP, De Vleeschauwer D, Bautsoens N, Hannah MA, Boer den B, Gallé A, Van Rie J. 2019b.** A single point mutation in the C-terminal extension of wheat Rubisco activase dramatically reduces ADP inhibition via enhanced ATP binding affinity. *The Journal of Biological Chemistry* **294**: 17931–17940.
- Scafaro AP, Gallé A, Van Rie J, Carmo-Silva E, Salvucci ME, Atwell BJ. 2016.** Heat tolerance in a wild *Oryza* species is attributed to maintenance of Rubisco activation by a thermally stable Rubisco activase ortholog. *New Phytologist* **211**: 899–911.
- Schrader SM, Kane HJ, Sharkey TD, Caemmerer von S. 2006.** High temperature enhances inhibitor production but reduces fallover in tobacco Rubisco. *Functional Plant Biology* **33**: 921–929.
- Semenov MA, Mitchell RAC, Whitmore AP, Hawkesford MJ, Parry MAJ, Shewry PR. 2012.** Shortcomings in wheat yield predictions. *Nature Climate Change* **2**: 380–382.

Sharwood RE, Sonawane BV, Ghannoum O, Whitney SM. 2016. Improved analysis of C4 and C3 photosynthesis via refined in vitro assays of their carbon fixation biochemistry

. *Journal of Experimental Botany* **67**: 3137–3148.

Shivhare D, Mueller-Cajar O. 2017. In vitro characterization of thermostable CAM rubisco activase reveals a rubisco interacting surface loop. *Plant Physiology* **174**: 1505–1516.

Simkin AJ, McAusland L, Headland LR, Lawson T, Raines CA. 2015. Multigene manipulation of photosynthetic carbon assimilation increases CO₂ fixation and biomass yield in tobacco. *Journal of Experimental Botany* **66**: 4075–4090.

Somerville CR, Archie R, Portis J, Ogren WL. 1982. A Mutant of *Arabidopsis thaliana* Which Lacks Activation of RuBP Carboxylase In Vivo. **70**: 381–387.

Spreitzer RJ. 2003. Role of the small subunit in ribulose-1,5-bisphosphate carboxylase/oxygenase. *Archives of Biochemistry and Biophysics* **414**: 141–149.

Stevenson JR, Villoria N, Byerlee D, Kelley T, Maredia M. 2013. Green Revolution research saved an estimated 18 to 27 million hectares from being brought into agricultural production. *Proceedings of the National Academy of Sciences* **110**: 8363–8368.

Tack J, Barkley A, Nalley LL. 2015. Effect of warming temperatures on US wheat yields. *Proceedings of the National Academy of Sciences* **112**: 6931–6936.

Tanaka A, Takahashi K, Masutomi Y, Hanasaki N, Hijioka Y, Shiogama H, Yamanaka Y. 2015. Adaptation pathways of global wheat production: Importance of strategic adaptation to climate change. *Scientific reports* **5**: 14312.

Taylor SH, Long SP. 2017. Slow induction of photosynthesis on shade to sun transitions in wheat may cost at least 21% of productivity. *Philosophical Transactions of the Royal Society B: Biological Sciences* **372**: 20160543.

Tilman D, Balzer C, Hill J, Belfort BL. 2011. Global food demand and the sustainable intensification of agriculture. *Proceedings of the National Academy of Sciences* **108**: 20260–20264.

Tsai YCC, Lapina MC, Bhushan S, Mueller-Cajar O. 2015. Identification and characterization of multiple rubisco activases in chemoautotrophic bacteria. *Nature Communications* **6**: 8883.

- Uematsu K, Suzuki N, Iwamae T, Inui M, Yukawa H. 2012.** Increased fructose 1,6-bisphosphate aldolase in plastids enhances growth and photosynthesis of tobacco plants. *Journal of Experimental Botany* **63**: 3001–3009.
- United Nations, Department of Economic and Social Affairs, Population Division. 2015.** *World Population Prospects: The 2015 Revision, Key Findings and Advance Tables*.
- Vinyard DJ, Ananyev GM, Charles Dismukes G. 2013.** Photosystem II: The Reaction Center of Oxygenic Photosynthesis*. *Annual Review of Biochemistry* **82**: 577–606.
- Walker BJ, VanLoocke A, Bernacchi CJ, Ort DR. 2016.** The Costs of Photorespiration to Food Production Now and in the Future. *Annual Review of Plant Biology* **67**: 107–129.
- Wang D, Portis AR. 2006.** Increased sensitivity of oxidized large isoform of ribulose-1,5-bisphosphate carboxylase/oxygenase (rubisco) activase to ADP inhibition is due to an interaction between its carboxyl extension and nucleotide-binding pocket. *The Journal of Biological Chemistry* **281**: 25241–25249.
- Wang Q, Serban AJ, Wachter RM, Moerner WE. 2018.** Single-molecule difusometry reveals the nucleotide-dependent oligomerization pathways of *Nicotiana tabacum* Rubisco activase. *Journal of Chemical Physics* **148**: 123319.
- Wendler P, Ciniawsky S, Kock M, Kube S. 2012.** Structure and function of the AAA+ nucleotide binding pocket. *Biochimica et Biophysica Acta* **1823**: 2–14.
- Whitney SM, Houtz RL, Alonso H. 2011.** Advancing our understanding and capacity to engineer nature's CO₂-sequestering enzyme, Rubisco. *Plant Physiology* **155**: 27–35.
- Zhang N, Portis AR. 1999.** Mechanism of light regulation of Rubisco: a specific role for the larger Rubisco activase isoform involving reductive activation by thioredoxin-f. *Proceedings of the National Academy of Sciences* **96**: 9438–9443.
- Zhang N, Kallis RP, Ewy RG, Portis AR. 2002.** Light modulation of Rubisco in *Arabidopsis* requires a capacity for redox regulation of the larger Rubisco activase isoform. *Proceedings of the National Academy of Sciences* **99**: 3330–3334.
- Zhang N, Schürmann P, Portis AR. 2001.** Characterization of the regulatory function of the 46-kDa isoform of Rubisco activase from *Arabidopsis*. *Photosynthesis Research* **68**: 29–37.

Zhu G, Jensen RG. 1991. Xylulose 1,5-Bisphosphate Synthesized by Ribulose 1,5-Bisphosphate Carboxylase/Oxygenase during Catalysis Binds to Decarbamylated Enzyme. *Plant Physiology* **97**: 1348–1353.

Zhu X-G, Long SP, Ort DR. 2008. What is the maximum efficiency with which photosynthesis can convert solar energy into biomass? *Current Opinion in Biotechnology* **19**: 153–159.

Figure 4 of the following chapter was published as part of

Perdomo, J.A., Degen, G.E., Worrall, D. and Carmo-Silva, E. (2019) Rubisco activation by wheat Rubisco activase isoform 2 β is insensitive to inhibition by ADP. *Biochem. J.*, **476**, 2595–2606.

Author contributions: E.C.S. designed the experiments and supervised the project. J.A.P. and G.D. carried out the experiments. D.W. prepared recombinant enzyme expression constructs. D.W., J.A.P. and G.D. purified recombinant proteins. J.A.P. and E.C.S. analysed the data. J.A.P. and E.C.S. wrote the manuscript with contributions from all authors. All authors discussed the results and provided critical feedback.

2. Chapter 2: Wheat Rca isoforms vary in their concentration-dependent activity and ADP sensitivity

Abstract

Rubisco, the central enzyme of carbon assimilation, can be inhibited by sugar phosphate derivatives. The ATPase Rubisco activase (Rca), removes these inhibitors by remodelling the active site of Rubisco. Rca has been characterised in many model plant species, but little is known about the concentration dependence and regulatory properties of Rca in wheat, a staple crop for human nutrition. Rca isoforms purified after expression in *E. coli* were shown to differ in their *in vitro* capacity to activate Rubisco and vary in concentration-dependence and regulatory properties. Rca2 β and α had faster Rubisco activation activities than Rca1 β . Rca specific activity showed that a Rubisco-Active sites:Rca ratio of 11-6:1 are most efficient for activating Rubisco *in vitro*. Rca2 β was insensitive to ADP inhibition, in contrast to Rca1 β and two amino acid residues involved in ADP sensitivity were identified. Improving Rca response to ADP:ATP ratios in combination with tuning Rubisco to Rca ratios will inform future efforts to improve Rubisco activation by Rca *in planta*.

2.1 Introduction

Rubisco activase (Rca), a key regulator of carbon assimilation, removes inhibitory sugar phosphate derivatives from the active site of Rubisco, thereby restoring catalytic capacity (Salvucci *et al.*, 1985; Salvucci & Anderson, 1987). Rca has been characterised from many model plants, such as tobacco and Arabidopsis (Carmo-Silva & Salvucci, 2013). This research investigated the regulatory properties of Rca from wheat, the most widely grown crop in the world, which provides 20 % of daily calories and protein to 4.5 billion people (FAOSTAT, 2019). Projected wheat yields are insufficient to meet future demands (Ray *et al.*, 2013), however, improving photosynthesis has been identified as a strategy to increase crop yields while minimising the use of agricultural resources (Long *et al.*, 2006; Ort *et al.*, 2015). Plants often experience non-steady state conditions in an agricultural setting, where shading and sun movement can drastically change light environments. Activation of Rubisco during shade to sun transitions has been identified as a bottleneck in wheat, with an estimated productivity cost of 21% (Taylor & Long, 2017). Hence, understanding the regulation of Rca is vital for improving Rubisco activity under increasingly variable environmental conditions in order to meet future food demands.

As a member of the AAA+ protein group, Rca uses the energy from ATP hydrolysis, which yields ADP and inorganic phosphate, to remove Rubisco inhibitors by remodelling the active site (Bhat *et al.*, 2017b). Plants contain different Rca isoforms, with some species containing only a short β version, such as tobacco, and others containing a β as well as a longer α isoform, such as Arabidopsis and wheat (Nagarajan & Gill, 2018). The longer α isoform, which is sensitive to ADP inhibition, contains a redox-sensitive C-terminal extension, which contains two cysteine residues. Upon oxidation, these form a disulfide bond, which results in lower Rca activity (Zhang & Portis, 1999; Zhang *et al.*, 2001). Activity can be restored by reducing the disulfide bond in the light (Portis *et al.*, 2008), via the thioredoxin-f system. It is well established that Rca functions as a hexamer (Bhat *et al.*, 2017a),

however, many questions remain on the precise mechanism of Rubisco activation due to limited structural information (Henderson *et al.*, 2011; Stotz *et al.*, 2011; Hasse *et al.*, 2015). Understanding how Rca concentration, ATP supply and ATP:ADP ratios affect Rca activity is important in order to improve catalytic properties.

Physiological ratios of ADP:ATP in the stroma of wheat protoplasts have been estimated to be ca. 0.33 in the light and 0.9 in the dark (Stitt *et al.*, 1982), although this could differ in intact plants. Activity of tobacco Rca has been shown to be inhibited by increasing ADP concentrations, whereas Rca isoforms from Arabidopsis differ in their response (Carmo-Silva & Salvucci, 2013). The longer α isoform from Arabidopsis exhibited ADP sensitivity, while the shorter β isoform was insensitive. By changing the composition of Rca isoforms, plants can adapt to the prevailing light environment by modulating Rubisco activation state (Zhang & Portis, 1999).

Wheat contains the *Rca1* and *Rca2* genes, which encode the isoforms Rca1 β and Rca2 β and Rca2 α (Carmo-Silva *et al.*, 2015; Nagarajan & Gill, 2018). The isoforms encoded by *Rca2* are the product of alternative splicing between exon 5 and 6. A C-terminal lysine residue has been found to increase ADP sensitivity in Rca (Hartl *et al.*, 2017; Scafaro *et al.*, 2019). The results both suggest that the C-terminal extension is a mechanism of modulating Rca activity in response to the redox status and ADP:ATP ratio in the leaf, which is ultimately affected by the light environment.

The aim of the work described in this chapter was to characterise the activities of wheat Rca isoforms *in vitro*, to evaluate the enzyme-concentration dependence of Rca activity and to understand diversity in the regulation of wheat Rca isoforms by ADP:ATP ratios.

2.2 Results

2.2.1 Rca ATPase and Rubisco activation activities

Rca isoforms from wheat B genome proteins were expressed in *E. coli* and purified (Barta *et al.*, 2011a). Recombinantly produced enzymes were assayed for ATP hydrolysis, by measuring the release of inorganic phosphate (Chifflet

et al., 1988) in the presence of 5 mM ATP at 25°C. Rca1 β , the isoform produced from the *Rca1* gene showed ATPase activity of ca. 45 $\mu\text{mol ATP min}^{-1} \mu\text{mol Rca}^{-1}$ (Fig. 1A). Rca2 β , the short isoform produced from the *Rca2* gene had significantly higher ATPase activity at ca. 50 $\mu\text{mol ATP min}^{-1} \mu\text{mol Rca}^{-1}$. Rca2 α , the long isoform produced via alternative splicing from the *Rca2* gene, had significantly lower ATPase activity of ca. 25 $\mu\text{mol ATP min}^{-1} \mu\text{mol Rca}^{-1}$, compared to Rca1 β and Rca2 α .

In order to fully characterise the properties and catalytic capacity of Rca, the rate of reactivation of pre-inhibited Rubisco was measured (Fig. 1B-D) using the assay described in (Barta *et al.*, 2011b). Rubisco activation is calculated from the activity of three reaction types (Fig. 1B). In the “ECM” assay, inhibited Rubisco (ER) is incubated with Rca2 β in the absence of RuBP in the first stage assay (Fig. 1B, C). Inhibited Rubisco (ER) was produced prior to the assay by incubating purified Rubisco with RuBP at 4°C for 48 h. Rubisco activase removes inhibitory RuBP from the active site, which allows for non-substrate CO₂ and Mg²⁺ to bind to the active site (termed carbamylation). After 1, 3 and 5 minutes, a fraction of the first stage is then added to the second stage to assay Rubisco activity for 30 s and determine the rate of CO₂ assimilation (Vi), expressed as $\mu\text{mol CO}_2 \text{ min}^{-1} \text{ mg}^{-1}$ Rubisco.

In the second reaction type “Rca”, pre-inhibited Rubisco, Rca and RuBP (which acts as an inhibitor here) are included in the first stage assay. After 0.5, 1.5 and 3 min, an aliquot of the first stage assay is added to the second stage in order to measure Rubisco activity and assess the increase in Vi over time due to the removal of RuBP from uncarbamyated Rubisco active sites (R_{A.S.}) by Rca (Fig. 1C). The first “ECM” assay is used to yield the maximum Rubisco activity and is used to calculate the fraction of Rubisco activated by Rca using Eq. 1 and expressed as $\mu\text{mol R}_{A.S.} \text{ min}^{-1} \mu\text{mol Rca}^{-1}$.

In the third reaction type “ER”, Rca is excluded in the first stage, and pre-inhibited Rubisco is incubated with 6 mM RuBP. Aliquots are added from the first stage to the second stage at the same times as for “Rca”. This reaction allows for the measurement of spontaneous release of RuBP and

consequent Rubisco activation and is calculated according to Eq. 2. V_i increases slightly over time, due to spontaneous release of RuBP from $R_{A,S}$ (Fig. 1C) and this is accounted for when calculating the rate of Rubisco activation by Rca. Rubisco activation by Rca is corrected for spontaneous activation by subtracting the activity calculated in Eq. 2 from Eq. 1 (Eq. 3, Fig. 1D). It should be highlighted that spontaneous activation increases with temperature because the active site becomes more mobile (Schrader *et al.*, 2006). Hence, it is important to measure the spontaneous reactivation of Rubisco when assaying Rubisco activation activity of Rca at various temperatures. Rca2 β and Rca2 α exhibited much greater capacity for Rubisco activation than Rca1 β , which had significantly lower activity (Fig. 1D).

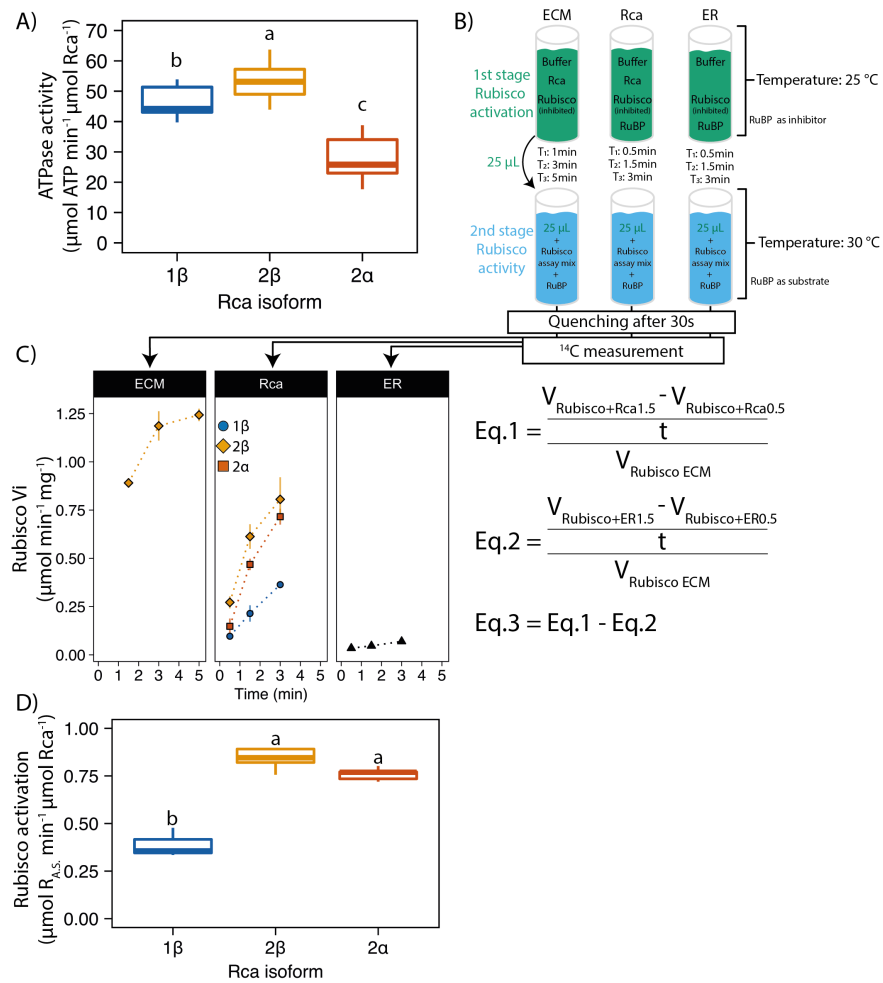


Fig. 1: Rubisco activase activities. A) ATP hydrolysis of the three wheat isoforms at 25°C containing 5mM ATP in the assay buffer. B) Scheme of the Rubisco activation assay. “ECM” is incubated for 1, 3 and 5 min in the first

stage, compared to “Rca” and “ER”, which are incubated for 0.5, 1.5 and 3 min (T1-3). 25 μL of the first stage is transferred to the second stage at the indicated times to initiate Rubisco carboxylation activity. Reactions are quenched after 30 s and incorporation of ^{14}C is measured by liquid scintillation counting. C) Rubisco activities at 30 °C in the second stage assays. “ECM” assay contained Rca2 β in the first stage buffer, “Rca” contained 6mM RuBP and different Rca proteins (indicated by three different colours) and ER contained 6mM RuBP in the first stage assay but no Rca. Rubisco activity was assayed for 30s after the three different assays had been incubated in the first stage assay for 0.5 – 5 min at T1,2 & 3. Final Rubisco and Rca concentrations of 0.5 mg mL^{-1} and 0.1 mg mL^{-1} were used, respectively, resulting in ca. 2 μM Rca monomer and ca. 6 μM Rubisco active sites in the first stage assays. D) Rubisco activation activities of the three native wheat isoforms expressed as $\mu\text{mol R}_{\text{A.S.}} \text{min}^{-1} \mu\text{mol Rca}^{-1}$, calculated from C) according to Eq. 1,2 and 3. Box lines represent the median, first and third quartiles, whiskers show the range, $n = 3\text{-}5$ technical replicates. ANOVA showed significant differences between Rca isoforms ($P > 0.05$) and different letters indicate significance groups (Tukey’s honestly significant difference [HSD] mean-separation test, $P < 0.05$).

2.2.2 Concentration-dependence of wheat Rca isoforms

Rca is active as a hexamer and activity is therefore concentration-dependent (Bhat *et al.*, 2017a; Wang *et al.*, 2018). Fig. 2 shows the effect of increasing Rca concentrations on ATP hydrolysis and increasing Rca concentration on Rubisco activation. All Rca isoforms showed highest ATPase activity at 1-2 μM and activity declined at higher concentrations (Fig. 2A, B). Rubisco activation expressed as μmol Rubisco active sites ($\text{R}_{\text{A.S.}}$) min^{-1} μmol Rca^{-1} , termed Rca specific activity, showed that Rubisco activation by Rca declined with increasing Rca concentration, suggesting an optimal $\text{R}_{\text{bisco}_{\text{A.S.}}}:\text{Rca}$ ratio of 11:1 for Rca1 β , 9:1 for Rca2 α and 6:1 for Rca2 β (Fig. 2E). Overall, Rca2 β and Rca2 α had similar Rubisco activation activities and exhibited a 2-fold higher activation capacity than Rca1 β . In contrast to Rca specific activity, Rubisco activation expressed as fraction of Rubisco activated (FA min^{-1}) showed that activity increased with increasing Rca concentration (Fig. 2F).

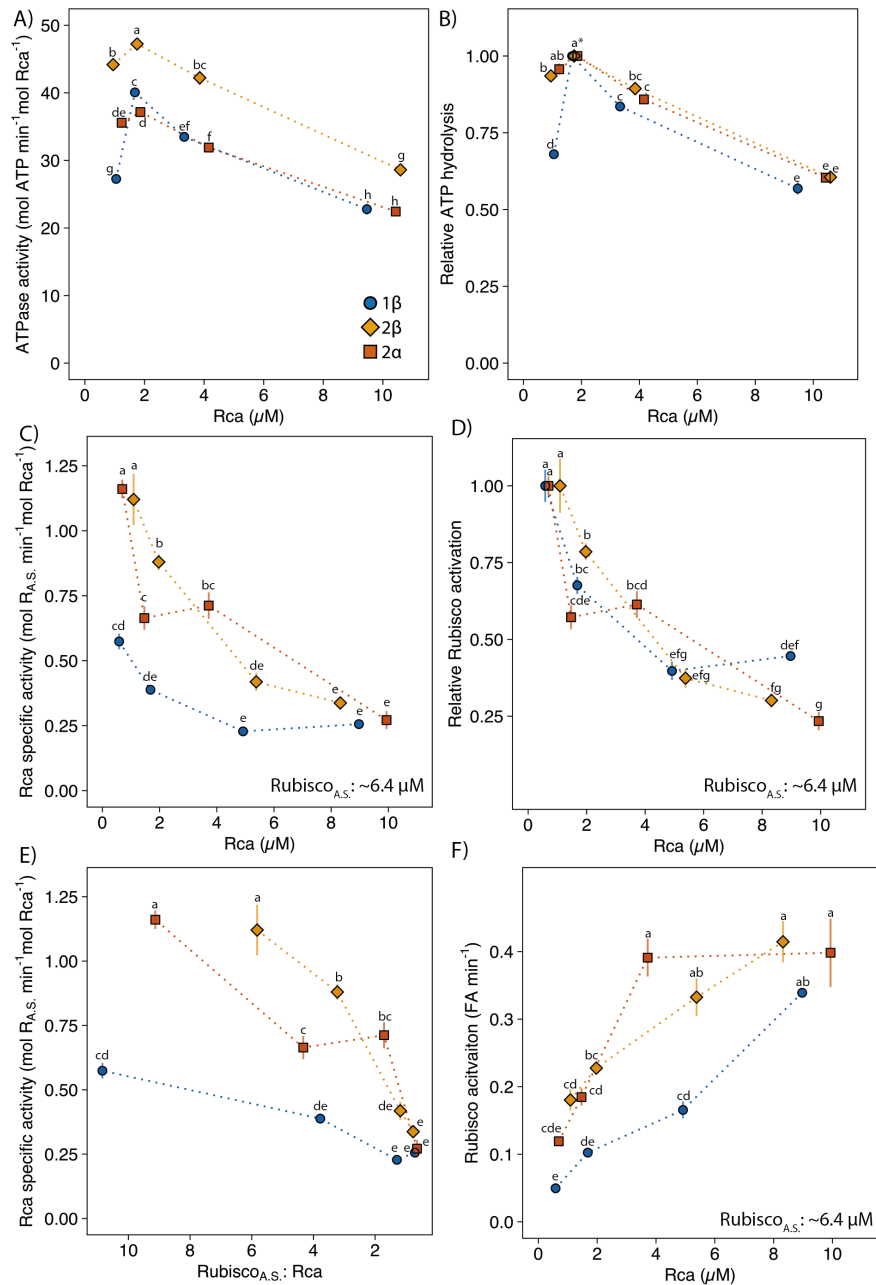


Fig. 2: Concentration-dependence of wheat Rca isoforms activity. A) ATP hydrolysis at various Rca concentrations. B) ATPase activity relative to the maximum activity measured in (A). C) Rca specific activity. Rca concentration was calculated using the protein molecular weight of the Rca monomer and ca. $6.4 \mu\text{M}$ Rubisco active sites (A.S.). D) Rubisco activation relative to the maximum activity measured in (C). E) Rca specific activity plotted against R.A.S.:Rca ratio. F) Fraction of Rubisco activated (FA) by Rca at various Rubisco concentrations. The second x-axis scale for E shows the R.A.S.:Rca ratio. Symbols represent the average calculated from $n = 3$ technical replicates. Some Error bars represent the standard error and in some cases are smaller than the symbol. ANOVA showed a significant effect of Rca concentration on the rates ($P < 0.05$) and different letters indicate significance groups (Tukey's HSD test, $P < 0.05$). * = all three isoforms have a Tukey group "a".

2.2.3 ADP sensitivity of wheat Rca isoforms

Rca activity is modulated by the ADP/ATP ratio of the chloroplast, and diversity in the regulatory properties of Rca has been reported for the isoforms from Arabidopsis and tobacco (Zhang & Portis, 1999; Carmo-Silva & Salvucci, 2013). The wheat Rca1 β and Rca2 β protein sequences were aligned with the Arabidopsis sequence, which contains an isoform that is insensitive to ADP inhibition and with tobacco Rca, which is sensitive (Fig. 3). This alignment was used to identify putative residues in wheat Rca that could confer ADP sensitivity.

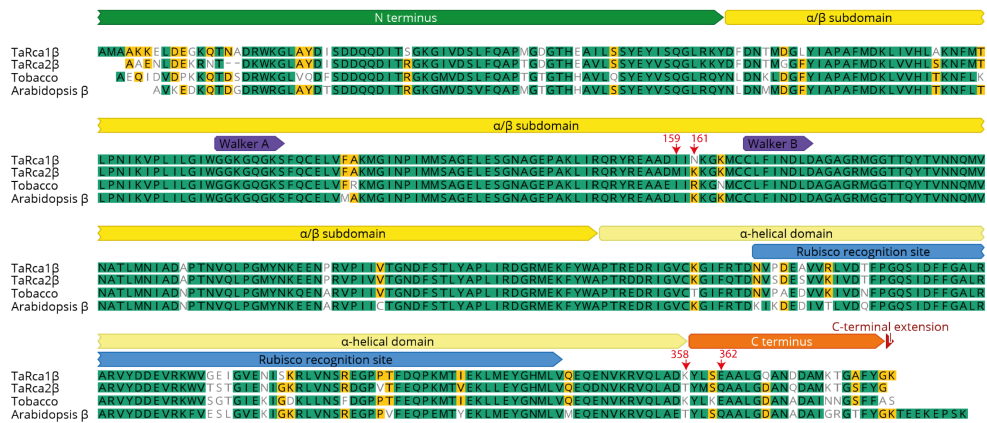


Fig. 3: Alignment of mature Rca isoforms from wheat, tobacco and Arabidopsis. The residues that were the target of site-directed mutagenesis are highlighted with red arrows. Alignment was made with Geneious. Sequences from (Carmo-Silva & Salvucci, 2013; Carmo-Silva *et al.*, 2015).

Sequence alignment revealed four residues of interest (Fig. 3), which were used to produce three mutants using site-directed mutagenesis. This resulted in two double mutants Rca2 β -M159I/K161N and Rca2 β -T358K/Q362T and one quadruple mutant which combined both double mutants (Rca2 β -M159I/K161N-T358K/Q362T).

In order to determine the effect of mutations on ADP sensitivity, ATP hydrolysis and Rubisco activation were assayed at ADP:ATP ratios of 0.00, 0.11 and 0.33. ATPase activity and Rubisco activation activity of Rca1 β and Rca2 α was sensitive to ADP inhibition, whereas Rubisco activation of Rca2 β was insensitive (Fig. 4). ATP hydrolysis of Rca2 β , however, was still inhibited by ADP and Rca2 α showed ADP sensitivity for both assays.

ATPase activity of the double mutant Rca2 β -M159I/K161N was less sensitive to ADP inhibition than Rca2 β . Rubisco activation by this mutant was also insensitive to ADP inhibition, showing a similar response to Rca2 β . Conversely, ATPase activity and Rubisco activation of Rca2 β -T358K/Q362T were much more sensitive to increasing ADP:ATP ratios than Rca2 β , suggesting that these residues are involved in ADP sensitivity. The ATPase activity of Rca2 β -M159I/K161N-T358K/Q362T exhibited ADP sensitivity similar to Rca2 β -M159I/K161N, whereas Rubisco activation was insensitive to ADP. ADP sensitivities of Rca isoforms from species and mutants discussed in this chapter are summarised in Table 1.

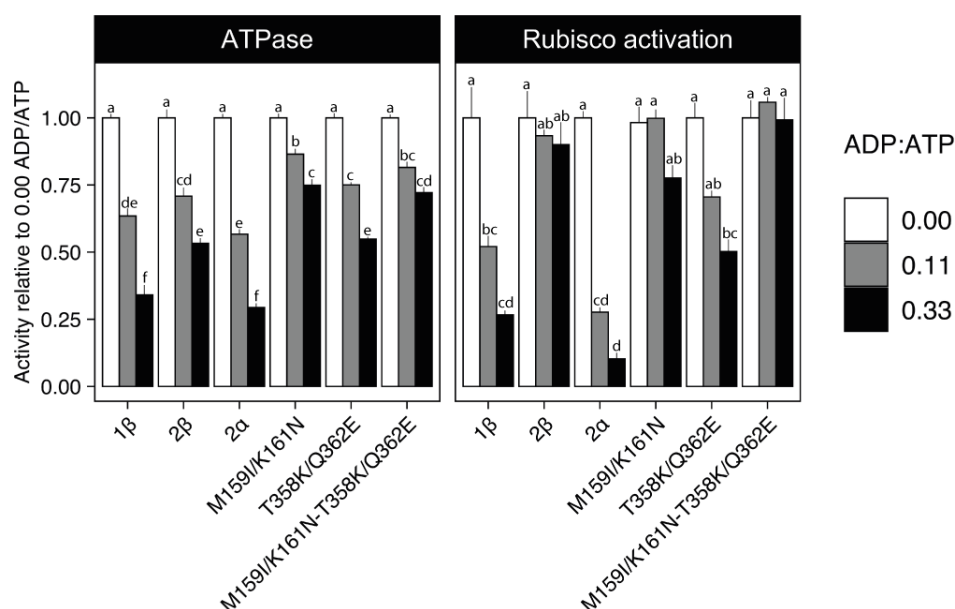


Fig. 4: ATPase activity and Rubisco activation in response to increasing ADP:ATP ratios relative to 0.00 ADP:ATP control of native wheat isoforms and three mutant proteins. ATPase assays contained 5 mM of ATP or 5 mM of 0.11 or 0.33 ADP:ATP and reactions were initiated by adding Rca to a final concentration of 2 μ M. Rubisco activation was assayed by using final concentrations of 2 μ M Rca and 6 μ M of active sites of inhibited Rubisco (ER) at the same ATP and ADP:ATP ratios. Bars represent the mean calculated from $n = 3-6$ technical replicates, bars represent the standard error. Two-way ANOVA showed significant effects of Rca isoform and ADP:ATP ratio, and a significant interaction ($P < 0.05$). Different letters indicate significance groups (Tukey's HSD test, $P < 0.05$). This data was published in Perdomo et al. (2019) as Figure 4.

Table 1: ADP sensitivity of Rubisco activation by Rca in different species.

Species	Rca isoform	ADP sensitivity	Reference
Tobacco	short	sensitive	(Carmo-Silva & Salvucci, 2013)
Ara- bidopsis	short (β)	insensitive	(Carmo-Silva & Salvucci, 2013)
	long (α)	sensitive	
Rice	2 β	sensitive	(Scafaro <i>et al.</i> , 2019)
	2 α	sensitive	
Wheat	1 β	sensitive	(Perdomo <i>et al.</i> , 2019)
	2 β	insensitive	
	2 β -M159I/K161N	insensitive	
	2 β -T358K/Q362T	sensitive	
	2 β -M159I/K161N-T358K/Q362T	insensitive	
	2 α	sensitive	

2.3 Discussion

Rubisco activase (Rca) plays a central role in the regulation of carbon assimilation. Diversity in the properties of Rca isoforms is known to exist but has received relatively little attention until recently (Carmo-Silva & Salvucci, 2013; Scafaro *et al.*, 2016; Perdomo *et al.*, 2019; Scafaro *et al.*, 2019; Degen *et al.*, 2020). Wheat Rca1 β and Rca2 β had similar rates of ATP hydrolysis, whereas Rca2 α activity was much lower. It could be speculated that the C-terminal extension of purified Rca2 α was oxidised (Zhang *et al.*, 2001; 2002), which resulted in low ATPase activity. However, Rubisco activation of Rca2 β and α showed similar activities (Fig. 1C), suggesting another mechanism that reduced activity in the ATPase assay or that larger protein molecular weight of Rca2 α could influence the capacity for ATP hydrolysis. Compared to the important crop rice (*O. sativa*), wheat Rca2 α exhibited much higher activity and rice Rca2 α was found to have much lower activation activity than Rca2 β (Scafaro *et al.*, 2016). A glutamic acid residue is present in the rice Rca2 α C-terminal extension (Degen *et al.*, 2020), which has been found to lower ATPase activity (Portis *et al.*, 2008) and likely also affects Rubisco activation activity. However, comparisons with data from other publications is complicated by the fact that other enzyme assays exist, which use different units such as ECM produced min^{-1} , and no consensus exists to report Rca and

Rubisco concentrations in μM or mg mL^{-1} . Using μM would control for differences in protein molecular weight and make activities of the shorter β and longer α isoforms more comparable. In addition, temperature responses of Rca isoform from different species would be comparable between studies.

Rca activity of multiple species has been found to be concentration-dependent (Keown *et al.*, 2013; Scales *et al.*, 2014; Wang *et al.*, 2018) and activity of wheat isoforms studied here peaked at around 2 μM Rca and declined with increasing Rca concentration. The decline in ATPase activity at high Rca concentration could be a result of increasing ADP levels as a result of ATP hydrolysis. Accumulating ADP could therefore inhibit ATPase activity and relative values show that the ADP-sensitive isoforms Rca2 α and Rca1 β have lower activities at 4 μM Rca, compared to the ADP-insensitive Rca2 β (Perdomo *et al.*, 2019). Rubisco activation, expressed as fraction of Rubisco activated min^{-1} , increased above 2 μM of Rca, however, Rca specific activity declined with increasing concentration. This finding confirms data shown for tobacco Rubisco and Rca (Scales *et al.*, 2014). It could be that with increasing Rca concentration, Rubisco becomes limiting and Rca is not saturated. This was highlighted in Scales *et al.* (2014), where increasing Rubisco concentration at a constant Rca concentration resulted in increased Rca specific activity. Previous results show that at 1-2 μM Rca forms hexamers (Keown *et al.*, 2013; Wang *et al.*, 2018), which is the optimal subunit arrangement for ATP hydrolysis and Rubisco activation (Bhat *et al.*, 2017a). Interestingly, wheat Rca isoforms exhibited different activities at the same R_{A.S.}:Rca ratios. Rca2 β and α had much higher activities at a 4:1 ratio compared to Rca1 β , highlighting the inefficiency of the latter isoform. Overall, this data suggests that ratios above 6:1-11:1 result in highest Rca specific activity. This should be considered when altering Rca expression *in plantae* in order to optimise Rubisco activation.

Rca activity is sensitive to ADP:ATP ratios, which can vary in the leaf as a result of the light environment. The sensitivity to ADP has been described previously for tobacco (sensitive) and Arabidopsis (β isoform is insensitive, α isoform is sensitive, summarised in Table 1) (Carmo-Silva & Salvucci, 2013). Wheat Rca1 β and Rca2 α showed ADP sensitivity in their

ATPase and Rubisco activation activities, whereas Rubisco activation by Rca2 β was insensitive to 0.33 ADP:ATP. This suggests that the C-terminal extension in 2 α and amino acid differences between 1 β and 2 β confer sensitivity. The C-terminal lysine residue of Rca1 β , which is also present in Rca2 α , confers ADP sensitivity (Scafaro *et al.*, 2019). While Rca2 β -M159I/K161N failed to show increased sensitivity to ADP, Rubisco activation by Rca2 β -T358K/Q362E was inhibited by increasing ADP in the assay, which contrasted with the lack of sensitivity in Rca2 β , suggesting that these residues also confer ADP sensitivity to Rca1 β . It could be speculated that additional residues in Rca1 β interact with the residues described and explain the difference in regulatory properties between the wheat Rca isoforms.

The results in this chapter show that Rca isoforms from wheat differ in their capacity to activate Rubisco and vary in their concentration-dependent activity. Furthermore, native wheat isoforms also differ in their ADP sensitivity and two amino acid residues were shown to influence enzyme activity in response to increasing ADP concentrations. These findings contribute to the understanding of the Rubisco activation mechanism of wheat and may inform future efforts to improve wheat productivity under variable light conditions.

2.4 Material and Methods

Purification of enzymes. Rubisco activase (Rca) enzymes were expressed in *E. coli* and purified as described by Barta *et al.* (Barta *et al.*, 2011a), with the following modifications. The frozen cell pellets were lysed and thawed by suspending the pellet in 130 mL of cell extraction buffer (50 mM HEPES-KOH pH 7.0, 5 mM MgCl₂, 1 mM EDTA, 0.1% (w/v) Triton X-100, 2 mM ATP, 5 mM DTT, 20 mM ascorbate, 1 mM PMSF, and 10 μM leupeptin) for 30 min on ice, and the protocol was followed hereafter. After adding ammonium sulphate to 37.5% (w/v), collecting the precipitated material and suspending in 10 mL of cell extraction buffer, the solution was centrifuged at 200,000 × *g* for 30 min in a Beckman centrifuge (Beckman Coulter) using a swinging bucket ultracentrifuge rotor SW 31 Ti. Rubisco was purified from wheat leaves according to Orr & Carmo-Silva (Orr & Carmo-Silva, 2018). Wheat (*Triticum aestivum* cultivar Cadenza) was grown in a glasshouse at ca. 22 °C and a light level of ca. 500 μmol m⁻² s⁻¹ (16h day, 8h night) for two weeks. Supplementary lighting was turned on once light inside the greenhouse fell below 200 μmol m⁻² s⁻¹. Leaf material was flash frozen in liquid nitrogen and stored at -80 °C until purification. Protein concentration was determined by the Bradford method (Bradford, 1976). Molecular weight of proteins was calculated from the respective amino acid sequence using The Sequence Manipulation Suite (Stothard, 2000) at https://www.bioinformatics.org/sms/prot_mw.html.

Site-directed mutagenesis Site-directed mutagenesis (SDM) was performed using the QuickChange Lightning Multi Site-Directed Mutagenesis Kit (Agilent Technologies) according to the manual (<https://www.agilent.com/cs/library/usermanuals/public/210513.pdf>). Primers were designed based on the coding sequence of Rca 2β from the B genome of wheat using the QuickChange Primer Design website (<https://www.agilent.com/store/primerDesignProgram.jsp>). The Rca 2β coding sequence was ligated into the pET-23(+) vector and used as a template to create the mutants described by (Perdomo *et al.*, 2019). After validation by sequencing of the Rca coding

region the plasmid was cloned into BL21(DE3)pLysS cells for expression and purification of the proteins.

Rubisco activase activity: ATP hydrolysis The rate of ATP hydrolysis by Rca isoforms was assayed using the method of (Chifflet *et al.*, 1988) with the following modifications. ATP hydrolysis was measured at a 25°C for 5 min in an assay mix (50 μ L) containing 100 mM Tricine-NaOH pH 8.0, 10 mM MgCl₂, 10 mM NaHCO₃, and 5 mM ATP or 5 mM of 0.11 and 0.33 ADP/ATP. The reaction was initiated by adding Rca at a final concentration of ca. 2 μ M and quenched after 5 min by adding 12% sodium dodecyl sulfate (SDS). Blanks were prepared by adding SDS to the reaction tube before adding the enzyme. Phosphate standards for a calibration curve were prepared by adding 0, 2.5, 5, 10, 15, 20, 32.5 and 50 mM KPi (final concentrations) to the reaction mixture described above (in the absence of Rca). Tubes containing the assay mix were incubated in a temperature block (Torrey Pines Scientific, Echotherm) until the desired temperature was reached before initiating the assay (typically 3 min). The temperature of 50 μ L H₂O incubated alongside the reaction tubes was monitored using a thermocouple (Omega Thermometer RDXL4SD, Omega Engineering). After the addition of SDS, all reactions and standards were kept in the fridge until Pi determination in a spectrophotometer (BMG Labtech) as detailed in (Perdomo *et al.*, 2019). For the three native wheat isoforms and the double mutant, enzymes from two independent purifications were used. For each ADP/ATP ratio, 3-6 technical replicates were used.

Rubisco activase activity: Rubisco reactivation. The rate of Rubisco reactivation by Rca was measured as described by Barta *et al.* (2011a) and Perdomo *et al.* (2019). To prepare inhibited Rubisco complexes (ER), purified Rubisco was first incubated in activation mix (500 mM Bicine-NaOH pH 8.0, 300 mM MgCl₂*6H₂O, 100 mM NaHcO₃) for 1h at 4 °C, followed by desalting in a spin column, protein concentration determination, and incubation of uncarbamylated enzyme with 0.5 mM RuBP at 4 °C overnight. The assay for Rubisco activation consisted of two stages (Barta *et al.*, 2011b) in the first stage, Rubisco (ER) was reactivated by Rca at 25°C and, in the second stage,

aliquots were taken from the first stage assay to measure Rubisco activity at 30°C. Temperature of Rubisco activation was controlled as described above for the ATP hydrolysis assay. Assays (90 µL final volume) contained 0.5 mg mL⁻¹ Rubisco (ER), 0.1 mg mL⁻¹ Rca, 5 mM ATP plus an ATP regenerating system, and 5 mM RuBP. Three variants of assays were performed for fully activated Rubisco (ECM, this contained no RuBP in the first stage assay), Rca (contained all components) and ER (contained no Rca, negative control). Rubisco activity (Vi) was calculated from the blank-corrected disintegrations per minute (DPM), adjusted for Rubisco concentration in the assay and expressed as µmol min⁻¹ mg⁻¹. The rate of Rubisco activation (fraction of Rubisco sites activated per minute) in the Rca reaction was calculated as:

$$\text{Eq.1: } \frac{(V_{\text{Rubisco+Rca } 1.5} - V_{\text{Rubisco+Rca } 0.5})/t}{V_{\text{Rubisco ECM}}}$$

, where $V_{\text{Rubisco+Rca } 0.5}$ and 1.5 are Rubisco activities of the Rca assays after having incubated 0.5 and 1.5 min in the first stage reaction and $V_{\text{RubiscoECM}}$ is the activity of fully activated Rubisco and t the difference in incubation time in the first stage assay (Carmo-Silva & Salvucci, 2011). Spontaneous activation of Rubisco was calculated as:

$$\text{Eq.2: } \frac{(V_{\text{Rubisco ER } 1.5} - V_{\text{Rubisco ER } 0.5})/t}{V_{\text{Rubisco ECM}}}$$

, where $V_{\text{RubiscoER } 0.5}$ and 1.5 are the activities of Rubisco in the ER assays after having incubated 0.5 and 1.5 min in the first stage reaction. The rate of Rubisco activation by Rca was calculated as:

$$\text{Eq.3: } \text{Eq.1} - \text{Eq.2}$$

The Rubisco activation activity was corrected for protein concentration in the assay, which takes into account the different protein molecular weights of each isoform and expressed as mol Rubisco active sites (R_{A.S.}) activated min⁻¹ mol Rca⁻¹.

For the three native wheat isoforms, the double and single mutant enzymes and Rubisco, one purification was used and for all assays, 3-4 technical repetitions were used.

Statistical analysis One-way ANOVA was used to test statistical significance of differences between means. This was followed by a Tukey's honestly significant difference [HSD] mean-separation test, where alpha level was set to

0.05 and letters were assigned to indicate significant differences. Statistical analysis was performed with R (version 3.6.0) and RStudio (version 1.2.5001). Box and whiskers plots were prepared using ggplot2 (Wickham, 2017).

2.5 References

- Barta C, Carmo-Silva E, Salvucci ME. 2011a.** Purification of Rubisco activase from leaves or after expression in *Escherichia coli*. *Methods in molecular biology* **684**: 363–374.
- Barta C, Carmo-Silva E, Salvucci ME. 2011b.** Rubisco activase activity assays. *Methods in molecular biology* **684**: 375–382.
- Bhat JY, Miličić G, Miličić G, Thieulin-Pardo G, Bracher A, Maxwell A, Maxwell A, Ciniawsky S, Mueller-Cajar O, Engen JR, et al. 2017a.** Mechanism of enzyme repair by the AAA(+) chaperone rubisco activase. *Molecular cell* **67**: 744–756.e6.
- Bhat JY, Thieulin-Pardo G, Hartl FU, Hayer-Hartl M. 2017b.** Rubisco activases: AAA+ chaperones adapted to enzyme repair. *Frontiers in Molecular Biosciences* **4**: 1555–10.
- Bradford MM. 1976.** A rapid and sensitive method for the quantitation of microgram quantities of protein utilizing the principle of protein-dye binding. *Analytical biochemistry* **72**: 248–254.
- Carmo-Silva E, Salvucci ME. 2011.** The activity of Rubisco's molecular chaperone, Rubisco activase, in leaf extracts. *Photosynthesis Research* **108**: 143–155.
- Carmo-Silva E, Salvucci ME. 2013.** The regulatory properties of Rubisco activase differ among species and affect photosynthetic induction during light transitions. *Plant Physiology* **161**: 1645–1655.
- Carmo-Silva E, Scales JC, Madgwick PJ, Parry MAJ. 2015.** Optimizing Rubisco and its regulation for greater resource use efficiency. *Plant, Cell & Environment* **38**: 1817–1832.
- Chifflet S, Torriglia A, Chiesa R, Tolosa S. 1988.** A method for the determination of inorganic phosphate in the presence of labile organic phosphate and high concentrations of protein: application to lens ATPases. *Analytical biochemistry* **168**: 1–4.
- Degen GE, Worrall D, Carmo-Silva E. 2020.** An isoleucine residue acts as a thermal and regulatory switch in wheat Rubisco activase. *The Plant Journal*.
- FAOSTAT. 2019.** *Crop Statistics*. Available at: <http://www.fao.org/faostat/en/#data/QC>.
- Hasse D, Larsson AM, Andersson I. 2015.** Structure of Arabidopsis thaliana Rubisco activase. *Acta crystallographica. Section D, Biological crystallography* **71**: 800–808.

- Henderson JN, Kuriata AM, Fromme R, Salvucci ME, Wachter RM. 2011.** Atomic resolution x-ray structure of the substrate recognition domain of higher plant ribulose-bisphosphate carboxylase/oxygenase (Rubisco) activase. *The Journal of Biological Chemistry* **286**: 35683–35688.
- Keown JR, Griffin MDW, Mertens HDT, Pearce FG. 2013.** Small oligomers of ribulose-bisphosphate carboxylase/oxygenase (Rubisco) activase are required for biological activity. *The Journal of Biological Chemistry* **288**: 20607–20615.
- Long SP, Zhu X-G, Naidu SL, Ort DR. 2006.** Can improvement in photosynthesis increase crop yields? *Plant, Cell & Environment* **29**: 315–330.
- Nagarajan R, Gill KS. 2018.** Evolution of Rubisco activase gene in plants. *Plant Molecular Biology* **96**: 69–87.
- Orr DJ, Carmo-Silva E. 2018.** Extraction of Rubisco to determine catalytic constants. Covshoff S ed. *Photosynthesis: Methods and Protocols*. Springer Protocols, 229–238.
- Ort DR, Merchant SS, Alric J, Barkan A, Blankenship RE, Bock R, Croce R, Hanson MR, Hibberd JM, Long SP, et al. 2015.** Redesigning photosynthesis to sustainably meet global food and bioenergy demand. *Proceedings of the National Academy of Sciences* **112**: 8529–8536.
- Perdomo JA, Degen GE, Worrall D, Carmo-Silva E. 2019.** Rubisco activation by wheat Rubisco activase isoform 2 β is insensitive to inhibition by ADP. *Biochemical Journal* **476**: 2595–2606.
- Portis AR, Li C, Wang D, Salvucci ME. 2008.** Regulation of Rubisco activase and its interaction with Rubisco. *Journal of Experimental Botany* **59**: 1597–1604.
- Ray DK, Mueller ND, West PC, Foley JA. 2013.** Yield trends are insufficient to double global crop production by 2050. *PLoS ONE* **8**: e66428.
- Salvucci ME, Anderson JC. 1987.** Factors affecting the activation state and the level of total activity of ribulose bisphosphate carboxylase in tobacco protoplasts. *Plant Physiology* **85**: 66–71.
- Salvucci ME, Portis AR, Ogren WL. 1985.** A soluble chloroplast protein catalyzes ribulosebisphosphate carboxylase/oxygenase activation in vivo. *Photosynthesis Research* **7**: 193–201.
- Scafaro AP, De Vleeschauwer D, Bautsoens N, Hannah MA, Boer den B, Gallé A, Van Rie J. 2019.** A single point mutation in the C-terminal extension of wheat Rubisco activase dramatically reduces ADP inhibition via enhanced ATP binding affinity. *The Journal of Biological Chemistry* **294**: 17931–17940.

- Scafaro AP, Gallé A, Van Rie J, Carmo-Silva E, Salvucci ME, Atwell BJ. 2016.** Heat tolerance in a wild *Oryza* species is attributed to maintenance of Rubisco activation by a thermally stable Rubisco activase ortholog. *New Phytologist* **211**: 899–911.
- Scales JC, Parry MAJ, Salvucci ME. 2014.** A non-radioactive method for measuring Rubisco activase activity in the presence of variable ATP: ADP ratios, including modifications for measuring the activity and activation state of Rubisco. *Photosynthesis Research* **119**: 355–365.
- Schrader SM, Kane HJ, Sharkey TD, Caemmerer von S. 2006.** High temperature enhances inhibitor production but reduces fallover in tobacco Rubisco. *Functional Plant Biology* **33**: 921–929.
- Stitt M, Lilley RM, Heldt HW. 1982.** Adenine nucleotide levels in the cytosol, chloroplasts, and mitochondria of wheat leaf protoplasts. **70**: 971–977.
- Stothard P. 2000.** The sequence manipulation suite: JavaScript programs for analyzing and formatting protein and DNA sequences. *BioTechniques* **28**: 1102–1104.
- Stotz M, Mueller-Cajar O, Ciniawsky S, Wendler P, Hartl FU, Bracher A, Hayer-Hartl M. 2011.** Structure of green-type Rubisco activase from tobacco. *Nature Structural & Molecular Biology* **18**: 1366–U78.
- Taylor SH, Long SP. 2017.** Slow induction of photosynthesis on shade to sun transitions in wheat may cost at least 21% of productivity. *Philosophical Transactions of the Royal Society B: Biological Sciences* **372**: 20160543.
- Wang Q, Serban AJ, Wachter RM, Moerner WE. 2018.** Single-molecule diffractometry reveals the nucleotide-dependent oligomerization pathways of *Nicotiana tabacum* Rubisco activase. *Journal of Chemical Physics* **148**: 123319.
- Wickham H. 2017.** *tidyverse: Easily install and load ‘Tidyverse’ packages.*
- Zhang N, Portis AR. 1999.** Mechanism of light regulation of Rubisco: a specific role for the larger Rubisco activase isoform involving reductive activation by thioredoxin-f. *Proceedings of the National Academy of Sciences* **96**: 9438–9443.
- Zhang N, Kallis RP, Ewy RG, Portis AR. 2002.** Light modulation of Rubisco in *Arabidopsis* requires a capacity for redox regulation of the larger Rubisco activase isoform. *Proceedings of the National Academy of Sciences* **99**: 3330–3334.
- Zhang N, Schürmann P, Portis AR. 2001.** Characterization of the regulatory function of the 46-kDa isoform of Rubisco activase from *Arabidopsis*. *Photosynthesis Research* **68**: 29–37.

The following chapter was published as

Degen, G.E., Worrall, D. and Carmo-Silva, E. (2020) An isoleucine residue acts as a thermal and regulatory switch in wheat Rubisco activase. *Plant J.*, 103, 742–751.

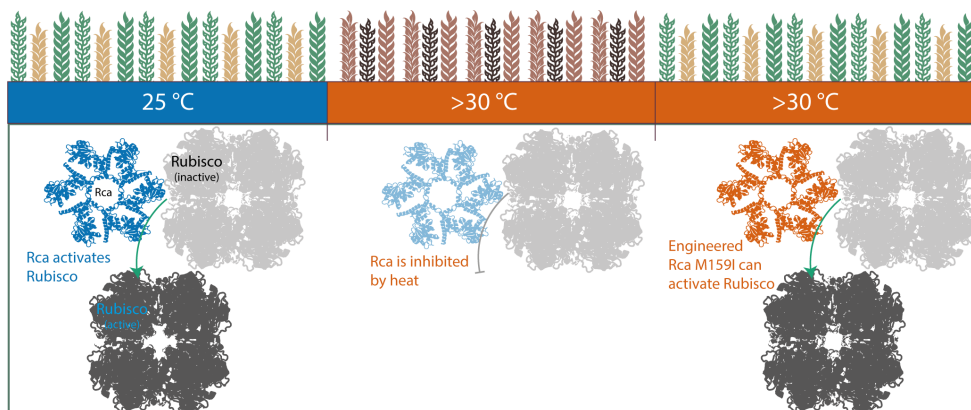
Author contributions: GED and ECS designed the research, GED performed the research with help from DW, ECS supervised the research, GED analysed the data, and GED and ECS wrote the article.

3. Chapter 3: An isoleucine residue acts as a thermal and regulatory switch in wheat Rubisco activase

Summary

Regulation of Rubisco, the gatekeeper of carbon fixation into the biosphere, by its molecular chaperone Rubisco activase (Rca) is essential for photosynthesis and plant growth. Using energy from ATP hydrolysis, Rca promotes the release of inhibitors and restores catalytic competence to Rubisco active sites. However, Rca is sensitive to moderate heat stress and becomes progressively inhibited as the temperature increases above the optimum for photosynthesis. Here, we identify a single amino acid substitution (M159I) that fundamentally alters the thermal and regulatory properties of Rca in bread wheat (*Triticum aestivum* L.). Using site-directed mutagenesis, we demonstrate that the M159I substitution extends the temperature optimum of the most abundant Rca isoform by 5°C *in vitro*, while maintaining the efficiency of Rubisco activation by Rca. The results suggest that this single amino acid substitution acts as a thermal and regulatory switch in wheat Rca that can be exploited to improve the climate resilience and efficiency of carbon assimilation of this cereal crop as temperatures become warmer and more volatile.

Graphical abstract



3.1 Introduction

Photosynthesis is the entry point of carbon into the biosphere. However, several processes of carbon fixation have been identified to operate below their theoretical maximum, limiting the efficiency of photosynthesis (Ort *et al.*, 2015). Therefore, strategies to optimise or redesign photosynthesis represent a promising opportunity to increase crop yields sustainably. Enhancing the efficiency of photosynthesis would lead to increased biomass production with equal or lower resource inputs, thereby helping to meet rising food demands from a growing world population and the shift to higher calorific diets (Asseng *et al.*, 2015), while minimising the negative impact of agriculture on the environment.

Wheat is one of the world's most important crops, providing over 20% of humanity's calories (Ray *et al.*, 2013) and in 2017 accounted for 15% of the global harvested agricultural area (FAOSTAT, 2019). Modern domesticated wheat is a temperate hexaploid cereal crop that emerged as a result of natural hybridization of three grasses (Mayer *et al.*, 2014). It grows optimally at 22°C and temperatures exceeding 25°C have been found to negatively impact wheat growth and productivity (Porter & Gawith, 1999). Decreased carbon assimilation has also been reported in wheat above this thermal threshold (Silva-Pérez *et al.*, 2017). Worryingly, climate resilience in European wheat has declined in recent years (Kahiluoto *et al.*, 2019) and climate change has already affected global wheat yields negatively (Asseng *et al.*, 2013; Ray *et al.*, 2019). Thus, efforts to increase wheat crop yields must be accompanied by improvements in yield stability during environmental oscillations (Pennacchi *et al.*, 2018).

Ribulose-1,5-bisphosphate carboxylase/oxygenase (Rubisco) plays a central role in carbon assimilation. Prior to the binding of ribulose-1,5-bisphosphate (RuBP) and subsequent reaction with the gaseous substrate, CO₂ or O₂, Rubisco catalytic sites must be carbamylated, via binding of non-substrate CO₂ and Mg²⁺ to form a stable carbamate (Lorimer and Miziorko, 1980). In addition, Rubisco activity *in vivo* is constrained by naturally occurring inhibitory phosphorylated compounds, including the substrate RuBP

when it binds to uncarbamylated active sites. A number of other sugar-phosphate derivatives have been described to inhibit Rubisco, including D-xylulose-1,5-bisphosphate (XuBP), a product of RuBP misprotonation that accumulates at elevated temperatures (Zhu & Jensen, 1991; Schrader *et al.*, 2006). To restore catalytic competence to Rubisco, inhibitory compounds must be removed from active sites by Rubisco activase (Rca). Rca is a member of the AAA+ protein family and uses energy from ATP hydrolysis to promote the release of such inhibitors (Salvucci *et al.*, 1985; Salvucci & Ogren, 1996). The activity of Rca is regulated by the redox status, the ADP:ATP ratio, and the Mg^{2+} concentration in the chloroplast (Robinson & Portis, 1989; Hazra *et al.*, 2015), thereby adjusting Rubisco activity to the prevailing irradiance level, e.g. during photosynthetic induction when leaves transition from low to high light (Taylor & Long, 2017). Post-translational modifications have also been shown to influence Rca activity and are likely to contribute to the regulation of carbon assimilation *in vivo* (Hartl *et al.*, 2017; Kim *et al.*, 2019).

The activity of Rubisco *in planta* declines as temperatures exceed the species-specific optimum temperature for plant growth (Carmo-Silva & Salvucci, 2012). For example, in the warm-adapted crop cotton, the activation state of Rubisco remains stable up to 35°C, while in the temperate crop wheat, Rubisco activation state decreases at temperatures above 30°C (Eckardt & Portis, 1997; Crafts-Brandner & Salvucci, 2000). *In vitro* experiments have shown that Rubisco itself is stable and remains active at temperatures up to 50°C (Crafts-Brandner & Salvucci, 2000). Conversely, Rca has been shown to be sensitive to elevated temperatures (Eckardt & Portis, 1997; Salvucci & Crafts-Brandner, 2004). In the warm-adapted species tobacco, Rca can hydrolyse ATP at temperatures up to 40°C, which is 20°C below Rubisco's denaturing temperature (Salvucci *et al.*, 2001). Hence, photosynthesis at high temperatures is not constrained by Rubisco itself, but by the inability of Rca to remove inhibitors and maintain Rubisco activity *in vivo*. It has been postulated that this thermolabile nature of Rca might act as a thermal fuse to limit carbon assimilation, and that tight-binding inhibitors might protect Rubisco from proteolysis during short periods at supra-optimal temperatures (Sage *et al.*, 2008), although this hypothesis remains to be tested.

Species from contrasting thermal environments have Rca isoforms with different thermal optima; i.e. Rca activated Rubisco best at 20°C in Antarctic hairgrass and 30°C in the desert dwelling creosote bush (Salvucci & Crafts-Brandner, 2004). In warm-adapted wild rice (*Oryza australiensis*), Rca has low catalytic activity but can promote Rubisco activation at warm temperatures when cultivated rice (*Oryza sativa*) Rca is largely inactive (Scafaro *et al.*, 2016). Importantly, maximum rates of ATP hydrolysis by the Rca isoforms present in these species were observed at temperatures 5-7°C higher than maximum rates of Rubisco activation by the same Rca isoforms (Salvucci & Crafts-Brandner, 2004; Scafaro *et al.*, 2016). This indicates that the two reactions catalysed by Rca, ATP hydrolysis and Rubisco activation, have different temperature profiles and both reactions must be taken into account to describe the temperature response of Rca activity.

Most plant species have two Rca isoforms, a shorter β isoform (~ 42 kDa) and a longer α isoform (~ 46 kDa), that are produced via alternative splicing of a single gene, while other species only have the short isoform or encode the long and short isoforms on separate genes (Nagarajan & Gill, 2018). In wheat, two genes encode three Rca isoforms: Rca1 β , Rca2 β and Rca2 α (Carmo-Silva *et al.*, 2015). Recently, Scafaro *et al.* (Scafaro *et al.*, 2019a) showed that Rca1 β was more thermostable by using differential scanning fluorimetry. In the same study, 11 amino acid residues that are present in Rca isoforms from warm-adapted species increased Rca thermostability by 7°C. However, the effect of the 11 amino acid residues on the temperature response of Rubisco activation by Rca was not tested and it remained unclear if all 11 residues were required for improved thermostability. In Arabidopsis, expression of thermostable Rca isoforms resulted in faster photosynthetic rates as well as increased plant biomass and seed yield during moderate heat stress (Kurek *et al.*, 2007; Kumar *et al.*, 2009), highlighting the importance and scope of increasing the temperature optimum of Rubisco activation by Rca to enhance plant resilience to global warming.

Wheat Rca isoforms have also been shown to differ in their response to increasing ADP:ATP ratios (Perdomo *et al.*, 2019; Scafaro *et al.*, 2019b), which are likely to change in wheat at high temperatures due to reduced

photosystem II efficiency and increased cyclic electron flow (Sharkey, 2005; Haque *et al.*, 2014). Combined, these observations suggest that Rca thermotolerance and ADP sensitivity might be co-regulated. Here, we identify a single isoleucine residue in the α/β -subdomain of Rca that increases the thermostability of Rubisco activation in wheat. Characterisation of the temperature response of both ATP hydrolysis and Rubisco activation for the three wheat Rca isoforms showed that Rca1 β was the most thermostable but was less efficient at activating Rubisco. Substitution of a methionine residue by an isoleucine in the wheat Rca2 β isoform (Rca2 β -M159I) improved the thermal optimum without affecting the efficiency of Rubisco activation.

3.2 Results

Identification of a residue putatively associated with the temperature optimum of Rca

The wheat Rca residue 159 (numbering of wheat Rca2 β lacking the chloroplast transit peptide) was identified as putatively associated with the temperature optimum of Rca (Figure 1). The Rca sequences from two warm-adapted rice species and the wheat Rca1 β isoform, which was recently shown to be more thermostable than the Rca2 β isoform (Scafaro *et al.*, 2019a), have an isoleucine at position 159, while the wheat Rca2 β contains a methionine at position 159 (Figure 1). This residue is located in the α/β subdomain of the Rca AAA+ module, between the Walker A and Walker B nucleotide binding motifs (Stotz *et al.*, 2011; Miller & Enemark, 2016).

To test the hypothesis that replacing the wheat Rca2 β methionine at position 159 by an isoleucine increases the temperature optimum of Rca activity, the single mutant Rca2 β -M159I was generated by site-directed mutagenesis. A double mutant of wheat Rca2 β with two residues changed to the corresponding amino acids in Rca1 β , including the residue change at position 159, was recently described (Rca2 β -M159I/K161N; (Perdomo *et al.*, 2019)). The mutation M159I was also present, while K161N was absent, in two recently characterized mutant proteins of wheat Rca containing 8- and 11-residue residue changes and characterized by enhanced thermal stability (Scafaro *et al.*, 2019a). These results suggest that the residue change M159I, rather than K161N, might be associated with the temperature optimum of Rca.

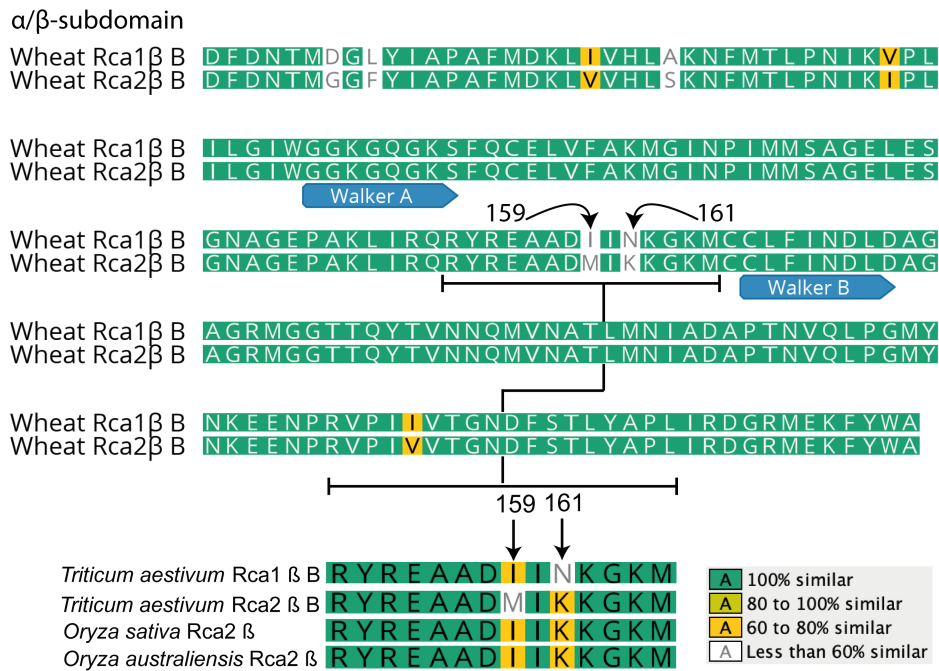


Figure 1. Selection of residues putatively involved in the temperature response of Rca. (Above) Amino acid sequence alignment of the α/β -subdomain of wheat Rca1 β and Rca2 β from the B genome (numbering according to wheat Rca2 β lacking the chloroplast transit peptide). The Walker A and Walker B motifs and two residues (159 and 161) differing between the two sequences are identified. (Below) Amino acid alignment of a short sequence within the α/β -subdomain of the two Rca isoforms from wheat and the Rca isoforms from two rice species that are adapted to warmer temperatures.

Wheat Rca2 β -M159I exhibits higher temperature optima of ATP hydrolysis and Rubisco activation

In order to verify that the residue change M159I is associated with the temperature optimum of Rca, the temperature response of ATP hydrolysis and Rubisco activation were determined for the Rca2 β -M159I single mutant and compared to the native wheat Rca isoforms and the double mutant Rca2 β -M159I/K161N (Figure 2). ATP hydrolysis peaked at lower temperatures for Rca2 β , intermediate for Rca2 β -M159I and Rca2 β -M159I/K161N, and higher temperatures for Rca1 β (Figure 2A), consistent with higher thermal stability of Rca1 β (Scafaro *et al.*, 2019a). Rca2 α hydrolysed ATP at slower rates (Figure S1A) but showed a similar temperature response profile to that of Rca2 β

at 20-40°C (Figure S1B). Maximum ATPase activity was highest for Rca1 β , Rca2 β -M159I had a maximum rate of ATP hydrolysis comparable to Rca2 β , and Rca2 β -M159I/K161N was intermediate to Rca2 β and Rca1 β (Table 1). The temperature at which Rca2 β -M159I and Rca2 β -M159I/K161N reached maximum rates of ATP hydrolysis (T_{\max}) was ca. 3°C higher than Rca2 β , but not as high as Rca1 β (Table 1).

The temperature optimum of ATPase activity of Rca2 β -M159I shifted towards higher temperatures compared to Rca2 β , with the mutant showing lower rates at temperatures up to 35°C and higher rates at 35-45°C (Figure 2A, Table S2). Shifts in temperature optimum are best visualised by considering the activity of each protein relative to the maximum activity (Figure 2B). Relative ATPase activities were not significantly different between Rca2 β -M159I and Rca2 β -M159I/K161N at temperatures between 20 and 37.5°C, however above 40°C Rca2 β -M159I presented significantly higher relative ATPase activity compared to Rca2 β -M159I/K161N (Figure 2B, Table S2). M159I also presented a shift towards a higher temperature optimum range (T_{opt}) and a higher temperature at which 50% of the maximum ATPase activity of remains ($T_{0.5}$) compared to Rca2 β -M159I/K161N (Table 1).

The rate of Rubisco activation by Rca2 β -M159I was intermediate to the slower Rca1 β and the faster Rca2 β at 20-25°C (Figure 2C, Table S3). The native wheat isoforms Rca2 β and Rca2 α activated Rubisco at comparable rates across the temperature range of 20-45°C (Figure S1C, Table S3), showing a similar temperature response profile (Figure S1D). The ER complex, consisting of uncarbamylated Rubisco bound to RuBP, is very stable at 20-25°C and remains inactive throughout the assay; however, as temperatures increase, RuBP spontaneously releases from Rubisco catalytic sites (Figure S2). The rate of Rca-dependent Rubisco reactivation was determined by the difference between the rates of Rubisco reactivation in presence and absence of Rca measured in parallel at each temperature (Figure S2A; Carmo-Silva and Salvucci, 2011) to account for the increase in spontaneous release of inhibitors from Rubisco active sites at high temperatures (Schrader et al., 2006). At 42.5-45°C, the rate of spontaneous Rubisco activation in assays

without Rca is significant and wheat Rca isoforms become unable to reactivate Rubisco, resulting in very low or even negative rates of Rubisco activation by Rca (Figure 2 and Figure S1).

Importantly, the temperature response of Rubisco activation by both Rca2 β -M159I and Rca2 β -M159I/K161N was characterised by a broader peak compared to the temperature response of Rca2 β , which peaked at 25.2°C (Figure 2D). The T_{opt} of Rubisco activation by Rca2 β -M159I and Rca2 β -M159I/K161N extended \sim 5°C above Rca2 β and \sim 5°C below Rca1 β (Table 1). The maximum rates of Rubisco activation by Rca2 β -M159I and Rca2 β -M159I/K161N were intermediate to the lower rates measured for Rca1 β and the higher rates measured for Rca2 α , and occurred at a temperature comparable to Rca2 β (Table 1). However, at 35°C Rca2 β -M159I had significantly higher relative Rubisco activation activity compared to Rca2 β (Figure 2D, Table S3), with a consequent increase in $T_{0.5}$ (Table 1).

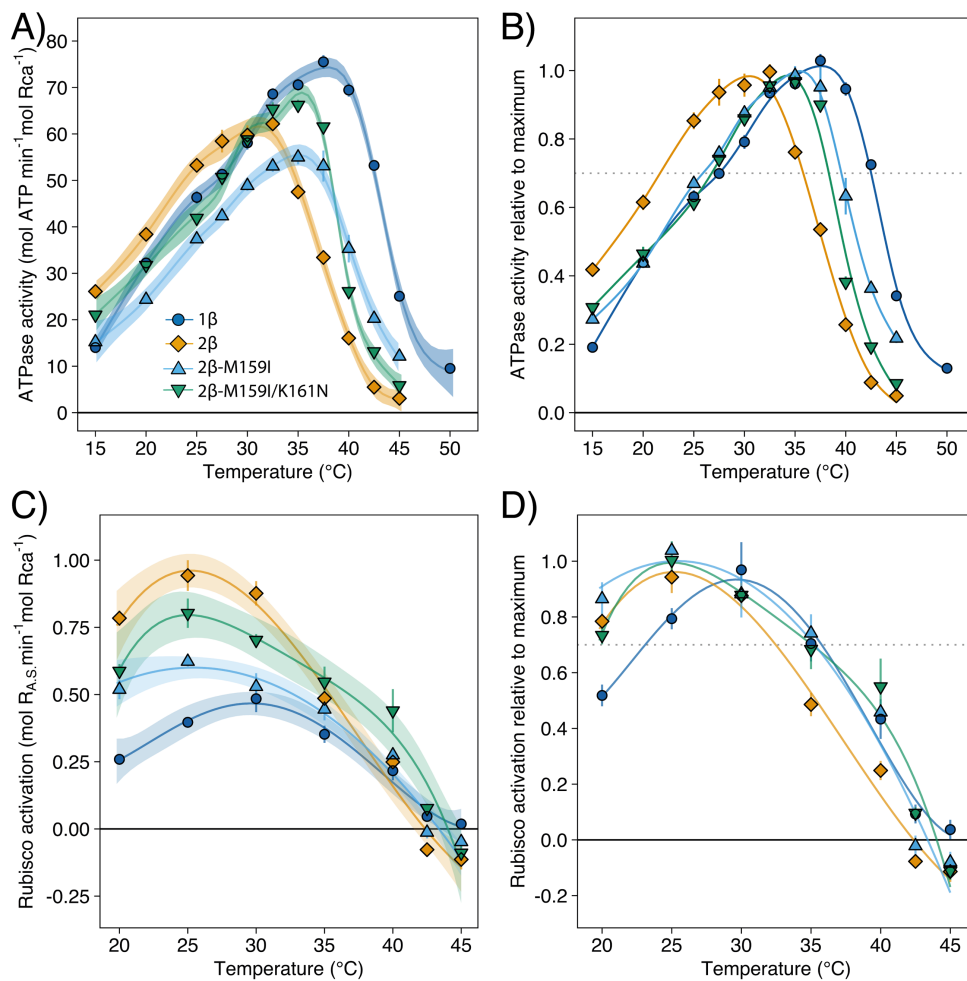


Figure 2. Temperature response of ATP hydrolysis and Rubisco activation by Rca. (A, C) Rates of ATP hydrolysis and Rubisco activation by wheat

Rca1 β (dark blue), Rca2 β (orange) and the mutant proteins Rca2 β -M159I (light blue) and Rca2 β -M159I/K161N (green). Assays were performed at the indicated temperatures using 2 μ M Rca monomer and 5 mM ATP. Activation of pre-inhibited Rubisco used 6 μ M Rubisco active sites (R_{A.S.}) in the ER form (1:3 Rca:R_{A.S.}). Values are means \pm standard error (n = 5-19 technical replicates in *A* and n = 3-15 technical replicates in *C*). Lines represent the best-fit for each enzyme (AIC, Table S1) and coloured areas denote the 95% confidence interval for each fit. (*B*, *D*) ATP hydrolysis and Rubisco activation relative to estimated maximum activities (Table 1).

Table 1. Temperature optimum of Rca activity. Maximum rate of ATP hydrolysis and Rubisco activation and corresponding temperature (T_{\max}), optimum temperature range (T_{opt} , above 70% activity) and temperature above the optimum at which 50% of the maximum activity remains ($T_{0.5}$) as estimated from the best-fit models applied to describe the temperature response of each Rca protein (Table S1).

Rca	Maximum ATPase activity			
	(mol ATP min ⁻¹ mol Rca ⁻¹)	T_{\max} (°C)	T_{opt} (°C)	$T_{0.5}$ (°C)
1 β	73.4 \pm 4.2	38.9 \pm 0.0	25-42.5	44.3 \pm 0.2
2 β	61.6 \pm 4.2	31.6 \pm 0.0	20-35	37.8 \pm 0.3
2 α	33.0 \pm 4.7	30.8 \pm 0.0	20-35	38.6 \pm 0.6
2β-M159I	55.5 \pm 4.6	35.0 \pm 0.0	25-40	41.0 \pm 0.4
2 β -M159I/K161N	68.4 \pm 3.9	35.3 \pm 0.0	20-37.5	39.5 \pm 0.1
Rca	Maximum Rubisco activation rate			
	(mol R _{A.S.} min ⁻¹ mol Rca ⁻¹)	T_{\max} (°C)	T_{opt} (°C)	$T_{0.5}$ (°C)
1 β	0.47 \pm 0.09	29.7 \pm 0.3	25-35	38.6 \pm 1.0
2 β	0.96 \pm 0.13	25.2 \pm 0.0	20-30	35.6 \pm 0.9
2 α	0.90 \pm 0.25	26.0 \pm 0.1	20-30	37.3 \pm 1.8
2β-M159I	0.60 \pm 0.08	25.4 \pm 2.2	20-35	37.9 \pm 0.9
2 β -M159I/K161N	0.80 \pm 0.18	25.0 \pm 1.2	20-35	39.2 \pm 1.8

M159I alters the regulatory properties of Rca

In addition to the increased temperature optimum of ATP hydrolysis and the broader temperature optimum of Rubisco activation, the residue substitution M159I also caused changes in the relative rates of Rca activity. To test the hypothesis that M159I might affect the regulation as well as the thermotolerance of Rca, the rates of ATP hydrolysis and Rubisco activation by Rca2 β -M159I were determined at 25°C in presence of increasing ratios of ADP:ATP. Rubisco activation by Rca2 β was previously shown to be insensitive to inhibition by ADP, in contrast to Rca1 β which shows inhibition of both ATP hydrolysis and Rubisco activation as the ADP:ATP ratio increases (Perdomo *et al.*, 2019). Rubisco activation by Rca2 β -M159I was inhibited to a greater extent than ATP hydrolysis in presence of increasing ADP:ATP ratios (Table 2), indicating that this amino acid substitution causes Rubisco activation by Rca to become more thermotolerant, but also more sensitive to inhibition by ADP.

The efficiency of Rubisco activation by Rca was estimated as the quantity of Rubisco active sites activated per quantity of ATP consumed, i.e. the rate of Rubisco activation divided by the rate of ATP hydrolysis for each enzyme at each temperature and nucleotide treatment. Rca1 β was the least efficient, especially as temperatures increased above 30°C (Figure 3A) and in presence of ADP (Figure 3B). Rca2 β -M159I and Rca2 β -M159I/K161N showed comparable efficiency to Rca2 β at 20-35°C (Figure 3A). The apparent increase in Rca efficiency at 40°C for Rca2 β and Rca2 β -M159I/K161N resulted from a more marked decrease in ATP hydrolysis than Rubisco activation activity at this temperature (Figure 2). The efficiency of Rca2 β also increased in presence of ADP (Figure 3B) due to the inhibition of ATP hydrolysis with no effect on Rubisco activation (Perdomo *et al.*, 2019). Rca2 β -M159I and Rca2 β -M159I/K161N maintained efficiency independent of ADP presence, because both ATP hydrolysis and Rubisco activation activities were inhibited (Rca2 β -M159I, Table 2) or very little affected (Rca2 β -M159I/K161N; (Perdomo *et al.*, 2019)) as ADP:ATP ratios increased. The response of Rca2 β -M159I to ADP contrasts with that observed for Rca2 β and

shows that the single mutation significantly affects both the regulatory properties and the temperature optimum of Rubisco activation by Rca.

Table 2. ADP sensitivity of Rca2 β -M159I. The rate of ATP hydrolysis and Rubisco activation by Rca was measured at 25°C with 2 μ M Rca monomer and (for Rubisco activation) 6 μ M Rubisco active sites (R_{A.S.}) (i.e., 1:3 Rca:R_{A.S.}). Adenine nucleotide concentration was maintained at 5mM. The 0.00 ADP:ATP control (v_c , 5 mM ATP and 0 ADP:ATP) contained ATP regeneration system, but this was absent in assays with 0.11 or 0.33 ADP:ATP (v_i). Values are means \pm standard error (n = 3 technical replicates) of rates normalised to the 0.00 ADP:ATP control. Different letters denote significant differences (Tukey HSD, $P < 0.05$).

ADP:ATP	ATP hydrolysis (v_i/v_c)	Rubisco activation (v_i/v_c)
0.00	1.00 \pm 0.007 a	1.00 \pm 0.010 a
0.11	0.83 \pm 0.029 b	0.62 \pm 0.048 b
0.33	0.71 \pm 0.019 c	0.53 \pm 0.004 b

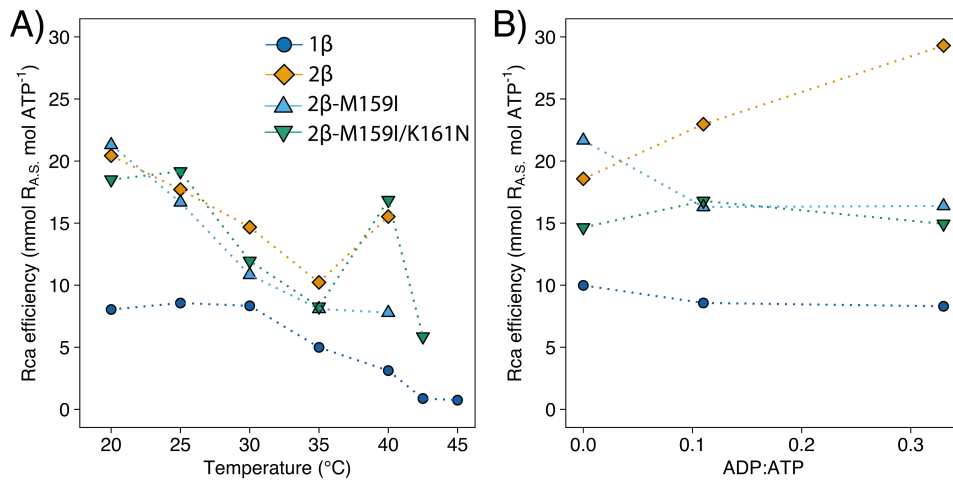


Figure 3. The efficiency of Rubisco activation by Rca. The efficiency of Rubisco activation by wheat Rca1 β (dark blue), Rca2 β (orange) and the mutant proteins Rca2 β -M159I (light blue) and Rca2 β -M159I/K161N (green). Rca efficiency was estimated by dividing the rate of Rubisco activation by the rate of ATP hydrolysis for each Rca isoform at each temperature (A; data from Figure 2) and ADP:ATP ratio (B; data for M159I from Table 2, for other Rca isoforms see (Perdomo *et al.*, 2019)).

3.3 Discussion

A single amino acid residue substitution in the wheat Rca2 β isoform (M159I) extended the temperature optimum while maintaining the efficiency of Rubisco activation by Rca. A previous study (Kurek *et al.*, 2007) showed an increase in the rate of ATP hydrolysis by Arabidopsis Rca at elevated temperature in a mutant protein with one single residue substitution. However, to the best of our knowledge, this is the first report of a specific amino acid residue in Rca that increases the thermostability of Rubisco activation specifically. Importantly, this residue substitution also altered the regulatory properties of Rca while resulting in a more efficient activation of Rubisco compared to the naturally occurring thermostable wheat Rca1 β .

Of the three native wheat isoforms, Rca1 β activated Rubisco at slower rates but exhibited high ATPase and Rubisco activation activities at higher temperatures compared to Rca2 β and Rca2 α . These results confirm and expand a recent observation that Rca1 β is more thermostable, obtained by incubating Rca at high temperatures and measuring at 25°C, and by inferring thermal midpoints from differential scanning fluorimetry (Scafaro *et al.*, 2019a). The higher temperature optimum of ATPase activity compared to Rubisco activation activity observed for all isoforms (Figure 2) suggests that the Rca-Rubisco interaction itself is sensitive to temperature and demonstrates that both Rca activities must be considered when assessing thermostability.

Wheat Rca1 β and the Rca isoforms in cultivated rice and in a wild rice species adapted to warm environments for which Rca has been characterised as thermotolerant contain an isoleucine residue at position 159, while a methionine is present in wheat Rca2 β (Figure 1). The two Rca genes in monocots are organised in tandem and are likely a result of a gene duplication (Nagarajan & Gill, 2018). Unlike wheat and other monocots, the *Rca1* gene in rice is not functional due to multiple deletions (Nagarajan & Gill, 2018), and only the products of *Rca2* expression are present. The presence of an isoleucine at position 159 in rice Rca2 (Scafaro *et al.*, 2016), may reflect an

adaptation to warm environments. A switch from methionine to isoleucine would occur when the third base in the methionine-coding ATG codon mutates to any of A, C or T, suggesting that this residue switch could occur relatively frequently. Thus, it could be speculated that the ancestral Rca of monocots contained a methionine residue at this position, since the reverse switch would be far less likely.

Two mutant wheat Rca2 β proteins containing 8 and 11 residues substitutions to amino acids found in warm-adapted species, including the mutation M159I, showed 5-7°C increases in thermostability (Scafaro *et al.*, 2019a). It is likely that some of the other amino acid changes may have contributed to increased Rca thermostability. However, the results presented here show that the single isoleucine residue substitution at position 159 likely contributed the majority of the thermostability increase observed in the more complex mutants. The increased thermostability in Rca2 β -M159I might result from increased hydrophobicity, since this amino acid change results in an increase of the hydropathy index (Kyte & Doolittle, 1982) from 1.9 to 4.5. Increased thermostability in response to a residue substitution causing increased hydrophobicity has previously been observed in the CutA1 protein from *E. coli* (Matsuura *et al.*, 2010; 2015).

In wheat, photosynthesis and Rubisco activation start to decline at leaf temperatures above 30°C (Feller *et al.*, 1998; Perdomo *et al.*, 2017). While gene expression of Rca1 β has recently been shown to increase with temperature (Scafaro *et al.*, 2019a), the rate of Rubisco activation by Rca1 β is considerably slower than by Rca2 β (Figure 2), suggesting that the amount of active Rca at high temperature would be insufficient to maintain Rubisco activity. Furthermore, Rca1 β is less efficient than Rca2 β due to its high ATPase activity (Figure 3), meaning that this isoform hydrolyzes ATP at high rates at elevated temperatures. Rca2 β -M159I on the other hand was much more efficient than Rca1 β , even at elevated temperatures (Figure 3), and less sensitive to ADP inhibition than Rca1 β (Table 2, (Perdomo *et al.*, 2019)). However, ADP inhibition may not constitute a bottle neck, since cyclic electron transport has been shown to increase at elevated temperatures

(Havaux *et al.*, 1991; Bukhov *et al.*, 1999; Bukhov & Carpentier, 2000). Measuring cyclic electron flow in plants expressing a genetically engineered Rca2 β -M159I would enable investigating changes in ATP demand as the temperature increases.

The redox-sensitive isoform Rca2 α exhibited considerably lower ATPase activity but comparable Rubisco activation activity to Rca2 β (Figure S1), suggesting that the C-terminal extension reduces ATP hydrolysis specifically, making Rca2 α more efficient (less ATP consumed per Rubisco activated). The difference in ATPase activity between Rca2 α and Rca2 β was greater in rice (Scafaro *et al.*, 2016), which might be associated with the presence of a glutamic acid (E) at the C-terminal extension position 392. Substitution of this glutamic acid in the rice Rca2 α by an alanine (which is present in wheat Rca2 α , Figure S3) to produce a mutant E392A increased ATPase activity by ca. 30% (Portis *et al.*, 2008), indicating that this residue may influence Rca2 α efficiency.

In addition to broadening the thermal optimum of Rubisco activation by 5°C, Rca2 β -M159I activated Rubisco at lower rates at 20-30°C and showed increased sensitivity of Rubisco activation to inhibition by ADP compared to Rca2 β (Table 2, (Perdomo *et al.*, 2019)). Recently, a single lysine residue in the C-terminal extension of Rca was also shown to decrease ADP sensitivity (Scafaro *et al.*, 2019b). Importantly, the double mutant Rca2 β -M159I/K161N was much less inhibited by ADP than Rca2 β -M159I, suggesting that the residue substitution K161N counteracts the ADP sensitivity induced by M159I. The efficiency of Rubisco activation by both Rca2 β -M159I and Rca2 β -M159I/K161N was unaffected in the presence of ADP, as both ATP hydrolysis and Rubisco activation were similarly affected.

In summary, we show that a single isoleucine residue substitution significantly alters the function of wheat Rca, a key regulator of Rubisco activity and carbon assimilation. Rca2 β -M159I showed a broadened temperature optimum compared to the native wheat Rca2 β , while maintaining a rate of Rubisco activation that is higher, less inhibited by ADP, and much more efficient than the thermostable native wheat Rca1 β . The findings suggest that the isoleucine residue at position 159 of Rca acts as a thermal and

regulatory switch that can be exploited to improve the efficiency and climate resilience of wheat carbon fixation.

3.4 Material and Methods

Protein sequences

Rubisco activase (Rca) protein sequences from *Triticum aestivum* (wheat) (Carmo-Silva *et al.*, 2015), *Oryza australiensis* and *Oryza sativa* (Feller *et al.*, 1998; Crafts-Brandner & Salvucci, 2000; Salvucci & Crafts-Brandner, 2004; Jurczyk *et al.*, 2015; 2016; Scafaro *et al.*, 2016) were aligned using Geneious 9.1.8 and edited with Adobe Illustrator 22.0. The MUSCLE algorithm (Edgar, 2004) was used and colour coding represents similarity (Henikoff & Henikoff, 1992). Sequence data for wheat Rca can be found in the GenBank data library under accession numbers LM992844 (Rca1 β), LM992846 (Rca2 β) and LM992845 (Rca2 α), corresponding to EnsemblPlants gene numbers TraesCS4B02G140200 (Rca1) and TraesCS4B02G140300 (Rca2).

Site-directed mutagenesis

Site-directed mutagenesis (SDM) was performed using the QuickChange Lightning Multi Site-Directed Mutagenesis Kit (Agilent Technologies) according to the manual (<https://www.agilent.com/cs/library/usermanuals/public/210513.pdf>). Primers were designed based on the coding sequence of Rca2 β from the B genome of wheat using the QuickChange Primer Design website (<https://www.agilent.com/store/primerDesignProgram.jsp>). The Rca2 β coding sequence was ligated into the pET-23(+) vector and used as a template to create the double mutant Rca2 β -M159I/K161N as described previously (Perdomo *et al.*, 2019) and the single mutant Rca2 β -M159I using the primer 5'-ACCGTGAGGCTGCAGACATA**A**ATCAAGAAGGGTAAG-3' (the base change is highlighted in bold). After validation by sequencing of the Rca coding region, the plasmid was cloned into BL21(DE3)pLysS cells for protein expression.

Purification of enzymes

Rubisco activase (Rca) enzymes were expressed in *E. coli* and purified as described by Barta *et al.* (Barta *et al.*, 2011a), with the following modifications. The frozen cell pellets from 10 L cultures were lysed and thawed by

suspending the pellet in 130 mL of cell extraction buffer (50 mM HEPES-KOH pH 7.0, 5 mM MgCl₂, 1 mM EDTA, 0.1% (w/v) Triton X-100, 2 mM ATP, 5 mM DTT, 20 mM ascorbate, 1 mM PMSF, and 10 μM leupeptin) for 30 min on ice. After adding ammonium sulphate to 37.5%, collecting the precipitated material and suspending in 10 mL of cell extraction buffer, the solution was centrifuged at 200,000 × g for 30 min in a Beckman centrifuge (Beckman Coulter) using a swinging bucket ultracentrifuge rotor SW 31 Ti. Rubisco was purified from wheat leaves according to Orr & Carmo-Silva (Orr & Carmo-Silva, 2018). Wheat (*Triticum aestivum* cultivar Cadenza) was grown in a glasshouse at ~22°C and a photosynthetic photon flux density of ~500 μmol m⁻² s⁻¹ (16h day, 8h night) for two weeks. Leaf material was flash frozen in liquid nitrogen and stored at -80°C until purification. Protein concentration was determined by the Bradford method (Bradford, 1976). Polypeptides present in the Rca and Rubisco preparations were separated by SDS-PAGE on 12% gels (Bio-Rad) and visualised by staining with Coomassie Blue (Figure S4). Molecular weight of proteins was calculated from the respective amino acid sequence using The Sequence Manipulation Suite (Stothard, 2000) at https://www.bioinformatics.org/sms/prot_mw.html. Two independent preparations of four of the recombinant Rca proteins showed no significant differences in ATPase activity (Figure S5, Table S4). Consequently, only one purification was used for the single mutant Rca2β-M159I and only one preparation per Rca was used for the Rubisco reactivation assays.

Rubisco activase activity: ATP hydrolysis

The rate of ATP hydrolysis by Rca isoforms was assayed using the method of Chifflet *et al.* (Chifflet *et al.*, 1988) with the following modifications. ATP hydrolysis was measured at a range of temperatures (15-50°C) over 5 min in an assay mix (50 μL) containing 100 mM Tricine-NaOH pH 8.0, 10 mM MgCl₂, 10 mM NaHCO₃, and 5 mM ATP. The reaction was initiated by adding Rca (final concentration = 2 μM Rca monomer) and quenched after 5 min by adding 12% SDS. Blanks were prepared by adding SDS to the reaction tube before adding Rca. Phosphate standards for a calibration curve were prepared by adding 0, 2.5, 5, 10, 15, 20, 32.5 and 50 mM KPi (final

concentrations) to the reaction mixture described above (in the absence of Rca). Tubes containing the assay mix were incubated in a temperature block (Torrey Pines Scientific, Echotherm) until the desired temperature was reached before initiating the assay (typically 3 min). The temperature of 50 μ L H₂O incubated alongside the reaction tubes was monitored using a thermocouple (Omega Thermometer RDXL4SD, Omega Engineering). After the addition of SDS, all reactions and standards were kept in the fridge until Pi determination in a spectrophotometer (BMG Labtech) as detailed in (Perdomo *et al.*, 2019).

Rubisco activase activity: Rubisco reactivation

The rate of Rubisco reactivation by Rca was measured as described by Barta *et al.* (Barta *et al.*, 2011b) and Perdomo *et al.* (Perdomo *et al.*, 2019). To prepare inhibited Rubisco complexes (ER), purified Rubisco was first incubated in activation mix (500 mM Bicine-NaOH pH 8.0, 300 mM MgCl₂*6 H₂O, 100 mM NaHCO₃) for 1h at 4 °C, followed by spin desalting, protein concentration determination, and incubation of uncarbamyated enzyme with 4 mM RuBP at 4 °C overnight. The assay for Rubisco activation consisted of two stages (Barta *et al.*, 2011b). In the first stage, Rubisco (ER) was reactivated by Rca at a range of temperatures (20-45 °C), and in the second stage, aliquots were taken from the first stage assay to measure Rubisco activity at 30°C by the incorporation of ¹⁴CO₂ into acid-stable compounds. Temperature of Rubisco activation was controlled as described above for the ATP hydrolysis assay. First stage assays (90 μ L final volume) contained 50 mM Tricine-NaOH pH 8.0, 10 mM MgCl₂, 10 mM NaHCO₃, 2 mM DTT, 5 mM ATP, an ATP regenerating system consisting of 40 U mL⁻¹ phosphocreatine kinase, 4 mM phosphocreatine, 5 % (w/v) PEG-3350, 6 μ M Rubisco active sites (ER), 2 μ M Rca monomer, 5 mM ATP plus an ATP regenerating system, and 6 mM RuBP. Three variants of assays were performed for determination of: fully activated Rubisco activity (ECM, this contained no RuBP in the first stage assay), Rca-dependent Rubisco activation (contained all components) and the spontaneous activation of ER (contained no Rca, negative control).

Second-stage assays to assess Rubisco activity in aliquots taken at time intervals from the first stage assays (Figure S2A) contained 100 mM Tricine-NaOH pH 8.0, 10 mM MgCl₂, 10 mM NaH¹⁴CO₃ (0.5 Ci mol⁻¹) and 0.4 mM RuBP. The rate of Rubisco activation (fraction of Rubisco sites activated per minute) in the Rca and ER reactions was calculated from the difference in Rubisco activity measured 1.5 and 0.5 min after starting the first stage assay, taking into account the activity of fully activated Rubisco (Carmo-Silva & Salvucci, 2011). The rate of Rubisco activation by Rca was calculated as the difference between the rate of increase in Rubisco activity measured at each temperature in presence and absence of Rca (Rca reaction minus spontaneous activation in the ER reaction; Figure S2), and corrected for the concentrations of Rubisco active sites and Rca in the assay.

Data analysis and modelling

Data was processed using R 3.5.1 and RStudio 1.1.463, and graphs were prepared using the ggplot2 package (Wickham, 2017). Outliers were detected using the ggstatsplot package using Tukey's fences method, where outliers are defined as extreme values that are 1.5 times the inter-quartile range (1.5 IQR) below the 1st quartile or 1.5 IQR above the 3rd quartile. To estimate maximum ATP hydrolysis and Rubisco activation activities and the corresponding temperatures at which the maximum values are attained, as well as the temperature above the peak at which half of the activity remains ($T_{0.5}$), 2nd – 4th order polynomials and generalised additive models (GAM) were fitted to the experimental data using the gam function from the mgcv 1.8-24 R package (Wood, 2017). The model that best fit the experimental data was selected based on the Akaike information criterion (Akaike, 1974) using the AIC function (Table S1). The *predict* function was used to estimate maximum activity values and corresponding temperatures for each Rca isoform (T_{\max}), and the *approx.* function was used to estimate the optimum temperature range (T_{opt} , above 70% activity) and the temperature above the peak at which 50% of activity remains ($T_{0.5}$). The standard error calculated for each model was used to predict 95% confidence intervals for each fit (dashed lines in the graphs). One-way ANOVA followed by Tukey posthoc tests were

used to test the significance of differences between Rca isoforms at each temperature and nucleotide treatment (Tables S2-S4).

3.5 References

- Akaike H. 1974.** A new look at the statistical model identification. *IEEE Transactions on Automatic Control* **19**: 716–723.
- Asseng S, Ewert F, Martre P, Rotter RP, Lobell DB, Cammarano D, Kimball BA, Ottman MJ, Wall GW, White JW, et al. 2015.** Rising temperatures reduce global wheat production. *Nature Climate Change* **5**: 143–147.
- Asseng S, Ewert F, Rosenzweig C, Jones JW, Hatfield JL, Ruane AC, Boote KJ, Thorburn PJ, Rotter RP, Cammarano D, et al. 2013.** Uncertainty in simulating wheat yields under climate change. *Nature Climate Change* **3**: 827–832.
- Barta C, Carmo-Silva E, Salvucci ME. 2011a.** Purification of Rubisco activase from leaves or after expression in *Escherichia coli*. *Methods in molecular biology* **684**: 363–374.
- Barta C, Carmo-Silva E, Salvucci ME. 2011b.** Rubisco activase activity assays. *Methods in molecular biology* **684**: 375–382.
- Bradford MM. 1976.** A rapid and sensitive method for the quantitation of microgram quantities of protein utilizing the principle of protein-dye binding. *Analytical biochemistry* **72**: 248–254.
- Bukhov NG, Carpentier R. 2000.** Heterogeneity of photosystem II reaction centers as influenced by heat treatment of barley leaves. *Physiologia Plantarum* **110**: 279–285.
- Bukhov NG, Wiese C, Neimanis S, Heber U. 1999.** Heat sensitivity of chloroplasts and leaves: Leakage of protons from thylakoids and reversible activation of cyclic electron transport. *Photosynthesis Research* **59**: 81–93.
- Carmo-Silva E, Salvucci ME. 2011.** The activity of Rubisco's molecular chaperone, Rubisco activase, in leaf extracts. *Photosynthesis Research* **108**: 143–155.
- Carmo-Silva E, Salvucci ME. 2012.** The temperature response of CO₂ assimilation, photochemical activities and Rubisco activation in *Camelina sativa*, a potential bioenergy crop with limited capacity for acclimation to heat stress. *Planta* **236**: 1433–1445.
- Carmo-Silva E, Scales JC, Madgwick PJ, Parry MAJ. 2015.** Optimizing Rubisco and its regulation for greater resource use efficiency. *Plant, Cell & Environment* **38**: 1817–1832.
- Chifflet S, Torriglia A, Chiesa R, Tolosa S. 1988.** A method for the determination of inorganic phosphate in the presence of labile organic phosphate and high concentrations of protein: application to lens ATPases. *Analytical biochemistry* **168**: 1–4.

- Crafts-Brandner SJ, Salvucci ME. 2000.** Rubisco activase constrains the photosynthetic potential of leaves at high temperature and CO₂. *Proceedings of the National Academy of Sciences* **97**: 13430–13435.
- Eckardt NA, Portis AR Jr. 1997.** Heat denaturation profiles of Ribulose-1,5-Bisphosphate Carboxylase/Oxygenase (Rubisco) and Rubisco activase and the inability of Rubisco activase to restore activity of heat-denatured Rubisco. **113**: 243–248.
- Edgar RC. 2004.** MUSCLE: multiple sequence alignment with high accuracy and high throughput. *Nucleic Acids Research* **32**: 1792–1797.
- FAOSTAT. 2019.** *Crop Statistics*.
- Feller U, Crafts-Brandner S, Salvucci M. 1998.** Moderately high temperatures inhibit Ribulose-1,5-Bisphosphate Carboxylase/Oxygenase (Rubisco) activase-mediated activation of Rubisco. *Plant Physiology* **116**: 539–546.
- Haque MS, Kjaer KH, Rosenqvist E, Sharma DK, Ottosen C-O. 2014.** Heat stress and recovery of photosystem II efficiency in wheat (*Triticum aestivum* L.) cultivars acclimated to different growth temperatures. *Environmental and Experimental Botany* **99**: 1–8.
- Havaux M, Greppin H, Strasser RJ. 1991.** Functioning of photosystems I and II in pea leaves exposed to heat stress in the presence or absence of light: Analysis using in-vivo fluorescence, absorbance, oxygen and photoacoustic measurements. *Planta* **186**: 88–98.
- Hazra S, Henderson JN, Liles K, Hilton MT, Wachter RM. 2015.** Regulation of ribulose-1,5-bisphosphate carboxylase/oxygenase (rubisco) activase: product inhibition, cooperativity, and magnesium activation. *The Journal of Biological Chemistry* **290**: 24222–24236.
- Henikoff S, Henikoff JG. 1992.** Amino acid substitution matrices from protein blocks. *Proceedings of the National Academy of Sciences* **89**: 10915–10919.
- Jurczyk B, Hura K, Trzemecka A, Rapacz M. 2015.** Evidence for alternative splicing mechanisms in meadow fescue (*Festuca pratensis*) and perennial ryegrass (*Lolium perenne*) Rubisco activase gene. *Journal of Plant Physiology* **176**: 61–64.
- Jurczyk B, Pocięcha E, Grzesiak M, Kalita K, Rapacz M. 2016.** Enhanced expression of Rubisco activase splicing variants differentially affects Rubisco activity during low temperature treatment in *Lolium perenne*. *Journal of Plant Physiology* **198**: 49–55.
- Kahiluoto H, Kaseva J, Balek J, Olesen JE, Ruiz-Ramos M, Gobin A, Kersebaum KC, Takáč J, Ruget F, Ferrise R, et al. 2019.** Decline in climate resilience of European wheat. *Proceedings of the National Academy of Sciences* **116**: 123–128.

- Kurek I, Chang TK, Bertain SM, Madrigal A, Liu L, Lassner MW, Zhu G. 2007. Enhanced thermostability of Arabidopsis Rubisco activase improves photosynthesis and growth rates under moderate heat stress. *The Plant Cell* **19**: 3230–3241.
- Kyte J, Doolittle R. 1982. A simple method for displaying the hydropathic character of a protein. *Journal of Molecular Biology* **157**: 105–132.
- Matsuura Y, Ota M, Tanaka T, Takehira M, Ogasahara K, Bagautdinov B, Kunishima N, Yutani K. 2010. Remarkable improvement in the heat stability of CutA1 from *Escherichia coli* by rational protein design. *Journal of Biochemistry* **148**: 449–458.
- Matsuura Y, Takehira M, Joti Y, Ogasahara K, Tanaka T, Ono N, Kunishima N, Yutani K. 2015. Thermodynamics of protein denaturation at temperatures over 100 °C: CutA1 mutant proteins substituted with hydrophobic and charged residues. *Scientific reports* **5**: 15545.
- Mayer KFX, Rogers J, Dole el J, Pozniak C, Eversole K, Feuillet C, Gill B, Friebe B, Lukaszewski AJ, Sourdille P, *et al.* 2014. A chromosome-based draft sequence of the hexaploid bread wheat (*Triticum aestivum*) genome. *Science* **345**: 1251788–1251788.
- Miller JM, Enemark EJ. 2016. Fundamental characteristics of AAA+ protein family structure and function. *Archaea* **2016**: 9294307–9294312.
- Nagarajan R, Gill KS. 2018. Evolution of Rubisco activase gene in plants. *Plant Molecular Biology* **96**: 69–87.
- Orr DJ, Carmo-Silva E. 2018. Extraction of Rubisco to determine catalytic constants. Covshoff S ed. *Photosynthesis: Methods and Protocols*. Springer Protocols, 229–238.
- Ort DR, Merchant SS, Alric J, Barkan A, Blankenship RE, Bock R, Croce R, Hanson MR, Hibberd JM, Long SP, *et al.* 2015. Redesigning photosynthesis to sustainably meet global food and bioenergy demand. *Proceedings of the National Academy of Sciences* **112**: 8529–8536.
- Pennacchi JP, Silva EC, Andralojc PJ, Lawson T, Allen AM, Raines CA, Parry MAJ. 2018. Stability of wheat grain yields over three field seasons in the UK. *Food and Energy Security* **24**: e00147.
- Perdomo JA, Capó-Bauçà S, Carmo-Silva E, Galmés J. 2017. Rubisco and Rubisco activase play an important role in the biochemical limitations of photosynthesis in rice, wheat, and maize under high temperature and water deficit. *Frontiers in Plant Science* **8**: 490.
- Perdomo JA, Degen GE, Worrall D, Carmo-Silva E. 2019. Rubisco activation by wheat Rubisco activase isoform 2 β is insensitive to inhibition by ADP. *Biochemical Journal* **476**: 2595–2606.

- Porter JR, Gawith M. 1999.** Temperatures and the growth and development of wheat: a review. *European Journal of Agronomy* **10**: 23–36.
- Portis AR, Li C, Wang D, Salvucci ME. 2008.** Regulation of Rubisco activase and its interaction with Rubisco. *Journal of Experimental Botany* **59**: 1597–1604.
- Ray DK, Mueller ND, West PC, Foley JA. 2013.** Yield trends are insufficient to double global crop production by 2050. *PLoS ONE* **8**: e66428.
- Ray DK, West PC, Clark M, Gerber JS, Prishchepov AV, Chatterjee S. 2019.** Climate change has likely already affected global food production (YH Jung, Ed.). *PLoS ONE* **14**: e0217148.
- Robinson SP, Portis AR. 1989.** Ribulose-1,5-bisphosphate carboxylase/oxygenase activase protein prevents the *in vitro* decline in activity of ribulose-1,5-bisphosphate carboxylase/oxygenase. *Plant Physiology* **90**: 968–971.
- Sage RF, Way DA, Kubien DS. 2008.** Rubisco, Rubisco activase, and global climate change. *Journal of Experimental Botany* **59**: 1581–1595.
- Salvucci ME, Crafts-Brandner SJ. 2004.** Relationship between the heat tolerance of photosynthesis and the thermal stability of Rubisco activase in plants from contrasting thermal environments. *Plant Physiology* **134**: 1460–1470.
- Salvucci ME, Ogren WL. 1996.** The mechanism of Rubisco activase: Insights from studies of the properties and structure of the enzyme. *Photosynthesis Research* **47**: 1–11.
- Salvucci ME, Osteryoung KW, Crafts-Brandner SJ, Vierling E. 2001.** Exceptional sensitivity of Rubisco activase to thermal denaturation *in vitro* and *in vivo*. *Plant Physiology* **127**: 1053–1064.
- Salvucci ME, Portis AR, Ogren WL. 1985.** A soluble chloroplast protein catalyzes ribulosebisphosphate carboxylase/oxygenase activation *in vivo*. *Photosynthesis Research* **7**: 193–201.
- Scafaro AP, Bautsoens N, Boer den B, Van Rie J, Gallé A. 2019a.** A Conserved sequence from heat-adapted species improves Rubisco activase thermostability in wheat. *Plant Physiology* **181**: 43–54.
- Scafaro AP, De Vleeschauwer D, Bautsoens N, Hannah MA, Boer den B, Gallé A, Van Rie J. 2019b.** A single point mutation in the C-terminal extension of wheat Rubisco activase dramatically reduces ADP inhibition via enhanced ATP binding affinity. *The Journal of Biological Chemistry* **294**: 17931–17940.
- Scafaro AP, Gallé A, Van Rie J, Carmo-Silva E, Salvucci ME, Atwell BJ. 2016.** Heat tolerance in a wild *Oryza* species is attributed to maintenance of

- Rubisco activation by a thermally stable Rubisco activase ortholog. *New Phytologist* **211**: 899–911.
- Schrader SM, Kane HJ, Sharkey TD, Caemmerer von S. 2006.** High temperature enhances inhibitor production but reduces fallover in tobacco Rubisco. *Functional Plant Biology* **33**: 921–929.
- Sharkey TD. 2005.** Effects of moderate heat stress on photosynthesis: importance of thylakoid reactions, rubisco deactivation, reactive oxygen species, and thermotolerance provided by isoprene. *Plant, Cell & Environment* **28**: 269–277.
- Silva-Pérez V, Furbank RT, Condon AG, Evans JR. 2017.** Biochemical model of C3 photosynthesis applied to wheat at different temperatures. *Plant, Cell & Environment* **40**: 1552–1564.
- Stothard P. 2000.** The sequence manipulation suite: JavaScript programs for analyzing and formatting protein and DNA sequences. *BioTechniques* **28**: 1102–1104.
- Stotz M, Mueller-Cajar O, Ciniawsky S, Wendler P, Hartl FU, Bracher A, Hayer-Hartl M. 2011.** Structure of green-type Rubisco activase from tobacco. *Nature Structural & Molecular Biology* **18**: 1366–U78.
- Taylor SH, Long SP. 2017.** Slow induction of photosynthesis on shade to sun transitions in wheat may cost at least 21% of productivity. *Philosophical Transactions of the Royal Society B: Biological Sciences* **372**: 20160543.
- Wickham H. 2017.** *tidyverse: Easily install and load ‘Tidyverse’ packages.*
- Wood SN. 2017.** *Generalized Additive Models: An Introduction with R.* Chapman and Hall/CRC.
- Zhu G, Jensen RG. 1991.** Xylulose 1,5-Bisphosphate Synthesized by Ribulose 1,5-Bisphosphate Carboxylase/Oxygenase during Catalysis Binds to Decarbamylated Enzyme. *Plant Physiology* **97**: 1348–1353.

3.6 Supplementary information

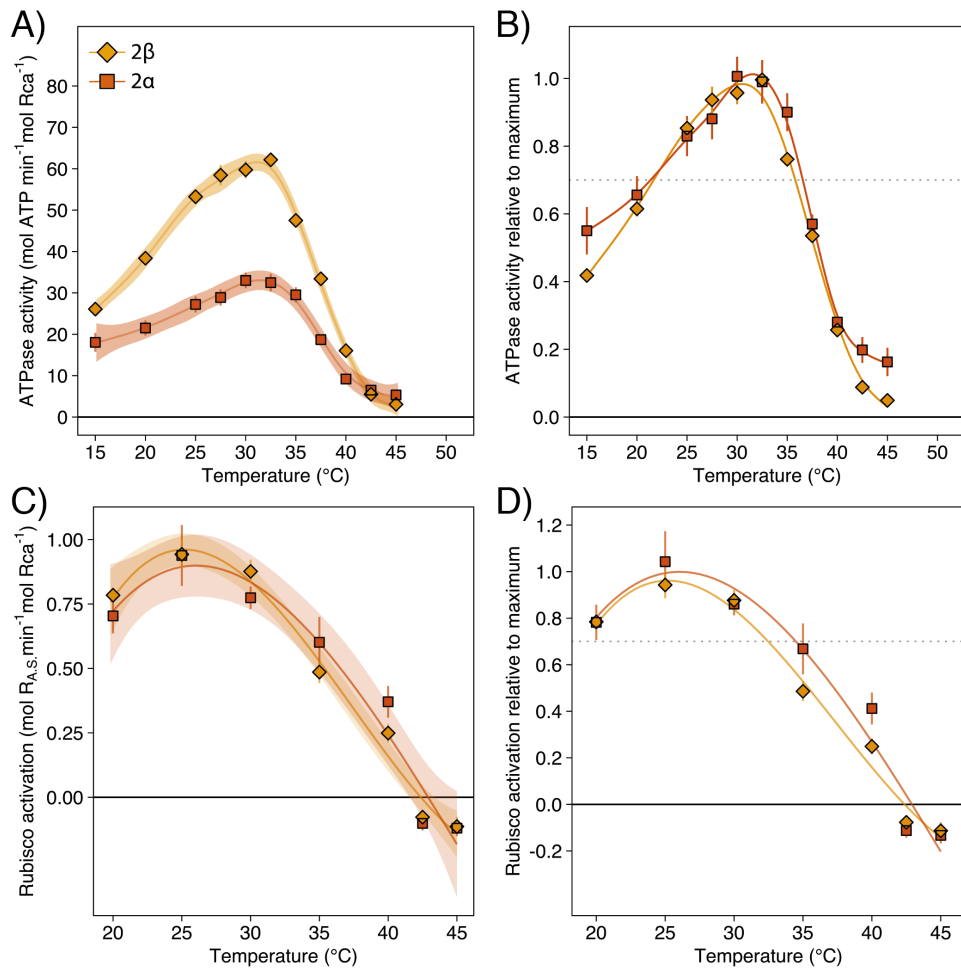


Figure S1. Temperature response of ATP hydrolysis and Rubisco activation by Rca. (A, C) Rates of ATP hydrolysis and Rubisco activation by wheat Rca2 β (orange) and Rca2 α (vermillion). Assays were performed at the indicated temperatures using 2 μ M Rca protomer and 5 mM ATP. Activation of pre-inhibited Rubisco used 6 μ M Rubisco active sites (R_{A.S.}) in the ER form (1:3 Rca:R_{A.S.}). Values are means \pm standard error ($n = 6-18$ technical replicates in A and $n = 3-8$ technical replicates in C). Lines represent the best-fit for each enzyme (AIC, Table S1) and coloured areas denote the 95% confidence interval for each fit. (B, D) ATP hydrolysis and Rubisco activation relative to estimated maximum activities (Table 1).

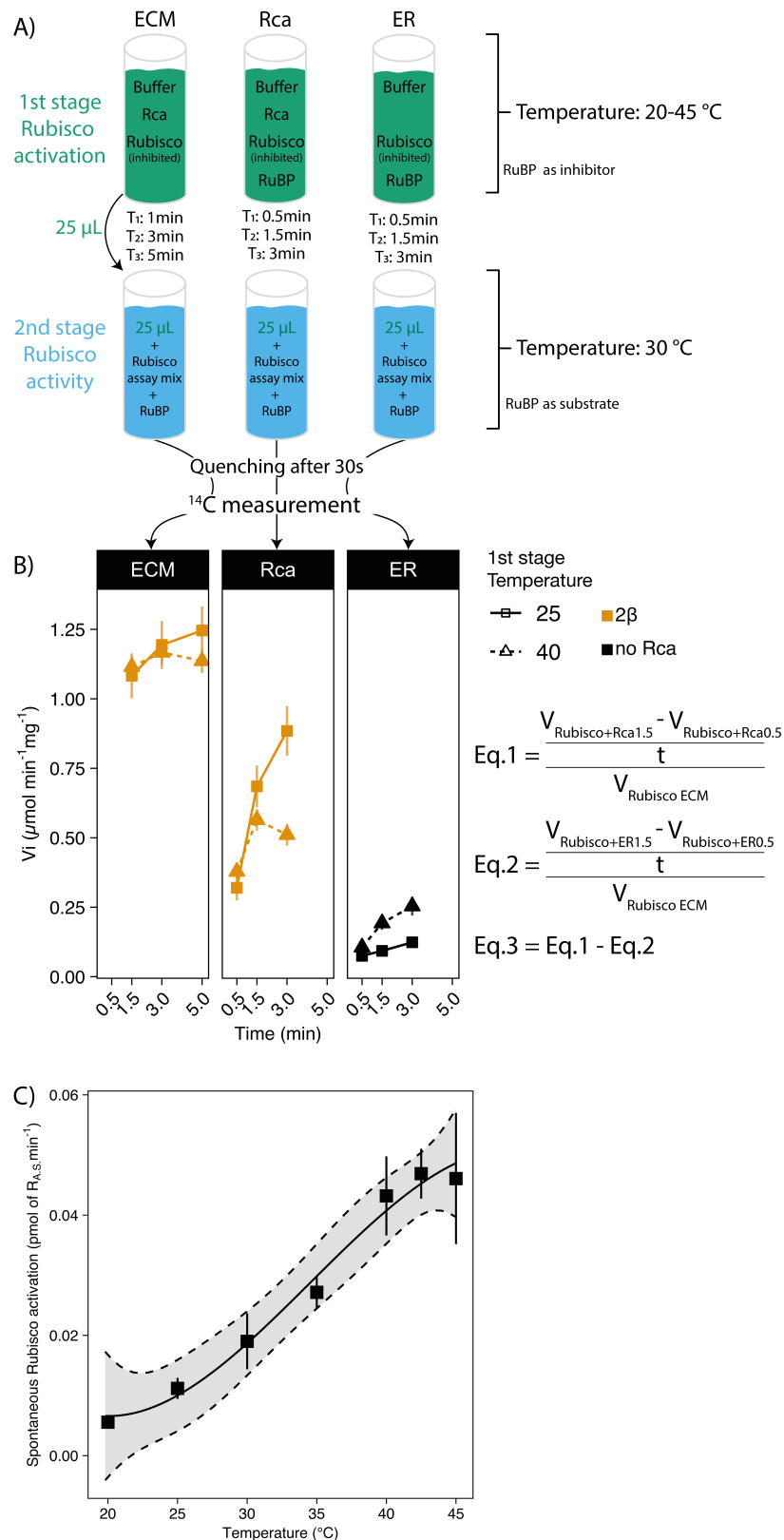


Figure S2. The spontaneous release of RuBP from inhibited Rubisco (ER) increases with temperature.

(A) Scheme of Rubisco activation assay. The 1st stage Rubisco activation assays were performed without addition of RuBP to allow Rubisco to fully

reactivate (ECM), in presence of all components to monitor the Rca-dependent increase in Rubisco activity (Rca), and in the absence of Rca to assess the extent of spontaneous release of inhibitors (ER). The 1st stage Rubisco activation assays were carried out at a range of temperatures (from 20-45°C). Aliquots (25 μ L) were taken from each 1st stage assay at specific time points to measure Rubisco activity in 2nd stage assays. The 2nd stage Rubisco activity assays were always carried out at 30°C and the carboxylation reaction was quenched after 30 s to determine acid-stable ¹⁴C by liquid scintillation counting.

(B) Representative example of time-course assays showing the increase in Rubisco activity (2nd stage assay) in aliquots taken from the 1st stage assays. Rubisco activation assays (1st stage) used 6 μ M Rubisco active sites (R_{A.S.}) in the presence/absence of 2 μ M Rca. Symbols represent means \pm standard error (n = 3-17 technical replicates). Using this data, rates of Rubisco activation were calculated from the increase in Rubisco activity between 0.5 and 1.5 min (Eq.1 & Eq.2). Calculation of the rate of Rubisco activation by Rca took into consideration the spontaneous release of inhibitors at each temperature (Eq.3).

(C) Rate of spontaneous Rubisco activation measured in the absence of Rca at 20-45°C (ER, Eq.2). Symbols represent means \pm standard error (n = 9-17 technical replicates). The line represents a best-fit model and the shaded area denotes the 95% confidence interval.

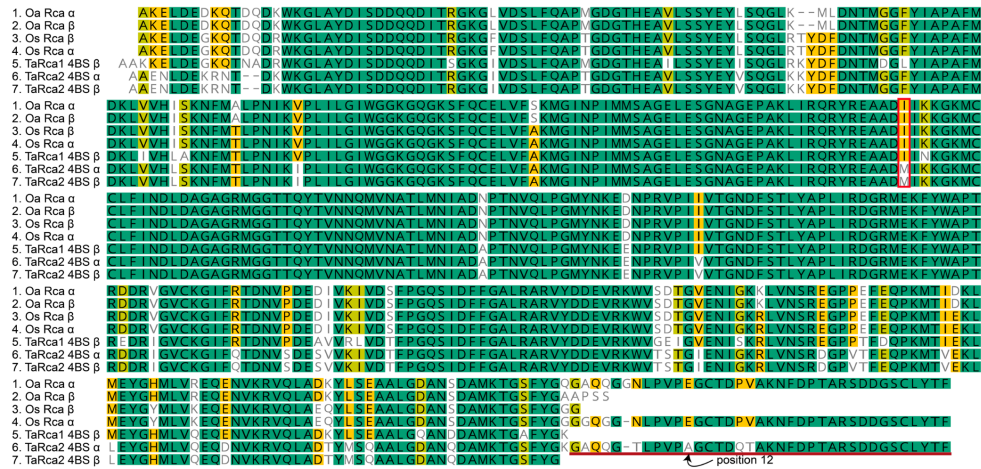


Figure S3. Amino acid sequence alignment of Rca isoforms from warm-adapted wild rice (*O. australiensis*, Oa), cultivated rice (*O. sativa*, Os) and bread wheat (*T. aestivum*, Ta). Rice sequences were obtained from Scafaro *et al.* (2016). The red line highlights the C-terminal extension and the arrow indicates the residue at position 12 of the C-terminal extension (corresponding to position 392 of the mature protein; numbering according to wheat Rca2 β lacking the chloroplast transit peptide). The residue at position 159 is identified by the red box.

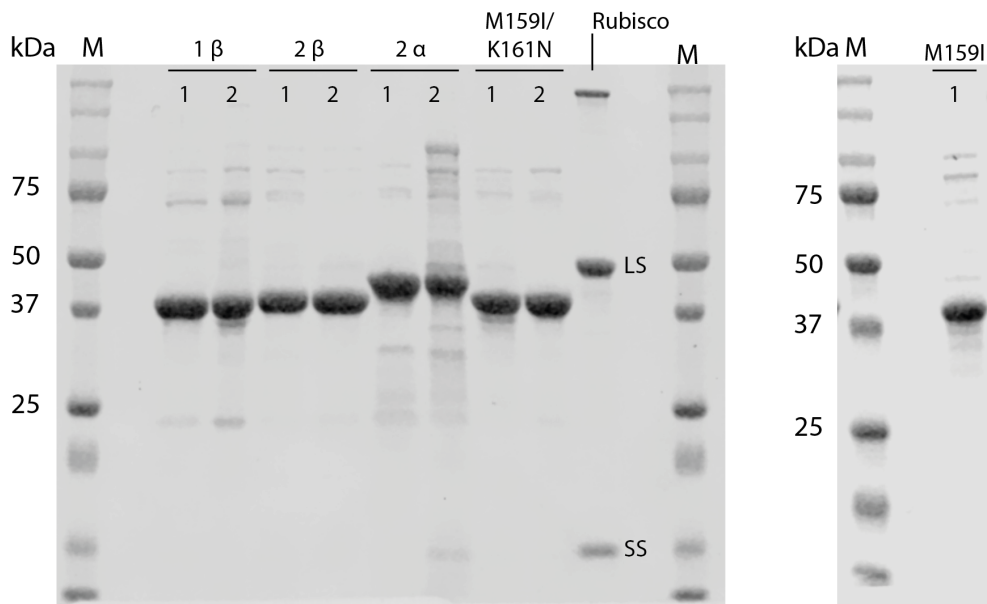


Figure S4. Separation of purified Rca and Rubisco proteins by SDS-Page. Rca isoforms were expressed in *E. coli* prior to purification and Rubisco was isolated from wheat leaves. The total soluble protein (TSP) concentration in each preparation was determined by the Bradford method, 3 μ g TSP was loaded in each lane prior to separation of proteins by SDS-PAGE. Gels were stained with Coomassie Blue. Two independent preparations of wheat Rca1 β (predicted Mw = 42.9 kDa), Rca2 β (42.3 kDa), Rca2 α (46.2 kDa) and Rca2 β -M159I/K161N (42.3 kDa), and one preparation of Rca2 β -M159I (42.3 kDa) were used. Abbreviations: LS = large subunit, SS = small subunit, M = molecular weight marker.

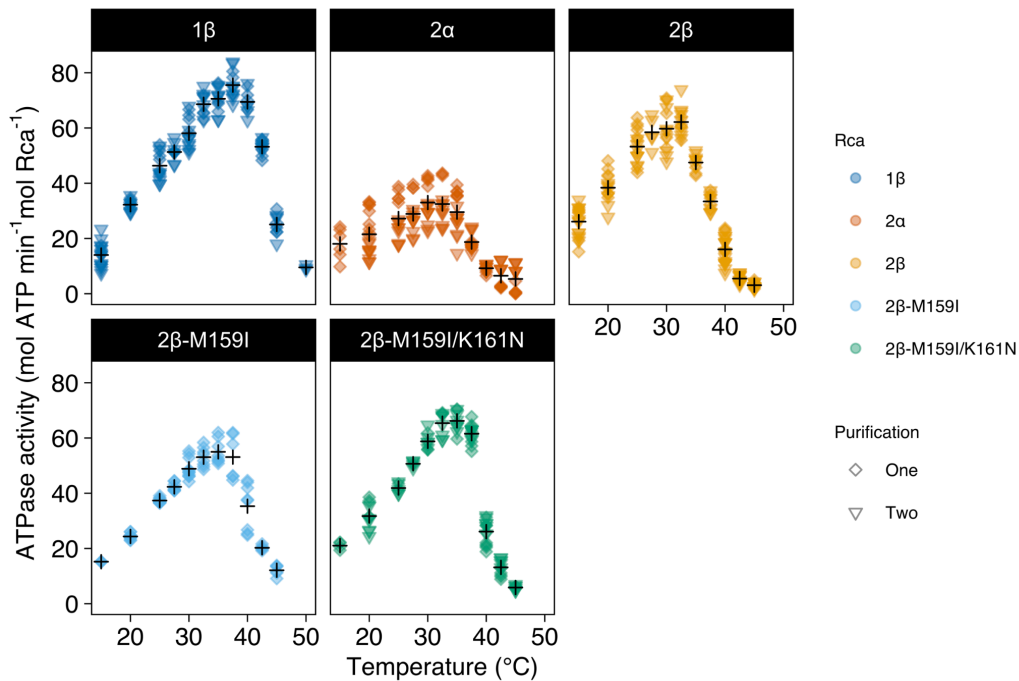


Figure S5. Temperature response of ATP hydrolysis by Rca proteins. The rate of ATP hydrolysis by Rca1 β (blue), Rca2 β (orange), Rca2 α (red), Rca2 β -M159I (light blue), Rca2 β -M159I/K161N (green). Assays were performed at the indicated temperatures with 2 μ M Rca protomer and 5 mM ATP. Squares represent the mean value of measurements at each temperature, circles and triangles represent technical replicates for each independent preparation of Rca. For Rca2 β -M159I there was only one preparation. The cross shows the average value for both purifications at the respective temperature.

Table S1. Modelling the temperature response of ATP hydrolysis and Rubisco activation by wheat Rca isoforms. The model providing the best fit to the data is highlighted in bold and was selected according to the lowest AIC score (Akaike information criterion) calculated according to (Akaike, 1974) using the AIC function in R. Models were applied to the full dataset shown in Figure 2 and Figure S1, using individual data points.

Rca	ATPase assay			Rubisco activation assay		
	Model	degrees of freedom (K)	AI C score	Model	degrees of freedom (K)	AIC score
1 β	2 nd order polynom	5.0	931	2 nd order polynom	5.0	-124
	3 rd order polynom	6.0	925	3rd order polynom	6.0	-125
	4 th order polynom	7.0	838	4 th order polynom	7.0	-123
	GAM	10.7	798	GAM	-	-
2 β	2 nd order polynom	5.0	1083	2nd order polynom	5.0	-64
	3 rd order polynom	6.0	963	3 rd order polynom	6.0	-62
	4 th order polynom	7.0	946	4 th order polynom	7.0	-60
	GAM	9.7	942	GAM	-	-
2 α	2 nd order polynom	5.0	944	2nd order polynom	5.0	-3
	3 rd order polynom	6.0	918	3 rd order polynom	6.0	-1
	4 th order polynom	7.0	911	4 th order polynom	7.0	-2
	GAM	8.3	910	GAM	-	-
2 β M15 9I/ K161 N	2 nd order polynom	5.0	778	2 nd order polynom	5.0	-36
	3 rd order polynom	6.0	753	3rd order polynom	6.0	-38
	4 th order polynom	7.0	666	4 th order polynom	7.0	-37
	GAM	10.8	597	GAM	-	-
2 β	2 nd order polynom	5.0	522	2nd order polynom	4.0	-89

M15 9I	3 rd order			3 rd order		
	polynom	6.0	519	polynom	5.0	-88
	4 th order			4 th order		
	polynom	7.0	500	polynom	6.0	-86
	GAM	9.9	491	GAM	4.7	-88

Table S2. Result of a Tukey's multiple comparison test of the Rca ATPase activity. For each temperature, Rca activities were compared pairwise and significant differences are denoted by different letters as determined using Tukey's multiple comparisons test ($P < 0.05$).

ATPase activity (mol ATP min⁻¹ mol⁻¹ Rca)											
Rca	Temperature (°C)										
	15	20	25	27.5	30	32.5	35	37.5	40	42.5	45
1 β	b	b	b	a	a	a	a	a	a	a	a
2 β	a	a	a	a	a	b	c	d	d	d	c
2 α	b	c	d	c	c	d	d	e	e	d	c
2 β -M159I	b	c	c	b	b	c	b	c	b	b	b
2 β -M159I/K161N	ab	b	bc	a	a	ab	a	b	c	c	c
ATPase activity (relative to maximum)											
Rca	Temperature (°C)										
	15	20	25	27.5	30	32.5	35	37.5	40	42.5	45
1 β	c	c	b	b	b	a	a	a	a	a	a
2 β	b	ab	a	a	a	a	b	c	d	d	d
2 α	a	a	a	a	a	a	ab	c	d	c	bc
2 β -M159I	bc	c	b	ab	ab	a	a	ab	b	b	b
2 β -M159I/K161N	bc	bc	b	ab	ab	a	a	b	c	c	cd

Table S3. Result of a Tukey's multiple comparison test of the Rubisco activation activity. For each temperature, Rca activities were compared pairwise and significant differences are denoted by different letters as determined using Tukey's multiple comparisons test ($P < 0.05$).

Rubisco activation (mol R_{A.S.} min⁻¹ mol⁻¹ Rca)							
Rca	Temperature (°C)						
	20	25	30	35	40	42.5	45
1 β	d	c	c	b	b	a	a
2 β	a	a	a	ab	b	b	b
2 α	ab	a	a	a	ab	b	b
2 β -M159I	c	b	bc	ab	ab	ab	ab
2 β -M159I/K161N	bc	ab	ab	ab	a	a	ab
Rubisco activation (relative to maximum)							
Rca	Temperature (°C)						
	20	25	30	35	40	42.5	45
1 β	b	ab	a	ab	ab	a	a
2 β	a	ab	a	b	b	b	b
2 α	a	a	a	ab	ab	b	b
2 β -M159I	a	a	a	a	ab	ab	ab
2 β -M159I/K161N	ab	ab	a	ab	a	a	ab

Table S4. Two-way ANOVA showed no significant differences between results obtained for ATPase activity using different preparations of Rca ($P > 0.05$). Two-way ANOVA was applied using the aov function of the R base package.

Rca		Df	Sum Sq	Mean Sq	F value	P value
1 β	Purification	1	239	239.4	0.523	0.471
	Residuals	135	61784	457.7		
2 β	Purification	1	239	1	0.002	0.962
	Residuals	153	70274	459.3		
2 α	Purification	1	163	162.8	1.241	0.267
	Residuals	137	17969	131.2		
2 β -M159I/K161N	Purification	1	533	532.8	1.41	0.288
	Residuals	105	49006	466.7		

References

- Akaike H.** 1974. A new look at the statistical model identification. *IEEE Transactions on Automatic Control* **19**: 716–723.
- Scafaro AP, Gallé A, Van Rie J, Carmo-Silva E, Salvucci ME, Atwell BJ.** 2016. Heat tolerance in a wild *Oryza* species is attributed to maintenance of Rubisco activation by a thermally stable Rubisco activase ortholog. *New Phytologist* **211**: 899–911.

The following chapter has been accepted will be published as

Degen, G.E., ORR, D.J. and Carmo-Silva, E. (2020) Heat-induced changes in the abundance of wheat Rubisco activase. *New Phytologist*

Author contributions: GED, DJO and ECS designed research; GED performed research with help from DJO; GED analysed data; and GED and ECS wrote the manuscript with help from DJO.

4. Chapter 4: Heat-induced changes in the abundance of wheat Rubisco activase isoforms

Summary

- The *Triticum aestivum* (wheat) genome encodes three isoforms of Rubisco activase (Rca) differing in thermostability, which could be exploited to improve the resilience of this crop to global warming. We hypothesised that elevated temperatures would cause an increase in the relative abundance of heat stable Rca1 β .
- Wheat plants were grown at 25/18°C (day/night) and exposed to heat stress (38/22°C) for up to 5 days at pre-anthesis. Carbon assimilation, Rubisco activity, CA1Pase activity, transcripts of Rca1 β , Rca2 β and Rca2 α , and the quantities of the corresponding protein products were measured during and after heat stress.
- The transcript of *Rca1 β* increased 40-fold in 4 hours at elevated temperatures, and returned to the original level 4 hours upon return of plants to control temperatures. Rca1 β comprised up to 2% of the total Rca protein in unstressed leaves, but increased 3-fold in leaves exposed to elevated temperatures for 5 days, and remained high 4 hours post heat stress.
- These results show that elevated temperatures cause rapid changes in *Rca* gene expression and adaptive changes in Rca isoform abundance. The improved understanding of the regulation of carbon assimilation under heat stress will inform efforts to improve wheat productivity and climate resilience.

4.1 Introduction

Wheat production is threatened by the increasing frequency of heat stress in combination with other abiotic factors (IPCC, 2014; Slattery & Ort, 2019; Ray *et al.*, 2019). Field studies show that predicted benefits of increasing atmospheric CO₂ for plant growth are offset by drought and heat stress (Ruiz-Vera *et al.*, 2013; 2015; Gray *et al.*, 2016). Moreover, increases in [CO₂] result in increased canopy temperature (Long *et al.*, 2006). Although plants can cool their leaves by transpiration (Ayeneh *et al.*, 2002), increased drought frequencies limit water availability and increase leaf temperature (Carmo-Silva *et al.*, 2012). As leaf temperature increases, respiration rates increase exponentially while photosynthesis declines above an optimum temperature threshold for each species (Way & Yamori, 2014). Acclimation of respiration to the growth temperature further compounds the balance between the two processes (Atkin *et al.*, 2005). The photosynthetic machinery also adapts to the growth environment (Berry & Bjorkman, 1980; Yamori *et al.*, 2013; Thomey *et al.*, 2019), and depending on the extent of temperature changes, photosynthetic limitations may be reversible or cause permanent damage. Broadening the temperature range for optimal carbon assimilation in wheat is important because global production is predicted to decline in response to rising temperatures (Asseng *et al.*, 2015; Liu *et al.*, 2016).

The activity of ribulose-1,5-bisphosphate (RuBP) carboxylase/oxygenase (Rubisco) has long been identified as the site of heat inactivation of the Calvin-Benson-Bassham Cycle (CBBC) (Weis, 1981). This inactivation is largely due to an inefficient regulation of Rubisco activity by the heat-sensitive molecular chaperone Rubisco activase, Rca (Crafts-Brandner & Salvucci, 2000; Salvucci *et al.*, 2001). Rubisco itself remains active up to 50°C (Salvucci & Crafts-Brandner, 2004b; Galmés *et al.*, 2016), but the reactions it catalyses are differently affected by temperature (Galmés *et al.*, 2019). In addition to CO₂ assimilation by reaction with RuBP, Rubisco can use O₂ as an alternative gaseous substrate, which initiates photorespiration and results in a net loss of CO₂ (Ogren, 1984). Oxygenation occurs at faster rates as temperature increases because the solubility of CO₂

decreases more rapidly than O₂ with temperature (Ku & Edwards, 1977; Bauwe *et al.*, 2010; Dusenge *et al.*, 2019), leading to substantial crop yield losses under future climate scenarios (Walker *et al.*, 2016).

Environmental factors such as [CO₂] and growth temperature have been shown to affect the expression of Rubisco small subunit genes (*RbcS*) in *Arabidopsis* (Cheng *et al.*, 1998; Yoon *et al.*, 2001; Cavanagh & Kubien, 2013), the relative abundance of *RbcS* isoforms in rye (Huner & Macdowall, 1979; Huner & Hayden, 1982), and Rubisco properties in spinach (Yamori *et al.*, 2006). Specific residues in the Rubisco large subunit (*rbcL*) have also been linked to improved catalytic capacity at high temperatures (Prins *et al.*, 2016; Sharwood *et al.*, 2016). Thus, the temperature dependence of Rubisco activity appears to be determined by the inherent properties of the amino acid residues that make up the protein, and by the combination of *rbcL* assembled with diverse *RbcS* isoforms. While phenotypic plasticity enables plants to adapt the photosynthetic machinery to warmer temperatures, short-term heat stress is likely to cause detrimental effects (Leakey *et al.*, 2003).

The regulation of Rubisco activity by *Rca* is particularly sensitive to temperature (Salvucci *et al.*, 2001; Carmo-Silva & Salvucci, 2011). The active site of Rubisco is prone to deactivation by tight-binding of inhibitory sugar-phosphate derivatives, the production of which increases with temperature (Salvucci & Crafts-Brandner, 2004c; Schrader *et al.*, 2006). Reactivation requires *Rca* to remodel the active site of Rubisco and facilitate the release of such inhibitors (Salvucci *et al.*, 1985; Bhat *et al.*, 2017). Subsequent removal of a phosphate group from these compounds by specific phosphatases, such as 2-carboxy-D-arabinitol-1-phosphate (CA1P) phosphatase (CA1Pase) and xylulose-1,5-bisphosphate (XuBP) phosphatase (XuBPase), renders them non-inhibitory (Andralojc *et al.*, 2012; Bracher *et al.*, 2015). Overexpression of *ca1pase* decreased Rubisco abundance and grain yields in wheat (Lobo *et al.*, 2019), but the temperature response of the phosphatases that act in concert with *Rca* to regulate the activity of Rubisco has received little attention to date. On the other hand, the temperature optimum of Rubisco activation by *Rca* has been shown to follow a pattern that resembles the species adaptation to growth at different temperatures

(Carmo-Silva & Salvucci, 2011). In wheat, the optimal leaf temperature for photosynthesis is between 20-25°C (Porter & Gawith, 1999; Silva-Pérez *et al.*, 2017) and decreased capacity for carbon assimilation at elevated temperatures has been linked to the heat sensitivity of Rca (Law & Crafts-Brandner, 2001; Yang *et al.*, 2020).

The potential for greater photosynthetic thermotolerance by improving Rca thermostability has been shown for Arabidopsis (Kurek *et al.*, 2007; Kumar *et al.*, 2009) and rice (Wang *et al.*, 2010; Scafaro *et al.*, 2016; Shivhare & Mueller-Cajar, 2017; Scafaro *et al.*, 2018), making it a promising target for improving photosynthesis at high temperatures in other crops. This could be achieved by exploiting natural diversity in species adapted to warm environments. Light activation of Rubisco by Rca was inhibited by moderately high temperatures to a greater extent in wheat than in heat-tolerant cotton (Feller *et al.*, 1998; Law *et al.*, 2001). In two wild rice species, higher capacity for Rubisco activation at high temperatures resulted in photosynthetic thermotolerance (Scafaro *et al.*, 2012), and was associated with improved Rca thermostability compared to cultivated rice (Scafaro *et al.*, 2016). Heat stress was also shown to increase abundance of the large Rca isoform in domesticated rice, with plants overexpressing this isoform having increased seedling aboveground biomass dry weight when exposed to heat stress (Wang *et al.*, 2010).

Wheat contains two Rca genes as do the majority of grass species, with exceptions including rice where the *OsRca1* gene is thought to be non-functional (Nagarajan & Gill, 2018). Wheat *Rca1* produces a 42.9 kDa Rca1 β isoform and *Rca2* produces a 42.3 kDa Rca2 β and a 46.2 kDa Rca2 α isoform via alternative splicing (Carmo-Silva *et al.*, 2015). Recent detailed analyses of the temperature response of wheat Rca isoforms showed that Rca1 β is more thermostable than Rca2 β and Rca2 α (Scafaro *et al.*, 2019; Degen *et al.*, 2020). However, Rubisco activation by Rca1 β is relatively inefficient at elevated temperature, due to high rates of ATPase activity in relation to Rubisco activation (Degen *et al.*, 2020). Gene expression of *Rca1 β* increased by varying extents in two wheat cultivars exposed to short-term (2 days) heat stress at two growth stages (Scafaro *et al.*, 2019). Rca protein abundance

may also be regulated post-transcriptionally as suggested by the observation of a decrease in total *Rca* transcript accompanied by an apparent increase in total Rca protein abundance under short-term heat stress (2 days; Law & Crafts-Brandner, 2001). Wheat leaves developed under longer-term heat stress (2 weeks) showed no significant change in Rca protein abundance, but Rca β was more abundant in leaves that were simultaneously exposed to drought and heat (Perdomo *et al.*, 2017). Importantly, studies to date did not distinguish between the abundance of the two short protein isoforms, Rca1 β and Rca2 β , which have similar molecular weights (Carmo-Silva *et al.*, 2015), but differ in heat sensitivity (Scafaro *et al.*, 2019; Degen *et al.*, 2020).

A detailed understanding of the temperature response of Rubisco regulation will become increasingly important with predictions of increased frequency of future heat waves (Slattery & Ort, 2019) and more variable leaf temperatures (Vico *et al.*, 2019). Given the previously characterised differences in the temperature response of Rubisco activation by wheat Rca isoforms (Degen *et al.*, 2020), here we set out to investigate how whole-plant heat stress impacts Rca protein levels. Specifically, we tested the hypothesis that the relative abundance of wheat Rca isoforms would change so that leaves of heat-stressed plants contain relatively more of the thermostable Rca1 β , and these changes would be accompanied by altered photosynthetic biochemistry, physiology and grain yield. This was tested by exposing plants to a five-day period of heat stress at pre-anthesis (a critical stage of wheat plant development). Net CO₂ assimilation, Rubisco activity and abundance, CA1Pase activity, and the abundance of the three Rca isoforms were determined during and immediately after heat stress. Findings are interpreted in relation to the thermostability of wheat Rca isoforms and will inform approaches to improve photosynthetic regulation under increasingly warm and variable temperatures for enhanced crop productivity and resilience to climate change.

4.2 Materials and Methods

Plant growth and heat stress conditions

Triticum aestivum L. cv. Cadenza seeds were soaked in de-ionised H₂O for 24h at 7°C prior to sowing in a wheat mix growth medium (Petersfield compost, Hewitt & Son Ltd., Cosby, UK). Twenty plants per experiment were grown in a heated glasshouse for three weeks in 3 L pots before being divided into two groups and transferred to two controlled environment cabinets (Snijders Labs, Tilburg, Netherlands). Cabinets were set to 25/18°C day/night, with a 16 h photoperiod, photosynthetic photon flux density (PPFD) at the plant level of 450 $\mu\text{mol m}^{-2} \text{s}^{-1}$, and 60% relative humidity until the flag leaf of the main tiller was fully expanded (approximately 3 weeks). For the heat stress treatment, once the flag leaves were visible, the temperature in one of the two cabinets was raised to 34/22°C day/night for one day, followed by five days at 38/22°C day/night (Fig. 1a). Night-time warming causes increased dark respiration (e.g. Rashid *et al.*, 2020) and decreased yields of crops such as wheat and rice (Sadok & Jagadish, 2020). Effects on productivity are complex, genotype-specific, and may be more pronounced when night-time elevated temperatures occur at the reproductive stage (Hein *et al.*, 2019; Impa *et al.*, 2019) compared to earlier growth stages (Frantz *et al.*, 2004; Peraudeau *et al.*, 2015). In the present study, both day- and night-time temperatures were increased in the heat stress cabinets to replicate real-world conditions, and measurements were taken during the day focusing on photosynthetic traits. After 5 days at 38/22°C, the cabinet was returned to control temperatures (25/18°C) at the end of the photoperiod on experiment day 7. Temperatures in each cabinet were increased over the course of 1 h at the start of the photoperiod and decreased over the course of 1 h at the end of the photoperiod. Air temperature and relative humidity in each cabinet were measured continuously during the course of the heat stress treatment (OM-EL-USB temperature and humidity data logger, Omega Engineering, UK; Fig. 1b, Fig. S1).

Two consecutive experiments were completed switching the cabinets used for control conditions and the heat stress treatment. In each experiment,

a set of 5 plants (i.e. 10 plants in total for control and 10 plants in total for heat stress) was used for non-destructive repeated measures of *in vivo* gas-exchange over the course of the heat stress treatment. This same set of plants was used for final biomass and grain yield. A separate set of 4 plants per experiment (i.e. 8 plants in total for control and 8 plants in total for heat stress) was used for collecting samples for biochemical analysis.

Measurements and samples were taken at four time-points during the experiment: (1) the day prior to the start of the heat treatment, corresponding to experiment day 1, when all plants were exposed to control conditions; (2) four hours and (3) five days into the heat stress exposure period, corresponding to experiment days 3 and 7, when plants were either exposed to control or elevated temperatures; and (4) the day after the end of the heat treatment, when plants were exposed to control conditions to assess recovery from heat stress, corresponding to experiment day 8 (Fig. 1a). No samples or measurements were taken on the other days of the experiment.

Samples were collected 4 hours into the beginning of the photoperiod and *in vivo* measurements were taken 5-6 hours into the photoperiod. At each of the four time-points, samples for biochemistry were taken from a flag leaf in a separate tiller of each plant (repeated sampling from each biological replicate throughout the experiment). Leaf segments of known area were immediately snap frozen in liquid nitrogen and kept at -80°C until analysis. Sampling for biochemistry resulted in approximately half of the flag leaf being removed from the sampled tiller and each plant contained on average 15 fertile tillers. Measurements and sampling were always taken from flag leaves of tillers at the booting stage, i.e. prior to ear emergence. Leaf temperature was measured before sampling using a thermocouple (CDH-SD1, Omega Engineering, UK; Fig. 1c) and light level was measured with a PAR meter (MQ-200, Apogee Instruments, Canada).

Gas-exchange measurements

Steady-state measurements of net CO₂ assimilation (*A*) and stomatal conductance to water vapour (*g_s*) used an open gas-exchange system (LI-6400XT, Li-COR, Lincoln, NE, USA) at a PPFD of 400 μmol m⁻² s⁻¹, a

reference CO₂ concentration of 400 μmol mol⁻¹ and a flow rate of 300 μmol s⁻¹. The gas-exchange system was placed inside the respective growth cabinets, under control or heat stress conditions. The temperature of the block in the leaf chamber was set to 25°C for plants in the control cabinet and to 38°C for plants in the heat stress cabinet (experiment days 3 and 7). The water vapour pressure deficit (VPD) was maintained at 1-1.6 kPa by adjusting the humidity inside the leaf chamber of the gas-exchange system as needed, and calculated from the leaf temperature during gas-exchange measurements.

Gene expression analyses

Gene expression of *ca1pase*, *Rca1β*, *Rca2β+a*, *Rca2a*, *RbcS1-25* and *rbcL*, were determined by reverse-transcription quantitative PCR (RT-qPCR). mRNA was extracted from plant tissue using a NucleoSpin® Tri Prep kit (Macherey-Nagel, Düren, Germany), including a DNase treatment. mRNA yield and purity were assessed using a spectrometer by measuring absorbance at 230, 260 and 280 nm (SpectroStar Nano, BMG Labtech GmbH, Ortenberg, Germany). cDNA synthesis used 1 μg mRNA and the Precision nanoScript™ 2 Reverse Transcription kit (Primer design Ltd., Camberley, UK). qPCR reactions used 40 ng of cDNA and the primer pair for the target gene in a Mx3005P qPCR system (Stratagene, Agilent Technologies, Stockport, UK). RT-qPCR details including cycle conditions are described in the MIQE checklist (Table **S1**). *Ta2291* (ADP-ribosylation factor) and *Ta2776* (similar to RNase L inhibitor-like protein) were used for normalisation due to their high expression stability across various environmental conditions (Paolacci *et al.*, 2009). Primer efficiency for each primer set was analysed according to Pfaffl *et al.* (2001). Primers were designed to bind to all three sub genomes (Table **S2**), except for *rbcL*, which is encoded in the chloroplast genome. Primers for *Rca2* amplified both splicing products. EnsemblPlants was used to search for genes annotated as *RbcS*; 25 genes were identified and divided into three groups according to the similarity of the respective protein sequences (Table **S3**). Primer pairs were designed to quantify the expression of each of the three *RbcS* groups (Table **S2**).

Enzyme activity assays

Photosynthetic proteins were extracted essentially as described by Carmo-Silva *et al.* (2017) with slight modifications, as follows. Leaf samples were ground using an ice-cold mortar and pestle containing 0.8 mL of (final concentrations) 50 mM Bicine-NaOH pH 8.2, 20 mM MgCl₂, 1 mM EDTA, 2 mM benzamidine, 5 mM ϵ -aminocaproic acid, 50 mM 2-mercaptoethanol, 10 mM dithiothreitol, 1% (v/v) plant protease inhibitor cocktail (Sigma-Aldrich Co., St Louis, MO, USA), and 1 mM phenylmethylsulphonyl fluoride.

Rubisco activity was determined by incorporation of ¹⁴CO₂ into acid-stable products at 30°C (Parry *et al.*, 1997; Carmo-Silva *et al.*, 2017) in reaction mixtures containing (final concentrations) 100 mM Bicine-NaOH pH 8.2, 20 mM MgCl₂, 10 mM NaH¹⁴CO₃ (9.25 kBq μ mol⁻¹), and 0.6 mM RuBP (added to tubes individually). Initial activity assays started with leaf extract addition, while total activity assays started with RuBP addition after allowing carbamylation of Rubisco for 3 min. Reactions were quenched after 30 s with 4N formic acid, then dried, rehydrated with de-ionised H₂O, mixed with scintillation cocktail (Gold Star Quanta, Meridian Biotechnologies, Epsom, UK) and subject to liquid scintillation counting (Packard Tri-Carb, PerkinElmer). Rubisco activation state was calculated from the ratio of initial/total Rubisco activity. Rubisco amounts were determined by a [¹⁴C]carboxyarabinitol-1,5-bisphosphate (¹⁴C-CABP) binding assay (Whitney *et al.*, 1999).

CA1Pase activity was measured according to Lobo *et al.* (2019) and Andralojc *et al.* (2012) in reaction mixtures (90 μ L) containing (final concentrations) 50 mM BisTrisPropane-HCl pH 7.0, 200 mM KCl, 1 mM EDTA, 1 mM ϵ -aminocaproic acid, 1 mM benzamidine, 10 mM CaCl₂, 0.5 mg mL⁻¹ BSA and 1% (v/v) protease inhibitor cocktail. For each sample, two technical replicates containing 0.5 mM 2-carboxy-D-ribitol-1,5-bisphosphate (CRBP, a substrate for CA1Pase) and two replicates without CRBP were prepared, in addition to a blank containing no leaf extract. Reactions were initiated by adding 5 μ L of leaf extract and quenched after 60 min at 22°C in a temperature-controlled dry bath (Echotherm, Torrey Pines Scientific, USA)

by adding 30 μL of 1 M trichloroacetic acid. Reactions were centrifuged for 3 min at 14,000 g to sediment BSA, then 100 μL of supernatant was transferred into a microplate well to determine inorganic phosphate by adding 200 μL of 2.2% (w/v) ammonium molybdate in 1.6 M H_2SO_4 , incubating 10 min, adding 50 μL of 0.035% (w/v) malachite green in 0.35% (w/v) polyvinyl alcohol, incubating 60 min at room temperature, and measuring absorbance at 610 nm. Inorganic phosphate in the samples was calculated from a standard curve of 0-10 nmol KH_2PO_4 .

Gel electrophoresis and immunoblotting

Total soluble proteins (TSP) in leaf extracts were quantified by the Bradford method (Bradford, 1976), then separated by sodium dodecyl sulfate polyacrylamide gel electrophoresis (SDS-PAGE) followed by immunoblotting, essentially as described by Perdomo *et al.* (2018). A primary antibody anti-Rca produced in rabbit against cotton Rca (Salvucci, 2008) was used for quantification of all Rca α and β isoforms using 2 μg TSP per sample. A primary polyclonal antibody that specifically detects the wheat Rca1 β isoform was produced in rabbit (Cambridge Research Biochemicals Ltd., Cleveland, UK) using a short peptide at the N-terminal region where the protein differed sufficiently from Rca2 β (KKELDEGKQTNADR, corresponding to residues 3-16 of the mature sequence, Fig. **S2**). Detection of Rca1 β required the use of 6 μg TSP per sample. A dilution series of 20, 50 and 100 ng purified recombinant Rca2 β + α at a 90:10 ratio was added to each gel for quantification of total Rca α and β isoforms; and a dilution series of 1, 5 and 20 ng purified recombinant Rca1 β was added to each gel for quantification of Rca1 β (Fig. **S2**). Recombinant Rca proteins used for standards were purified as described in Barta *et al.* (2011). A fluorescent secondary antibody (anti-rabbit, 800CW, Li-COR Biosciences) was used to detect Rca by imaging blots at 800 nm using an Odyssey system (Li-COR Biosciences, Lincoln, NE, USA). Protein levels were calculated from the standard curves of purified Rca. Quantities of Rca2 β were calculated by subtracting Rca1 β from the total Rca β isoform.

Biomass and yield traits

After the heat stress treatment, at the end of experiment day 8, plants were transferred back into the glasshouse and kept well-watered until reaching full maturity. Aboveground biomass and grain yield traits were determined for each plant as described by Lobo *et al.* (2019).

Statistical analysis

Significance of differences between control and heat stress plants was analysed using Restricted Maximum Likelihood (REML), which gives the same *P* values and multiple comparisons tests as repeated measures ANOVA. The mixed model was fitted in GraphPad Prism 8 using the Geisser-Greenhouse correction to account for possible violations of sphericity. The lack of significant differences in biochemical (destructive flag leaf sampling) and physiological (non-destructive flag leaf sampling) traits between control plants analysed at different time-points suggests that repeated sampling caused no significant wounding effect on *Rca* gene expression and protein levels in flag leaves from adjacent tillers. Significance of differences in grain yield and biomass between treatments was assessed by two-sided t-tests with alpha set to 0.05 using R (version 3.6.0; R Core Development Team, 2013) and RStudio (version 1.2.5001; R Studio Team, 2019). Box and whiskers plots were prepared using ggplot2 (Wickham, 2017); boxes show medians and first and third quartiles (25th and 75th percentiles), and whiskers extend from the hinge to the largest or smallest value. Symbols represent individual data points and black diamonds represent the mean values. Plants in the two cabinets on the day prior to the onset of heat stress (i.e. under control conditions) were not statistically different in their rates of CO₂ assimilation or Rubisco properties and were combined for data analysis (Table S4).

4.3 Results

Wheat plants were exposed to heat stress conditions over a period of 5 days before reaching anthesis (booting stage) in a pot experiment and using plant growth cabinets for environmental control. The air temperature in the control cabinet corresponded with the set temperatures of 25/18°C, while the day temperature in the heat stress cabinet was slightly below the setting of 38/22°C (Fig. **1a, b**). Leaf temperature (T_{leaf}) was measured to assess the extent to which plants experienced heat stress. Plants in the control cabinet had mean T_{leaf} of 22.5°C and plants in the heat stress cabinet had mean T_{leaf} of 28.7°C, corresponding to a difference between air temperature (T_{air}) and T_{leaf} of 2.5°C for control and 9.3°C for heat stress plants (Fig. **1c**). Plants were maintained well-watered and in a humid environment (Fig. **S1**) throughout the experiment, which would have enabled the greater extent of evaporative cooling during heat stress (Carmo-Silva *et al.*, 2012). Once T_{air} returned to control values on experiment day 8, T_{leaf} in the heat stress cabinet (22.6°C) was again comparable to control plants.

In order to assess the effect of heat stress on carbon assimilation, gas exchange measurements were taken under steady-state conditions resembling those used for plant growth, i.e. a PPFD of 400 $\mu\text{mol m}^{-2} \text{s}^{-1}$ and 25°C for control or 38°C for heat stress plants (Fig. **2**). Net CO_2 assimilation (A) in the wheat flag leaves remained unchanged throughout the experiment days for control plants but decreased significantly in plants measured after 4 h of heat stress. The decline in A was greater after 5 days of heat stress, and still observed after the cabinet temperature was returned to control levels (4 h of recovery at control temperatures; Fig. **2a**). Stomatal conductance to water vapour (g_s) was highly variable but remained unchanged in control plants and after 4 h of heat. However, g_s was reduced after 5 days of heat stress and remained significantly lower after 4 h of recovery compared to control plants (Fig. **2b**). Despite attempts to maintain constant cabinet humidity, the vapour pressure deficit based on leaf temperature (VPD_L) increased after 5 days of heat stress compared to control conditions (Fig. **2c**). The intercellular CO_2 concentration did not decrease in response to heat stress, in fact after 4

h of heat there was a slight increase relative to the values prior to heat stress (Fig. 2d), likely as a result of decreased assimilation (Fig. 2a).

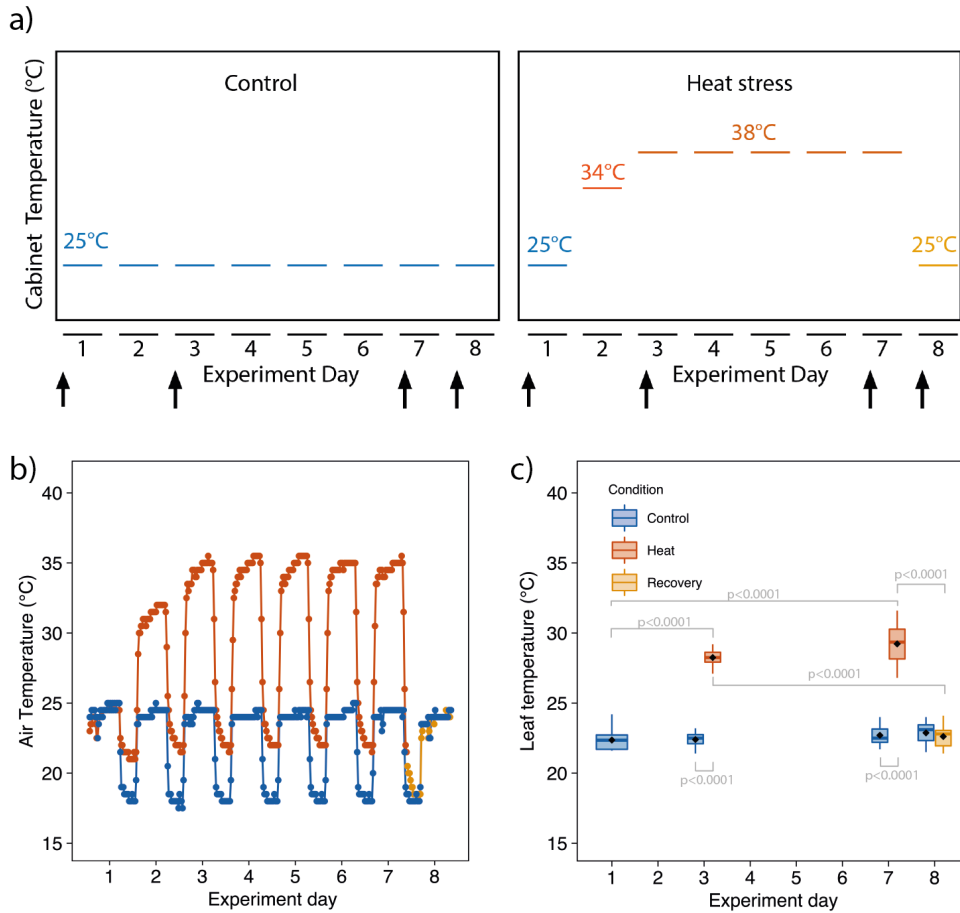


Figure 1. Experimental design, air and leaf temperatures of wheat plants during heat stress. Plants were grown at 25/18°C day/night (control conditions); at booting stage one of the two plant growth cabinets was set to 34/22°C for 1 day (experiment day 2) followed by 38/22°C for 5 days (heat stress, experiment days 3-7), then back to control temperatures (recovery, experiment day 8). Blue = control, red = heat stress, orange = recovery. (a) Experimental setup of control and heat stress cabinets. The cabinet temperature during the day is indicated and was gradually increased to induce heat stress in the respective cabinet, then maintained for 5 days prior to returning to control conditions. Vertical arrows indicate experiment days when measurements and sampling took place. (b) Air temperature in the two plant growth cabinets. (c) Leaf temperature of wheat plants, measured before sampling. Over the course of the experiment, mean leaf temperature (black diamond) \pm SD was $22.5 \pm 0.7^\circ\text{C}$ for control, $28.7 \pm 1.3^\circ\text{C}$ for heat stress and $22.6 \pm 0.9^\circ\text{C}$ for recovery. Significant *P*-values for pairwise comparisons are shown (REML, $\alpha = 0.05$).

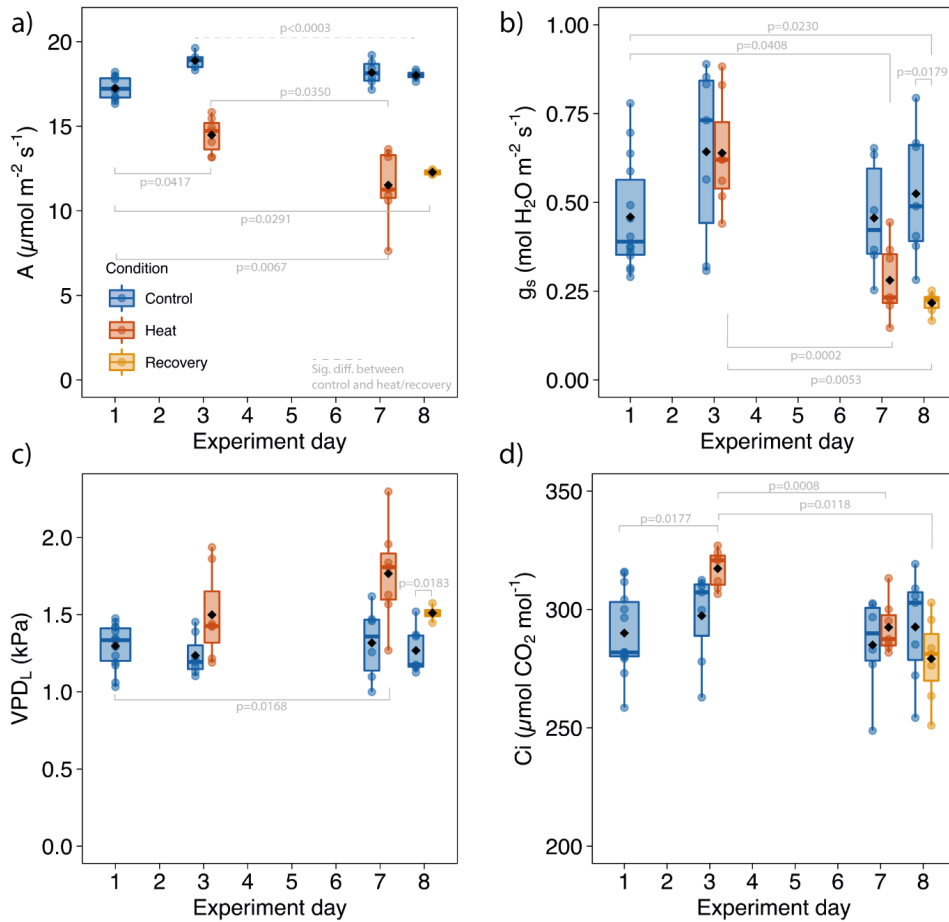


Figure 2. (a) Net CO₂ assimilation (A), (b) stomatal conductance to water vapour (g_s), (c) vapour pressure deficit (VPD) based on leaf temperature, and (d) intercellular CO₂ concentration (C_i) in wheat plants under heat stress. Measurements were taken under steady-state conditions at PPFD = 400 $\mu\text{mol m}^{-2} \text{s}^{-1}$, reference $[\text{CO}_2] = 400 \mu\text{mol mol}^{-1}$ and $T_{\text{block}} = 25^\circ\text{C}$ for control plants and 38°C for heat-stress plants. T_{leaf} during measurements was $25.3 \pm 0.5^\circ\text{C}$ for control, $37.1 \pm 0.8^\circ\text{C}$ for heat stress and $25.7 \pm 0.3^\circ\text{C}$ for recovery plants. Box lines represent the median, first and third quartiles, whiskers the range, black diamonds the mean, and circles individual samples ($n = 4$ –12 biological replicates). Significant P -values for pairwise comparisons are shown (REML, $\alpha = 0.05$).

After the heat stress exposure, all plants were transferred to the glasshouse until maturity to determine the effect of the 5 days heat stress exposure during booting on final biomass and grain yield. Aboveground

biomass at 100% dry matter (DM) showed no significant difference between control and heat stress plants (Table 1). However, the grain weight per plant at 85% DM was significantly lower in plants exposed to the heat treatment. The number of spikes per plant remained constant, suggesting that grain weight per spike was negatively impacted by the heat stress exposure pre-anthesis.

Table 1. Final biomass and yield traits of wheat plants exposed to heat stress for five days during booting. Plants were grown at 25/18°C day/night (control) and at booting stage half of the plants were exposed to heat stress (1 day at 34/22°C, 5 days at 38/22°C, then returned to 25/18°C). Values are means \pm SEM ($n = 10$ biological replicates). The heat stress treatment had no significant effect on aboveground biomass or number of spikes, but significantly affected grain yield (two-sided t-tests).

Treatment	n	Aboveground bio-	Grain Yield	Spike no.
		mass (g plant ⁻¹ @100% DM)	(g plant ⁻¹ @85% DM)	(plant ⁻¹)
Control	10	38.2 \pm 4.3	11.2 \pm 2.5	14.5 \pm 2.9
Heat stress	10	38.1 \pm 2.6	8.4 \pm 1.8	16.6 \pm 2.8
<i>P-value</i>		0.9608	0.0139	0.1129

To investigate the impact of heat stress on the regulation of Rubisco activity, flag leaf samples of plants in the control and heat conditions were taken prior to, during, and after the exposure to stress. Initial and total activities and content of Rubisco were not significantly affected during heat stress (Fig. 3), but total activity and Rubisco content declined slightly in recovery plants on experiment day 8 compared to control plants on experiment day 1 (Fig. 3b, c, $P = 0.0062$ and $P = 0.0451$, respectively). When expressing the activities of Rubisco per quantity of enzyme (specific activities), no significant differences were observed throughout the experiment (Fig. S3). The same was largely true for total soluble protein

(TSP), Rubisco content as a fraction of TSP (Fig. **S3**), and chlorophyll a, chlorophyll b and total carotenoids (Fig. **S4**).

Initial and total activities were used to calculate Rubisco activation states (Fig. **3d**), which declined significantly after 4h of heat stress ($P = 0.0006$) but showed no significant difference to control after 5 days of heat stress ($P > 0.05$). Rubisco activation state increased after 4h of recovery on experiment day 8, compared to control plants at the start of the experiment ($P = 0.0014$) and to heat stress plants on experiment day 3 ($P = 0.0044$).

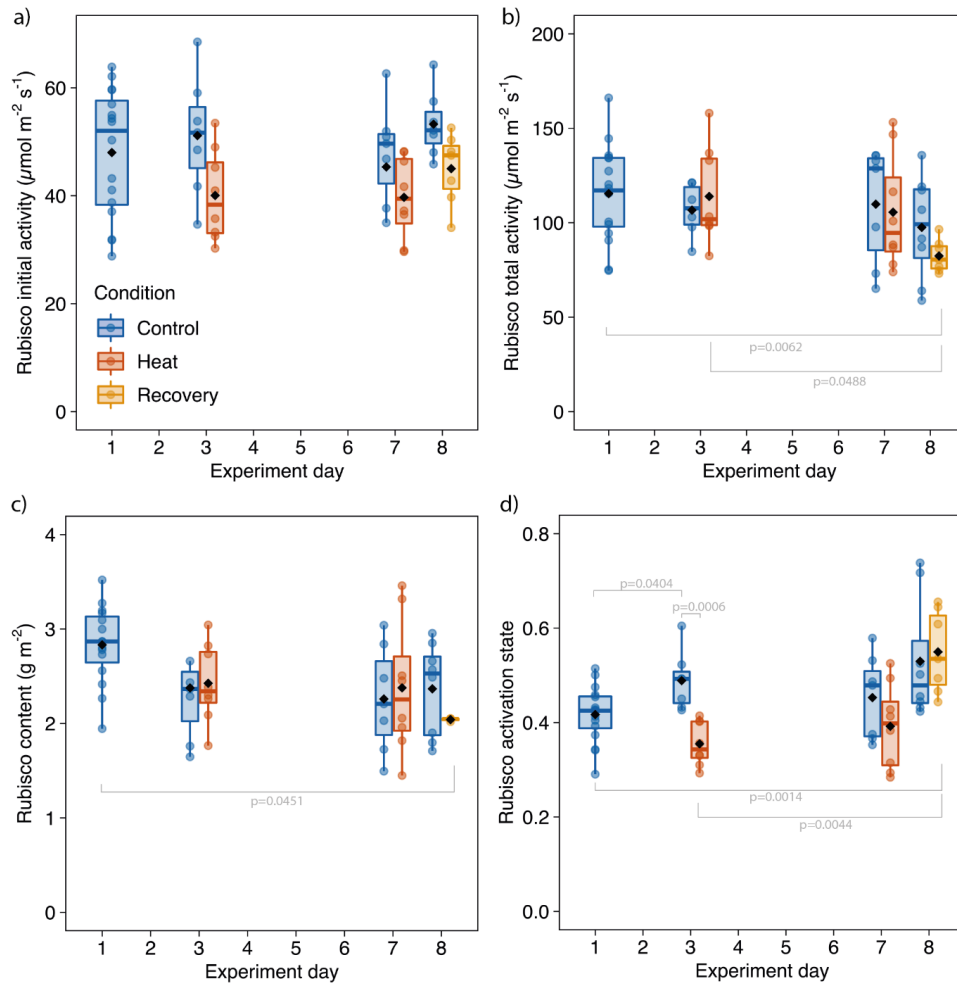


Figure 3. Rubisco activities and content in wheat plants under heat stress. Rubisco initial and total activities, content, and activation state in flag leaves of wheat plants exposed to control (25°C), heat (38°C), and recovery (25°C) conditions. Box lines represent the median, first and third quartiles, whiskers the range, black diamonds the mean, and circles individual samples ($n = 4-16$ biological replicates). Significant *P*-values for pairwise comparisons are shown (REML, $\alpha = 0.05$).

The activation state of Rubisco reflects the balance between inhibition due to binding of inhibitors to active sites, and activation via removal of such inhibitors by Rca and subsequent dephosphorylation of inhibitors by enzymes such as CA1Pase. The activity of CA1Pase remained constant in control plants throughout the experiment, showed a mild, non-significant increase after 5 days of heat stress and was significantly increased in recovery plants post heat stress, on experiment day 8 (Fig. 4; $P = 0.0442$). These results suggest increased capacity to dephosphorylate sugar-phosphate derivatives that would otherwise inhibit Rubisco activity upon stress relief.

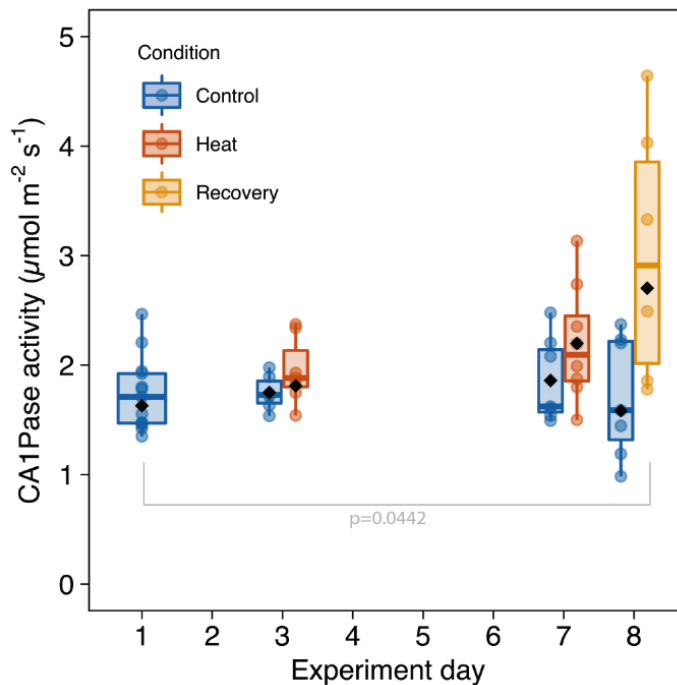


Figure 4. CA1Pase activity in wheat plants under heat stress. Activity of CA1Pase was measured in flag leaves of wheat plants exposed to control (25°C), heat (38°C), and recovery (25°C) conditions. Box lines represent the median, first and third quartiles, whiskers the range, black diamonds the mean, and circles individual samples ($n = 7-16$ biological replicates). Significant P -values for pairwise comparisons are shown (REML, $\alpha = 0.05$).

Wheat Rca isoforms differ in their regulatory and thermal properties (Scafaro *et al.*, 2019; Perdomo *et al.*, 2019; Degen *et al.*, 2020). Wheat flag leaves presented very little Rca1 β protein compared to both Rca2 β , which

was most abundant, and Rca2 α (Fig. 5). The amount of Rca1 β remained similar to control levels after 4 h of heat stress, but after 5 days of heat stress (68 h of cumulative heat), Rca1 β protein levels increased ca. 2.5-fold, and remained at this level the day after heat stress (4 h of recovery at control temperatures). Rca2 β and Rca2 α abundance remained similar between control and heat stress. The relative abundance of each wheat Rca isoform in the flag leaf highlighted that under control conditions Rca1 β was only 1% of the total Rca pool, and that Rca2 β was the most abundant isoform corresponding to more than 85% of the total Rca pool (Fig. 6). The relative abundance of Rca2 α appeared to decline slightly as the leaves aged (from experiment day 3 to experiment day 8), but this was not significant ($P > 0.05$). While the total Rca pool size (ca. $6.5 \pm 0.9 \text{ mg m}^{-2}$) was unaffected by heat stress, the relative abundance of Rca1 β increased from 1% in leaves under control conditions to 6% after 5 days of heat stress (Fig. 6, Fig. S5). The abundance of Rubisco active sites relative to total Rca monomers ($R_{A.S.}:Rca_{total}$) in wheat flag leaves did not change significantly throughout the experiment and remained at $103 \pm 11 \text{ mol R}_{A.S.} \text{ mol}^{-1} Rca_{total}$ (Table S5). Because of the increase in Rca1 β abundance during heat stress, the abundance of $R_{A.S.}:Rca1\beta$ decreased ca. 5-fold under heat stress.

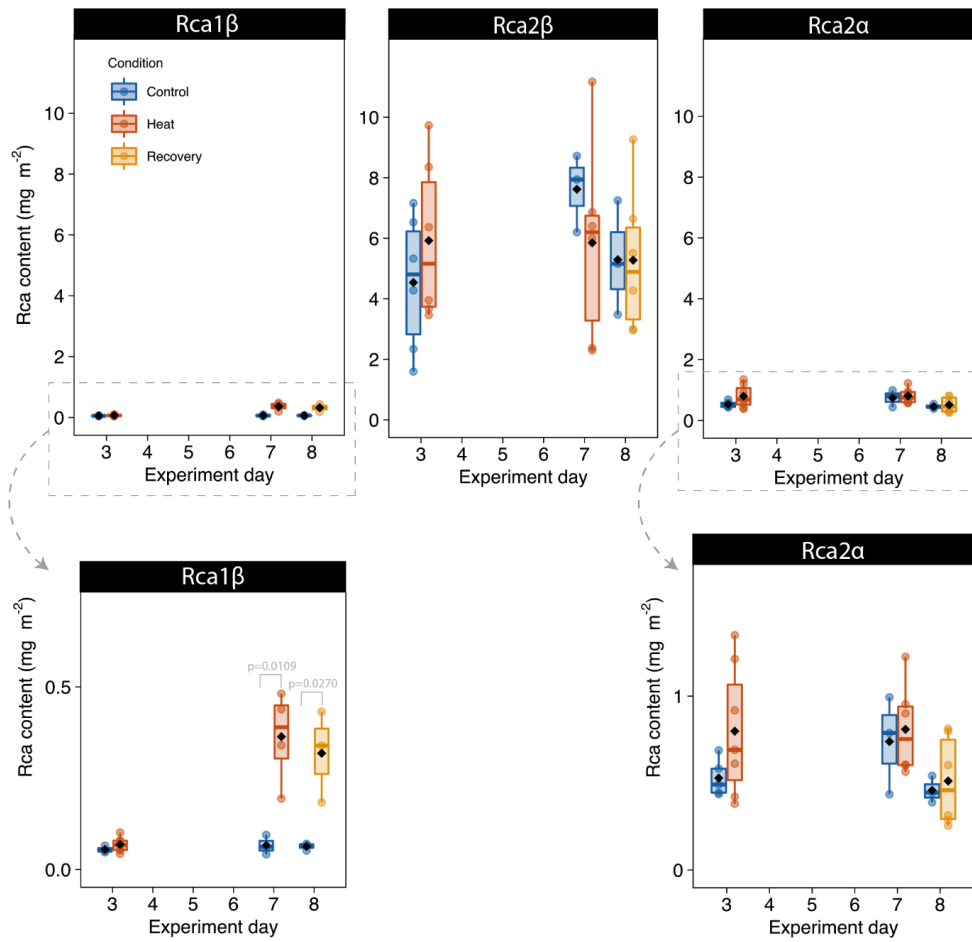


Figure 5. Rca protein amounts in wheat plants under heat stress. Protein levels in flag leaves of wheat plants exposed to control (25°C), heat (38°C), and recovery (25°C) conditions were quantified using Rca1β-specific and Rca polyclonal antibodies, and purified Rca proteins as standards (Fig. S2). Box lines represent the median, first and third quartiles, whiskers the range, black diamonds the mean, and circles individual samples ($n = 4-8$ biological replicates). Significant P -values for pairwise comparisons are shown (REML, $\alpha = 0.05$).

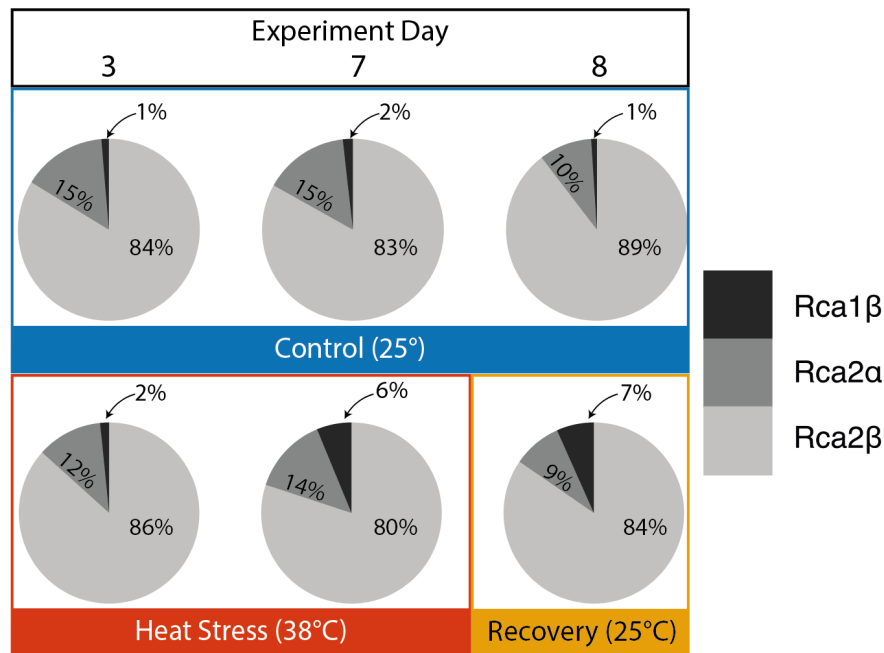


Figure 6. Relative abundance of *Rca* isoforms in wheat plants under heat stress. The abundance of *Rca1β*, *Rca2β* and *Rca2α* is shown as a percentage of the total *Rca* pool in flag leaves of wheat plants exposed to control (25°C), heat stress (38°C), and recovery (25°C) conditions.

The timing of changes in *Rca* gene expression during and post heat stress was investigated to assess whether gene expression might contribute to explain the observed changes in relative abundance of the three isoforms. Control plants showed virtually no expression of *Rca1β*, whereas heat-stressed plants showed a ca. 40-fold increase in *Rca1β* expression after 4 h of heat (Fig. 7). *Rca1β* expression was still increased relative to control plants after 5 days of heat stress exposure, and decreased to near-control levels the day after heat stress. By comparison, expression of the *Rca2* gene splice variants *Rca2β* and *Rca2α* showed less clear changes in response to heat stress. To investigate the possibility that heat responsive elements could be driving the change in *Rca1β* expression in response to heat stress, the promoter regions of *Rca* were investigated for presence of such elements based to consensus sequences identified by Jung *et al.* (2013). This revealed the presence of a heat responsive element upstream of *Rca1* genes in all three genomes and interestingly also upstream of the *Rca2* gene copy in the A genome only (Fig. S6).

The expression of other genes related to Rubisco function was investigated after 5 days of heat stress exposure only (experiment day 7; Fig. 7). Despite some heat stress plants showing higher values of *rbcL* expression, there were no significant differences in the expression of *ca1pase*, *rbcL* or *RbcS* genes between control and heat stress plants. The wheat genome encodes at least 25 *RbcS* genes (Table S2), which were divided into three groups based on sequence similarity (Fig. S7, Table S3). The relative expression of *RbcS G2* and *G3* was 4-fold higher than *G1*, and none of the groups showed changes in expression in response to heat stress. Based on data available in the gene expression atlas expVIP (Borrill *et al.*, 2016; Ramirez-Gonzalez *et al.*, 2018), *RbcS G3* appears to be the *RbcS* group most consistently highly expressed in all wheat plant organs, including roots, and across different plant developmental stages and growth conditions (Fig. S8). Interestingly, the predicted wheat RbcS G3 protein sequences share an isoleucine residue with the unusual T-type *RbcS1* variant from rice (Morita *et al.*, 2014; Pottier *et al.*, 2018), while the other wheat and rice RbcS isoforms share a valine in the same residue position (Fig. S9). The functional significance of this isoleucine residue and potential significance of RbcS presence in non-photosynthetic tissue could warrant further study.

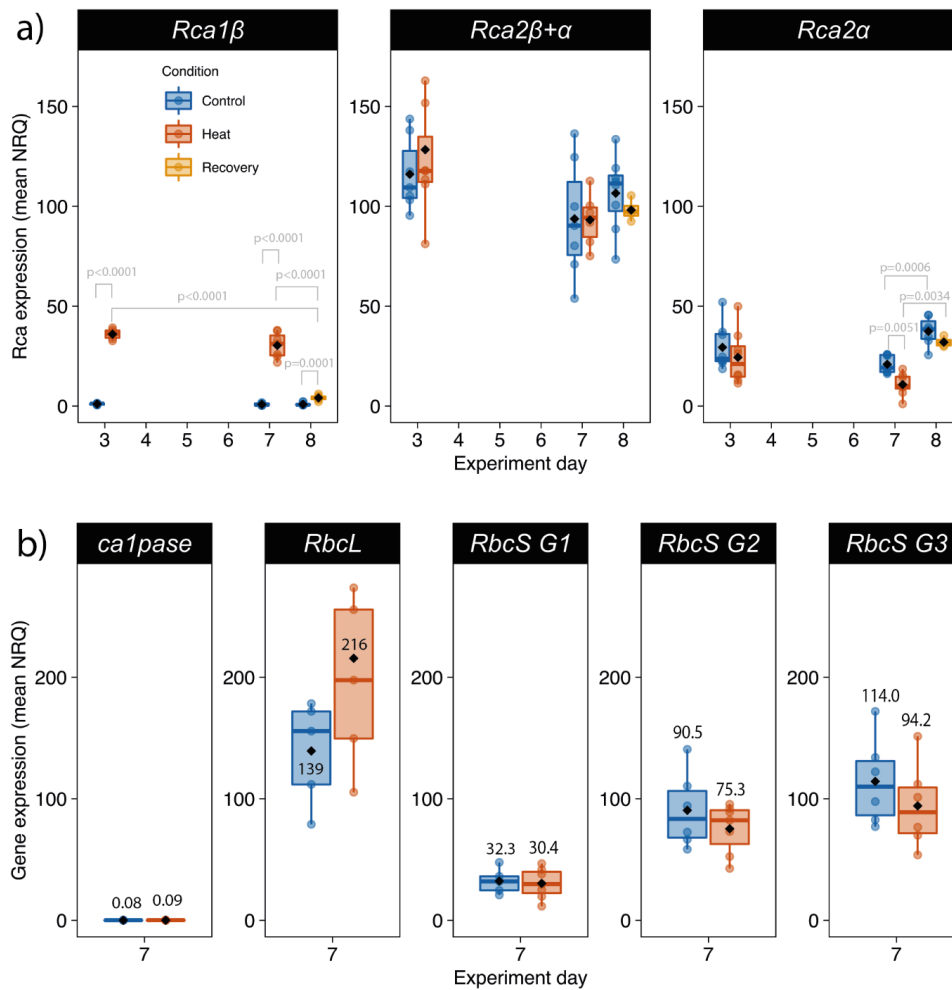


Figure 7. Relative expression of *Rca*, *ca1pase*, *RbcL* and *RbcS* genes in wheat plants under heat stress. Gene expression was determined in flag leaves of wheat plants exposed to control (25°C), heat (38°C), and recovery (25°C) conditions on experiment days 3, 7 and 8 for *Rca* (a), and solely on experiment day 7 for the other genes (b). Normalised relative quantification (NRQ) was estimated for each gene using both *Ta2291* and *Ta2776* as reference genes. Box lines represent the median, first and third quartiles, whiskers the range, black diamonds the mean, and circles individual samples ($n = 5-8$ biological replicates). Significant P -values for pairwise comparisons are shown (REML, $\alpha = 0.05$).

4.4 Discussion

Rubisco activation is sensitive to moderate heat stress due to the thermolabile nature of Rca (Salvucci *et al.*, 2001; Salvucci & Crafts-Brandner, 2004a,c; Scafaro *et al.*, 2012; 2016; Shivhare & Mueller-Cajar, 2017; Degen *et al.*, 2020). In wheat, the isoform Rca1 β has recently been shown to be more thermostable than the other two native isoforms, Rca2 β and Rca2 α (Scafaro *et al.*, 2019, Degen *et al.*, 2020). Here, pre-anthesis heat stress promoted a rapid increase in gene expression and a longer-term adaptive increase in protein abundance of Rca1 β compared to the less thermostable wheat Rca isoforms.

Wheat plants exposed to 38°C during the day had leaf temperatures around 28°C and showed a large (40-fold) increase in *Rca1 β* expression after 4 h heat stress, with expression remaining high after 5 days heat stress. These findings agree with previous studies in wheat (Law & Crafts-Brandner, 2001; Scafaro *et al.*, 2019). In cotton, there were no significant changes in either mRNA or protein levels of constitutive Rca β or Rca α isoforms, but an additional Rca isoform was found to account for 5% of the total Rca pool after 2 days heat stress (Law *et al.*, 2001). These findings suggest that synthesis of heat-inducible isoforms of Rca may occur and be wide-spread among plant species. The promoter region of the wheat gene *Rca1* contains a heat responsive element in all three genomes, whilst this is only present in the A genome for *Rca2*. These regions have been associated with increased *Rca* expression under heat stress in Arabidopsis (Jung *et al.*, 2013), and are likely related to the increased *Rca1 β* expression in wheat.

Rca1 β protein abundance did not increase significantly at the onset of heat stress (4 h), but increased 3-fold after 5 days heat stress. Young wheat plants at the 3rd leaf stage showed increased abundance of the 42 kDa protein (Rca1 β +Rca2 β) after 24-48 h exposure to a 38/34°C day/night heat stress (Law & Crafts-Brandner, 2001). The relative abundance of Rca1 β and Rca2 β was not assessed in that study, and was only assessed after 4 h and 5 days heat stress in the present study. Further research is required to test whether abundance of thermostable Rca1 β protein in wheat increases within 24 h of exposure to heat stress during the day and/or in response to elevated

temperatures during the night. The observed response might also differ between cultivars and wheat growth stages (Scafaro *et al.*, 2019). The much larger fold-change in Rca abundance at the transcript level compared to the protein level shows that gene expression and protein abundance are not directly coupled, and suggest that Rca protein abundance might be regulated by a post-transcriptional mechanism (Law & Crafts-Brandner 2001; Law *et al.*, 2001). Understanding such regulatory mechanisms warrants further investigation to inform efforts aimed at optimising Rca levels and Rubisco activation *in planta*.

Leaf temperatures in plants experiencing heat stress (Fig. 1c) closely matched the temperature optimum for Rubisco activation by Rca1 β *in vitro*, whereas in control plants leaf temperatures approximated those at which Rca2 β and Rca2 α are most active *in vitro* (Degen *et al.*, 2020). The activation state of Rubisco was lower after 4 h heat stress compared to control plants analysed on the same day, but after 5 days heat stress was not significantly different from control plants. It is possible that the increase in the abundance of the thermostable Rca1 β protein contributed to maintaining Rubisco activity during heat stress. It has recently been shown that while Rca2 β and Rca2 α become unable to activate Rubisco at moderately high temperatures (Scafaro *et al.*, 2019; Degen *et al.*, 2020), Rca1 β continues to operate at higher temperatures, but is relatively inefficient compared to the other two isoforms. An increase in Rubisco activation state was observed in both control plants and heat-stressed plants at the end of the experiment (following a 4 h recovery period under control conditions). As the wheat flag leaves age, decreasing Rubisco abundance can be accompanied by an increase in Rubisco activation state (Carmo-Silva *et al.*, 2017). In addition, increased Rubisco activation in recovery plants could also be partly explained by the increase in CA1Pase activity, decreasing the abundance of Rubisco inhibitors.

The properties of a particular Rca isoform can impact the overall properties of the Rca holoenzyme composed of a mixture of isoforms, both *in vitro* and *in vivo* (Zhang *et al.*, 2001; 2002). Scafaro *et al.* (2019) showed that the effects of mixing wheat Rca β isoforms *in vitro* were strongly temperature-dependent. At leaf temperatures up to ca. 30°C, it is possible that the small

increase in the relative abundance of Rca1 β in wheat flag leaves observed in the present study could confer stability to the Rca holoenzyme during heat stress. Testing this hypothesis more thoroughly warrants further detailed study as it raises the possibility that the combination of Rca isoforms present in the leaf might be adjustable to maximise overall efficiency of Rubisco activation in wheat. Importantly, our previous *in vitro* study highlighted that the two activities of Rca have different temperature optima, with fast rates of ATP hydrolysis continuing well above the moderately high temperatures that cause a 50% decrease in Rubisco activation rates (Degen *et al.*, 2020). ATP levels do not decrease under heat stress (Schrader *et al.*, 2004) and the ability of Rca to continue hydrolysing ATP above 30°C may act as a significant ATP sink during heat stress, contributing to prevent irreversible damage of thylakoid membranes (Sharkey & Zhang, 2010).

Catalytic misfire events by Rubisco increase with temperature, resulting in increased production of inhibitory sugar-phosphate derivatives (Schrader *et al.*, 2006; Parry *et al.*, 2008). *In vitro* inhibition of Rubisco by these compounds, termed fallover (Edmondson *et al.*, 1990), declines at high temperature due to a more flexible active site (Schrader *et al.*, 2006; Parry *et al.*, 2008). *In planta*, accumulation of these inhibitors is thought to occur under heat stress due to increased proportion of oxygenation to carboxylation and increased misfire events. Inhibitors that accumulate during heat stress may still be present in increased levels after plants are returned to control conditions, potentially preventing rapid recovery of Rubisco activity. CA1Pase metabolises sugar-phosphate derivatives (Andralojc *et al.*, 2012), and there was significantly more CA1Pase activity in wheat the day after heat stress compared to plants that did not experience heat stress, suggesting up-regulation of the capacity to restore Rubisco activity for continued carbon assimilation upon relief from stress.

In addition to regulation by Rca and CA1Pase, variations in Rubisco subunit composition have been proposed as a mechanism for adaption to growth temperature (Yoon *et al.*, 2001; Yamori *et al.*, 2006; Cavanagh & Kubien, 2013). Although expression of *rbcL* and *RbcS* groups was not significantly different between plants exposed to control temperatures and

heat stress, there was a trend for increased expression of *rbcL* and decreased expression of *RbcS G2* and *G3* under heat stress. These trends might become significant in wheat plants exposed to prolonged heat stress, and could result in altered Rubisco catalytic properties, as shown by Yamori *et al.* (2006). Rubisco is highly abundant (Ellis, 1979; Carmo-Silva *et al.*, 2015; Lobo *et al.*, 2019) and constituted 30-40% of the total soluble protein in the flag leaf of the wheat plants studied here. Therefore, variation in Rubisco subunit composition is likely to be a long-term adaptation response, in part because of the large amount of protein synthesis required. Changes in Rca and CA1Pase activity, on the other hand, could be regarded as a shorter-term mechanism for mitigating the impact of heat stress and maintaining Rubisco functionality.

Carbon assimilation decreased throughout heat stress exposure, and remained low the day after heat stress, which was accompanied by reduced stomatal conductance, in line with previous reports (Law & Crafts-Brandner, 1999; Galmés *et al.*, 2007; Silva-Pérez *et al.*, 2017; Lawson & Vialet-Chabrand, 2018). The intercellular CO₂ concentration (C_i) remained above 250 μmol mol⁻¹ throughout the experiment, which is well above the level thought to promote Rubisco decarbamylation and consequent inactivation (Galmés *et al.*, 2010). At high light, the transition of photosynthetic limitation by Rubisco activity to electron transport (and RuBP regeneration) has been reported to occur at C_i values around 300 μmol mol⁻¹ (Silva-Pérez *et al.*, 2017). At a non-saturating PPF of ~400 μmol mol⁻¹, used for both plant growth and gas-exchange measurements in this study, photosynthesis would be more likely limited by the rate of RuBP regeneration than by Rubisco activity (Lauerer *et al.* 1993, von Caemmerer 2000). The large decrease in A observed under heat stress cannot be directly compared to the observed effect of heat stress on productivity traits or Rubisco biochemistry, since gas-exchange was measured at a higher leaf temperature (ca. 37.1°C) than the leaf temperature of plants during the heat stress treatment (ca. 28.7°C). The 5-day heat stress treatment pre-anthesis significantly decreased plant grain weight at full maturity; a similar impact on grain yield was reported in wheat plants exposed to 5 days heat stress at anthesis (Chavan

et al., 2019). These findings support other studies suggesting that flag leaf photosynthesis makes a significant contribution towards grain yield (e.g. Carmo-Silva *et al.*, 2017). Heat priming wheat plants at pre-anthesis has been shown to result in reduced damage to the flag leaf and increased carbon assimilation in plants exposed to post-anthesis heat stress (Wang *et al.*, 2011). While the priming study was conducted at moderate heat stress (34/30°C day/night for 7 days), it suggests wheat plants can, to some extent, adapt to the growth temperature. However, current evidence and the findings reported herein suggest that isolated events of heat stress affecting flag leaf photosynthetic properties cause a significant decline in wheat productivity.

In summary, the biochemical and molecular responses of pre-anthesis wheat plants exposed to heat stress showed short-term increased gene expression and longer-term increased protein abundance of the more thermostable wheat Rca1 β isoform. These findings support previous wheat heat stress reports (Law & Crafts-Brandner, 1999; 2001; Silva-Pérez *et al.*, 2017; Yang *et al.*, 2020) and *in vitro* wheat Rca temperature responses (Scafaro *et al.*, 2019; Degen *et al.*, 2020) suggesting that Rubisco activity and regulation by Rca in wheat are primarily optimised for leaf temperatures between 20-25°C, but with room to improve climate resilience. Manipulation of the relative abundance of Rca isoforms, alongside introduction of superior forms of Rca, through breeding or genetic engineering, offers scope to make Rubisco regulation in wheat more resilient to an increasingly warm and variable climate.

4.5 References

- Andralojc PJ, Madgwick PJ, Tao Y, Keys A, Ward JL, Beale MH, Loveland JE, Jackson PJ, Willis AC, Gutteridge S, *et al.* 2012. 2-Carboxy-D-arabinitol 1-phosphate (CA1P) phosphatase: evidence for a wider role in plant Rubisco regulation. *Biochemical Journal* **442**: 733–742.
- Asseng S, Ewert F, Martre P, Rotter RP, Lobell DB, Cammarano D, Kimball BA, Ottman MJ, Wall GW, White JW, *et al.* 2015. Rising temperatures reduce global wheat production. *Nature Climate Change* **5**: 143–147.
- Atkin OK, Bruhn D, Hurry VM, Tjoelker MG. 2005. Evans Review No. 2: The hot and the cold: unravelling the variable response of plant respiration to temperature. *Functional Plant Biology* **32**: 87–105.
- Ayeneh A, van Ginkel M, Reynolds MP, Ammar K. 2002. Comparison of leaf, spike, peduncle and canopy temperature depression in wheat under heat stress. *Field Crops Research* **79**: 173–184.
- Barta C, Carmo-Silva E, Salvucci ME. 2011. Purification of Rubisco activase from leaves or after expression in *Escherichia coli*. *Methods in Molecular Biology* **684**: 363–374.
- Bauwe H, Hagemann M, Fernie AR. 2010. Photorespiration: players, partners and origin. *Trends in Plant Science* **15**: 330–336.
- Berry J, Bjorkman O. 1980. Photosynthetic Response and Adaptation to Temperature in Higher-Plants. *Annual Review of Plant Physiology* **31**: 491–543.
- Bhat JY, Miličić G, Thieulin-Pardo G, Bracher A, Maxwell A, Ciniawsky S, Mueller-Cajar O, Engen JR, Hartl FU, Wendler P, Hayer-Hartl M. 2017. Mechanism of enzyme repair by the AAA(+) chaperone Rubisco activase. *Molecular Cell* **67**: 744–756.e6.

- Borrill P, Ramirez-Gonzalez R, Uauy C. 2016.** expVIP: a customizable RNA-seq data analysis and visualization platform. *Plant Physiology* **170**: 2172–2186.
- Bracher A, Sharma A, Starling-Windhof A, Hartl FU, Hayer-Hartl M. 2015.** Degradation of potent Rubisco inhibitor by selective sugar phosphatase. *Nature Plants* **1**: 14002.
- Bradford MM. 1976.** A rapid and sensitive method for the quantitation of microgram quantities of protein utilizing the principle of protein-dye binding. *Analytical biochemistry* **72**: 248–254.
- Carmo-Silva AE, Salvucci ME. 2011.** The activity of Rubisco's molecular chaperone, Rubisco activase, in leaf extracts. *Photosynthesis Research* **108**: 143–155.
- Carmo-Silva E, Salvucci ME. 2012.** The temperature response of CO₂ assimilation, photochemical activities and Rubisco activation in *Camelina sativa*, a potential bioenergy crop with limited capacity for acclimation to heat stress. *Planta* **236**: 1433–1445.
- Carmo-Silva E, Andralojc PJ, Scales JC, Driever SM, Mead A, Lawson T, Raines CA, Parry MAJ. 2017.** Phenotyping of field-grown wheat in the UK highlights contribution of light response of photosynthesis and flag leaf longevity to grain yield. *Journal of Experimental Botany* **68**: 3473–3486.
- Carmo-Silva E, Gore MA, Andrade-Sanchez P, French AN, Hunsaker DJ, Salvucci ME. 2012.** Decreased CO₂ availability and inactivation of Rubisco limit photosynthesis in cotton plants under heat and drought stress in the field. *Environmental and Experimental Botany* **83**: 1–11.
- Carmo-Silva E, Scales JC, Madgwick PJ, Parry MAJ. 2015.** Optimizing Rubisco and its regulation for greater resource use efficiency. *Plant, Cell & Environment* **38**: 1817–1832.

- Cavanagh AP, Kubien DS. 2013.** Can phenotypic plasticity in Rubisco performance contribute to photosynthetic acclimation? *Photosynthesis Research* **119**: 203–214.
- Chavan SG, Duursma RA, Tausz M, Ghannoum O. 2019.** Elevated CO₂ alleviates the negative impact of heat stress on wheat physiology but not on grain yield. *Journal of Experimental Botany* **70**: 6447–6459.
- Cheng SH, Moore B, Seemann JR. 1998.** Effects of short- and long-term elevated CO₂ on the expression of ribulose-1,5-bisphosphate carboxylase/oxygenase genes and carbohydrate accumulation in leaves of *Arabidopsis thaliana* (L.) Heynh. *Plant Physiology* **116**: 715–723.
- Crafts-Brandner SJ, Salvucci ME. 2000.** Rubisco activase constrains the photosynthetic potential of leaves at high temperature and CO₂. *Proceedings of the National Academy of Sciences* **97**: 13430–13435.
- Degen GE, Worrall D, Carmo-Silva E. 2020.** An isoleucine residue acts as a thermal and regulatory switch in wheat Rubisco activase. *The Plant Journal* **103**: 742–751.
- Dusenge ME, Duarte AG, Way DA. 2019.** Plant carbon metabolism and climate change: elevated CO₂ and temperature impacts on photosynthesis, photorespiration and respiration. *New Phytologist* **221**: 32–49.
- Edmondson DL, Badger MR, Andrews TJ. 1990.** Slow inactivation of ribulosebisphosphate carboxylase during catalysis is not due to decarbamylation of the active site. *Plant Physiology* **93**: 1383–1389.
- Ellis RJ. 1979.** The most abundant protein in the world. *Trends in Biochemical Sciences* **4**: 241–244.
- Feller U, Crafts-Brandner S, Salvucci M. 1998.** Moderately high temperatures inhibit ribulose-1,5-bisphosphate carboxylase/oxygenase (Rubisco) activase-mediated activation of Rubisco. *Plant Physiology* **116**: 539–546.

- Frantz, J., Cometti, N., Bugbee, B. 2004.** Night temperature has a minimal effect on respiration and growth in rapidly growing plants. *Annals of Botany* **94**: 155–166.
- Galmés J, Capó-Bauçà S, Niinemets Ü, Iñiguez C. 2019.** Potential improvement of photosynthetic CO₂ assimilation in crops by exploiting the natural variation in the temperature response of Rubisco catalytic traits. *Current Opinion in Plant Biology* **49**: 60–67.
- Galmés J, Hermida-Carrera C, Laanisto L, Niinemets Ü. 2016.** A compendium of temperature responses of Rubisco kinetic traits: variability among and within photosynthetic groups and impacts on photosynthesis modeling. *Journal of Experimental Botany* **67**: 5067–5091.
- Galmés J, Medrano H, Flexas J. 2007.** Photosynthetic limitations in response to water stress and recovery in Mediterranean plants with different growth forms. *New Phytologist* **175**: 81–93.
- Galmés J, Ribas-Carbó M, Medrano H, Flexas J. 2010.** Rubisco activity in Mediterranean species is regulated by the chloroplastic CO₂ concentration under water stress. *Journal of Experimental Botany* **62**: 653–665.
- Gray SB, Dermody O, Klein SP, Locke AM, McGrath JM, Paul RE, Rosenthal DM, Ruiz-Vera UM, Siebers MH, Strellner R, et al. 2016.** Intensifying drought eliminates the expected benefits of elevated carbon dioxide for soybean. *Nature Plants* **2**: 16132.
- Hein NT, Wagner D, Bheemanahalli R, Šebela D, Bustamante C, Chiluwal A, Neilsen ML, Jagadish SK. 2019.** Integrating field-based heat tents and cyber-physical system technology to phenotype high night-time temperature impact on winter wheat. *Plant Methods* **15**: 41.
- Huner NPA, Hayden DB. 1982.** Changes in the heterogeneity of ribulosebiphosphate carboxylase–oxygenase in winter rye induced by cold hardening. *Canadian Journal of Biochemistry* **60**: 897–903.

- Huner NPA, Macdowall FD. 1979.** Changes in the net charge and subunit properties of ribulose biphosphate carboxylase–oxygenase during cold hardening of Puma rye. *Canadian Journal of Biochemistry* **57**: 155–164.
- Impa SM, Sunoj VJ, Krassovskaya I, Bheemanahalli R, Obata T, Jagadish SK. 2019.** Carbon balance and source-sink metabolic changes in winter wheat exposed to high night-time temperature. *Plant, Cell & Environment* **42**: 1233–1246.
- IPCC. 2014.** Climate change 2014. Mitigation of Climate Change—Working group III contribution to the fifth assessment report of the intergovernmental panel on climate change. *Cambridge University Press*.
- Jung H-S, Crisp PA, Estavillo GM, Cole B, Hong F, Mockler TC, Pogson BJ, Chory J. 2013.** Subset of heat-shock transcription factors required for the early response of Arabidopsis to excess light. *Proceedings of the National Academy of Sciences* **110**: 14474–14479.
- Ku SB, Edwards GE. 1977.** Oxygen inhibition of photosynthesis: I. Temperature dependence and relation to O₂/CO₂ solubility ratio. *Plant Physiology* **59**: 986–990.
- Kumar A, Li C, Portis AR. 2009.** *Arabidopsis thaliana* expressing a thermostable chimeric Rubisco activase exhibits enhanced growth and higher rates of photosynthesis at moderately high temperatures. *Photosynthesis Research* **100**: 143–153.
- Kurek I, Chang TK, Bertain SM, Madrigal A, Liu L, Lassner MW, Zhu G. 2007.** Enhanced thermostability of *Arabidopsis* Rubisco activase improves photosynthesis and growth rates under moderate heat stress. *The Plant Cell* **19**: 3230–3241.
- Lauerer M, Saftic D, Quick WP, Labate C, Fichtner K, Schulze E-D, Rodermel SR, Bogorad L, Stitt M. 1993.** Decreased ribulose-1,5-

bisphosphate carboxylase-oxygenase in transgenic tobacco transformed with “antisense” rbcS. *Planta* **190**: 332–345.

Law R, Crafts-Brandner S. 1999. Inhibition and acclimation of photosynthesis to heat stress is closely correlated with activation of ribulose-1,5-bisphosphate carboxylase/oxygenase. *Plant Physiology* **120**: 173–182.

Law RD, Crafts-Brandner SJ. 2001. High temperature stress increases the expression of wheat leaf ribulose-1,5-bisphosphate carboxylase/oxygenase activase protein. *Archives of Biochemistry and Biophysics* **386**: 261–267.

Law RD, Crafts-Brandner SJ, Salvucci ME. 2001. Heat stress induces the synthesis of a new form of ribulose-1,5-bisphosphate carboxylase/oxygenase activase in cotton leaves. *Planta* **214**: 117–125.

Lawson T, Vialet-Chabrand S. 2018. Speedy stomata, photosynthesis and plant water use efficiency. *New Phytologist* **221**: 93–98.

Leakey ADB, Press MC, Scholes JD. 2003. High-temperature inhibition of photosynthesis is greater under sunflecks than uniform irradiance in a tropical rain forest tree seedling. *Plant, Cell and Environment* **26**: 1681–1690.

Liu B, Asseng S, Müller C, Ewert F, Elliott J, Lobell DB, Martre P, Ruane AC, Wallach D, Jones JW, et al. 2016. Similar estimates of temperature impacts on global wheat yield by three independent methods. *Nature Climate Change* **6**: 1130–1136.

Lobo AKM, Orr DJ, Gutierrez MO, Andralojc PJ, Sparks C, Parry MAJ, Carmo-Silva E. 2019. Overexpression of *ca1pase* decreases Rubisco abundance and grain yield in wheat. *Plant Physiology* **181**: 471–479.

Long SP, Ainsworth EA, Leakey ADB, Nösberger J, Ort DR. 2006. Food for thought: lower-than-expected crop yield stimulation with rising CO₂ concentrations. *Science* **312**: 1918–1921.

- Morita K, Hatanaka T, Misoo S, Fukayama H. 2014.** Unusual small subunit that is not expressed in photosynthetic cells alters the catalytic properties of Rubisco in rice. *Plant Physiology* **164**: 69–79.
- Nagarajan R, Gill KS. 2018.** Evolution of Rubisco activase gene in plants. *Plant Molecular Biology* **96**: 69–87.
- Ogren W. 1984.** Photorespiration: pathways, regulation, and modification. *Annual Review of Plant Physiology*: 415–442.
- Paolacci AR, Tanzarella OA, Porceddu E, Ciaffi M. 2009.** Identification and validation of reference genes for quantitative RT-PCR normalization in wheat. *BMC Molecular Biology* **10**: 11–27.
- Parry MAJ, Keys AJ, Madgwick PJ, Carmo-Silva AE, Andralojc PJ. 2008.** Rubisco regulation: a role for inhibitors. *Journal of Experimental Botany* **59**: 1569–1580.
- Peraudeau S, Lafarge T, Roques S, Quiñones CO, Clement-Vidal A, Ouwerkerk PBF, Van Rie J, Fabre D, Jagadish KSV, Dingkuhn M. 2015.** Effect of carbohydrates and night temperature on night respiration in rice. *Journal of Experimental Botany* **66**: 3931–3944.
- Perdomo JA, Capó-Bauçà S, Carmo-Silva E, Galmés J. 2017.** Rubisco and Rubisco activase play an important role in the biochemical limitations of photosynthesis in rice, wheat, and maize under high temperature and water deficit. *Frontiers in Plant Science* **8**: 490.
- Perdomo JA, Degen GE, Worrall D, Carmo-Silva E. 2019.** Rubisco activation by wheat Rubisco activase isoform 2 β is insensitive to inhibition by ADP. *Biochemical Journal* **476**: 2595–2606.
- Perdomo JA, Sales CRG, Carmo-Silva E. 2018.** Quantification of photosynthetic enzymes in leaf extracts by immunoblotting. *Methods in Molecular Biology* **1770**: 215–227.

- Pfaffl MW. 2001.** A new mathematical model for relative quantification in real-time RT-PCR. *Nucleic Acids Research* **29**: e45–45.
- Porter JR, Gawith M. 1999.** Temperatures and the growth and development of wheat: a review. *European Journal of Agronomy* **10**: 23–36.
- Pottier M, Gilis D, Boutry M. 2018.** The hidden face of Rubisco. *Trends in Plant Science* **23**: 382–392.
- Prins A, Orr DJ, Andralojc PJ, Reynolds MP, Carmo-Silva E, Parry MAJ. 2016.** Rubisco catalytic properties of wild and domesticated relatives provide scope for improving wheat photosynthesis. *Journal of Experimental Botany* **67**: 1827–1838.
- R Core Development Team. 2013.** A language and environment for statistical computing. <http://www.r-project.org/>
- R Studio Team. 2019.** RStudio Cloud: Integrated Development for R. <https://www.rstudio.com/>
- Ramirez-Gonzalez RH, Borrill P, Lang D, Harrington SA, Brinton J, Venturini L, Davey M, Jacobs J, van Ex F, Pasha A, et al. 2018.** The transcriptional landscape of polyploid wheat. *Science* **361**: eaar6089.
- Rashid FAA, Scafaro AP, Asao S, Fenske R, Dewar RC, Masle J, Taylor NL, Atkin OK. 2020.** Diel and temperature driven variation of leaf dark respiration rates and metabolite levels in rice. *New Phytologist* <https://doi.org/10.1111/nph.16661>
- Ray DK, West PC, Clark M, Gerber JS, Prishchepov AV, Chatterjee S. 2019.** Climate change has likely already affected global food production. *PLoS ONE* **14**: e0217148.
- Ruiz-Vera UM, Siebers M, Gray SB, Drag DW, Rosenthal DM, Kimball BA, Ort DR, Bernacchi CJ. 2013.** Global warming can negate the expected

CO₂ stimulation in photosynthesis and productivity for soybean grown in the Midwestern United States. *Plant Physiology* **162**: 410–423.

Ruiz-Vera UM, Siebers MH, Drag DW, Ort DR, Bernacchi CJ. 2015. Canopy warming caused photosynthetic acclimation and reduced seed yield in maize grown at ambient and elevated [CO₂]. *Global Change Biology* **21**: 4237–4249.

Sadok W, Jagadish SK. 2020. The hidden costs of nighttime warming on yields. *Trends in Plant Science* **25**: 644–651.

Salvucci ME. 2008. Association of Rubisco activase with chaperonin-60 beta: a possible mechanism for protecting photosynthesis during heat stress. *Journal of Experimental Botany* **59**: 1923–1933.

Salvucci ME, Crafts-Brandner SJ. 2004a. Inhibition of photosynthesis by heat stress: the activation state of Rubisco as a limiting factor in photosynthesis. *Physiologia Plantarum* **120**: 179–186.

Salvucci ME, Crafts-Brandner SJ. 2004b. Relationship between the heat tolerance of photosynthesis and the thermal stability of Rubisco activase in plants from contrasting thermal environments. *Plant Physiology* **134**: 1460–1470.

Salvucci ME, Crafts-Brandner SJ. 2004c. Mechanism for deactivation of Rubisco under moderate heat stress. *Physiologia Plantarum* **122**: 513–519.

Salvucci ME, Osteryoung KW, Crafts-Brandner SJ, Vierling E. 2001. Exceptional sensitivity of Rubisco activase to thermal denaturation *in vitro* and *in vivo*. *Plant Physiology* **127**: 1053–1064.

Salvucci ME, Portis AR, Ogren WL. 1985. A soluble chloroplast protein catalyzes ribulosebisphosphate carboxylase/oxygenase activation *in vivo*. *Photosynthesis Research* **7**: 193–201.

- Scafaro AP, Atwell BJ, Muylaert S, Reusel BV, Ruiz GA, Van Rie J, Gallé A. 2018.** A thermotolerant variant of Rubisco activase from a wild relative improves growth and seed yield in rice under heat stress. *Frontiers in Plant Science* **871**: 1663.
- Scafaro AP, Bautsoens N, den Boer B, Van Rie J, Gallé A. 2019.** A conserved sequence from heat-adapted species improves Rubisco activase thermostability in wheat. *Plant Physiology* **181**: 43–54.
- Scafaro AP, Gallé A, Van Rie J, Carmo-Silva E, Salvucci ME, Atwell BJ. 2016.** Heat tolerance in a wild *Oryza* species is attributed to maintenance of Rubisco activation by a thermally stable Rubisco activase ortholog. *New Phytologist* **211**: 899–911.
- Scafaro AP, Yamori W, Carmo-Silva E, Salvucci ME, von Caemmerer S, Atwell BJ. 2012.** Rubisco activity is associated with photosynthetic thermotolerance in a wild rice (*Oryza meridionalis*). *Physiologia Plantarum* **146**: 99–109.
- Schrader SM, Kane HJ, Sharkey TD, von Caemmerer S. 2006.** High temperature enhances inhibitor production but reduces fallover in tobacco Rubisco. *Functional Plant Biology* **33**: 921–929.
- Schrader SM, Wise RR, Wacholtz WF, Ort DR, Sharkey TD. 2004.** Thylakoid membrane responses to moderately high leaf temperature in Pima cotton. *Plant, Cell & Environment* **27**: 725–735.
- Sharkey TD, Zhang R. 2010.** High temperature effects on electron and proton circuits of photosynthesis. *Journal of Integrative Plant Biology* **52**: 712–722.
- Sharwood RE, Ghannoum O, Kapralov MV, Gunn LH, Whitney SM. 2016.** Temperature responses of Rubisco from Paniceae grasses provide opportunities for improving C3 photosynthesis. *Nature Plants* **2**: 1–9.

- Shivhare D, Mueller-Cajar O. 2017.** In vitro characterization of thermostable CAM Rubisco activase reveals a Rubisco interacting surface loop. *Plant Physiology* **174**: 1505–1516.
- Silva-Pérez V, Furbank RT, Condon AG, Evans JR. 2017.** Biochemical model of C3 photosynthesis applied to wheat at different temperatures. *Plant, Cell & Environment* **40**: 1552–1564.
- Slattery RA, Ort DR. 2019.** Carbon assimilation in crops at high temperatures. *Plant, Cell & Environment* **42**: 2750–2758.
- Thomey ML, Slattery RA, Köhler IH, Bernacchi CJ, Ort DR. 2019.** Yield response of field-grown soybean exposed to heat waves under current and elevated [CO₂]. *Global Change Biology* **25**: 4352–4368.
- Vico G, Way DA, Hurry V, Manzoni S. 2019.** Can leaf net photosynthesis acclimate to rising and more variable temperatures? *Plant, Cell & Environment* **42**: 1913–1928.
- von Caemmerer S. 2000.** *Biochemical Models of Leaf Photosynthesis*. CSIRO Publishing.
- Walker BJ, VanLoocke A, Bernacchi CJ, Ort DR. 2016.** The costs of photorespiration to food production now and in the future. *Annual Review of Plant Biology* **67**: 107–129.
- Wang D, Li X-F, Zhou Z-J, Feng X-P, Yang W-J, Jiang D-A. 2010.** Two Rubisco activase isoforms may play different roles in photosynthetic heat acclimation in the rice plant. *Physiologia Plantarum* **139**: 55–67.
- Wang X, Cai J, Jiang D, Liu F, Dai T, Cao W. 2011.** Pre-anthesis high-temperature acclimation alleviates damage to the flag leaf caused by post-anthesis heat stress in wheat. *Journal of Plant Physiology* **168**: 585–593.

- Way DA, Yamori W. 2014.** Thermal acclimation of photosynthesis: On the importance of adjusting our definitions and accounting for thermal acclimation of respiration. *Photosynthesis Research* **119**: 89–100.
- Weis E. 1981.** Reversible heat-inactivation of the Calvin cycle: A possible mechanism of the temperature regulation of photosynthesis. *Planta* **151**: 33–39.
- Whitney SM, von Caemmerer S, Hudson GS, Andrews TJ. 1999.** Directed mutation of the Rubisco large subunit of tobacco influences photorespiration and growth. *Plant Physiology* **121**: 579–588.
- Wickham H. 2017.** *tidyverse: Easily install and load ‘Tidyverse’ packages.*
<https://www.tidyverse.org>
- Yamori W, Hikosaka K, Way DA. 2013.** Temperature response of photosynthesis in C3, C4, and CAM plants: temperature acclimation and temperature adaptation. *Photosynthesis Research* **119**: 101–117.
- Yamori W, Suzuki K, Noguchi KO, Nakai M, Terashima I. 2006.** Effects of Rubisco kinetics and Rubisco activation state on the temperature dependence of the photosynthetic rate in spinach leaves from contrasting growth temperatures. *Plant, Cell & Environment* **29**: 1659–1670.
- Yang Y, Zhang Q, Huang G, Peng S, Li Y. 2020.** Temperature responses of photosynthesis and leaf hydraulic conductance in rice and wheat. *Plant, Cell and Environment* **43**: 1437–1451.
- Yoon M, Putterill JJ, Ross GS, Laing WA. 2001.** Determination of the relative expression levels of rubisco small subunit genes in Arabidopsis by rapid amplification of cDNA ends. *Analytical Biochemistry* **291**: 237–244.
- Zhang N, Schürmann P, Portis AR. 2001.** Characterization of the regulatory function of the 46-kDa isoform of Rubisco activase from Arabidopsis. *Photosynthesis Research* **68**: 29–37.

Zhang N, Kallis RP, Ewy RG, Portis AR. 2002. Light modulation of Rubisco in Arabidopsis requires a capacity for redox regulation of the larger Rubisco activase isoform. *Proceedings of the National Academy of Sciences* **99**: 3330-3334.

4.6 Supporting Information

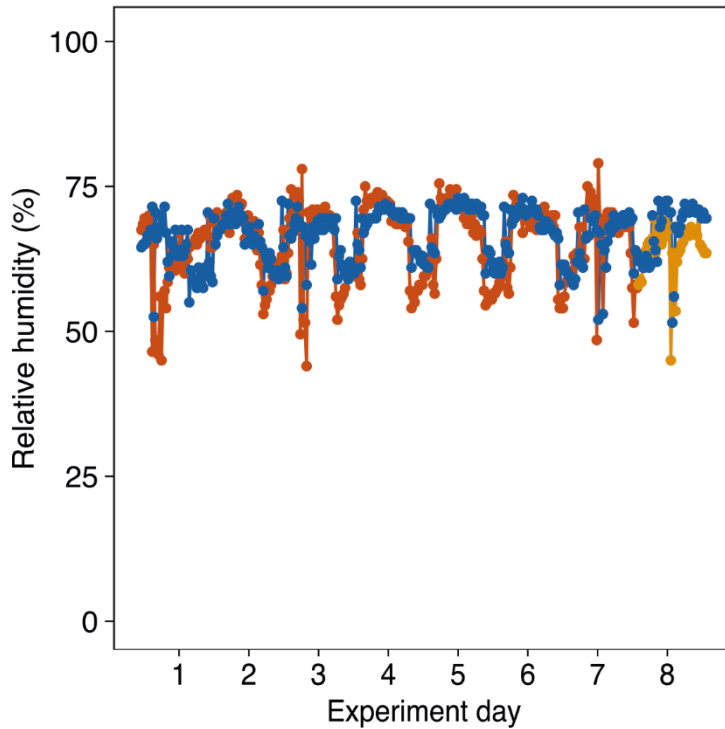


Fig. S1 Profile of relative humidity in the plant growth cabinets. Plants were grown at 25/18°C day/night (control conditions); at booting stage (experiment day 0), one of the two plant growth cabinets was set to 34/22°C for 1 day (experiment day 2) followed by 38/22°C for 5 days (heat stress, experiment days 3-7), then back to control temperatures (recovery, experiment day 8). Blue = control, red = heat stress, orange = recovery. Relative humidity in each cabinet was measured continuously throughout the heat treatment (OM-EL-USB temperature and humidity data logger, Omega Engineering, UK).

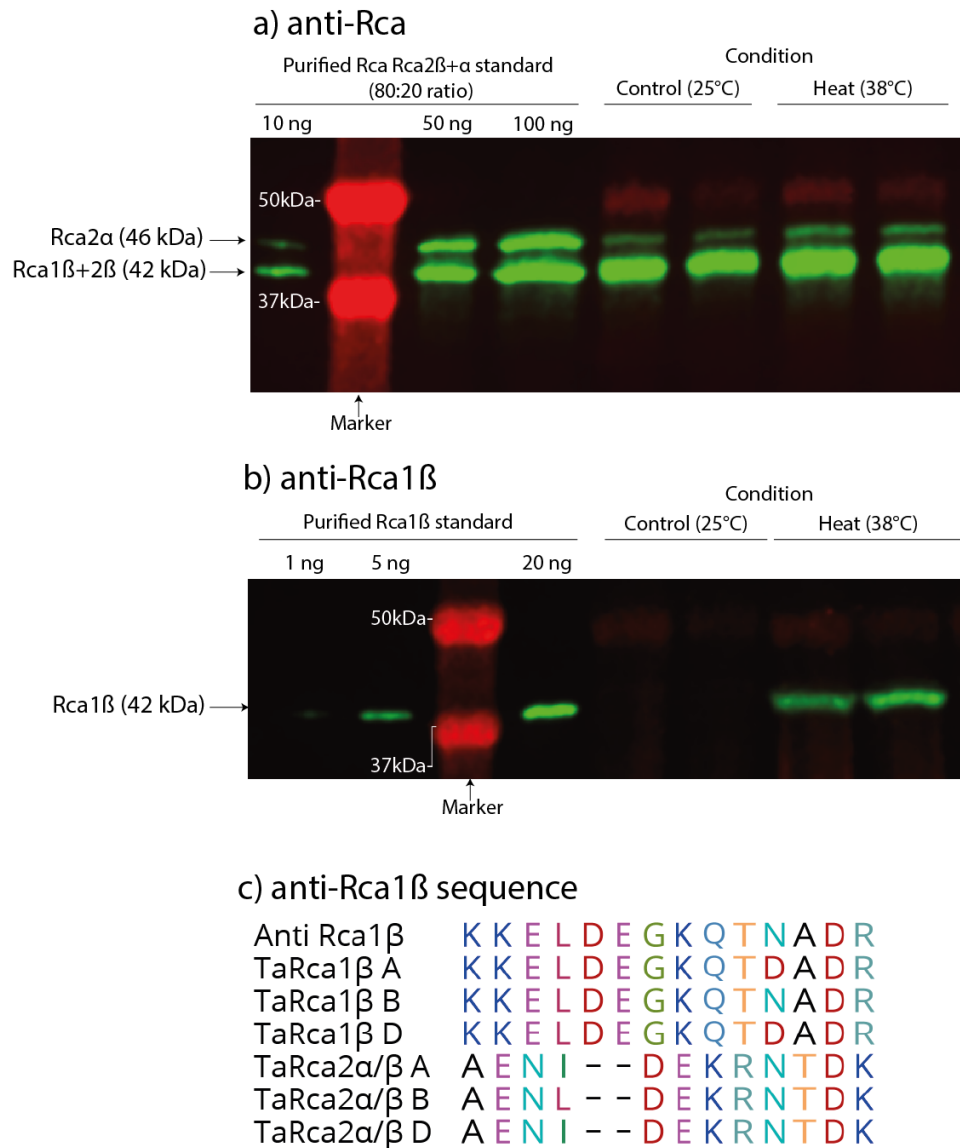


Fig. S2 Immunoblot detection and quantification of Rca using purified Rca standards. a) Detection of the three Rca isoforms using the polyclonal anti-Rca primary antibody. Purified Rca2 β + α (80:20 ratio) were used as a standard to quantify Rca in leaf samples. Two examples of control and heat stressed plants are shown. b) Detection of Rca1 β using a specific anti-Rca1 β antibody and purified Rca1 β as a standard. The same control and heat stress samples shown in a) were used to illustrate the ability to detect Rca1 β in leaf samples. c) The sequence alignment of the peptide used to produce the anti-Rca1 β antibody shows specificity to the N-terminal sequence of Rca1 β from wheat.

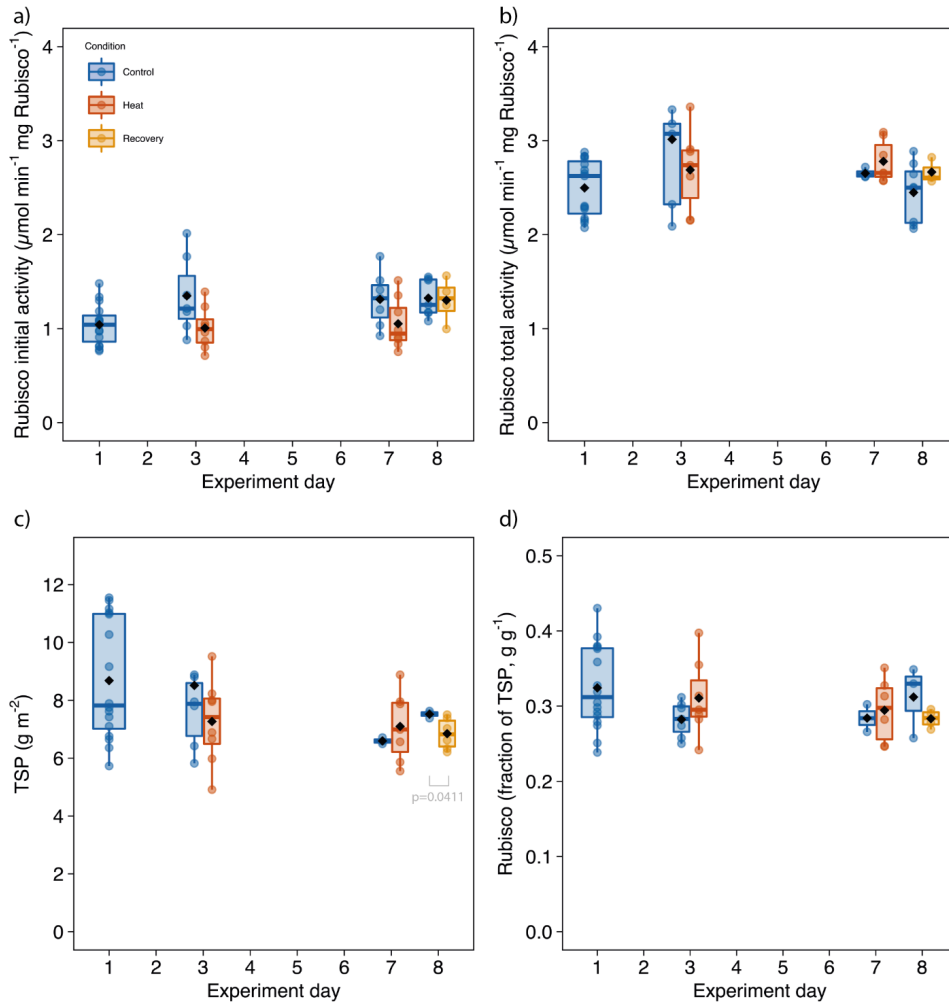


Fig. S3 Rubisco specific activities, total soluble protein and Rubisco content in wheat plants under heat stress. Rubisco (a) initial and (b) total activities per quantity of Rubisco, (c) total soluble protein (TSP) content and (d) Rubisco content as a fraction of TSP. Box lines represent the median, first and third quartiles, whiskers the range, black diamonds the mean, and circles individual samples ($n = 4-8$ biological replicates). Significant P-values for pairwise comparisons are shown (REML, $\alpha = 0.05$); there was no significant effect of treatment on the specific activity of Rubisco or the amount of Rubisco relative to TSP ($P > 0.05$).

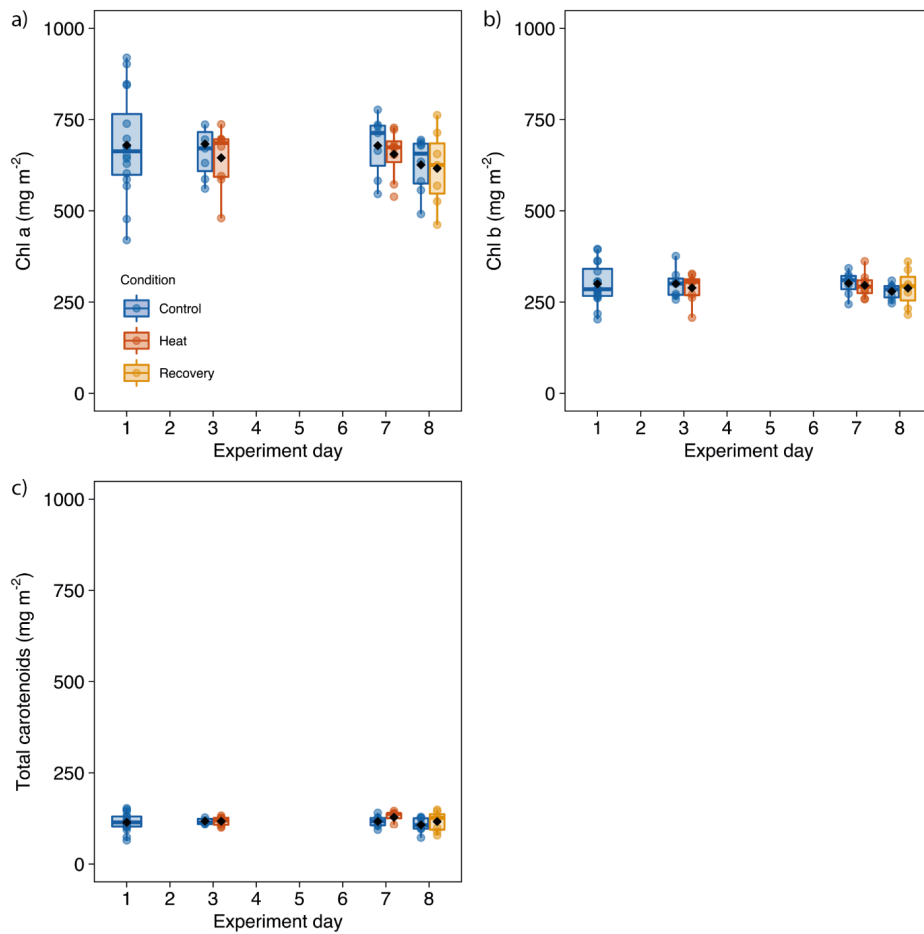


Fig. S4 Chlorophyll a, chlorophyll b and total carotenoids in wheat plants under heat stress. Chlorophyll (Chl) and carotenoid contents were quantified in flag leaves of wheat plants under control conditions, exposed to heat stress (experiment days 3 and 7) and upon recovery to control conditions (day 8). Box lines represent the median, first and third quartiles, whiskers the range, black diamonds the mean, and circles individual samples ($n = 4-8$ biological replicates). There was no significant effect of heat stress on chlorophyll and carotenoid levels (REML, $P > 0.05$).

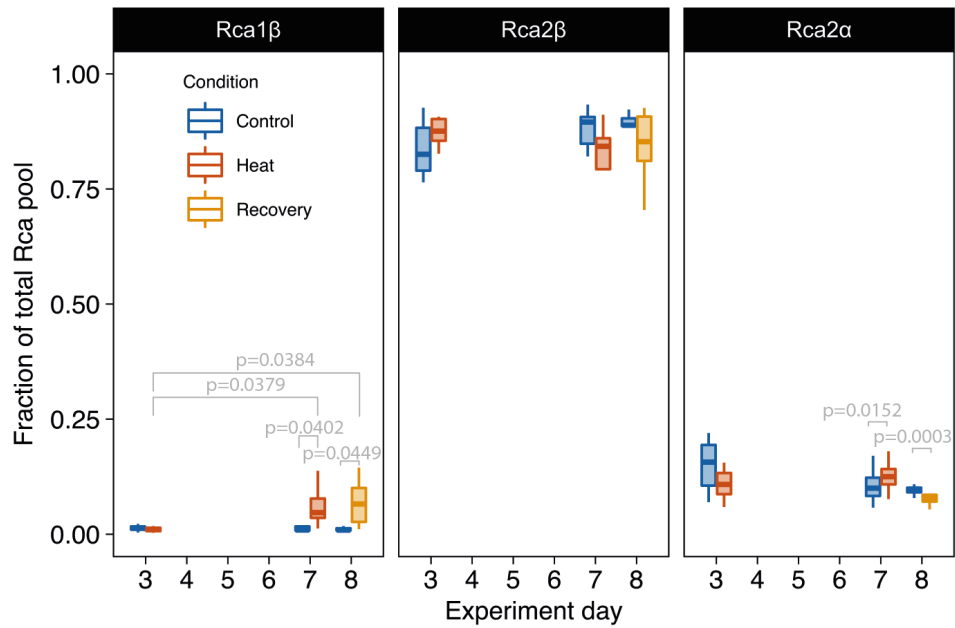


Fig. S5 Relative Rca isoform abundance in wheat plants under heat stress.

The abundance of Rca1 β , Rca2 β and Rca2 α is shown as a fraction of the total Rca pool in flag leaves of wheat plants exposed to control (25°C), heat stress (38°C) and recovery (25°C) conditions. Box lines represent the median, first and third quartiles, whiskers the range, and black diamonds the mean ($n = 3-8$ biological replicates). There was a significant effect of treatment for Rca1 β ($P < 0.05$), but not for Rca2 β and Rca2 α ($P > 0.05$). Significant P-values for pairwise comparisons are shown (REML, alpha = 0.05).

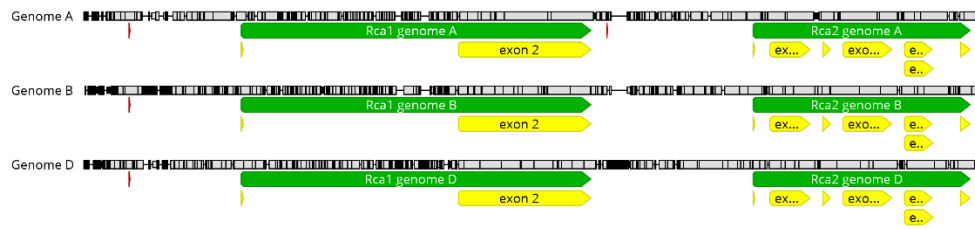


Fig. S6 Location of putative heat responsive elements in wheat *Rca* genes. Heat responsive elements are indicated in red and were identified based on consensus sequences identified in Jung *et al.* (2013). HSE2 was identified upstream of *Rca2 A* using the consensus sequence TTCnnGAA. HSE4 was identified upstream of *Rca1* copies from all three genomes using the consensus sequence TCCnnGAAnnTTC.

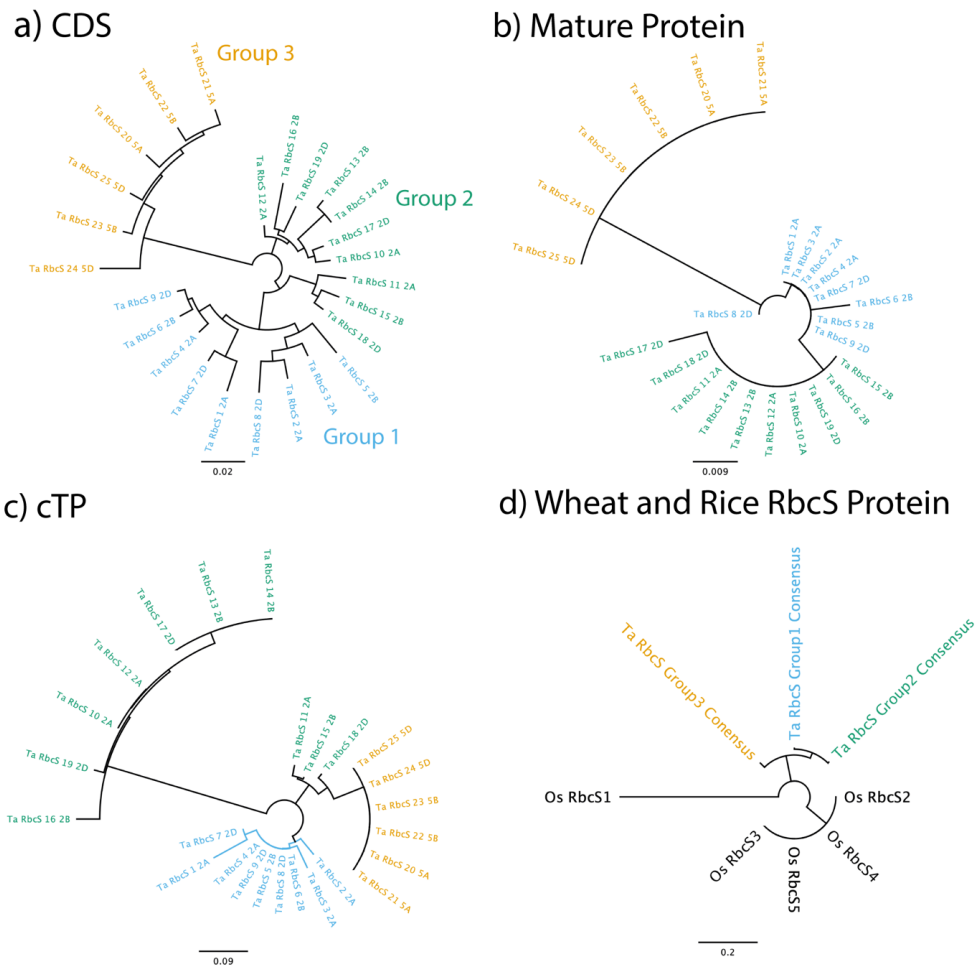


Fig. S7 Phylogenetics of wheat *RbcS*. Phylogenetic trees based on (a) the coding sequences (CDS) of *RbcS* genes in wheat, (b) the respective mature protein sequences, or (c) the chloroplast transit peptide (cTP) for each protein. (d) Phylogenetic relationships of wheat *RbcS* protein groups and rice *RbcS* protein isoforms. *RbcS* sequences were obtained from EnsemblPlants (accessions listed in Table S3) and phylogenetic trees built using the neighbour-joining method in Geneious 9.1.8. Black lines represent substitutions per site. Based on genetic similarity, wheat *RbcS* genes were divided into three groups (blue, green and yellow) for gene expression analysis.

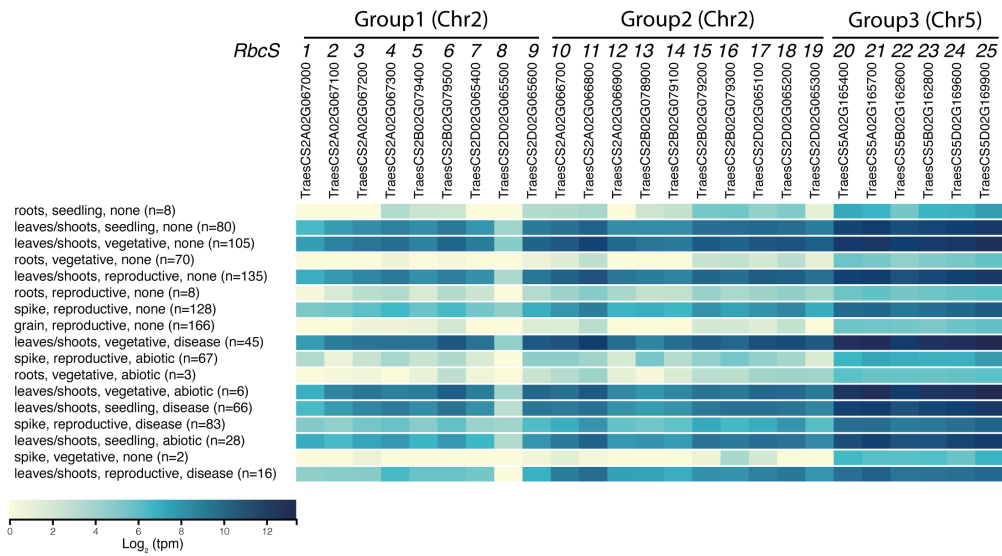


Fig. S8 *RbcS* gene expression in wheat. Gene expression data for each *RbcS* gene in different plant organs, at various growth stages and environmental conditions, as indicated to the left, was obtained from expVIP (<http://wheat-expression.com>). Colour scale indicates the Log_2 of transcripts per million (tpm).



Fig. S9 Alignment of RbcS protein sequences from rice and wheat. (a) Full sequences for each rice RbcS protein and consensus sequences for each of the three wheat RbcS protein groups are shown. The isoleucine residue at position 51 is highlighted in red. (b) Percentage of amino acid sequence similarity.

Table S1 MIQE guidelines for gene expression analyses.

MIQE guidelines (as per Bustin <i>et al.</i> 2009)	
Experimental design	
Definition of experimental and control groups	Experimental group: wheat plants exposed to heat stress, control group: wheat plants grown under control conditions
Number within group	8 biological replicates per group, consisting of 4 biological replicates from each of two replicate experiments. 2-3 technical replicates per biological replicate.
Sample	
Description	Leaf material from wheat plants
Processing	Leaf material was cut with a razor blade and immediately snap frozen in liquid nitrogen and stored at -80°C.
Nucleic acid extraction	
Procedure	Frozen leaf material was ground with a chilled pestle and mortar to a fine powder. 15-20 mg were used for RNA extraction.
Kit	NuceloSpin® Tri Prep kit (Macherey-Nagel, Düren, Germany)
DNase treatment	An on-column treatment included as part of the kit mentioned above. 95 µL DNase solution per sample for 15 min at room temperature.
RNA concentration, purity	Measured with SpectroStar Nano microplate reader (BMG Labtech GmbH, Ortenberg, Germany). RNA purity and yield were assessed by evaluating absorbance ratios at 260/280 and 260/230 nm; pure RNA was defined as 260/280 around 2.0 and 260/230 above 1.8, respectively.
Reverse transcription	
Complete reaction conditions	1 µg of RNA was added to a 10 µL reaction containing 1 µL of Oligo-dT primer, which was incubated for 5 min at 65°C and immediately cooled on ice. nanoScript™ buffer, dNTPs, RNase/DNAase free water and nanoScript2 were added according the instructions of the Precision nanoScript™ 2 Reverse Transcription kit (Primer design Ltd., Camberley, UK). The 20 µL reaction was incubated for 20 min at 42°C, followed

	by heat inactivation for 10 min at 75°C. cDNA was stored at -20 °C.
qPCR target information and qPCR oligonucleotides	
See table S2 for genes, primer sequences and product sizes and further information. Primers were manufactured by Sigma-Aldrich (Sigma-Aldrich Company Ltd, Gillingham, UK). Primers were purified by desalting.	
qPCR protocol	
qPCR conditions	95°C for 2 min, 40 cycles at 95°C for 15 sec and 60°C for 1 min
Melting curves	95°C for 1 min, 60°C for 30 sec and 95°C for 30 sec
Reaction volume and cDNA amount	15 µL, 40 ng
Master mix	PrecisionPLUS qPCR Master Mix (Primer design Ltd., Camberley, UK)
Nucleic acid extraction	
Procedure	Frozen leaf material was ground with a chilled pestil and mortar to a fine powder. 15-20 mg were used for RNA extraction.
Kit	NuceloSpin® Tri Prep kit (Macherey-Nagel, Düren, Germany)
DNase treatment	95 µL DNase per sample for 15 min at room temperature
RNA concentration, purity	Measured with SpectroStar Nano microplate reader (BMG Labtech GmbH, Ortenberg, Germany). RNA purity and yield were assessed by evaluating absorbance ratios at 260/280 and 260/230 nm; pure RNA was defined as 260/280 around 2.0 and 260/230 above 1.8, respectively.
Reverse transcription	
Complete reaction conditions	1 µg of RNA was added to a 10 µL reaction containing 1 µL of RT primer, which was incubated for 5 min at 65°C and immediately cooled on ice. nanoScript™ buffer, dNTPs, RNase/DNAase free water and nanoScript2 were added according the instructions of the Precision nanoScript™ 2 Reverse Transcription kit (Primer design Ltd., Camberley, UK). The 20 µL reaction was incubated for 20 min at 42°C, followed by heat inactivation for 10 min at 75°C. cDNA was stored at -20 °C.
qPCR target information and qPCR oligonucleotides	

See table S2 for genes, primer sequences and product sizes and further information. Primers were manufactured by Sigma-Aldrich (Sigma-Aldrich Company Ltd, Gillingham, UK). Primers were purified by desalting.	
qPCR protocol	
qPCR conditions	95°C for 2 min, 40 cycles at 95°C for 15 sec and 60°C for 1 min
Melting curves:	95°C for 1 min, 60°C for 30 sec and 95°C for 30 sec
Reaction volume and cDNA amount	15 µL, 40 ng
Master mix	PrecisionPLUS qPCR Master Mix (Primer design Ltd., Camberley, UK)
Primer concentration	0.467 µM
qPCR instrument	Mx3005P qPCR system (Stratagene Inc, Agilent Technologies, Stockport, UK)
qPCR validation	
Specificity	Melt curve
Primer efficiency/slope/y-intercept/R ² of linear regression of C _q /ln(cDNA)// C _q for NTC (threshold 350, NA where C _q was too low):	
<i>ca1pase</i>	1.85/-1.62/23.65/0.9960//NA
<i>Rca1β</i>	1.67/-1.96/16.73/0.9957//NA
<i>Rca2a+β</i>	1.61/-2.09/15.91/0.9941//35.63
<i>Rca2a</i>	1.82/-1.66/17.08/0.9952//34.93
<i>rbcL</i>	1.87/-1.59/13.73/0.9931//NA
<i>RbcSG1</i>	1.87/-1.59/15.32/0.9858//NA
<i>RbcSG2</i>	1.80/-1.70/14.26/0.9742//35.77
<i>RbcSG3</i>	1.78/-1.74/14.59/0.9896//NA
<i>Ta2291</i> (reference gene 1)	1.72/-1.85/19.70/0.9955//NA
<i>Ta2776</i> (reference gene 2)	1.77/-1.75/22.14/0.9986//NA
Data analysis	
qPCR analysis program	MxPro (Stratagene, Inc)
C _q determination	Followed protocol in the Manual
Normalisation method	As described by Rieu and Powers (2009)
Number and justification of choice of reference genes	Based on the recommendation by Paolacci <i>et al.</i> (2009). Two reference genes were chosen due to their high expression stability, including heat stress.

Statistical method	REML analysis to test significance of differences between treatments and experiment days.
--------------------	---

Table S2 Sequences of qPCR primers used in this study.

Gene	Accession no.	qPCR primer	Sequence	Product size
<i>ca1pas</i> <i>e</i>	Gen bank: HE603918	qGDCA1Pase _F	TATTCCTTCCAGGGGC TCTT	119
		qGDCA1Pase _R	AGCTCCCCGCACTGGGT AGT	
<i>Rca1β</i>	EnsemblPlants: TraesCS4B02G14 0200	qGDRca1_F	GCTTCTGCTTTTCRT CCAC	224
		qGDRca1_R	TGGTCRTCGGAGATGT CGTA	
<i>rbcL</i>	Gen bank: LN626616	qGDRbcL_F	TATCACATCGAGCCTG TTGC	146
		qGDRbcL_R	AGAGCACGTAGGGCTT TGAA	
<i>Rca2a</i>	EnsemblPlants: TraesCS4B02G14 0300	qGD011	GGGTGATGCTAACCAG GATG	117
		qGD010	GGGTCTGAAGTTCTTGG CAGT	
<i>Rca2β</i> <i>+a</i>	0300	GD009	GACTTCGACAACACCA TGGG	146
		GD008	TTTCCTTGACCCTTGC CTCC	
	See Table S4	RbcS1_F	AGATGCATGCAGGTGT GG	173

<i>RbcS</i> (Group 1)		RbcS1_R	CTGTTGTGCTCACGGA AGAC	
<i>RbcS</i> (Group 2)		RbcS2_F	CGGAAGGATCAGGTGC AT	138
		RbcS2_R	CAGGGCACCCACTTKG AG	
<i>RbcS</i> (Group 3)		RbcS3_F	AACGGTGGAAGGATCA GGT	183
		RbcS3_R	GTGCTCACGGAAGATR AACC	

Table S3 Wheat *RbcS* gene groups. Genes that were annotated as *RbcS* on EnsemblPlants were divided into three groups according to their phylogenetic similarity. For each *RbcS* group, one primer pair was designed to amplify all genes in the group.

<i>RbcS</i> gene	Genome	EnsemblPlants accession code	Group
1	2A	TraesCS2A02G067000	1
2	2A	TraesCS2A02G067100	1
3	2A	TraesCS2A02G067200	1
4	2A	TraesCS2A02G067300	1
5	2B	TraesCS2B02G079400	1
6	2B	TraesCS2B02G079500	1
7	2D	TraesCS2D02G065400	1
8	2D	TraesCS2D02G065500	1
9	2D	TraesCS2D02G065600	1
10	2A	TraesCS2A02G066700	2
11	2A	TraesCS2A02G066800	2
12	2A	TraesCS2A02G066900	2
13	2B	TraesCS2B02G078900	2
14	2B	TraesCS2B02G079100	2
15	2B	TraesCS2B02G079200	2
16	2B	TraesCS2B02G079300	2
17	2D	TraesCS2D02G065100	2
18	2D	TraesCS2D02G065200	2
19	2D	TraesCS2D02G065300	2
20	5A	TraesCS5A02G165400	3
21	5A	TraesCS5A02G165700	3
22	5B	TraesCS5B02G162600	3
23	5B	TraesCS5B02G162800	3
24	5D	TraesCS5D02G169600	3
25	5D	TraesCS5D02G169900	3

Table S4 Comparison of wheat plants in the two cabinets prior to heat stress. Plants in each of the two plant growth cabinets were analysed prior to the onset of heat stress, when both cabinets were set to 25°C. Values are means \pm SEM. There was no significant effect of cabinet on gas-exchange and biochemical traits (two-sided t-test, $P > 0.05$), showing that the plants in the two plant growth cabinets were comparable prior to heat stress treatment.

Treatment	<i>n</i>	Net CO₂ assimilation ($\mu\text{mol m}^{-2} \text{s}^{-1}$)	Rubisco activation state (%)	Rubisco content (g m^{-2})
Control	6- 8	17.5 \pm 0.5	0.4 \pm 0.1	2.6 \pm 0.6
Heat stress	5- 8	17.0 \pm 0.8	0.4 \pm 0.1	3.0 \pm 0.3
<i>P-value</i>		0.2316	0.4077	0.2584

Table S5 Ratio of Rubisco active sites to Rca (R_{A.S.}:Rca) in wheat flag

leaves. The amounts of Rubisco and Rca were converted to mol active sites (R_{A.S.}) and mol monomer, respectively, and expressed per leaf area. The ratios of R_{A.S.} to each individual Rca isoform and to the total Rca amount in the flag leaves of wheat plants under control (25°C) and heat (38°C) conditions were calculated for experiment days 3, 7 and 8. Values are means ± SEM ($n = 3-8$ biological replicates). R_{A.S.}:Rca1 β was significantly lower in heat stress compared to control plants in experiment days 7 (** $P < 0.0001$) and 8 (** $P = 0.0028$); the ratios of R_{A.S.}:Rca2 β , R_{A.S.}:Rca2 α , and R_{A.S.}:Rca_{total} were not significantly affected by heat stress (REML, $P > 0.05$).

Exp. day	Condition	n	R _{A.S.} :Rca1 β	R _{A.S.} :Rca2 β	R _{A.S.} :Rca2 α	R _{A.S.} :Rca _{total}
3	Control	7	10937±1436	172±54	1194±156	145±41
	Heat	8	10714±1160	137±25	1112±189	117±20
7	Control	7	10453±3105	72±8	852±100	65±7
	Heat	8	1716±394***	138±43	726±68	104±27
8	Control	8	8594±867	102±4	1236±35	93±3
	Recovery	7	1779±346**	104±14	1283±251	91±11

5. Chapter 5: Low genetic diversity in cereal Rubisco activase might still offer scope for crop improvement

Abstract

Rubisco activase (Rca) plays a central role in the regulation of carbon assimilation. The three isoforms present in wheat differ in regulatory properties and thermal optimum. The thermostable Rca1 β is only expressed during heat and contains an isoleucine switch that increases the temperature optimum. Here, we explored the possibility that wheat wild relatives would show genetic diversity in Rca that would be exploitable for crop improvement. The expression of Rca in wheat was comparable between the three genomes in the most highly expressed isoforms, Rca2 β and Rca2 α . Rca1 β was characterised by low expression levels, which increased slightly under abiotic stress. The three isoforms were highly conserved showing only 1-5 amino acid differences between wheat, wild relatives and the crop relatives rye and barley, across the whole protein sequence. The isoforms encoded by the B genome of bread wheat presented most of the variation, with the A and D genome encoding near identical Rca proteins that closely resemble the isoforms in the bread wheat wild relative progenitors. Interestingly, the Rca isoforms present in cultivated rice, a warm-adapted species, were more similar to Rca1 β than Rca2 β . The findings show that genetic diversity in Rca is limited but might be exploitable for enhancing wheat resilience to global warming.

5.1 Introduction

Adaption of crops to fast-changing environments is vital given the threat posed by global climate change on crop yields (Ray *et al.*, 2012; 2019). Breeding has narrowed genetic diversity of crops over time, therefore wild relatives and locally adapted varieties, called landraces, have been suggested as a resource for crop improvement (Wingen *et al.*, 2014; King *et al.*, 2017b; Zaïm *et al.*, 2017; King *et al.*, 2017a).

Bread wheat (*Triticum aestivum*) is a hexaploid cereal and the product of natural hybridisation as shown by Marcussen *et al.* (2014). It contains the diploid genomes A, B and D, which derived from its progenitors and are related to wheat wild relatives that still occur in nature. Three hybridisation events contributed to the hexaploid nature of wheat. Firstly, the formation of *Aegilops tauschii* (DD genome) by homoploid hybrid speciation of *Triticum urartu* (AA genome) and a relative of *Aegilops speltoides* (BB genome) ca. 5.5 million years ago (mya). *T. urartu* and the relative of *Ae. speltoides* then formed the allotetraploid *Triticum durum* (AABB genome, also known as pasta wheat) ca 0.8 mya. Finally, the hybridisation of *T. durum* and *Ae. tauschii* gave rise to the hexaploid *T. aestivum* (AABBDD) ca. 0.4 mya. Analysis of gene distribution showed that the three sub-genomes have 99% similarity, 35% of genes are located on the B genome, whereas the A and D genomes contain 33% and 32%, respectively (Mayer *et al.*, 2014).

Despite the high similarity between the three bread wheat genomes and between each genome and their wild relative progenitors, adaption to local environments requires fine-tuning of plant metabolism. This either requires a change in gene and protein expression levels or adaption via mutations to increase fitness. For example, wild emmer (*T. turgidum*) populations show increased mutation and selection in response to global warming (Fu *et al.*, 2019) and a screen of *Aegilops* species showed high tolerance to heat stress (Pradhan *et al.*, 2012). Furthermore, diversity in drought-adaption of Mexican land races has been shown to exist, which were attributed to improved water extraction by roots and superior water use efficiency (Reynolds *et al.*,

2007). These findings emphasise the potential of wheat wild relatives and cultivar diversity as a resource for crop improvement.

The photosynthetic machinery can adapt to environmental factors such as temperature (Berry & Bjorkman, 1980) and diversity has been observed in Rubisco catalytic properties of wheat wild relatives and domesticated wheat (Prins *et al.*, 2016). Specifically, Prins *et al.*, (2016) showed that *Hordeum vulgare* and *Ae. cylindrica* had higher Rubisco carboxylation velocities at 25 and 35°C compared to other species, and this was possibly associated with a specific amino acid change from lysine to glutamine at position 14 of the Rubisco large subunit compared to Cadenza wheat. This highlights the impact a single amino acid change can have on catalytic properties and temperature response of an enzyme. Similarly, an isoleucine residue in wheat Rubisco activase (Rca) has been shown using directed mutagenesis to contribute to increased thermostability of Rubisco activase (Degen *et al.*, 2020)Chapter 3).

In this chapter we investigated the hypothesis that wheat wild relatives would present significant diversity in Rubisco activase that may be exploitable to enhance the resilience of wheat crop production to climate change. Firstly, publicly available gene expression data was used to compare the expression of the *T. aestivum* Rca isoforms encoded by the three genomes. This was followed by a gene sequence analysis of the wheat Rca isoforms alongside Rca isoforms of wheat wild relatives, including the crop progenitors, and the cereal crop relatives rye, barley and rice.

5.2 Results

5.2.1 Wheat Rca gene expression

Rca gene expression of the three wheat sub-genomes A, B and D was determined by using data available in the wheat expression atlas expVIP (Borrill *et al.*, 2016; Ramirez-Gonzalez *et al.*, 2018). Rca transcript IDs and homoeologues of Rca genes were identified on EnsemblPlants (Howe *et al.*, 2019). In order to differentiate Rca expression across plant tissues and between control and abiotic stress, four studies were selected (Fig. 1). Data consists of expression levels for roots, leaves/shoots, spikes and grains under control conditions (or in the absence of stress, i.e. “none” in Fig. 1) and for leaves/shoots under abiotic stress consisting of heat and drought conditions (“abiotic” in Fig. 1). A total of 17 transcripts were found for the three wheat Rca isoforms, including one in each genome for *Rca1 β* , one to seven transcripts per genome for *Rca2 β* , and one to two transcripts per genome for *Rca2a*. Some transcripts were much less expressed than others, but significant expression was observed for more than one *Rca2 β* transcript in genomes A and D. The presence of multiple transcripts was based on predictions from EnsemblPlants and do not necessarily result in multiple Rca isoforms.

Studies selected:

- ✓ Grain tissue-specific developmental timecourse
- ✓ Developmental time-course of Chinese Spring
- ✓ Chinese Spring leaves and roots from seven leaf stage
- ✓ Drought and heat stress time-course in seedlings

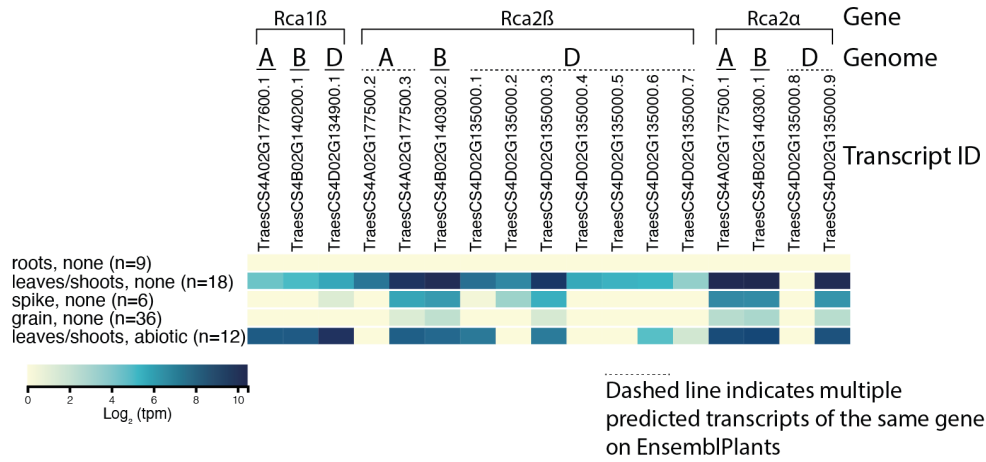


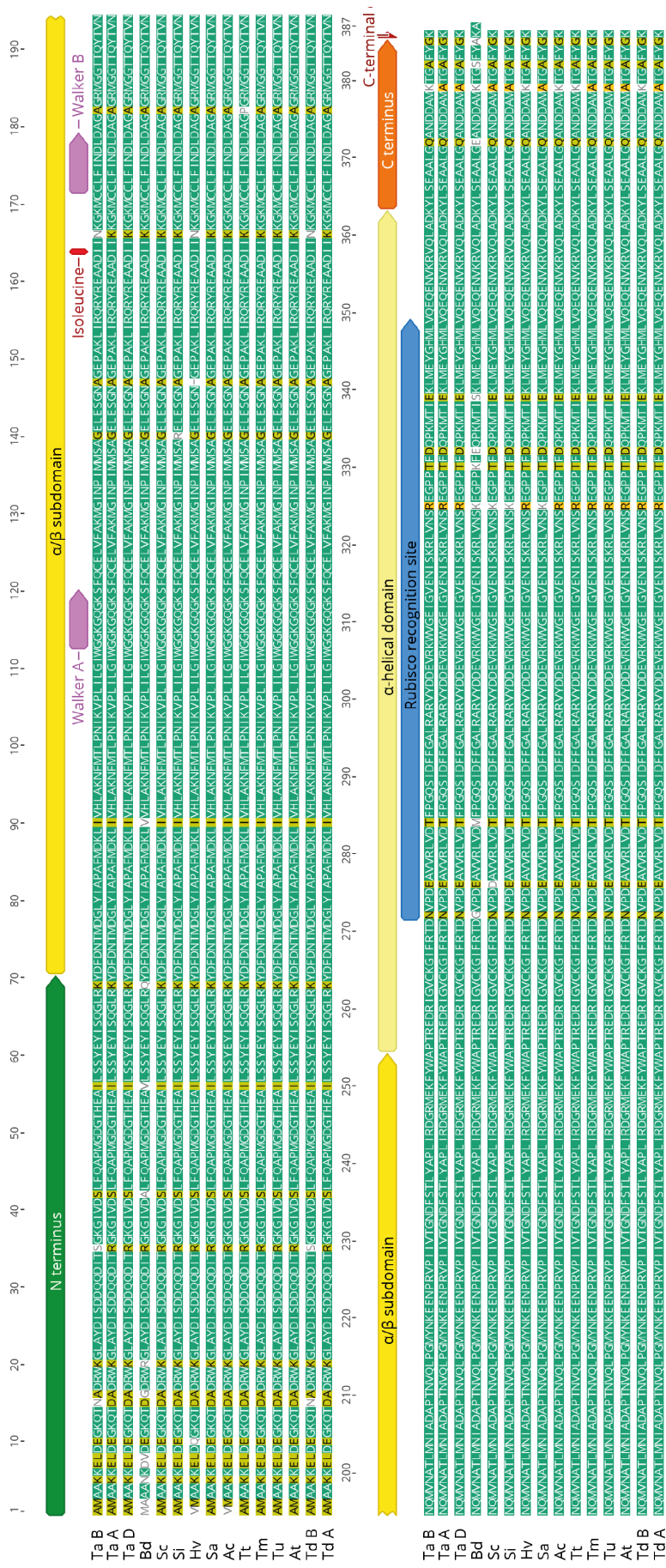
Fig. 1. Gene expression of Rca isoforms of the three wheat sub-genomes A, B and D. Data was obtained from expVIP. The colour scale indicates the log₂ of transcript per millions (tpm). Four tissue types were selected for control conditions (“none”) and leaves/shoots was selected for abiotic stress conditions. Transcript IDs of Rca isoforms were obtained from EnsemblPlants.

Rca expression was absent in roots and was primarily detected in leaves and shoots, with significant expression also detected in spikes and to a lesser extent in grains (Fig. 1). *Rca1β* showed significant expression in leaves and shoots under non-abiotic (control) conditions, with expression showing a gradient from the A genome (lowest) to the D genome (highest). During abiotic stress, expression in leaves and shoots increased substantially compared to control conditions. *Rca2a* and *Rca2β* were more highly expressed than *Rca1β* and also showed highest expression in the leaves and shoots than in spikes or grains under control conditions. Overall, expression of *Rca2a* and *Rca2β* was comparable across genomes A, B and D, appeared to decrease under abiotic stress compared to control conditions. Where multiple transcripts were present, these showed different expression across tissues and during abiotic stress.

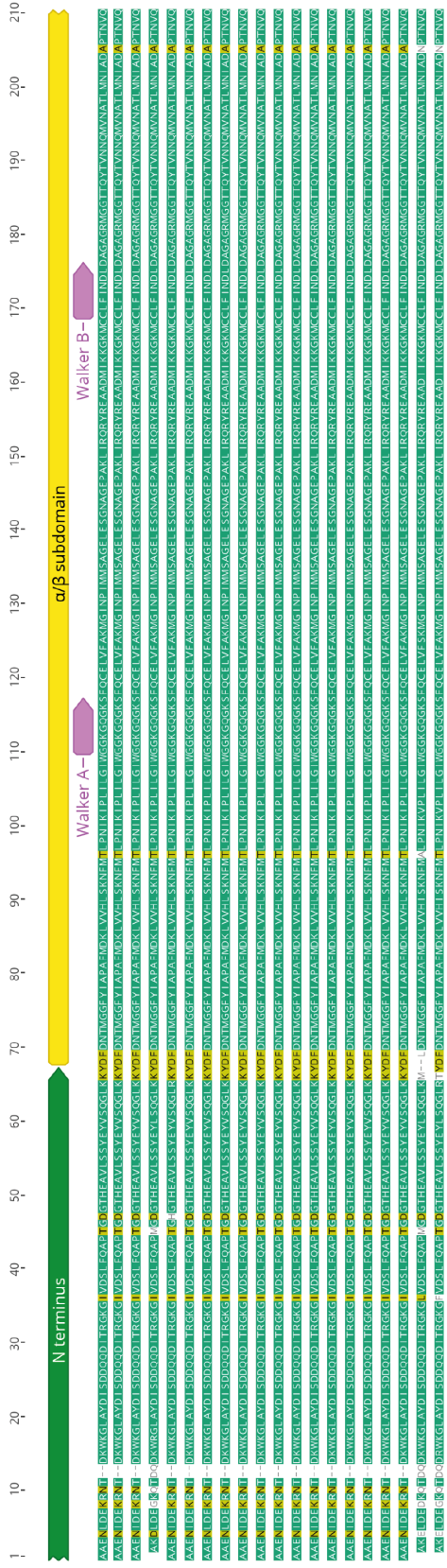
5.2.2 Rca genetic diversity in wheat and its wild relatives

In order to establish genetic diversity of Rca, genes of wheat wild relatives were sequenced. Predicted mature protein sequences of Rca1 β from the *T. aestivum* A and D genomes and from their respective donor species as well as *T. monococcum* were identical (Fig. 2A, 3A). The B genome copy, however, presented a few amino acid differences and was more similar to *H. vulgare* and *Ae. caudata*. Sequences of Rca2 β and Rca2 α were highly conserved between wheat wild relatives, with only 3 (β) and 5 (α) amino acid residues differing between *T. aestivum* and *H. vulgare*, and 1 amino acid residue differing between *T. aestivum* and *Ae. speltooides* (Fig. 2B, 3B, 3C). Rca2 sequences of each genome were (near) identical to the respective genome donors (Fig. 3B, 3C), *T. urartu* A genome (Mayer *et al.*, 2014), *Ae. speltooides* B genome (Miki *et al.*, 2019), and *Ae. tauschii* D genome (Mayer *et al.*, 2014). Overall, the A and D genomes are near identical, and the B genome is slightly more distantly related.

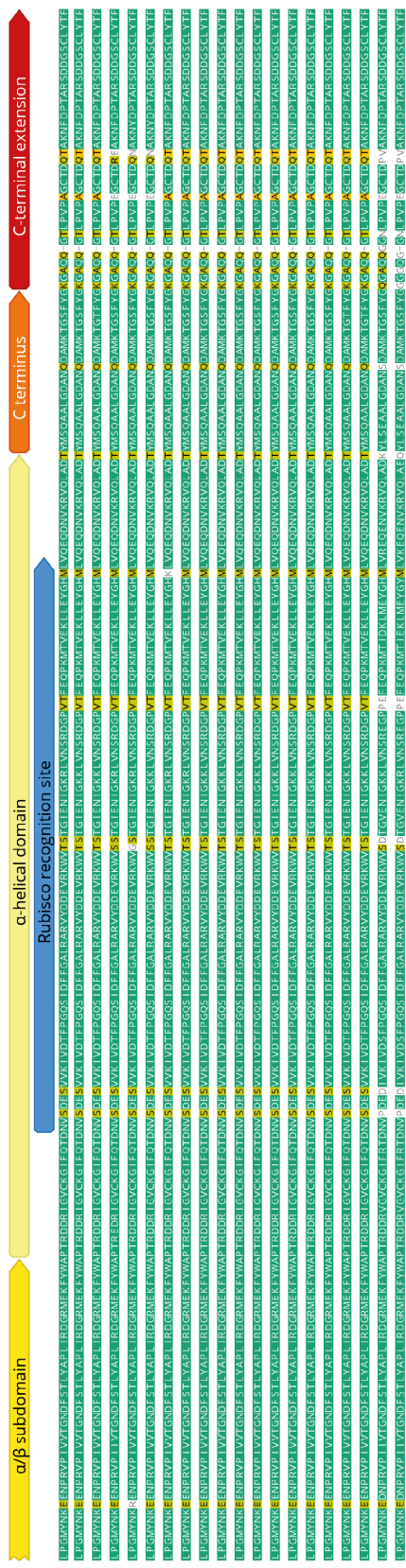
A)



B)



Ta B
Ta A
Ta D
Lp
Hv
Sc
As
Td B
Ac
Aco
Am
Ash
Tu
Tm
Tb
Td A
Acy
Oa
Os



Ta B
Ta A
Ta D
Lp
Hv
Sc
As
Td B
Ac
Aco
Am
Ash
Tu
Tm
Tb
Td A
Acy
Oa
Os

D)

<i>B. distachyon Rca16</i>	89.76	87.17	86.23	87.17	86.49	86.91	86.65	86.65	Ae. cylindrica Rca2ß	86.91	86.91	86.91	86.91	86.91	86.91	86.91	86.91	86.91	Th. bessarabium Rca2ß	86.91	86.91	86.23	87.14	88.51	89.56	
<i>T. aestivum B Rca16</i>	89.76	87.96	87.27	88.22	87.53	87.7	87.7	87.7	Ae. tauschii Rca2ß	86.91	86.91	86.91	86.91	86.91	86.91	86.91	86.91	86.91	86.91	T. durum A Rca2ß	86.91	86.91	87.01	87.66	88.48	90.05
<i>T. durum B Rca16</i>	89.76	87.96	87.27	88.22	87.53	87.7	87.7	87.7	Ae. mutica Rca2ß	86.91	86.91	86.91	86.91	86.91	86.91	86.91	86.91	86.91	86.91	T. durum A Rca2ß	86.91	86.91	87.01	87.66	88.48	90.05
<i>S. triticum Rca16</i>	89.76	87.7	87.01	87.96	87.27	87.43	87.43	87.43	Ae. columnaris Rca2ß	86.91	86.91	86.91	86.91	86.91	86.91	86.91	86.91	86.91	86.91	T. durum A Rca2ß	86.91	86.91	86.75	87.4	88.48	90.05
<i>S. cereale Rca16</i>	89.76	87.7	87.01	87.96	87.27	87.43	87.43	87.43	Ae. caudata Rca2ß	86.91	86.91	86.91	86.91	86.91	86.91	86.91	86.91	86.91	86.91	T. durum A Rca2ß	86.91	86.91	86.75	87.4	88.48	90.05
<i>Ae. tauschii Rca16</i>	90.29	88.22	87.53	88.48	87.79	87.96	87.96	87.96	T. aestivum D Rca2ß	86.91	86.91	86.91	86.91	86.91	86.91	86.91	86.91	86.91	86.91	Th. bessarabium Rca2ß	86.91	86.91	87.27	87.93	89.01	90.58
<i>T. aestivum A Rca16</i>	90.29	88.22	87.53	88.48	87.79	87.96	87.96	87.96	T. aestivum D Rca2ß	86.91	86.91	86.91	86.91	86.91	86.91	86.91	86.91	86.91	86.91	Th. bessarabium Rca2ß	86.91	86.91	87.27	87.93	89.01	90.58
<i>T. aestivum D Rca16</i>	90.29	88.22	87.53	88.48	87.79	87.96	87.96	87.96	T. aestivum D Rca2ß	86.91	86.91	86.91	86.91	86.91	86.91	86.91	86.91	86.91	86.91	Th. bessarabium Rca2ß	86.91	86.91	87.27	87.93	89.01	90.58
<i>T. monococcum Rca16</i>	90.29	88.22	87.53	88.48	87.79	87.96	87.96	87.96	T. aestivum D Rca2ß	86.91	86.91	86.91	86.91	86.91	86.91	86.91	86.91	86.91	86.91	Th. bessarabium Rca2ß	86.91	86.91	87.27	87.93	89.01	90.58
<i>T. urartu Rca16</i>	90.29	88.22	87.53	88.48	87.79	87.96	87.96	87.96	T. aestivum D Rca2ß	86.91	86.91	86.91	86.91	86.91	86.91	86.91	86.91	86.91	86.91	Th. bessarabium Rca2ß	86.91	86.91	87.27	87.93	89.01	90.58
<i>T. durum A Rca16</i>	90.29	88.22	87.53	88.48	87.79	87.96	87.96	87.96	T. aestivum D Rca2ß	86.91	86.91	86.91	86.91	86.91	86.91	86.91	86.91	86.91	86.91	Th. bessarabium Rca2ß	86.91	86.91	87.27	87.93	89.01	90.58
<i>S. anatolicum Rca16</i>	90.03	87.96	87.27	88.22	87.53	87.7	87.7	87.7	Ae. caudata Rca2ß	86.91	86.91	86.91	86.91	86.91	86.91	86.91	86.91	86.91	86.91	T. durum A Rca2ß	86.91	86.91	87.27	87.93	89.01	90.58
<i>H. vulgare Rca16</i>	89.76	87.7	87.01	87.96	87.27	87.43	87.43	87.43	T. aestivum D Rca2ß	86.91	86.91	86.91	86.91	86.91	86.91	86.91	86.91	86.91	86.91	T. durum A Rca2ß	86.91	86.91	87.27	87.93	89.01	90.58
<i>Ae. vulgare Rca2ß</i>	90.55	88.48	87.79	88.74	88.05	88.22	88.22	88.22	T. aestivum D Rca2ß	86.91	86.91	86.91	86.91	86.91	86.91	86.91	86.91	86.91	86.91	T. durum A Rca2ß	86.91	86.91	87.53	88.19	89.27	90.84
<i>Th. turgidum Rca16</i>	90.29	88.22	87.53	88.48	87.79	87.96	87.96	87.96	T. aestivum D Rca2ß	86.91	86.91	86.91	86.91	86.91	86.91	86.91	86.91	86.91	86.91	Th. bessarabium Rca2ß	86.91	86.91	87.27	87.93	89.01	90.58
<i>L. perenne Rca2ß</i>	95.54	96.33	96.59	96.59	96.59	96.33	95.8	95.8	L. perenne Rca2ß	96.06	96.06	96.06	96.06	96.06	96.06	96.06	96.06	96.06	96.06	T. durum A Rca2ß	96.06	96.06	96.06	96.05	90.29	91.08
<i>H. vulgare Rca2ß</i>	96.33	98.42	98.68	98.68	98.68	98.68	98.42	98.42	H. vulgare Rca2ß	98.68	98.68	98.68	98.68	98.68	98.68	98.68	98.68	98.68	98.68	T. durum A Rca2ß	98.68	98.68	98.68	98.68	87.4	88.98
<i>Ae. speltoides Rca2ß</i>	96.33	98.42	98.68	98.68	98.68	98.68	98.42	98.42	Ae. speltoides Rca2ß	98.68	98.68	98.68	98.68	98.68	98.68	98.68	98.68	98.68	98.68	T. durum A Rca2ß	98.68	98.68	98.68	98.68	87.4	88.98
<i>T. aestivum B Rca2ß</i>	96.59	98.68	99.74	99.74	100	99.21	99.21	99.21	T. aestivum B Rca2ß	99.21	99.21	99.21	99.21	99.21	99.21	99.21	99.21	99.21	99.21	T. durum A Rca2ß	99.21	99.21	99.21	99.21	88.45	89.5
<i>T. durum B Rca2ß</i>	96.59	98.68	99.74	99.74	100	99.21	99.21	99.21	T. durum B Rca2ß	99.21	99.21	99.21	99.21	99.21	99.21	99.21	99.21	99.21	99.21	T. durum A Rca2ß	99.21	99.21	99.21	99.21	88.45	89.5
<i>S. cereale Rca2ß</i>	96.33	98.68	99.74	99.74	100	99.21	99.21	99.21	S. cereale Rca2ß	99.21	99.21	99.21	99.21	99.21	99.21	99.21	99.21	99.21	99.21	T. durum A Rca2ß	99.21	99.21	99.21	99.21	88.45	89.5
<i>Ae. cylindrica Rca2ß</i>	95.8	98.42	98.95	99.21	99.21	99.47	99.47	100	Ae. cylindrica Rca2ß	99.47	99.47	99.47	99.47	99.47	99.47	99.47	99.47	99.47	99.47	T. durum A Rca2ß	99.47	99.47	99.47	99.47	88.71	89.24
<i>Ae. tauschii Rca2ß</i>	95.8	98.42	98.95	99.21	99.21	99.47	99.47	100	Ae. tauschii Rca2ß	99.47	99.47	99.47	99.47	99.47	99.47	99.47	99.47	99.47	99.47	T. durum A Rca2ß	99.47	99.47	99.47	99.47	88.71	89.24
<i>T. aestivum D Rca2ß</i>	95.8	98.42	98.95	99.21	99.21	99.47	99.47	100	T. aestivum D Rca2ß	99.47	99.47	99.47	99.47	99.47	99.47	99.47	99.47	99.47	99.47	T. durum A Rca2ß	99.47	99.47	99.47	99.47	88.71	89.24
<i>Ae. caudata Rca2ß</i>	96.06	98.68	99.21	99.47	99.47	99.74	99.74	99.74	Ae. caudata Rca2ß	99.74	99.74	99.74	99.74	99.74	99.74	99.74	99.74	99.74	99.74	T. durum A Rca2ß	99.74	99.74	99.74	99.74	88.19	88.71
<i>Ae. columnaris Rca2ß</i>	96.06	98.68	99.21	99.47	99.47	99.74	99.74	99.74	Ae. columnaris Rca2ß	99.74	99.74	99.74	99.74	99.74	99.74	99.74	99.74	99.74	99.74	T. durum A Rca2ß	99.74	99.74	99.74	99.74	88.19	88.71
<i>Ae. mutica Rca2ß</i>	96.06	98.68	99.21	99.47	99.47	99.74	99.74	99.74	Ae. mutica Rca2ß	99.74	99.74	99.74	99.74	99.74	99.74	99.74	99.74	99.74	99.74	T. durum A Rca2ß	99.74	99.74	99.74	99.74	88.19	88.71
<i>T. aestivum A Rca2ß</i>	96.06	98.68	99.21	99.47	99.47	99.74	99.74	99.74	T. aestivum A Rca2ß	99.74	99.74	99.74	99.74	99.74	99.74	99.74	99.74	99.74	99.74	T. durum A Rca2ß	99.74	99.74	99.74	99.74	88.19	88.71
<i>T. monococcum Rca2ß</i>	96.06	98.68	99.21	99.47	99.47	99.74	99.74	99.74	T. monococcum Rca2ß	99.74	99.74	99.74	99.74	99.74	99.74	99.74	99.74	99.74	99.74	T. durum A Rca2ß	99.74	99.74	99.74	99.74	88.19	88.71
<i>Th. bessarabium Rca2ß</i>	96.06	98.68	99.21	99.47	99.47	99.74	99.74	99.74	Th. bessarabium Rca2ß	99.74	99.74	99.74	99.74	99.74	99.74	99.74	99.74	99.74	99.74	T. durum A Rca2ß	99.74	99.74	99.74	99.74	88.19	88.71
<i>T. durum A Rca2ß</i>	96.06	98.68	99.21	99.47	99.47	99.74	99.74	99.74	T. durum A Rca2ß	99.74	99.74	99.74	99.74	99.74	99.74	99.74	99.74	99.74	99.74	T. durum A Rca2ß	99.74	99.74	99.74	99.74	88.19	88.71
<i>T. urartu Rca2ß</i>	96.05	98.68	99.21	99.47	99.47	99.74	99.74	99.74	T. urartu Rca2ß	99.74	99.74	99.74	99.74	99.74	99.74	99.74	99.74	99.74	99.74	T. durum A Rca2ß	99.74	99.74	99.74	99.74	88.42	88.95
<i>O. australiensis Rca2ß</i>	90.29	87.4	88.19	88.45	88.45	88.71	88.19	88.19	O. australiensis Rca2ß	88.45	88.45	88.45	88.45	88.45	88.45	88.45	88.45	88.45	88.45	T. durum A Rca2ß	88.45	88.45	88.45	88.42	95.04	95.04
<i>O. sativa Rca2ß</i>	91.08	88.98	89.24	89.5	89.5	89.24	88.71	88.71	O. sativa Rca2ß	88.98	88.98	88.98	88.98	88.98	88.98	88.98	88.98	88.98	88.98	T. durum A Rca2ß	88.98	88.98	88.98	88.95	95.04	95.04

Fig. 2. Alignment of mature protein sequences of A) Rca1 β , B) Rca2 β /Rca2 α of the three wheat sub-genomes and selected wheat wild relatives. Sequences of *Ae. tauschii*, *B. distachyon*, *H. vulgare*, *O. australiensis*, *O. sativa*, *T. urartu*, *T. durum* and *T. aestivum* were obtained from EnsemblPlants. Abbreviations: Ta, *T. aestivum*; Ac, *Ae. caudata*; Acy, *Ae. cylindrica*; Aco, *Ae. columnaris*; Am, *Ae. mutica*; Ash, *Ae. sharonensis*; As, *Ae. speltoides*; At, *Ae. tauschii*; Bd, *B. distachyon*; Hv, *H. vulgare*; Lp, *L. perenne*; Oa, *O. australiensis*; Os, *O. sativa*; Sc, *S. cereale*; Sa, *S. anatolicum*; Si, *S. iranicum*; Td, *T. durum*; Tm, *T. monoccoccum*; Tu, *T. urartu*; Tb, *Th. bessarabium*; Tt, *Th. turgidum*. Rca domains are annotated in different colours. Alignment was created using the ClustalW algorithm in Geneious 9.1.8. C, D) Percentage identity of Rca isoforms based on protein sequence.

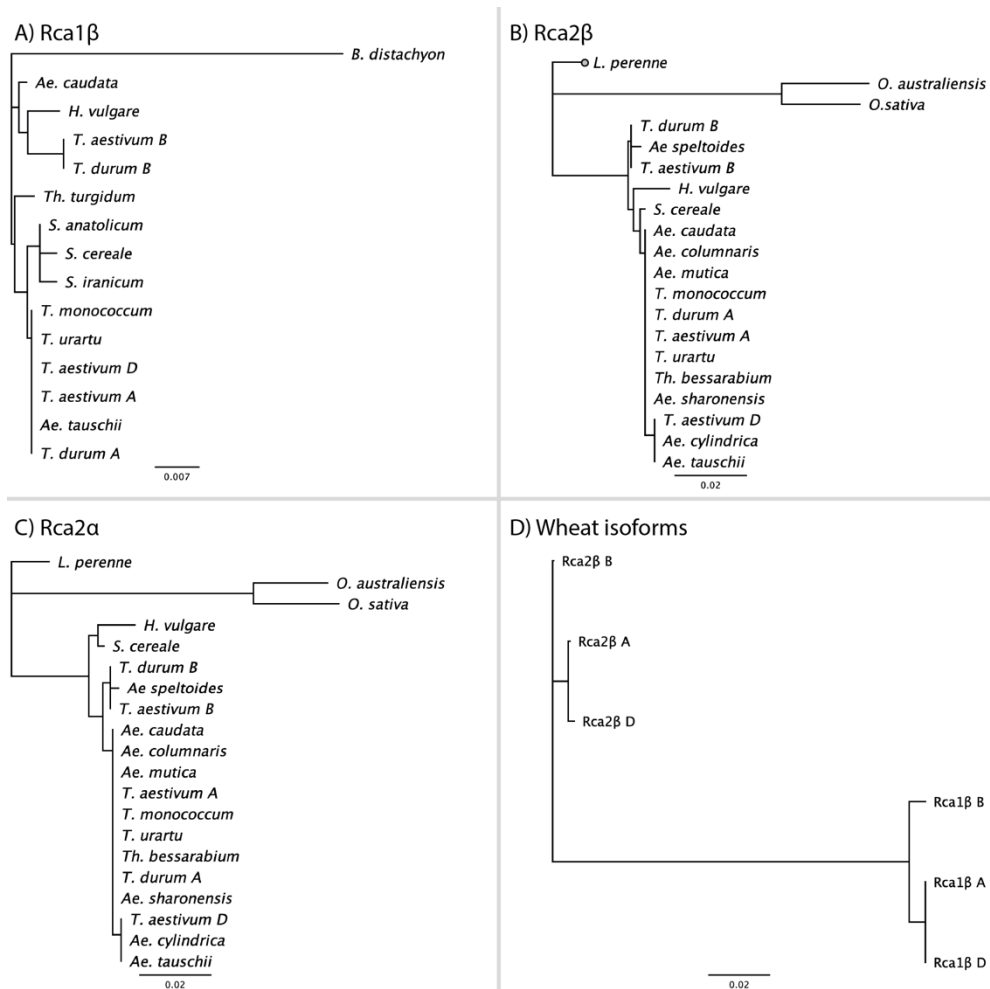


Fig. 3. Phylogenetic trees of mature protein sequences. A) Rca1 β , B) Rca2 β , C) Rca2 α of wheat and wild relatives and D) of wheat sub-genomes. Phylogenetic tree was constructed based on the sequence alignment in Fig. 2 using the Jukes-Cantor genetic distance model and the neighbour-joining tree build method in Geneious 9.1.8. Scale represents amino substitutions per site.

While *Rca* and the Rubisco small subunit (*RbcL*) genes are encoded in the nucleus, the Rubisco large subunit (*rbcL*) is encoded in the chloroplast genome, which has been suggested to have been maternally inherited from an *Ae. speltoides* relative, the donor of the B genome (Middleton *et al.*, 2014). A phylogenetic tree of the RbcL protein sequences from wheat and sub-genome donors (*Ae. speltoides* and *T. urartu*) showed that these were closely related (Fig. 4). Overall, protein sequence identity was >99 % for all six species.

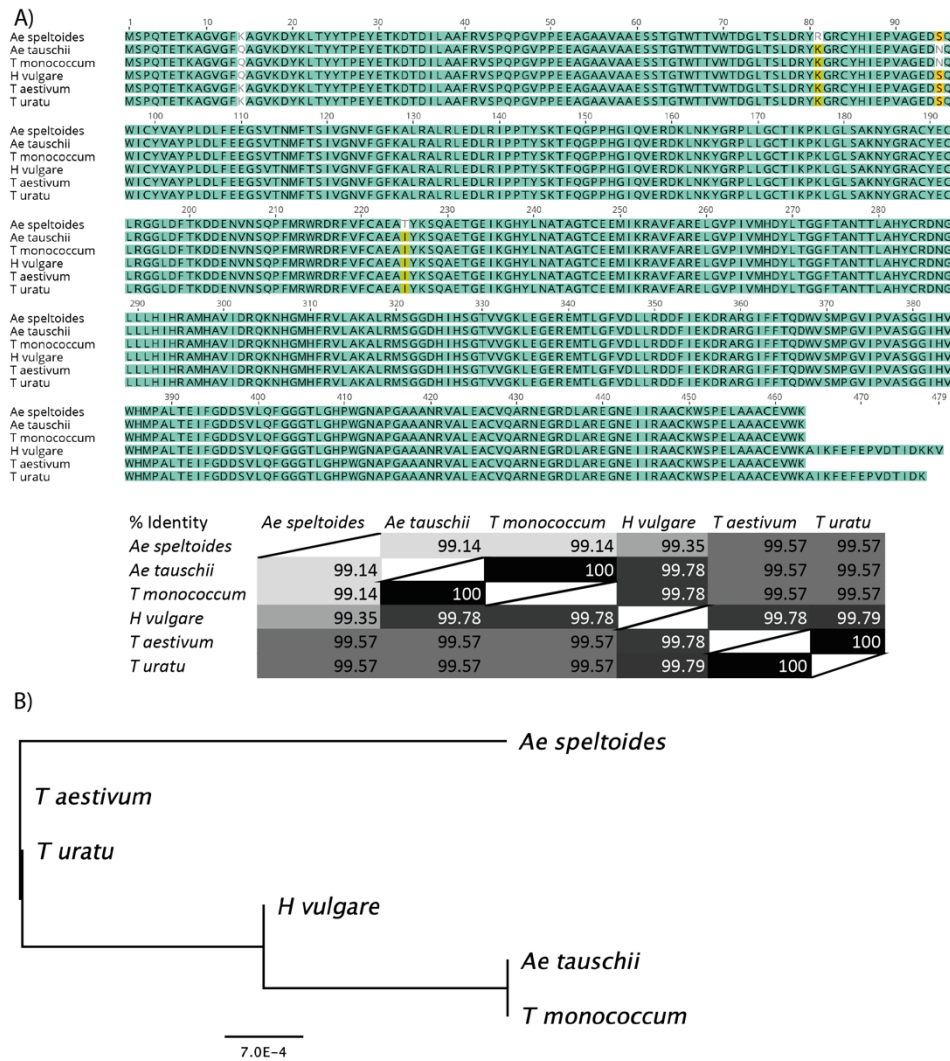


Fig. 4: Sequence analysis of Rubisco large subunits of wheat and related species. A) Protein sequence alignment of RbcL from wheat and related species and percentage identity, B) Phylogenetic tree of RbcL protein sequences. Phylogenetic tree was constructed based on the sequence alignment in A) using the Jukes-Cantor genetic distance model and the neighbour-joining tree build method in Geneious 9.1.8. Scale represents amino substitutions per site.

To reconstruct the evolution of Rca in wheat and wild progenitors, protein sequence flows (Fig. 5) were derived from sequence alignments (Fig. 2) and phylogenetic analysis (Fig. 3). *T. aestivum* Rca1 β in the A genome was identical to the genome donor species, *T. urartu*, and to the tetraploid wheat relative *T. durum*. *T. aestivum* Rca1 β in the B genome was also identical to *T. durum*, however, it was not possible to obtain the Rca1 β sequence for *Ae. speltooides* due to insufficient genomic data available. *T. aestivum* Rca1 β in

the D genome was identical to *Ae. tauschii* and *T. urartu*, as indicated by the blue arrow in Fig. 5. Rca2 β / α in the A and B genomes of *T. aestivum* were identical to the respective donor species, *T. urartu* and *Ae. speltooides*. *T. aestivum* Rca2 β / α in the D genome was identical to *Ae. tauschii*, the donor species. Rca1 β , Rca2 β / α in *Ae. tauschii* showed minimal amino acid difference from *T. urartu*, as indicated by the blue to green colour gradient in Fig. 5. This suggests that during the speciation event of *Ae. tauschii*, Rca copies from *T. urartu* were retained and copies from the relative of *Ae. speltooides* were lost, indicated by the red horizontal line in Fig. 5.

The two tandemly organised *Rca* genes in grasses have been suggested to be the result of a duplication event (Nagarajan & Gill, 2018). To assess similarity of Rca isoforms, Rca1 β and Rca2 β of selected species were aligned (Fig. 6), including Rca from domesticated (*O. sativa*) and wild rice (*O. australiensis*), which have been studied in detail and shown to be thermostable (Scafaro *et al.*, 2012; 2016; Shivhare & Mueller-Cajar, 2017; Scafaro *et al.*, 2018). *T. aestivum* Rca1 β showed >94% sequence identity with Rca1 β and >85% identity with Rca2 β from other species (Fig. 2C, D). Strikingly, the wheat Rca1 β shared >90% identity, while the wheat Rca2 β was slightly less related, to the thermostable Rca2 β from *O. sativa*. A similar pattern was observed when comparing the two wheat isoforms with the isoform from *O. australiensis*.

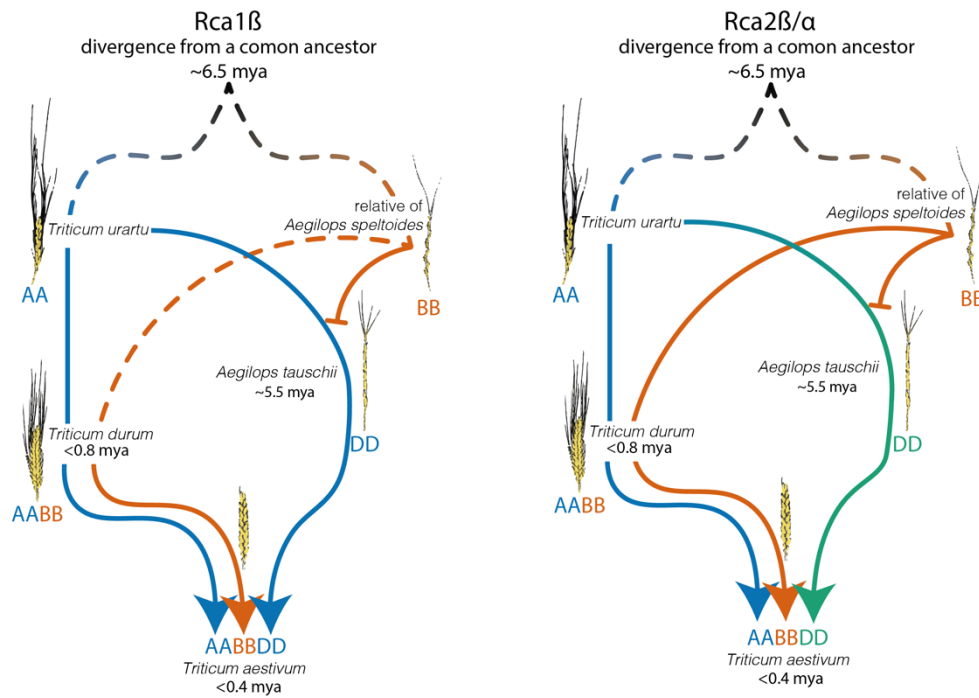


Fig. 5. Protein sequence flow of Rca from wild relatives to wheat. Arrows indicate the direction of flow from ancestral grasses. Colours indicate whether Rca proteins sequence changed between species. The dashed line indicates unclear phylogenetic relationship due to lack of sequence data. Red horizontal line indicates that Rca from the BB genome donor was lost during speciation of *Ae. tauschii*. Phylogeny and timescale in million years ago (mya) is based on Marcussen *et al.* (2014).

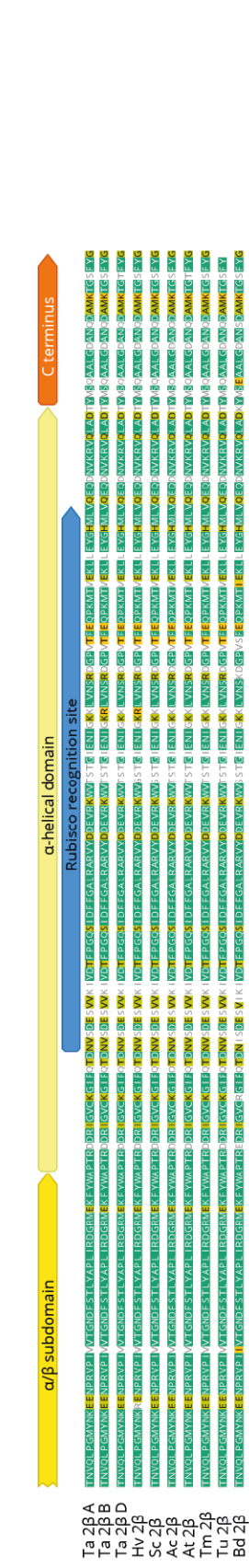
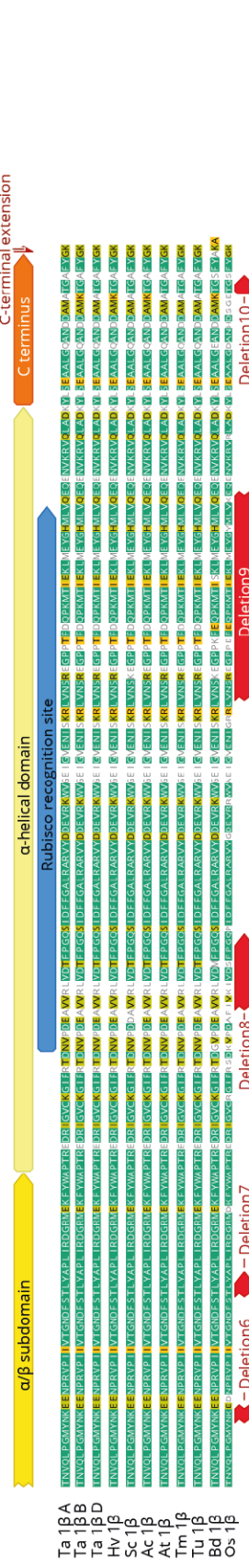
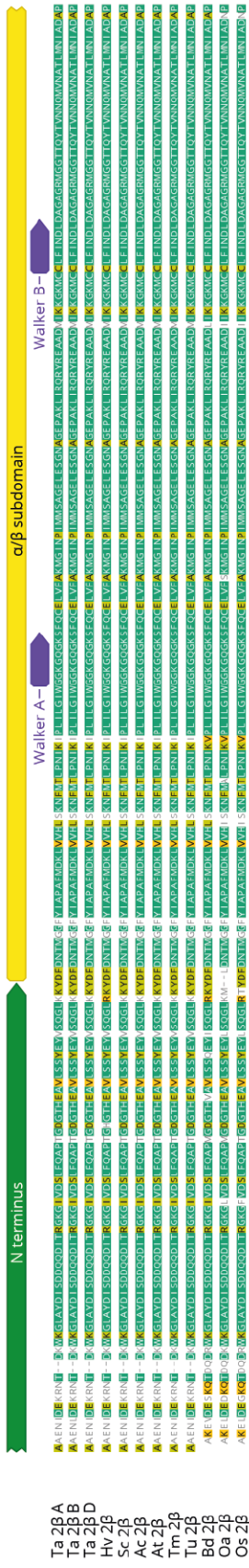
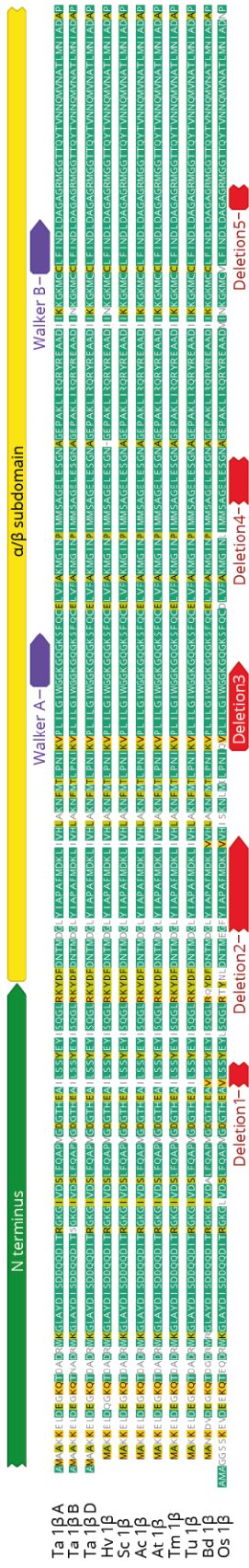


Fig. 6. Alignment of Rca protein sequences from selected grass species. *O. sativa* Rca1 β protein sequence was reconstructed using genomic sequences from the *O. sativa* Rca2 β according to (Nagarajan & Gill, 2018).

5.3 Discussion

Expression of Rca isoforms was found to be similar between the three wheat sub-genomes in leaves. Rca2 β and α had similar expression between genome and were higher expressed than Rca1 β . This isoform showed an expression gradient of A>B>D between genomes and expression increased under abiotic stress. Rca sequences were highly conserved between wheat and wild relatives and only showed 1-5 amino acid differences. Isoforms from the A and D genome were nearly identical and highly conserved amongst wheat progenitors, whereas the B genome showed slightly more diversity. Interestingly, Rca2 β from rice was found to be more similar to wheat Rca1 β than Rca2 β .

Rca expression was predominantly found in photosynthetic vegetative tissue, with only minor expression in reproductive tissue. Findings from the wheat expression database for the heat responsive *Rca1 β* are in line with previous reports (Scafaro *et al.*, 2019) and Chapter 4. Interestingly, no Rca expression was found in roots, in contrast to some unusual Rubisco small subunits in rice, Arabidopsis and tobacco (Morita *et al.*, 2014; Laterre *et al.*, 2017; Pottier *et al.*, 2018), which was also shown for wheat *RbcS* group 3 (Chapter 4). This could indicate that the small subunits expressed in roots, assuming these are assembled into a Rubisco holoenzyme, is not activated by Rca and serves another still unclear function.

Rca1 β has been identified as a thermostable isoform (Scafaro *et al.*, 2019; Degen *et al.*, 2020). An isoleucine residue (Fig. 3A, indicated in red) has been shown to substantially contribute to Rca1 β thermostability, by producing the thermostable mutant Rca2 β -M159I (Degen *et al.*, 2020). This isoleucine residue is highly conserved in wheat wild relatives and likely confers thermostability to Rca1 β from wheat wild relatives as well. *Rca1 β* expression

and protein levels in wild relatives could be higher in order to sustain photosynthesis at higher temperatures. This should be investigated in future studies, as well as screening for heat responsive elements in the *Rca1* promoter region. Furthermore, Rca1 β from the B genome and from barley share an asparagine residue at position 166, which is not present in other wild relatives. Barley Rubisco exhibited increased catalysis at 35°C compared to wheat and modelling showed that replacing native wheat *rbcl* with the barley protein would increase photosynthesis at 35 °C (Prins *et al.*, 2016). This suggests that barley might be adapted to higher temperatures. This is supported by the fact that the double mutant Rca2 β -M159I/K161N, which contained the asparagine residue, had higher Rubisco activation activity than Rca2 β and Rca2 β -M159I at elevated temperatures (Degen *et al.*, 2020)(Chapter 3). Interestingly, this asparagine residue is not conserved in Rca1 β from the A and D genome. Hence, enzymatic properties of Rca1 β from the three genomes might be different and it could be speculated that Rubisco activation by Rca1 β from the A/D genomes is likely lower than for the B genome variant (Degen *et al.*, 2020).

Rca from wild and domesticated rice (*O. australiensis* and *O. sativa*) diverged from barley and other wheat grasses and is more similar to *L. perenne*. Since Rca genes in grasses are arranged in tandem, these are most likely the result of a duplication event (Nagarajan & Gill, 2018). Rice only expresses *Rca2 β* and *Rca2a*, the *Rca1* copy contains 10 deletions and is silent. The predicted rice Rca1 β protein sequence and the wheat Rca2 β contain a methionine at position 166 (red arrow in Fig. 2A). Conversely, the functional rice Rca2 β and the little abundant wheat Rca1 β contain an isoleucine that confers thermotolerance (Degen *et al.*, 2020; Chapter 3). Rice grows in hotter climates compared to the temperate cereal wheat. Therefore, heat-induced expression of thermotolerant Rca is not necessary in rice, whereas heat-stress events require expression of a more thermostable isoform in wheat. Introducing the rice Rca into wheat could in theory improve thermotolerance of Rubisco activation. However, the more thermostable Rca from wild rice was less efficient at activating *O. sativa* Rubisco than the native Rca isoform (Scafaro

et al., 2016). Rca from *Agave tequilana*, however, was shown to be very thermostolerant and was more effective at activating *O. sativa* Rubisco than the respective native isoform (Shivhare & Mueller-Cajar, 2017). This could be a result of the environment *Agave tequilana* evolved in, which required more thermostable Rca isoforms than rice. These results show that *in vitro* studies would be required to test the compatibility of rice Rca and wheat Rubisco. A more promising strategy might be to engineer the isoleucine residue into Rca2 β and to tune *Rca1 β* expression, if genome copies are proven to have different catalytic properties.

Overall, Rca protein sequences are highly conserved between wheat genomes, only differing in 1-5 amino acid residues. In addition, wheat wild relatives were identical or very similar to wheat genomes. This could suggest that capacity for improving thermotolerance is limited. However, results from Degen *et al.* (2020) indicate a single amino acid change at another position could still result in superior thermotolerance. Future research should include research on the thermal environment of wild relatives as well as the presence of heat inducible elements in the promoter regions of Rca and levels of the thermostable Rca1 β isoform. The findings in this chapter show that wheat wild relatives might still prove a valuable resource for wheat improvement.

5.4 Material and Methods

Plant growth Seeds of wheat wild relatives were germinated on filter paper soaked in dH₂O for four days at room temperature. Germinated seeds were transferred to 2 L pots containing a wheat mix growth medium (Petersfield compost, Hewitt & Son Ltd., Cosby, UK) in a glasshouse at the Lancaster Environment Centre. Minimum temperatures were set to 24°C day/18°C night. The photoperiod was set to 16 h and supplementary lights were used when the light level inside the glasshouse fell below 200 $\mu\text{mol m}^{-2} \text{s}^{-1}$. Leaf material was collected for DNA extraction after two weeks, snap frozen in liquid nitrogen and stored at -80°C.

Genomic DNA extraction Genomic DNA was extracted according to (Edwards *et al.*, 1991). Leaf material was homogenised in 1.5 mL DNA extraction buffer, which contained 200 mM Tris (pH 7.5, HCl), 250 mM NaCl, 0.5% (w/v) SDS and 25 mM EDTA (pH 8.0, NaOH), followed by centrifugation at 14,000 x *g* for 10 min. The supernatant was transferred into a sterile 1.5 mL tube and centrifuged again at the above conditions. 350 μL of clear supernatant were transferred to a new tube, mixed with an equal volume of 100% isopropanol and incubated at room temperature for 30 min to allow genomic DNA to precipitate. Genomic DNA was collected by centrifugation at 14,000 x *g* for 10 min. The pellet was washed with 70% ethanol three times and dried in a flow hood until all ethanol was removed. The pellet was resuspended overnight at 4°C in 80 μL TER buffer, containing 10 mM Tris, 1 mM EDTA and 25 $\mu\text{L mL}^{-1}$ RNase. Genomic DNA was stored at -20°C.

PCR and Sequencing Genomic sequences of *Rca* genes from wheat wild relatives were obtained by amplifying three overlapping parts of the *Rca1* and *Rca2* genes, using primers from Table S1. PCR was performed in a thermocycler (Agilent SureCycler 8800, Agilent, CA, USA) using Phusion polymerase (Thermo Fisher Scientific, MA, USA). PCR cycling conditions for all species were identical, except for different annealing temperatures (Table S1) and

extension times (15s/1kb, Table S1): initial denaturation for 5 min at 98°C; cycle conditions were 15 s at 98°C, 15 s at 61-67°C, 15-60 s at 72°C, repeated 35-40 times. Final extension was 5 min at 72°C, followed by a hold step at 20°C.

The PCR products were visualised on a 0.7% (w/v) agarose gel and the DNA band of interest was excised on a UV table. DNA was extracted using a Wizard® Genomic DNA Purification Kit (Promega, WI, USA) according to the manufacturer's instructions. The PCR product was cloned into the pGEM®-T Easy vector (Promega, WI, USA) for sequencing (the protocol can be found here dx.doi.org/10.17504/protocols.io.hqab5se). 100 ng μL^{-1} of plasmid containing the Rca sequences were sent for Sanger sequencing (Source Biosciences, UK) using the M13 lacZ gene primers (CCCAGTCAC-GACGTTGTAAAACG, AGCGGATAACAATTTTCACACAGG). Sequencing data was analysed and assembled in Geneious 9.1.8.

Table.S1: Primer sequences used for sequencing wheat wild relative Rubisco activase genes. For some species, a different primer was used, indicated with a /. The corresponding annealing temperatures and product sizes are also given.

Gene	Primer sequence	Annealing Temperature	Product size
<i>TaRca1</i>	F: AAGTTRTCAGGTGCGGGGAG R: CGCTCCTCAACTCAYACCAGGA/ CTTCACCTTCTTCCCGAGGA	65/65	1260/2015
	F: CCCCACTCCCCTCAACAC R: GGGTTCTCCTCCTTGTTGTAC	61	1397
	F: TGCCTCTTCATCAACGACCT/ ATGAATCTGGTTGGGGCTGA R: TGTGCGGCGATGAATCAAAA	65/67	750/1263
<i>TaRca2</i>	F: AGAACCCAATCTCCAGCGTG R: TTCCTTGACCCTTGCCCTCC/ TAACAAAACATGCCAGCAA	66/64	973/2338
	F: GACTTCGACAACACCATGGG R: GGGAAGGTGTCGACGATCTT	65	850
	F: AGAAGTTCTACTGGGCTCCC R: TTGGCATGCTTAAAAGGTGT	61	866

5.5 References

- Berry J, Bjorkman O. 1980.** Photosynthetic response and adaptation to temperature in higher plants. *Annual Review of Plant Physiology* **31**: 491–543.
- Borrill P, Ramirez-Gonzalez R, Uauy C. 2016.** expVIP: a customizable RNA-seq data analysis and visualization platform. *Plant Physiology* **170**: 2172–2186.
- Degen GE, Worrall D, Carmo-Silva E. 2020.** An isoleucine residue acts as a thermal and regulatory switch in wheat Rubisco activase. *The Plant Journal* **103**: 742–751.
- Edwards K, Johnstone C, Thompson C. 1991.** A simple and rapid method for the preparation of plant genomic DNA for PCR analysis. *Nucleic Acids Research* **19**: 1349–1349.
- Fu Y-B, Peterson GW, Horbach C, Konkin DJ, Beiles A, Nevo E. 2019.** Elevated mutation and selection in wild emmer wheat in response to 28 years of global warming. *Proceedings of the National Academy of Sciences* **116**: 20002–20008.
- Howe KL, Contreras-Moreira B, De Silva N, Maslen G, Akanni W, Allen J, Alvarez-Jarreta J, Barba M, Bolser DM, Cambell L, *et al.* 2019.** Ensembl Genomes 2020—enabling non-vertebrate genomic research. *Nucleic Acids Research* **48**: D689–D695.
- King J, Grewal S, Yang C-Y, Hubbart Edwards S, Scholefield D, Ashling S, Harper JA, Allen AM, Edwards KJ, Burr ridge AJ, *et al.* 2017a.** Introgression of *Aegilops speltoides* segments in *Triticum aestivum* and the effect of the gametocidal genes. *Annals of Botany* **121**: 229–240.
- King J, Grewal S, Yang C-Y, Hubbart S, Scholefield D, Ashling S, Edwards KJ, Allen AM, Burr ridge A, Bloor C, *et al.* 2017b.** A step change in the transfer of interspecific variation into wheat from *Amblyopyrum muticum*. *Plant Biotechnology Journal* **15**: 217–226.
- Laterre R, Pottier M, Remacle C, Boutry M. 2017.** Photosynthetic trichomes contain a specific rubisco with a modified pH-dependent activity. *Plant Physiology* **173**: 2110–2120.
- Marcussen T, Sandve SR, Heier L, Spannagl M, Pfeifer M, Jakobsen KS, Wulff BBH, Steuernagel B, Mayer KFX, Olsen O-A, *et al.* 2014.** Ancient

hybridizations among the ancestral genomes of bread wheat. *Science* **345**: –1250092.

Mayer KFX, Rogers J, Dole el J, Pozniak C, Eversole K, Feuillet C, Gill B, Friebe B, Lukaszewski AJ, Sourdille P, et al. 2014. A chromosome-based draft sequence of the hexaploid bread wheat (*Triticum aestivum*) genome. *Science* **345**: 1251788–1251788.

Middleton CP, Senerchia N, Stein N, Akhunov ED, Keller B, Wicker T, Kilian B. 2014. Sequencing of chloroplast genomes from wheat, barley, rye and their relatives provides a detailed insight into the evolution of the triticeae tribe (MW Davey, Ed.). *PLoS ONE* **9**: e85761.

Miki Y, Yoshida K, Mizuno N, Nasuda S, Sato K, Takumi S. 2019. Origin of wheat B-genome chromosomes inferred from RNA sequencing analysis of leaf transcripts from section Sitopsis species of *Aegilops*. *DNA research : an international journal for rapid publication of reports on genes and genomes* **26**: 171–182.

Morita K, Hatanaka T, Misoo S, Fukayama H. 2014. Unusual small subunit that is not expressed in photosynthetic cells alters the catalytic properties of rubisco in rice. *Plant Physiology* **164**: 69–79.

Nagarajan R, Gill KS. 2018. Evolution of Rubisco activase gene in plants. *Plant Molecular Biology* **96**: 69–87.

Pottier M, Gilis D, Boutry M. 2018. The hidden face of Rubisco. *Trends in Plant Science* **23**: 382–392.

Pradhan GP, Prasad P, Fritz AK, Kirkham MB, Gill BS. 2012. High temperature tolerance in *Aegilops* species and its potential transfer to wheat. *Crop Science*: 292–304.

Prins A, Orr DJ, Andralojc PJ, Reynolds MP, Carmo-Silva E, Parry MAJ. 2016. Rubisco catalytic properties of wild and domesticated relatives provide scope for improving wheat photosynthesis. *Journal of Experimental Botany* **67**: 1827–1838.

Ramirez-Gonzalez RH, Borrill P, Lang D, Harrington SA, Brinton J, Venturini L, Davey M, Jacobs J, van Ex F, Pasha A, et al. 2018. The transcriptional landscape of polyploid wheat. *Science* **361**: eaar6089.

Ray DK, Ramankutty N, Mueller ND, West PC, Foley JA. 2012. Recent patterns of crop yield growth and stagnation. *Nature Communications* **3**: 1293.

Ray DK, West PC, Clark M, Gerber JS, Prishchepov AV, Chatterjee S. 2019. Climate change has likely already affected global food production (YH Jung, Ed.). *PLoS ONE* **14**: e0217148.

- Reynolds M, Dreccer F, Trethowan R. 2007. Drought-adaptive traits derived from wheat wild relatives and landraces. *Journal of Experimental Botany* **58**: 177–186.
- Scafaro AP, Atwell BJ, Muylaert S, Reusel BV, Ruiz GA, Rie JV, Gallé A. 2018. A thermotolerant variant of rubisco activase from a wild relative improves growth and seed yield in rice under heat stress. *Frontiers in Plant Science* **871**: 1663.
- Scafaro AP, Bautsoens N, Boer den B, Van Rie J, Gallé A. 2019. A conserved sequence from heat-adapted species improves rubisco activase thermostability in wheat. *Plant Physiology* **181**: 43–54.
- Scafaro AP, Gallé A, Van Rie J, Carmo-Silva E, Salvucci ME, Atwell BJ. 2016. Heat tolerance in a wild *Oryza* species is attributed to maintenance of Rubisco activation by a thermally stable Rubisco activase ortholog. *New Phytologist* **211**: 899–911.
- Scafaro AP, Yamori W, Carmo-Silva E, Salvucci ME, Caemmerer von S, Atwell BJ. 2012. Rubisco activity is associated with photosynthetic thermotolerance in a wild rice (*Oryza meridionalis*). *Physiologia Plantarum* **146**: 99–109.
- Shivhare D, Mueller-Cajjar O. 2017. In vitro characterization of thermostable CAM rubisco activase reveals a rubisco interacting surface loop. *Plant Physiology* **174**: 1505–1516.
- Wingen LU, Orford S, Goram R, Leverington-Waite M, Bilham L, Patsiou TS, Ambrose M, Dicks J, Griffiths S. 2014. Establishing the A. E. Watkins landrace cultivar collection as a resource for systematic gene discovery in bread wheat. *Theoretical and Applied Genetics* **127**: 1831–1842.
- Zaïm M, Hassouni El K, Gamba F, Filali-Maltouf A, Belkadi B, Sourour A, Amri A, Nachit M, Taghouti M, Bassi FM. 2017. Wide crosses of durum wheat (*Triticum durum Desf.*) reveal good disease resistance, yield stability, and industrial quality across Mediterranean sites. *Field Crops Research* **214**: 219–227.

6. General discussion

Wheat is a hexaploid temperate cereal and a staple of human nutrition. It provides 20% of daily calories and 19% of protein (Parry *et al.*, 2011). However, climate change threatens future wheat yields and population growth will increase demand (Ray *et al.*, 2013; IPCC, 2014; Ray *et al.*, 2019). Cultivars from varying climates have shown to vary in their response to heat stress (Stone & Nicolas, 1994), suggesting there is scope for improving heat sensitivity. A strategy of heat-adapted European cultivars is a quicker maturation, which comes with the penalty of reduced yield (Semenov *et al.*, 2014). Therefore, this is not a sustainable approach to improve thermotolerance in wheat. One promising strategy to create climate-resilient and high-yielding wheat varieties is to improve photosynthesis and in particular the regulation of carbon assimilation (Crafts-Brandner & Salvucci, 2000; Salvucci & Crafts-Brandner, 2004a; Carmo-Silva *et al.*, 2015), in concert with optimising heat-tolerance of grain filling. This thesis aimed to broaden the understanding of the regulation of carbon assimilation in wheat by Rubisco activase (Rca).

Rca has been identified as a temperature-sensitive enzyme that limits photosynthesis at during moderate heat stress (Crafts-Brandner & Salvucci, 2000; Salvucci & Crafts-Brandner, 2004a). This is supported by research in *Arabidopsis* and rice, where expressing a more thermostable Rca isoform improved growth at elevated temperatures (Kurek *et al.*, 2007; Kumar *et al.*, 2009; Scafaro *et al.*, 2018). Therefore, optimising the temperature range of Rca in wheat is also predicted to contribute towards making wheat more resilient to global warming.

In order to improve Rca properties, a better understanding of the catalytic properties of wheat Rca isoforms was required. In the second chapter, Rca activity was shown to vary between isoforms and to be concentration dependent. The three isoforms behaved similarly in their relative concentration-dependent ATPase activity, which decreased with increasing enzyme concentration. In contrast, the fraction of Rubisco activation by Rca increased with increasing Rca concentrations. However, Rca specific activity declined with increasing Rca concentrations and optimal Rubisco activation

rates were observed when Rubisco and Rca in the assay were present at a ratio above 6-11 mol R_{A.S.} to mol⁻¹ Rca monomer. Moreover, the results of the *in vitro* characterisation showed that Rca1 β exhibited much lower Rubisco activation activity than Rca2 β and Rca2 α . As shown in chapter 4, *in planta* ratios of R_{A.S.}:Rca_{total} are around 100:1, suggesting that Rca is saturated with Rubisco. Here, it was also shown that the majority of the Rca pool in wheat flag leaves is comprised of the catalytically superior Rca2 β isoform. The decline of Rca specific activity shown in chapter 2 is supported by results for tobacco Rca shown in Scales *et al.* (2014) and expand the understanding of isoform variation within a species. Furthermore, results from chapter 2 highlight the importance of using protein molecular weight when calculating Rca activity. Identification of the optimal Rubisco:Rca ratio will be valuable for future research on Rca of wheat and other species. In addition, this work showed that Rubisco activation by Rca2 β was insensitive to ADP inhibition, in contrast to Rca1 β and 2 α (Perdomo *et al.*, 2019).

As shown in chapter 3 (Degen *et al.*, 2020) Rca1 β is more thermostable than the other two isoforms, however, its capacity for Rubisco activation and efficiency is much lower (chapters 2 and 3). Results from Degen *et al.* (2020) also highlight the importance of measuring ATPase and Rubisco activation activity and show that these are not interchangeable. In particular, wheat Rca was still able to hydrolyse ATP at higher temperatures compared to the optimum of Rubisco activation activity. This was also observed for Rca isoform from *O. sativa* and *O. australiensis* (Scafaro *et al.*, 2016) and for the cold-adapted species Antarctic hairgrass and the desert-dwelling creosote bush (Salvucci & Crafts-Brandner, 2004b). This should be considered in future studies of Rca activities when assessing temperature response. The difference in optimum temperature of these two activities also highlights that the Rca-Rubisco interaction and removal of inhibitors might be much more sensitive to temperature than ATP hydrolysis, which should be regarded as a proxy for maximum thermostability of the enzyme. Since the distantly related species mentioned above all exhibit a similar difference in temperature optimums of the two assays, this could be considered an inherent property of

Rubisco activation by Rca, rather than a species-specific effect. Finally, including Rubisco in the ATPase assay might affect the observed response and should be investigated in future research efforts, in order to establish whether the presence of Rubisco has an effect on ATP hydrolysis at different temperatures.

To gain a better understanding of Rubisco regulation during heat stress, protein levels of the three Rca isoforms were determined in heat-stressed wheat. Increased protein synthesis of the thermostable Rca1 β isoform was observed during moderate heat stress. However, this was insufficient to fully restore Rubisco activation to control levels. In light of the concentration-dependence of Rca, this suggests that simply increasing Rca1 β levels might not be a viable strategy to improve thermotolerance of Rubisco activation in wheat. In fact, even during heat stress, Rca1 β only increased to 6% of the total Rca pool, and R_{A.S.}:Rca1 β ratios were at around 2000:1. These results indicate that there is an inherent trade-off between thermostability and catalytic capacity, in contrast to suggestions made by Scafaro *et al.* (2019). Here only thermostability was assessed and not Rubisco activation activity itself, which, as discussed above, is a key assay when assessing Rca temperature response. The catalytic properties of Rca1 β are therefore in line with the current understanding of the relationship between enzyme rigidity, reduced activity and thermostability (Vieille & Zeikus, 2001).

Analysis of *RbcS* expression in chapter 4 showed that the three wheat *RbcS* groups identified based on sequence similarity respond differently to heat stress. Although expression changes were not significant, prolonged heat stress might result in significant changes. This suggests that Rubisco itself can change its subunit composition and possibly catalytic properties in response to heat stress, as demonstrated by Yamori *et al.* (2006). In light of the temperature response of wheat Rca isoforms, future research should include Rubisco extracted from wheat grown at different temperatures. This could give insight into the influence of Rubisco thermostability on Rca activity. In addition, this highlights the importance of growth temperature on Rubisco properties and it is important to consider this for future research on

Rubisco activation and Rca thermostability in other species closely related to wheat.

Wheat wild relatives and crops such as rye and barley have been suggested as a resource to enhance genetic diversity for crop improvement (Wingen *et al.*, 2014; Prins *et al.*, 2016; Riaz *et al.*, 2016; Castaneda-Alvarez *et al.*, 2016). Chapter 5 showed that Rca protein sequences were highly conserved in wheat wild relatives. It could be speculated that wild relatives adapt to diverse environments by tuning *Rca* expression, in particular levels of *Rca1 β* in response to heat stress. This was shown for the different expression of splice variants in low and high freezing tolerant *Lolium perenne* genotypes, which was accompanied by increased Rubisco activity in the high freezing tolerant genotype during low temperature (Jurczyk *et al.*, 2016). However, as highlighted above, *Rca1 β* appears to be a catalytically poor enzyme and always exhibited lower Rca specific activity compared to *Rca2 β* and *Rca2 α* when assayed at various concentrations. Yet, even a single amino acid residue difference in wild relatives could change thermotolerance, as shown for *Rca2 β -M159I* in Degen *et al.* (2020).

If Rca isoforms in wild relatives differ in their temperature response, however, requires further investigation. Wild relatives might also differ in other physiological traits such as transpiration in order to cool leaves to optimal temperatures. In addition, grain maturation might be faster than in domesticated wheat, which would come at the penalty of reduced yield. Producing enough seed for the next generation and not maximising seed quantity itself might be sufficient for the survival of wheat wild relatives. Thus, selective pressure does not necessarily select traits of value for maximising yield. Therefore, this strategy is not compatible with increasing wheat yield. Since the bulk of the Rca pool in wheat is made up of Rca 2 β (chapter 4) and heat stress only marginally increased *Rca1 β* levels, altering isoform levels as a response to heat stress would require a substantial alteration of the Rca pool in wheat. These findings indicate that there might be limited scope in improving the temperature response of Rubisco activation in wheat by altering protein levels of the native enzymes.

A way of improving Rca activity in wheat might be to transplant more thermostable Rca isoforms from other cereals such as rice, as discussed in chapter 5. However, compatibility with native wheat Rubisco might be a bottleneck as has been shown for Rca and Rubisco from wild and domesticated rice (Scafaro *et al.*, 2016; Shivhare & Mueller-Cajar, 2017). Therefore, a more promising strategy might be to engineer the superior Rca2 β isoform to be more thermostable, as demonstrated in chapter 3 (Degen *et al.*, 2020) and supported by results from Kumar *et al.* (2009) and Scafaro *et al.* (2019).

The results from Degen *et al.* (2020) show that the Rca2 β -M159I mutant is more thermostable whilst maintaining superior Rubisco activation activity compared to Rca1 β . This would allow for increased Rubisco activation during heat stress *in planta*. Changing only one amino acid is more straightforward than changing 7 or 11 amino acids, which also contained the switch from methionine to isoleucine, as was the case for Scafaro *et al.* (2019). Results from Degen *et al.* (2020) demonstrate that a majority of thermostability gained in mutants investigated in the study by Scafaro *et al.* (2019) can be attributed to the single isoleucine switch. Hence, engineering this Rca variant under the control of a heat-inducible promoter into wheat could improve resilience to heat waves.

In order to optimise Rubisco activation for a higher overall growth temperature, it would be more beneficial to use gene-editing to engineer the single isoleucine switch into *Rca2* genome copies. Furthermore, Rca2 β -M159I also exhibited reduced ADP-sensitivity and high activation efficiency, in contrast to Rca1 β and 2 α as shown in chapter 2. This would speed up Rubisco activation during shade to sun transitions and make Rubisco activation more thermotolerant. Improving Rubisco regulation by Rca should also be viewed in the context of the light reactions of photosynthesis. Since Rca uses the energy from ATP hydrolysis and ATP is supplied by ATP synthase, the possible effect of changes in Rca activity on ATP synthesis have to be taken into account. During heat stress, cyclic electron transport has been shown to increase (Bukhov *et al.*, 1999), which results in increased ATP production without producing NADPH. Therefore, the ATP:NADPH ratio is altered, and

more ATP is available for the CBBC (Sharkey, 2005). The inhibition of Rubisco at elevated temperature as a result of heat sensitive Rca might be a regulatory mechanism to protect the CBBC from this altered ATP:NADPH ratio. Since ATP hydrolysis by Rca still occurs above temperatures optimal for Rubisco activation (Degen *et al.*, 2020), Rca might act as an ATP sink at high temperatures, without activating Rubisco. Increased cyclic electron flow around PSI also constitutes a photoprotective mechanism, since PSI is prone to inhibition by overreduction (Bukhov *et al.*, 1999; Munekage *et al.*, 2002). Therefore, Rca may act as a thermal fuse during stressful high temperature conditions (Sharkey, 2005; Mueller-Cajar, 2017), however, this might be disadvantageous when growth temperatures of plants increase quickly as a result of anthropogenic climate change (IPPC, 2014).

Conclusion

This work advanced the understanding of wheat Rca. Differences in the activities of the three native Rca isoforms in wheat were characterised alongside the effect of ADP:ATP ratios. Residues were identified that conferred ADP-sensitivity. Results in this thesis demonstrate that Rca isoforms from wheat have different temperature responses and site-directed mutagenesis was used to produce more thermostable Rca variants. In addition, this work improves understanding of Rubisco regulation in wheat during pre-anthesis heat stress, including impact on the abundance of the three Rca isoforms and CA1Pase activity. Finally, screening for genetic diversity of Rca revealed high conservation amongst wheat wild relatives and other closely related crop species, with only a few residues differing between isoforms of the cereal species studied. Taken together, the findings presented in this work will inform production of more efficient and thermostable elite wheat cultivars.

References

- Bukhov NG, Wiese C, Neimanis S, Heber U. 1999.** Heat sensitivity of chloroplasts and leaves: Leakage of protons from thylakoids and reversible activation of cyclic electron transport. *Photosynthesis Research* **59**: 81–93.
- Carmo-Silva E, Scales JC, Madgwick PJ, Parry MAJ. 2015.** Optimizing Rubisco and its regulation for greater resource use efficiency. *Plant, Cell & Environment* **38**: 1817–1832.
- Castaneda-Alvarez NP, Khoury CK, Achicanoy HA, Bernau V, Dempewolf H, Eastwood RJ, Guarino L, Harker RH, Jarvis A, Maxted N, et al. 2016.** Global conservation priorities for crop wild relatives. *Nature Plants* **2**.
- Crafts-Brandner SJ, Salvucci ME. 2000.** Rubisco activase constrains the photosynthetic potential of leaves at high temperature and CO₂. *Proceedings of the National Academy of Sciences* **97**: 13430–13435.
- Degen GE, Worrall D, Carmo-Silva E. 2020.** An isoleucine residue acts as a thermal and regulatory switch in wheat Rubisco activase. *The Plant Journal* **103**: 742–751.
- IPPC. 2014.** Climate Change 2014. The Physical Basis of Climate Change—Working Group I Contribution to the Fifth Assessment Report of the Intergovernmental Panel on Climate Change. *Cambridge University Press*.
- Jurczyk B, Pocięcha E, Grzesiak M, Kalita K, Rapacz M. 2016.** Enhanced expression of Rubisco activase splicing variants differentially affects Rubisco activity during low temperature treatment in *Lolium perenne*. *Journal of Plant Physiology* **198**: 49–55.
- Kumar A, Li C, Portis AR. 2009.** Arabidopsis thaliana expressing a thermostable chimeric Rubisco activase exhibits enhanced growth and higher rates of photosynthesis at moderately high temperatures. *Photosynthesis Research* **100**: 143–153.

- Kurek I, Chang TK, Bertain SM, Madrigal A, Liu L, Lassner MW, Zhu G. 2007.** Enhanced thermostability of Arabidopsis Rubisco activase improves photosynthesis and growth rates under moderate heat stress. *The Plant Cell* **19**: 3230–3241.
- Mueller-Cajar O. 2017.** The diverse AAA+ machines that repair inhibited rubisco active sites. *Frontiers in Molecular Biosciences* **4**: 2–18.
- Munekage Y, Hojo M, Meurer J, Endo T, Tasaka M, Shikanai T. 2002.** PGR5 is involved in cyclic electron flow around photosystem I and is essential for photoprotection in Arabidopsis. *Cell* **110**: 361–371.
- Parry MAJ, Reynolds M, Salvucci ME, Raines C, Andralojc PJ, Zhu X-G, Price GD, Condon AG, Furbank RT. 2011.** Raising yield potential of wheat. II. Increasing photosynthetic capacity and efficiency. *Journal of Experimental Botany* **62**: 453–467.
- Perdomo JA, Degen GE, Worrall D, Carmo-Silva E. 2019.** Rubisco activation by wheat Rubisco activase isoform 2 β is insensitive to inhibition by ADP. *Biochemical Journal* **476**: 2595–2606.
- Prins A, Orr DJ, Andralojc PJ, Reynolds MP, Carmo-Silva E, Parry MAJ. 2016.** Rubisco catalytic properties of wild and domesticated relatives provide scope for improving wheat photosynthesis. *Journal of Experimental Botany* **67**: 1827–1838.
- Ray DK, Mueller ND, West PC, Foley JA. 2013.** Yield trends are insufficient to double global crop production by 2050. *PLoS ONE* **8**: e66428.
- Ray DK, West PC, Clark M, Gerber JS, Prishchepov AV, Chatterjee S. 2019.** Climate change has likely already affected global food production (YH Jung, Ed.). *PLoS ONE* **14**: e0217148.
- Riaz A, Hathorn A, Dinglasan E, Ziemls L, Richard C, Singh D, Mitrofanova O, Afanasenko O, Aitken E, Godwin I, et al. 2016.** Into the vault of

the Vavilov wheats: old diversity for new alleles. *Genetic Resources and Crop Evolution* **64**: 1–14.

Salvucci ME, Crafts-Brandner SJ. 2004a. Inhibition of photosynthesis by heat stress: the activation state of Rubisco as a limiting factor in photosynthesis. *Physiologia Plantarum* **120**: 179–186.

Salvucci ME, Crafts-Brandner SJ. 2004b. Relationship between the heat tolerance of photosynthesis and the thermal stability of Rubisco activase in plants from contrasting thermal environments. *Plant Physiology* **134**: 1460–1470.

Scafaro AP, Atwell BJ, Muylaert S, Reusel BV, Ruiz GA, Rie JV, Gallé A. 2018. A thermotolerant variant of rubisco activase from a wild relative improves growth and seed yield in rice under heat stress. *Frontiers in Plant Science* **871**: 1663.

Scafaro AP, Bautsoens N, Boer den B, Van Rie J, Gallé A. 2019. A conserved sequence from heat-adapted species improves rubisco activase thermostability in wheat. *Plant Physiology* **181**: 43–54.

Scafaro AP, Gallé A, Van Rie J, Carmo-Silva E, Salvucci ME, Atwell BJ. 2016. Heat tolerance in a wild *Oryza* species is attributed to maintenance of Rubisco activation by a thermally stable Rubisco activase ortholog. *New Phytologist* **211**: 899–911.

Scales JC, Parry MAJ, Salvucci ME. 2014. A non-radioactive method for measuring Rubisco activase activity in the presence of variable ATP: ADP ratios, including modifications for measuring the activity and activation state of Rubisco. *Photosynthesis Research* **119**: 355–365.

Semenov MA, Stratonovitch P, Alghabari F, Gooding MJ. 2014. Adapting wheat in Europe for climate change. *Journal of Cereal Science* **59**: 245–256.

Sharkey TD. 2005. Effects of moderate heat stress on photosynthesis: importance of thylakoid reactions, rubisco deactivation, reactive oxygen species, and thermotolerance provided by isoprene. *Plant, Cell & Environment* **28**: 269–277.

Shivhare D, Mueller-Cajal O. 2017. In vitro characterization of thermostable CAM rubisco activase reveals a rubisco interacting surface loop. *Plant Physiology* **174**: 1505–1516.

Stone PJ, Nicolas ME. 1994. Wheat cultivars vary widely in their responses of grain yield and quality to short periods of post-anthesis heat stress. *Functional Plant Biology* **21**: 887.

Vieille C, Zeikus GJ. 2001. Hyperthermophilic enzymes: sources, uses, and molecular mechanisms for thermostability. *Microbiology and Molecular Biology Reviews* **65**: 1–43.

Wingen LU, Orford S, Goram R, Leverington-Waite M, Bilham L, Patsiou TS, Ambrose M, Dicks J, Griffiths S. 2014. Establishing the A. E. Watkins landrace cultivar collection as a resource for systematic gene discovery in bread wheat. *Theoretical and Applied Genetics* **127**: 1831–1842.

Yamori W, Suzuki K, Noguchi KO, Nakai M, Terashima I. 2006. Effects of Rubisco kinetics and Rubisco activation state on the temperature dependence of the photosynthetic rate in spinach leaves from contrasting growth temperatures. *Plant, Cell & Environment* **29**: 1659–1670.

7. Complete reference list

- Akaike H. 1974.** A new look at the statistical model identification. *IEEE Transactions on Automatic Control* **19**: 716–723.
- Ammelburg M, Frickey T, Lupas AN. 2006.** Classification of AAA+ proteins. *Journal of Structural Biology* **156**: 2–11.
- Andralojc PJ, Carmo-Silva E, Degen GE, Parry MAJ. 2018.** Increasing metabolic potential: C-fixation. *Essays In Biochemistry* **62**: 109–118.
- Andralojc PJ, Madgwick PJ, Tao Y, Keys A, Ward JL, Beale MH, Loveland JE, Jackson PJ, Willis AC, Gutteridge S, et al. 2012.** 2-Carboxy-D-arabinitol 1-phosphate (CA1P) phosphatase: evidence for a wider role in plant Rubisco regulation. *Biochemical Journal* **442**: 733–742.
- Asseng S, Ewert F, Martre P, Rotter RP, Lobell DB, Cammarano D, Kimball BA, Ottman MJ, Wall GW, White JW, et al. 2014.** Rising temperatures reduce global wheat production. *Nature Climate Change* **5**: 143–147.
- Asseng S, Ewert F, Rosenzweig C, Jones JW, Hatfield JL, Ruane AC, Boote KJ, Thorburn PJ, Rotter RP, Cammarano D, et al. 2013.** Uncertainty in simulating wheat yields under climate change. *Nature Climate Change* **3**: 827–832.
- Atkin OK, Bruhn D, Hurry VM, Tjoelker MG. 2005.** Evans Review No. 2: The hot and the cold: unravelling the variable response of plant respiration to temperature. *Functional Plant Biology* **32**: 87–105.
- Ayeneh A, van Ginkel M, Reynolds MP, Ammar K. 2002.** Comparison of leaf, spike, peduncle and canopy temperature depression in wheat under heat stress. *Field Crops Research* **79**: 173–184.
- Barta C, Carmo-Silva E, Salvucci ME. 2011a.** Purification of Rubisco activase from leaves or after expression in *Escherichia coli*. *Methods in molecular biology* **684**: 363–374.

- Barta C, Carmo-Silva E, Salvucci ME. 2011b.** Rubisco activase activity assays. *Methods in molecular biology* **684**: 375–382.
- Bauwe H, Hagemann M, Fernie AR. 2010.** Photorespiration: players, partners and origin. *Trends in Plant Science* **15**: 330–336.
- Berry J, Bjorkman O. 1980.** Photosynthetic response and adaptation to temperature in higher plants. *Annual Review of Plant Physiology* **31**: 491–543.
- Bhat JY, Miličić G, Miličić G, Thieulin-Pardo G, Bracher A, Maxwell A, Maxwell A, Ciniawsky S, Mueller-Cajar O, Engen JR, et al. 2017a.** Mechanism of enzyme repair by the AAA(+) chaperone rubisco activase. *Molecular cell* **67**: 744–756.e6.
- Bhat JY, Thieulin-Pardo G, Hartl FU, Hayer-Hartl M. 2017b.** Rubisco activases: AAA+ chaperones adapted to enzyme repair. *Frontiers in Molecular Biosciences* **4**: 1555–10.
- Borrill P, Ramirez-Gonzalez R, Uauy C. 2016.** expVIP: a customizable RNA-seq data analysis and visualization platform. *Plant Physiology* **170**: 2172–2186.
- Bracher A, Sharma A, Starling-Windhof A. Hartl FU, Hayer-Hartl M. 2015.** Degradation of potent Rubisco inhibitor by selective sugar phosphatase. *Nature Plants* **1**: 14002.
- Bracher A, Whitney SM, Hartl FU, Hayer-Hartl M. 2017.** Biogenesis and Metabolic Maintenance of Rubisco. *Annual Review of Plant Biology* **68**: 29–60.
- Bradford MM. 1976.** A rapid and sensitive method for the quantitation of microgram quantities of protein utilizing the principle of protein-dye binding. *Analytical biochemistry* **72**: 248–254.
- Bukhov NG, Carpentier R. 2000.** Heterogeneity of photosystem II reaction centers as influenced by heat treatment of barley leaves. *Physiologia Plantarum* **110**: 279–285.

- Bukhov NG, Wiese C, Neimanis S, Heber U. 1999.** Heat sensitivity of chloroplasts and leaves: Leakage of protons from thylakoids and reversible activation of cyclic electron transport. *Photosynthesis Research* **59**: 81–93.
- Calvin M, Benson AA. 1948.** The Path of Carbon in Photosynthesis. *Science* **107**: 476–480.
- Carmo-Silva AE, Salvucci ME. 2011.** The activity of Rubisco's molecular chaperone, Rubisco activase, in leaf extracts. *Photosynthesis Research* **108**: 143–155.
- Carmo-Silva E, Andralojc PJ, Scales JC, Driever SM, Mead A, Lawson T, Raines CA, Parry MAJ. 2017.** Phenotyping of field-grown wheat in the UK highlights contribution of light response of photosynthesis and flag leaf longevity to grain yield. *Journal of Experimental Botany* **68**: 3473–3486.
- Carmo-Silva E, Gore MA, Andrade-Sanchez P, French AN, Hunsaker DJ, Salvucci ME. 2012.** Decreased CO₂ availability and inactivation of Rubisco limit photosynthesis in cotton plants under heat and drought stress in the field. *Environmental and Experimental Botany* **83**: 1–11.
- Carmo-Silva E, Salvucci ME. 2011.** The activity of Rubisco's molecular chaperone, Rubisco activase, in leaf extracts. *Photosynthesis Research* **108**: 143–155.
- Carmo-Silva E, Salvucci ME. 2012.** The temperature response of CO₂ assimilation, photochemical activities and Rubisco activation in *Camelina sativa*, a potential bioenergy crop with limited capacity for acclimation to heat stress. *Planta* **236**: 1433–1445.
- Carmo-Silva E, Salvucci ME. 2013.** The regulatory properties of Rubisco activase differ among species and affect photosynthetic induction during light transitions. *Plant Physiology* **161**: 1645–1655.
- Carmo-Silva E, Scales JC, Madgwick PJ, Parry MAJ. 2015.** Optimizing Rubisco and its regulation for greater resource use efficiency. *Plant, Cell & Environment* **38**: 1817–1832.

- Castaneda-Alvarez NP, Khoury CK, Achicanoy HA, Bernau V, Dempe-
wolf H, Eastwood RJ, Guarino L, Harker RH, Jarvis A, Maxted N, et al.**
2016. Global conservation priorities for crop wild relatives. *Nature Plants*
2: 16022
- Cavanagh AP, Kubien DS. 2013.** Can phenotypic plasticity in Rubisco
performance contribute to photosynthetic acclimation? *Photosynthesis*
Research **119**: 203–214.
- Chavan SG, Duursma RA, Tausz M, Ghannoum O. 2019.** Elevated CO₂
alleviates the negative impact of heat stress on wheat physiology but not
on grain yield. *Journal of Experimental Botany* **70**: 6447–6459.
- Cheng SH, Moore B, Seemann JR. 1998.** Effects of short- and long-term
elevated CO₂ on the expression of ribulose-1,5-bisphosphate carbox-
ylase/oxygenase genes and carbohydrate accumulation in leaves of *Ara-
bidopsis thaliana* (L.) Heynh. *Plant Physiology* **116**: 715–723.
- Chifflet S, Torriglia A, Chiesa R, Tolosa S. 1988.** A method for the deter-
mination of inorganic phosphate in the presence of labile organic phos-
phate and high concentrations of protein: application to lens ATPases.
Analytical biochemistry **168**: 1–4.
- Crafts-Brandner SJ, Salvucci ME. 2000.** Rubisco activase constrains the
photosynthetic potential of leaves at high temperature and CO₂. *Pro-
ceedings of the National Academy of Sciences* **97**: 13430–13435.
- Dawson IA, Wardlaw IF. 1989.** The tolerance of wheat to high tempera-
tures during reproductive growth. III. Booting to anthesis. *Australian*
Journal of Agricultural Research **40**: 965–980.
- Degen GE, Worrall D, Carmo-Silva E. 2020.** An isoleucine residue acts as
a thermal and regulatory switch in wheat Rubisco activase. *The Plant*
Journal **103**: 742–751.
- Driever SM, Simkin AJ, Alotaibi S, Fisk SJ, Madgwick PJ, Sparks CA,
Jones HD, Lawson T, Parry MAJ, Raines CA. 2017.** Increased SBPase
activity improves photosynthesis and grain yield in wheat grown in green-
house conditions. *Philosophical transactions of the Royal Society of Lon-
don. Series B, Biological sciences* **372**: 20160384.

- Dusenge ME, Duarte AG, Way DA. 2019.** Plant carbon metabolism and climate change: elevated CO₂ and temperature impacts on photosynthesis, photorespiration and respiration. *New Phytologist* **221**: 32–49.
- Eberhard S, Finazzi G, Wollman F-A. 2008.** The dynamics of photosynthesis. *Annual Review of Genetics* **42**: 463–515.
- Eckardt NA, Portis AR Jr. 1997.** Heat denaturation profiles of Ribulose-1,5-Bisphosphate Carboxylase/Oxygenase (Rubisco) and Rubisco activase and the inability of Rubisco activase to restore activity of heat-denatured Rubisco. **113**: 243–248.
- Edgar RC. 2004.** MUSCLE: multiple sequence alignment with high accuracy and high throughput. *Nucleic Acids Research* **32**: 1792–1797.
- Edmondson DL, Badger MR, Andrews TJ. 1990.** Slow inactivation of ribulosebisphosphate carboxylase during catalysis is not due to decarbamylation of the active site. *Plant Physiology* **93**: 1383–1389.
- Edwards K, Johnstone C, Thompson C. 1991.** A simple and rapid method for the preparation of plant genomic DNA for PCR analysis. *Nucleic Acids Research* **19**: 1349–1349.
- Ellis RJ. 1979.** The most abundant protein in the world. *Trends in Biochemical Sciences* **4**: 241–244.
- Evans JR, Lawson T. 2020.** From green to gold: agricultural revolution for food security. *Journal of Experimental Botany* **71**: 2211–2215.
- FAOSTAT 2014.** Food and Agriculture Organization of the United Nations Statistics Division.
- FAOSTAT. 2019.** *Crop Statistics*. Available at: <http://www.fao.org/faostat/en/#data/QC>.
- Fedoroff NV, Battisti DS, Beachy RN, Cooper PJM, Fischhoff DA, Hodges CN, Knauf VC, Lobell D, Mazur BJ, Molden D, et al. 2010.** Radically rethinking agriculture for the 21st century. *Science* **327**: 833–834.
- Feller U, Anders I, Mae T. 2008.** Rubiscolytics: fate of Rubisco after its enzymatic function in a cell is terminated. *Journal of Experimental Botany* **59**: 1615–1624.

Feller U, Crafts-Brandner S, Salvucci M. 1998. Moderately high temperatures inhibit ribulose-1,5-bisphosphate carboxylase/oxygenase (Rubisco) activase-mediated activation of Rubisco. *Plant Physiology* **116**: 539–546.

Flexas J, Díaz-Espejo A, Conesa MA, Coopman RE, Douthe C, Gago J, Gallé A, Galmés J, Medrano H, Ribas-Carbo M, et al. 2016. Mesophyll conductance to CO₂ and Rubisco as targets for improving intrinsic water use efficiency in C₃ plants. *Plant, Cell and Environment* **39**: 965–982.

Frantz, J., Cometti, N., Bugbee, B. 2004. Night temperature has a minimal effect on respiration and growth in rapidly growing plants. *Annals of Botany* **94**: 155–166.

Fu Y-B, Peterson GW, Horbach C, Konkin DJ, Beiles A, Nevo E. 2019. Elevated mutation and selection in wild emmer wheat in response to 28 years of global warming. *Proceedings of the National Academy of Sciences* **116**: 20002–20008.

Galmés J, Capó-Bauçà S, Niinemets Ü, Iñiguez C. 2019. Potential improvement of photosynthetic CO₂ assimilation in crops by exploiting the natural variation in the temperature response of Rubisco catalytic traits. *Current Opinion in Plant Biology* **49**: 60–67.

Galmés J, Hermida-Carrera C, Laanisto L, Niinemets Ü. 2016. A compendium of temperature responses of Rubisco kinetic traits: variability among and within photosynthetic groups and impacts on photosynthesis modeling. *Journal of Experimental Botany* **67**: 5067–5091.

Galmés J, Medrano H, Flexas J. 2007. Photosynthetic limitations in response to water stress and recovery in Mediterranean plants with different growth forms. *New Phytologist* **175**: 81–93.

Galmés J, Ribas-Carbó M, Medrano H, Flexas J. 2010. Rubisco activity in Mediterranean species is regulated by the chloroplastic CO₂ concentration under water stress. *Journal of Experimental Botany* **62**: 653–665.

Gourdji SM, Mathews KL, Reynolds M, Crossa J, Lobell DB. 2013. An assessment of wheat yield sensitivity and breeding gains in hot environments. *Proceedings. Biological sciences / The Royal Society* **280**: 20122190–20122190.

- Govindjee, Whitmarsh J. 1999.** Photosynthesis and Photomorphogenesis: Section I.2: The Photosynthetic process. *Concepts in Photobiology*: **13**.
- Gray SB, Dermody O, Klein SP, Locke AM, McGrath JM, Paul RE, Rosenthal DM, Ruiz-Vera UM, Siebers MH, Strellner R, et al. 2016.** Intensifying drought eliminates the expected benefits of elevated carbon dioxide for soybean. *Nature Plants* **2**: 16132.
- Haque MS, Kjaer KH, Rosenqvist E, Sharma DK, Ottosen C-O. 2014.** Heat stress and recovery of photosystem II efficiency in wheat (*Triticum aestivum* L.) cultivars acclimated to different growth temperatures. *Environmental and Experimental Botany* **99**: 1–8.
- Harrison EP, Olcer H, Lloyd JC, Long SP, Raines CA. 2001.** Small decreases in SBPase cause a linear decline in the apparent RuBP regeneration rate, but do not affect Rubisco carboxylation capacity. *Journal of Experimental Botany* **52**: 1779–1784.
- Harrison EP, Willingham NM, Lloyd JC, Raines CA. 1997.** Reduced sedoheptulose-1,7-bisphosphatase levels in transgenic tobacco lead to decreased photosynthetic capacity and altered carbohydrate accumulation. *Planta* **204**: 27–36.
- Hartl M, Füll M, Boersema PJ, Jost JO, Kramer K, Bakirbas A, Sindlinger J, Plöschinger M, Leister D, Uhrig G, et al. 2017.** Lysine acetylome profiling uncovers novel histone deacetylase substrate proteins in Arabidopsis. *Molecular Systems Biology* **13**: 949–16.
- Hasse D, Larsson AM, Andersson I. 2015.** Structure of Arabidopsis thaliana Rubisco activase. *Acta crystallographica. Section D, Biological crystallography* **71**: 800–808.
- Havaux M, Greppin H, Strasser RJ. 1991.** Functioning of photosystems I and II in pea leaves exposed to heat stress in the presence or absence of light: Analysis using in-vivo fluorescence, absorbance, oxygen and photoacoustic measurements. *Planta* **186**: 88–98.

- Hazra S, Henderson JN, Liles K, Hilton MT, Wachter RM. 2015.** Regulation of ribulose-1,5-bisphosphate carboxylase/oxygenase (rubisco) activase: product inhibition, cooperativity, and magnesium activation. *The Journal of Biological Chemistry* **290**: 24222–24236.
- Hein NT, Wagner D, Bheemanahalli R, Šebela D, Bustamante C, Chiluwal A, Neilsen ML, Jagadish SK. 2019.** Integrating field-based heat tents and cyber-physical system technology to phenotype high night-time temperature impact on winter wheat. *Plant Methods* **15**: 41.
- Henderson JN, Kuriata AM, Fromme R, Salvucci ME, Wachter RM. 2011.** Atomic resolution x-ray structure of the substrate recognition domain of higher plant ribulose-bisphosphate carboxylase/oxygenase (Rubisco) activase. *The Journal of Biological Chemistry* **286**: 35683–35688.
- Henikoff S, Henikoff JG. 1992.** Amino acid substitution matrices from protein blocks. *Proceedings of the National Academy of Sciences* **89**: 10915–10919.
- Hermida-Carrera C, Kapralov MV, Galmés J. 2016.** Rubisco Catalytic Properties and Temperature Response in Crops. **171**: 2549–2561.
- Hochman Z, Gobbett DL, Horan H. 2017.** Climate trends account for stalled wheat yields in Australia since 1990. *Global Change Biology* **23**: 2071–2081.
- Howe KL, Contreras-Moreira B, De Silva N, Maslen G, Akanni W, Allen J, Alvarez-Jarreta J, Barba M, Bolser DM, Cambell L, et al. 2019.** Ensembl Genomes 2020—enabling non-vertebrate genomic research. *Nucleic Acids Research* **48**: D689–D695.
- Huner NPA, Hayden DB. 1982.** Changes in the heterogeneity of ribulose-bisphosphate carboxylase–oxygenase in winter rye induced by cold hardening. *Canadian Journal of Biochemistry* **60**: 897–903.
- Huner NPA, Macdowall FD. 1979.** Changes in the net charge and subunit properties of ribulose bisphosphate carboxylase–oxygenase during cold hardening of Puma rye. *Canadian Journal of Biochemistry* **57**: 155–164.
- Impa SM, Sunoj VJ, Krassovskaya I, Bheemanahalli R, Obata T, Jagadish SK. 2019.** Carbon balance and source-sink metabolic changes in

winter wheat exposed to high night-time temperature. *Plant, Cell & Environment* **42**: 1233–1246.

IPCC. 2014. Climate change 2014. Mitigation of Climate Change—Working Group III Contribution to the Fifth Assessment Report of the Intergovernmental Panel on Climate Change. *Cambridge University Press*.

IPCC. 2014. Climate Change 2014. The Physical Basis of Climate Change—Working Group I Contribution to the Fifth Assessment Report of the Intergovernmental Panel on Climate Change. *Cambridge University Press*.

Ishijima S, Uchibori A, Takagi H, Maki R, Ohnishi M. 2003. Light-induced increase in free Mg²⁺ concentration in spinach chloroplasts: Measurement of free Mg²⁺ by using a fluorescent probe and necessity of stromal alkalization. *Archives of Biochemistry and Biophysics* **412**: 126–132.

Ishikawa C, Hatanaka T, Misoo S, Miyake C, Fukayama H. 2011. Functional Incorporation of Sorghum Small Subunit Increases the Catalytic Turnover Rate of Rubisco in Transgenic Rice. *Plant Physiology* **156**: 1603–1611.

Jarvis P, Soll J. 2002. Toc, Tic, and chloroplast protein import. *Biochimica et Biophysica Acta* **1590**: 177–189.

Jung H-S, Crisp PA, Estavillo GM, Cole B, Hong F, Mockler TC, Pogson BJ, Chory J. 2013. Subset of heat-shock transcription factors required for the early response of Arabidopsis to excess light. *Proceedings of the National Academy of Sciences* **110**: 14474–14479.

Jurczyk B, Hura K, Trzemecka A, Rapacz M. 2015. Evidence for alternative splicing mechanisms in meadow fescue (*Festuca pratensis*) and perennial ryegrass (*Lolium perenne*) Rubisco activase gene. *Journal of Plant Physiology* **176**: 61–64.

Jurczyk B, Pocięcha E, Grzesiak M, Kalita K, Rapacz M. 2016. Enhanced expression of Rubisco activase splicing variants differentially affects Rubisco activity during low temperature treatment in *Lolium perenne*. *Journal of Plant Physiology* **198**: 49–55.

- Kahiluoto H, Kaseva J, Balek J, Olesen JE, Ruiz-Ramos M, Gobin A, Kersebaum KC, Takáč J, Ruget F, Ferrise R, et al. 2019.** Decline in climate resilience of European wheat. *Proceedings of the National Academy of Sciences* **116**: 123–128.
- Kaiser E, Correa-Galvis V, Armbruster U. 2019.** Efficient photosynthesis in dynamic light environments: a chloroplast's perspective. *Biochemical Journal* **476**: 2725–2741.
- Keown JR, Griffin MDW, Mertens HDT, Pearce FG. 2013.** Small oligomers of ribulose-bisphosphate carboxylase/oxygenase (Rubisco) activase are required for biological activity. *The Journal of Biological Chemistry* **288**: 20607–20615.
- King J, Grewal S, Yang C-Y, Hubbart Edwards S, Scholefield D, Ashling S, Harper JA, Allen AM, Edwards KJ, Burridge AJ, et al. 2017a.** Introgression of *Aegilops speltoides* segments in *Triticum aestivum* and the effect of the gametocidal genes. *Annals of Botany* **121**: 229–240.
- King J, Grewal S, Yang C-Y, Hubbart S, Scholefield D, Ashling S, Edwards KJ, Allen AM, Burridge A, Bloor C, et al. 2017b.** A step change in the transfer of interspecific variation into wheat from *Amblyopyrum muticum*. *Plant Biotechnology Journal* **15**: 217–226.
- Ku SB, Edwards GE. 1977. Oxygen inhibition of photosynthesis: I. Temperature dependence and relation to O₂/CO₂ solubility ratio. *Plant Physiology* **59**: 986–990.
- Kumar A, Li C, Portis AR. 2009.** *Arabidopsis thaliana* expressing a thermostable chimeric Rubisco activase exhibits enhanced growth and higher rates of photosynthesis at moderately high temperatures. *Photosynthesis Research* **100**: 143–153.
- Kurek I, Chang TK, Bertain SM, Madrigal A, Liu L, Lassner MW, Zhu G. 2007.** Enhanced thermostability of *Arabidopsis* Rubisco activase improves photosynthesis and growth rates under moderate heat stress. *The Plant Cell* **19**: 3230–3241.
- Kyte J, Doolittle R. 1982.** A simple method for displaying the hydrophobic character of a protein. *Journal of Molecular Biology* **157**: 105–132.

- Laterre R, Pottier M, Remacle C, Boutry M. 2017.** Photosynthetic trichomes contain a specific rubisco with a modified pH-dependent activity. *Plant Physiology* **173**: 2110–2120.
- Lauerer M, Saftic D, Quick WP, Labate C, Fichtner K, Schulze E-D, Rodermeel SR, Bogorad L, Stitt M. 1993.** Decreased ribulose-1,5-bisphosphate carboxylase-oxygenase in transgenic tobacco transformed with “antisense” rbcS. *Planta* **190**: 332–345.
- Law R, Crafts-Brandner S. 1999.** Inhibition and acclimation of photosynthesis to heat stress is closely correlated with activation of ribulose-1,5-bisphosphate carboxylase/oxygenase. *Plant Physiology* **120**: 173–182.
- Law RD, Crafts-Brandner SJ, Salvucci ME. 2001.** Heat stress induces the synthesis of a new form of ribulose-1,5-bisphosphate carboxylase/oxygenase activase in cotton leaves. *Planta* **214**: 117–125.
- Lawson T, Vialet-Chabrand S. 2018.** Speedy stomata, photosynthesis and plant water use efficiency. *New Phytologist* **221**: 93–98.
- Leakey ADB, Press MC, Scholes JD. 2003.** High-temperature inhibition of photosynthesis is greater under sunflecks than uniform irradiance in a tropical rain forest tree seedling. *Plant, Cell and Environment* **26**: 1681–1690.
- Liu B, Asseng S, Müller C, Ewert F, Elliott J, Lobell DB, Martre P, Ruane AC, Wallach D, Jones JW, *et al.* 2016.** Similar estimates of temperature impacts on global wheat yield by three independent methods. *Nature Climate Change* **6**: 1130–1136.
- Lobo AKM, Orr DJ, Gutierrez MO, Andralojc PJ, Sparks C, Parry MAJ, Carmo-Silva E. 2019.** Overexpression of calpase Decreases Rubisco Abundance and Grain Yield in Wheat. *Plant Physiology* **181**: 471–479.
- Long SP, Ainsworth EA, Leakey ADB, Nösberger J, Ort DR. 2006a.** Food for thought: lower-than-expected crop yield stimulation with rising CO₂ concentrations. *Science* **312**: 1918–1921.
- Long SP, Zhu X-G, Naidu SL, Ort DR. 2006b.** Can improvement in photosynthesis increase crop yields? *Plant, Cell & Environment* **29**: 315–330.

- Lorimer GH, Badger MR, Andrews TJ. 1976.** The activation of ribulose-1,5-bisphosphate carboxylase by carbon dioxide and magnesium ions. Equilibria, kinetics, a suggested mechanism, and physiological implications. *Biochemistry* **15**: 529–536.
- Lorimer GH, Miziorko HM. 1980.** Carbamate formation on the epsilon-amino group of a lysyl residue as the basis for the activation of ribulose-bisphosphate carboxylase by CO₂ and Mg²⁺. *Biochemistry* **19**: 5321–5328.
- Marcussen T, Sandve SR, Heier L, Spannagl M, Pfeifer M, Jakobsen KS, Wulff BBH, Steuernagel B, Mayer KFX, Olsen O-A, et al. 2014.** Ancient hybridizations among the ancestral genomes of bread wheat. *Science* **345**: –1250092.
- Matsuura Y, Ota M, Tanaka T, Takehira M, Ogasahara K, Bagautdinov B, Kunishima N, Yutani K. 2010.** Remarkable improvement in the heat stability of CutA1 from *Escherichia coli* by rational protein design. *Journal of Biochemistry* **148**: 449–458.
- Matsuura Y, Takehira M, Joti Y, Ogasahara K, Tanaka T, Ono N, Kunishima N, Yutani K. 2015.** Thermodynamics of protein denaturation at temperatures over 100 °C: CutA1 mutant proteins substituted with hydrophobic and charged residues. *Scientific reports* **5**: 15545.
- Mayer KFX, Rogers J, Dole el J, Pozniak C, Eversole K, Feuillet C, Gill B, Friebe B, Lukaszewski AJ, Sourdille P, et al. 2014.** A chromosome-based draft sequence of the hexaploid bread wheat (*Triticum aestivum*) genome. *Science* **345**: 1251788–1251788.
- McKay RML, Gibbs SP, Vaughn KC. 1991.** RuBisCo activase is present in the pyrenoid of green algae. *Protoplasma* **162**: 38–45.
- Michelet L, Zaffagnini M, Morisse S, Sparla F, Perez-Perez ME, Francia F, Danon A, Marchand CH, Fermani S, Trost P, et al. 2013.** Redox regulation of the Calvin-Benson cycle: something old, something new. *Frontiers in Plant Science* **4**: 470.
- Middleton CP, Senerchia N, Stein N, Akhunov ED, Keller B, Wicker T, Kilian B. 2014.** Sequencing of chloroplast genomes from wheat, barley,

rye and their relatives provides a detailed insight into the evolution of the triticeae tribe (MW Davey, Ed.). *PLoS ONE* **9**: e85761.

Miki Y, Yoshida K, Mizuno N, Nasuda S, Sato K, Takumi S. 2019.

Origin of wheat B-genome chromosomes inferred from RNA sequencing analysis of leaf transcripts from section Sitopsis species of *Aegilops*. *DNA research : an international journal for rapid publication of reports on genes and genomes* **26**: 171–182.

Miller JM, Enemark EJ. 2016. Fundamental characteristics of AAA+ protein family structure and function. *Archaea* 2016: 9294307–9294312.

Morita K, Hatanaka T, Misoo S, Fukayama H. 2014. Unusual small subunit that is not expressed in photosynthetic cells alters the catalytic properties of Rubisco in rice. *Plant Physiology* **164**: 69–79.

Mueller-Cajar O, Stotz M, Wendler P, Hartl FU, Bracher A, Hayer-Hartl M. 2011. Structure and function of the AAA+ protein CbbX, a red-type Rubisco activase. *Nature* **479**: 194–199.

Mueller-Cajar O. 2017. The diverse AAA+ machines that repair inhibited rubisco active sites. *Frontiers in Molecular Biosciences* **4**: 2–18.

Munekage Y, Hojo M, Meurer J, Endo T, Tasaka M, Shikanai T. 2002.

PGR5 is involved in cyclic electron flow around photosystem I and is essential for photoprotection in Arabidopsis. *Cell* **110**: 361–371.

Nagarajan R, Gill KS. 2018. Evolution of Rubisco activase gene in plants. *Plant Molecular Biology* **96**: 69–87.

Neuwald AF, Aravind L, Spouge JL, Koonin EV. 1999. AAA+: A class of chaperone-like ATPases associated with the assembly, operation, and disassembly of protein complexes. *Genome research* **9**: 27–43.

Ogren W. 1984. Photorespiration: pathways, regulation, and modification. *Annual Review of Plant Physiology*: 415–442.

Ogura T, Whiteheart SW, Wilkinson AJ. 2004. Conserved arginine residues implicated in ATP hydrolysis, nucleotide-sensing, and inter-subunit interactions in AAA and AAA+ ATPases. *Journal of Structural Biology* **146**: 106–112.

- Ogura T, Wilkinson AJ. 2001.** AAA+ superfamily ATPases: common structure--diverse function. *Genes to cells : devoted to molecular & cellular mechanisms* **6**: 575–597.
- Orr DJ, Alcântara A, Kapralov MV, John Andralojc P, Carmo-Silva E, Parry MAJ. 2016.** Surveying rubisco diversity and temperature response to improve crop photosynthetic efficiency. *Plant Physiology* **172**: 707–717.
- Orr DJ, Carmo-Silva E. 2018.** Extraction of Rubisco to determine catalytic constants. Covshoff S ed. *Photosynthesis: Methods and Protocols*. Springer Protocols, 229–238.
- Ort DR, Merchant SS, Alric J, Barkan A, Blankenship RE, Bock R, Croce R, Hanson MR, Hibberd JM, Long SP, et al. 2015.** Redesigning photosynthesis to sustainably meet global food and bioenergy demand. *Proceedings of the National Academy of Sciences* **112**: 8529–8536.
- Paolacci AR, Tanzarella OA, Porceddu E, Ciaffi M. 2009.** Identification and validation of reference genes for quantitative RT-PCR normalization in wheat. *BMC Molecular Biology* **10**: 11–27.
- Parry MAJ, Keys AJ, Madgwick PJ, Carmo-Silva AE, Andralojc PJ. 2008.** Rubisco regulation: a role for inhibitors. *Journal of Experimental Botany* **59**: 1569–1580.
- Parry MAJ, Reynolds M, Salvucci ME, Raines C, Andralojc PJ, Zhu X-G, Price GD, Condon AG, Furbank RT. 2011.** Raising yield potential of wheat. II. Increasing photosynthetic capacity and efficiency. *Journal of Experimental Botany* **62**: 453–467.
- Pearce FG. 2006.** Catalytic by-product formation and ligand binding by ribulose biphosphate carboxylases from different phylogenies. *Biochemical Journal* **399**: 525–534.
- Pennacchi JP, Silva EC, Andralojc PJ, Lawson T, Allen AM, Raines CA, Parry MAJ. 2018.** Stability of wheat grain yields over three field seasons in the UK. *Food and Energy Security* **24**: e00147.
- Peraudeau S, Lafarge T, Roques S, Quiñones CO, Clement-Vidal A, Ouwerkerk PBF, Van Rie J, Fabre D, Jagadish KSV, Dingkuhn M. 2015.**

- Effect of carbohydrates and night temperature on night respiration in rice. *Journal of Experimental Botany* **66**: 3931–3944.
- Perdomo JA, Capó-Bauçà S, Carmo-Silva E, Galmés J. 2017.** Rubisco and Rubisco activase play an important role in the biochemical limitations of photosynthesis in rice, wheat, and maize under high temperature and water deficit. *Frontiers in Plant Science* **8**: 490.
- Perdomo JA, Degen GE, Worrall D, Carmo-Silva E. 2019.** Rubisco activation by wheat Rubisco activase isoform 2 β is insensitive to inhibition by ADP. *Biochemical Journal* **476**: 2595–2606.
- Perdomo JA, Sales CRG, Carmo-Silva E. 2018.** Quantification of photosynthetic enzymes in leaf extracts by immunoblotting. *Methods in Molecular Biology* **1770**: 215–227.
- Pfaffl MW. 2001. A new mathematical model for relative quantification in real-time RT-PCR. *Nucleic Acids Research* **29**: e45–45.
- Porter JR, Gawith M. 1999.** Temperatures and the growth and development of wheat: a review. *European Journal of Agronomy* **10**: 23–36.
- Porter JR, Xie L, Challinor AJ, Cochrane K, Howden SM, Iqbal MM, Lobell DB, Travasso MI. 2014.** Food security and food production systems. In: *Climate Change 2014: Impacts, Adaptation, and Vulnerability. Part A: Global and Sectoral Aspects. Contribution of Working Group II to the Fifth Assessment Report of the Intergovernmental Panel on Climate Change.*
- Portis AR, Li C, Wang D, Salvucci ME. 2008.** Regulation of Rubisco activase and its interaction with Rubisco. *Journal of Experimental Botany* **59**: 1597–1604.
- Pottier M, Gilis D, Boutry M. 2018.** The hidden face of Rubisco. *Trends in Plant Science* **23**: 382–392.
- Pradhan GP, Prasad P, Fritz AK, Kirkham MB, Gill BS. 2012.** High temperature tolerance in *Aegilops* species and its potential transfer to wheat. *Crop Science*: 292–304.

- Prins A, Orr DJ, Andralojc PJ, Reynolds MP, Carmo-Silva E, Parry MAJ. 2016.** Rubisco catalytic properties of wild and domesticated relatives provide scope for improving wheat photosynthesis. *Journal of Experimental Botany* **67**: 1827–1838.
- R Core Development Team. 2013.** A language and environment for statistical computing. <http://www.r-project.org/>
- R Studio Team. 2019.** RStudio Cloud: Integrated Development for R. <https://www.rstudio.com/>
- Ramirez-Gonzalez RH, Borrill P, Lang D, Harrington SA, Brinton J, Venturini L, Davey M, Jacobs J, van Ex F, Pasha A, et al. 2018.** The transcriptional landscape of polyploid wheat. *Science* **361**: eaar6089.
- Rashid FAA, Scafaro AP, Asao S, Fenske R, Dewar RC, Masle J, Taylor NL, Atkin OK. 2020.** Diel and temperature driven variation of leaf dark respiration rates and metabolite levels in rice. *New Phytologist*
<https://doi.org/10.1111/nph.16661>
- Ray DK, Mueller ND, West PC, Foley JA. 2013.** Yield trends are insufficient to double global crop production by 2050. *PLoS ONE* **8**: e66428.
- Ray DK, Ramankutty N, Mueller ND, West PC, Foley JA. 2012.** Recent patterns of crop yield growth and stagnation. *Nature Communications* **3**: 1293.
- Ray DK, West PC, Clark M, Gerber JS, Prishchepov AV, Chatterjee S. 2019.** Climate change has likely already affected global food production (YH Jung, Ed.). *PLoS ONE* **14**: e0217148.
- Reynolds M, Dreccer F, Trethowan R. 2007.** Drought-adaptive traits derived from wheat wild relatives and landraces. *Journal of Experimental Botany* **58**: 177–186.
- Riaz A, Hathorn A, Dinglasan E, Ziemis L, Richard C, Singh D, Mitrofanova O, Afanasenko O, Aitken E, Godwin I, et al. 2016.** Into the vault of the Vavilov wheats: old diversity for new alleles. *Genetic Resources and Crop Evolution* **64**: 1–14.
- Robinson SP, Portis AR. 1989.** Ribulose-1,5-bisphosphate carboxylase/oxygenase activase protein prevents the in vitro decline in activity

of ribulose-1,5-bisphosphate carboxylase/oxygenase. *Plant Physiology* **90**: 968–971.

Rosenthal DM, Locke AM, Khozaei M, Raines CA, Long SP, Ort DR.

2011. Over-expressing the C3 photosynthesis cycle enzyme Sedoheptulose-1-7 Bisphosphatase improves photosynthetic carbon gain and yield under fully open air CO₂ fumigation (FACE). *BMC Plant Biology* **11**: 123.

Ruiz-Vera UM, Siebers M, Gray SB, Drag DW, Rosenthal DM, Kimball BA, Ort DR, Bernacchi CJ. 2013. Global warming can negate the expected CO₂ stimulation in photosynthesis and productivity for soybean grown in the Midwestern United States. *Plant Physiology* **162**: 410–423.

Ruiz-Vera UM, Siebers MH, Drag DW, Ort DR, Bernacchi CJ. 2015. Canopy warming caused photosynthetic acclimation and reduced seed yield in maize grown at ambient and elevated [CO₂]. *Global Change Biology* **21**: 4237–4249.

Sadok W, Jagadish SK. 2020. The hidden costs of nighttime warming on yields. *Trends in Plant Science* **25**: 644–651.

Sage RF, Way DA, Kubien DS. 2008. Rubisco, Rubisco activase, and global climate change. *Journal of Experimental Botany* **59**: 1581–1595.

Salvucci ME, Anderson JC. 1987. Factors affecting the activation state and the level of total activity of ribulose bisphosphate carboxylase in tobacco protoplasts. *Plant Physiology* **85**: 66–71.

Salvucci ME, Crafts-Brandner SJ. 2004a. Inhibition of photosynthesis by heat stress: the activation state of Rubisco as a limiting factor in photosynthesis. *Physiologia Plantarum* **120**: 179–186.

Salvucci ME, Crafts-Brandner SJ. 2004b. Relationship between the heat tolerance of photosynthesis and the thermal stability of Rubisco activase in plants from contrasting thermal environments. *Plant Physiology* **134**: 1460–1470.

Salvucci ME, Crafts-Brandner SJ. 2004c. Mechanism for deactivation of Rubisco under moderate heat stress. *Physiologia Plantarum* **122**: 513–519.

- Salvucci ME, DeRidder BP, Portis AR. 2006.** Effect of activase level and isoform on the thermotolerance of photosynthesis in Arabidopsis. *Journal of Experimental Botany* **57**: 3793–3799.
- Salvucci ME, Ogren WL. 1996.** The mechanism of Rubisco activase: Insights from studies of the properties and structure of the enzyme. *Photosynthesis Research* **47**: 1–11.
- Salvucci ME, Osteryoung KW, Crafts-Brandner SJ, Vierling E. 2001.** Exceptional sensitivity of Rubisco activase to thermal denaturation *in vitro* and *in vivo*. *Plant Physiology* **127**: 1053–1064.
- Salvucci ME, Portis AR, Ogren WL. 1985.** A soluble chloroplast protein catalyzes ribulosebisphosphate carboxylase/oxygenase activation *in vivo*. *Photosynthesis Research* **7**: 193–201.
- Salvucci ME, Portis AR, Ogren WL. 1986.** Light and CO₂ Response of Ribulose-1,5-Bisphosphate Carboxylase/Oxygenase Activation in Arabidopsis Leaves. **80**: 655–659.
- Salvucci ME, van de Loo FJ, Stecher D. 2003.** Two isoforms of Rubisco activase in cotton, the products of separate genes not alternative splicing. *Planta* **216**: 736–744.
- Salvucci ME, Werneke JM, Ogren WL, Portis AR. 1987.** Purification and Species Distribution of Rubisco Activase. *Plant Physiology* **84**: 930–936.
- Salvucci ME. 2008.** Association of Rubisco activase with chaperonin-60 beta: a possible mechanism for protecting photosynthesis during heat stress. *Journal of Experimental Botany* **59**: 1923–1933.
- Scafaro AP, Atwell BJ, Muylaert S, Reusel BV, Ruiz GA, Rie JV, Gallé A. 2018.** A thermotolerant variant of rubisco activase from a wild relative improves growth and seed yield in rice under heat stress. *Frontiers in Plant Science* **871**: 1663.
- Scafaro AP, Bautsoens N, Boer den B, Van Rie J, Gallé A. 2019.** A conserved sequence from heat-adapted species improves rubisco activase thermostability in wheat. *Plant Physiology* **181**: 43–54.
- Scafaro AP, De Vleeschauwer D, Bautsoens N, Hannah MA, Boer den B, Gallé A, Van Rie J. 2019b.** A single point mutation in the C-terminal

extension of wheat Rubisco activase dramatically reduces ADP inhibition via enhanced ATP binding affinity. *The Journal of Biological Chemistry* **294**: 17931–17940.

Scafaro AP, Gallé A, Van Rie J, Carmo-Silva E, Salvucci ME, Atwell BJ. 2016. Heat tolerance in a wild *Oryza* species is attributed to maintenance of Rubisco activation by a thermally stable Rubisco activase ortholog. *New Phytologist* **211**: 899–911.

Scafaro AP, Yamori W, Carmo-Silva E, Salvucci ME, von Caemmerer S, Atwell BJ. 2012. Rubisco activity is associated with photosynthetic thermotolerance in a wild rice (*Oryza meridionalis*). *Physiologia Plantarum* **146**: 99–109.

Scales JC, Parry MAJ, Salvucci ME. 2014. A non-radioactive method for measuring Rubisco activase activity in the presence of variable ATP: ADP ratios, including modifications for measuring the activity and activation state of Rubisco. *Photosynthesis Research* **119**: 355–365.

Schrader SM, Kane HJ, Sharkey TD, von Caemmerer S. 2006. High temperature enhances inhibitor production but reduces fallover in tobacco Rubisco. *Functional Plant Biology* **33**: 921–929.

Schrader SM, Wise RR, Wacholtz WF, Ort DR, Sharkey TD. 2004. Thylakoid membrane responses to moderately high leaf temperature in Pima cotton. *Plant, Cell & Environment* **27**: 725–735.

Semenov MA, Mitchell RAC, Whitmore AP, Hawkesford MJ, Parry MAJ, Shewry PR. 2012. Shortcomings in wheat yield predictions. *Nature Climate Change* **2**: 380–382.

Semenov MA, Stratonovitch P, Alghabari F, Gooding MJ. 2014. Adapting wheat in Europe for climate change. *Journal of Cereal Science* **59**: 245–256.

Sharkey TD, Zhang R. 2010. High temperature effects on electron and proton circuits of photosynthesis. *Journal of Integrative Plant Biology* **52**: 712–722.

- Sharkey TD. 2005.** Effects of moderate heat stress on photosynthesis: importance of thylakoid reactions, rubisco deactivation, reactive oxygen species, and thermotolerance provided by isoprene. *Plant, Cell & Environment* **28**: 269–277.
- Sharwood RE, Ghannoum O, Kapralov MV, Gunn LH, Whitney SM. 2016.** Temperature responses of Rubisco from Paniceae grasses provide opportunities for improving C3 photosynthesis. *Nature Plants* **2**: 1–9.
- Sharwood RE, Sonawane BV, Ghannoum O, Whitney SM. 2016.** Improved analysis of C4 and C3 photosynthesis via refined in vitro assays of their carbon fixation biochemistry. *Journal of Experimental Botany* **67**: 3137–3148
- Shivhare D, Mueller-Cajar O. 2017.** In vitro characterization of thermostable CAM rubisco activase reveals a rubisco interacting surface loop. *Plant Physiology* **174**: 1505–1516.
- Silva-Pérez V, Furbank RT, Condon AG, Evans JR. 2017.** Biochemical model of C3 photosynthesis applied to wheat at different temperatures. *Plant, Cell & Environment* **40**: 1552–1564.
- Simkin AJ, McAusland L, Headland LR, Lawson T, Raines CA. 2015.** Multigene manipulation of photosynthetic carbon assimilation increases CO₂ fixation and biomass yield in tobacco. *Journal of Experimental Botany* **66**: 4075–4090.
- Slattery RA, Ort DR. 2019.** Carbon assimilation in crops at high temperatures. *Plant, Cell & Environment* **42**: 2750–2758.
- Somerville CR, Archie R, Portis J, Ogren WL. 1982.** A Mutant of *Arabidopsis thaliana* Which Lacks Activation of RuBP Carboxylase In Vivo. *Plant Physiology* **70**: 381–387.
- Spreitzer RJ. 2003.** Role of the small subunit in ribulose-1,5-bisphosphate carboxylase/oxygenase. *Archives of Biochemistry and Biophysics* **414**: 141–149.

- Stevenson JR, Villoria N, Byerlee D, Kelley T, Maredia M. 2013.** Green Revolution research saved an estimated 18 to 27 million hectares from being brought into agricultural production. *Proceedings of the National Academy of Sciences* **110**: 8363–8368.
- Stitt M, Lilley RM, Heldt HW. 1982.** Adenine nucleotide levels in the cytosol, chloroplasts, and mitochondria of wheat leaf protoplasts. **70**: 971–977.
- Stone PJ, Nicolas ME. 1994.** Wheat cultivars vary widely in their responses of grain yield and quality to short periods of post-anthesis heat stress. *Functional Plant Biology* **21**: 887.
- Stothard P. 2000.** The sequence manipulation suite: JavaScript programs for analyzing and formatting protein and DNA sequences. *BioTechniques* **28**: 1102–1104.
- Stotz M, Mueller-Cajar O, Ciniawsky S, Wendler P, Hartl FU, Bracher A, Hayer-Hartl M. 2011.** Structure of green-type Rubisco activase from tobacco. *Nature Structural & Molecular Biology* **18**: 1366–U78.
- Tack J, Barkley A, Nalley LL. 2015.** Effect of warming temperatures on US wheat yields. *Proceedings of the National Academy of Sciences* **112**: 6931–6936.
- Tanaka A, Takahashi K, Masutomi Y, Hanasaki N, Hijioka Y, Shiogama H, Yamanaka Y. 2015.** Adaptation pathways of global wheat production: Importance of strategic adaptation to climate change. *Scientific reports* **5**: 14312.
- Taylor SH, Long SP. 2017.** Slow induction of photosynthesis on shade to sun transitions in wheat may cost at least 21% of productivity. *Philosophical Transactions of the Royal Society B: Biological Sciences* **372**: 20160543.
- Thomey ML, Slattery RA, Köhler IH, Bernacchi CJ, Ort DR. 2019.** Yield response of field-grown soybean exposed to heat waves under current and elevated [CO₂]. *Global Change Biology* **25**: 4352–4368.

- Tilman D, Balzer C, Hill J, Befort BL. 2011.** Global food demand and the sustainable intensification of agriculture. *Proceedings of the National Academy of Sciences* **108**: 20260–20264.
- Tsai YCC, Lapina MC, Bhushan S, Mueller-Cajar O. 2015.** Identification and characterization of multiple rubisco activases in chemoautotrophic bacteria. *Nature Communications* **6**: 8883.
- Uematsu K, Suzuki N, Iwamae T, Inui M, Yukawa H. 2012.** Increased fructose 1,6-bisphosphate aldolase in plastids enhances growth and photosynthesis of tobacco plants. *Journal of Experimental Botany* **63**: 3001–3009.
- United Nations, Department of Economic and Social Affairs, Population Division. 2015.** *World Population Prospects: The 2015 Revision, Key Findings and Advance Tables*.
- Vico G, Way DA, Hurry V, Manzoni S. 2019.** Can leaf net photosynthesis acclimate to rising and more variable temperatures? *Plant, Cell & Environment* **42**: 1913–1928.
- Vieille C, Zeikus GJ. 2001.** Hyperthermophilic enzymes: sources, uses, and molecular mechanisms for thermostability. *Microbiology and Molecular Biology Reviews* **65**: 1–43.
- Vinyard DJ, Ananyev GM, Charles Dismukes G. 2013.** Photosystem II: The Reaction Center of Oxygenic Photosynthesis*. *Annual Review of Biochemistry* **82**: 577–606.
- von Caemmerer S. 2000.** *Biochemical Models of Leaf Photosynthesis*. CSIRO Publishing.
- Walker BJ, VanLoocke A, Bernacchi CJ, Ort DR. 2016.** The costs of photorespiration to food production now and in the future. *Annual Review of Plant Biology* **67**: 107–129.
- Wang D, Li X-F, Zhou Z-J, Feng X-P, Yang W-J, Jiang D-A. 2010.** Two Rubisco activase isoforms may play different roles in photosynthetic heat acclimation in the rice plant. *Physiologia Plantarum* **139**: 55–67.
- Wang D, Portis AR. 2006.** Increased sensitivity of oxidized large isoform of ribulose-1,5-bisphosphate carboxylase/oxygenase (rubisco) activase to

ADP inhibition is due to an interaction between its carboxyl extension and nucleotide-binding pocket. *The Journal of Biological Chemistry* **281**: 25241–25249.

Wang Q, Serban AJ, Wachter RM, Moerner WE. 2018. Single-molecule diffusometry reveals the nucleotide-dependent oligomerization pathways of *Nicotiana tabacum* Rubisco activase. *Journal of Chemical Physics* **148**: 123319.

Wang X, Cai J, Jiang D, Liu F, Dai T, Cao W. 2011. Pre-anthesis high-temperature acclimation alleviates damage to the flag leaf caused by post-anthesis heat stress in wheat. *Journal of Plant Physiology* **168**: 585–593.

Way DA, Yamori W. 2014. Thermal acclimation of photosynthesis: On the importance of adjusting our definitions and accounting for thermal acclimation of respiration. *Photosynthesis Research* **119**: 89–100.

Weis E. 1981. Reversible heat-inactivation of the Calvin cycle: A possible mechanism of the temperature regulation of photosynthesis. *Planta* **151**: 33–39.

Wendler P, Ciniawsky S, Kock M, Kube S. 2012. Structure and function of the AAA+ nucleotide binding pocket. *Biochimica et Biophysica Acta* **1823**: 2–14.

Whitney SM, Houtz RL, Alonso H. 2011. Advancing our understanding and capacity to engineer nature's CO₂-sequestering enzyme, Rubisco. *Plant Physiology* **155**: 27–35.

Whitney SM, von Caemmerer S, Hudson GS, Andrews TJ. 1999. Directed mutation of the Rubisco large subunit of tobacco influences photorespiration and growth. *Plant Physiology* **121**: 579–588.

Wickham H. 2017. tidyverse: Easily install and load ‘Tidyverse’ packages. <https://www.tidyverse.org>

Wingen LU, Orford S, Goram R, Leverington-Waite M, Bilham L, Patsiou TS, Ambrose M, Dicks J, Griffiths S. 2014. Establishing the A. E. Watkins landrace cultivar collection as a resource for systematic gene

- discovery in bread wheat. *Theoretical and Applied Genetics* **127**: 1831–1842.
- Wood SN. 2017.** *Generalized Additive Models: An Introduction with R*. Chapman and Hall/CRC.
- Yamori W, Hikosaka K, Way DA. 2013.** Temperature response of photosynthesis in C3, C4, and CAM plants: temperature acclimation and temperature adaptation. *Photosynthesis Research* **119**: 101–117.
- Yamori W, Suzuki K, Noguchi KO, Nakai M, Terashima I. 2006.** Effects of Rubisco kinetics and Rubisco activation state on the temperature dependence of the photosynthetic rate in spinach leaves from contrasting growth temperatures. *Plant, Cell & Environment* **29**: 1659–1670.
- Yang Y, Zhang Q, Huang G, Peng S, Li Y. 2020.** Temperature responses of photosynthesis and leaf hydraulic conductance in rice and wheat. *Plant, Cell and Environment* **43**: 1437–1451.
- Yoon M, Putterill JJ, Ross GS, Laing WA. 2001.** Determination of the relative expression levels of rubisco small subunit genes in Arabidopsis by rapid amplification of cDNA ends. *Analytical Biochemistry* **291**: 237–244.
- Zaïm M, Hassouni El K, Gamba F, Filali-Maltouf A, Belkadi B, Sourour A, Amri A, Nachit M, Taghouti M, Bassi FM. 2017.** Wide crosses of durum wheat (*Triticum durum Desf.*) reveal good disease resistance, yield stability, and industrial quality across Mediterranean sites. *Field Crops Research* **214**: 219–227.
- Zhang N, Kallis RP, Ewy RG, Portis AR. 2002.** Light modulation of Rubisco in Arabidopsis requires a capacity for redox regulation of the larger Rubisco activase isoform. *Proceedings of the National Academy of Sciences* **99**: 3330–3334.
- Zhang N, Portis AR. 1999.** Mechanism of light regulation of Rubisco: a specific role for the larger Rubisco activase isoform involving reductive activation by thioredoxin-f. *Proceedings of the National Academy of Sciences* **96**: 9438–9443.

Zhang N, Schürmann P, Portis AR. 2001. Characterization of the regulatory function of the 46-kDa isoform of Rubisco activase from Arabidopsis. *Photosynthesis Research* **68**: 29–37.

Zhu G, Jensen RG. 1991. Xylulose 1,5-Bisphosphate Synthesized by Ribulose 1,5-Bisphosphate Carboxylase/Oxygenase during Catalysis Binds to Decarbamylated Enzyme. *Plant Physiology* **97**: 1348–1353.

Zhu G, Long SP, Ort DR. 2008. What is the maximum efficiency with which photosynthesis can convert solar energy into biomass? *Current Opinion in Biotechnology* **19**: 153–159.